UNIVERSIDADE DE LISBOA
FACULDADE DE CIÊNCIAS

Harmful Algal Blooms (HAB) in a changing world: the case of S and W Iberian Bays

"Documento Definitivo"

Doutoramento em Ciências do Mar

Mariana Santinho Vieira dos Santos

Tese orientada por:
Prof. Doutora Ana Amorim
Doutora Maria Teresa Moita
Doutor Paulo Brás de Oliveira

Documento especialmente elaborado para a obtenção do grau de doutor

2020

UNIVERSIDADE DE LISBOA

FACULDADE DE CIÊNCIAS

Harmful Algal Blooms (HAB) in a changing world: the case of S and W Iberian Bays

Doutoramento em Ciências do Mar

Mariana Santinho Vieira dos Santos

Tese orientada por:

Prof. Doutora Ana Amorim, Doutora Maria Teresa Moita e Doutor Paulo Brás de Oliveira

Júri:

Presidente:

- Doutor Rui Manuel dos Santos Malhó, Professor Catedrático e Presidente do Departamento de Biologia Vegetal da Faculdade de Ciências da Universidade de Lisboa

Vogais:

- Doutor Emilio Fernández Suárez, Catedrático de Universidad, Facultade de Ciencias do Mar da Universidade de Vigo (Espanha)
- Doutor Henrique Queiroga, Professor Associado com Agregação, Departamento de Biologia da Universidade de Aveiro
- Doutora Ana Maria Branco Barbosa, Professora Auxiliar, Faculdade de Ciências e Tecnologia da Universidade do Algarve
- Doutor Paulo Nogueira Brás de Oliveira, Investigador Auxiliar, IPMA- Instituto Português do Mar e da Atmosfera (orientador)
- Doutora Vanda Costa Brotas Gonçalves, Professora Catedrática, Faculdade de Ciências da Universidade de Lisboa

Documento especialmente elaborado para a obtenção do grau de doutor

Fundação para a Ciência e Tecnologia, Bolsa SFRH/BD/52560/2014

2020

Aos meus pais…

☆♡

"There are some four million different kinds of animals and plants in the world. Four million different solutions to the problems of staying alive"

David Attenborough

AGRADECIMENTOS

Gostaria de deixar aqui o meu agradecimento especial aos meus orientadores, Prof. Doutora Ana Amorim, Doutora Teresa Moita e Doutor Paulo Oliveira, pelo apoio e amizade demonstrados no decorrer desta longa jornada. Os conhecimentos diversos dos três permitiram-me evoluir na minha perspetiva multidisciplinar de avaliar cada novo desafio e permitiram-me chegar a bom porto neste Doutoramento. À Doutora Teresa Moita por tudo, desde 2010, mas especialmente pelo entusiasmo, carinho e amizade que me fizeram ganhar um gosto especial pelas algas nocivas ao longo do meu percurso no IPMA. À Doutora Ana Amorim por tão bem me ter recebido na FCUL, pela sua amizade e por todos os conhecimentos que tem partilhado comigo. Sem dúvida que me tem ajudado a crescer imenso enquanto cientista. Ao Doutor Paulo Oliveira por toda a sua paciência, por me ouvir nas minhas partilhas várias de ânimos e desânimos, por ser o meu "buddy" de mergulho, mas acima de tudo por ser um excelente professor de oceanografia. Aos três, muito obrigada!

Aos meus amigos que estiveram sempre presentes, permanecendo como pilares de força e motivação, tanto no IPMA como na FCUL. Não posso deixar de mencionar uma amiga especial, sem a qual este trabalho não teria sido possível, obrigada Lia Godinho…saudades!

Durante o decorrer desta tese passei pelos melhores e pelos piores momentos da minha vida. Os melhores momentos foram sem dúvida proporcionados pelo meu filho Simão, pilar da minha força. Mas elaborar uma tese de doutoramento quando o mundo nos coloca constantes dificuldades no caminho foi sem dúvida um desafio. Deixo por isso o meu agradecimento de coração à minha família que, apesar de tudo o que temos passado esteve sempre presente para me apoiar em todos os momentos. Obrigado Alexandre Medeiros, por nunca teres permitido que desistisse mesmo quando isso significava um elevado esforço familiar.

Um agradecimento também especial à Professora Doutora Vanda Brotas por todo o apoio e motivação, à Doutora Ana Brito pelo seu incentivo e por ter permitido que dedicasse parte do meu tempo de bolsa à fase final da escrita desta tese, e à Vera Veloso por tanto me ensinar e tantas vezes me chamar à razão.

O presente trabalho foi financiado pelo Programa de Doutoramento da Fundação para a Ciência e Tecnologia (FCT) - PD/143/2012 - Lisbon Doctoral School on Earth System Science, Instituto Dom Luiz (IDL) através da bolsa SFRH/BD/52560/2014. Este trabalho foi também financeiramente suportado pelo Instituto Português do Mar e da Atmosfera (MAR2020-P02M01-1490P), pelo Centro de Ciências do Mar e do Ambiente da Faculdade de

Ciências da Universidade de Lisboa (UIDB/04292/2020) e pelo Centro de Ciências do Mar da Universidade do Algarve (UID/Multi/04326/2020). O trabalho foi ainda cofinanciado pela União Europeia através do FEDER pelo Programa Operacional Regional de Lisboa, Portugal 2020 e por Fundos Nacionais através da FCT no âmbito do projeto HABWAVE, LISBOA-01-0145-FEDER-031265.

ABSTRACT

This thesis aimed to investigate, in two wide-open sheltered bays (Lisbon and Lagos) influenced by upwelling, how the meteorological and oceanographic (MetOc) setting may affect phytoplankton communities. Results of a 9-year time series data showed a high interannual variability of phytoplankton biomass, estimated as chlorophyll *a* (Chl-*a*). Nevertheless, the Chl-*a* sinusoidal model showed different temporal variability patterns in each bay: a uni-modal pattern with a short peak and low Chl-*a* concentrations in Lagos, and a weak bi-modal pattern with a long period of high Chl-*a* concentrations in Lisbon. Cross-correlation analyses performed for Chl-*a* and different MetOc variables indicated that PAR contributed most to Chl-*a* in winter/early-spring, while upwelling and SST were the main drivers in late-spring/summer.

Analysis performed during 1-year showed significant spatial differences in phytoplankton assemblages between the bays. On a temporal scale, significant differences were observed on phytoplankton communities in both bays in the 4-meteorological seasons. However, results from a nearshore station studied in Lagos only indicated the occurrence of 3-biological seasons, with no significant differences between summer and autumn communities. This study suggests that Lagos region has a higher probability for the occurrence of HABs (in higher cell concentrations and persistence). The ecology of the benthic genus *Ostreopsis* was studied based on 7-years of water samples. Two species were identified reaching maximum cell densities in late-summer/early-autumn: *Ostreopsis* cf. *ovata* restricted to the south coast and *Ostreopsis* cf. *siamensis* present in both Portuguese coasts. *Ostreopsis* was much more abundant in Lagos (nearshore) and maxima concentrations were related to positive SST anomalies. High densities in the plankton were often recorded after a period of more than 2-weeks of low sea state, followed by short-time events of onshore wind and moderate waves. In Lisbon, *O.* cf. *siamensis* was seldom recorded in the plankton and no clear relationship could be established with the studied MetOc drivers. The recent records of *Ostreopsis* in this bay are interpreted as an early colonization stage of an invasion process.

The present work highlights the relevance of the peculiarities of regional setting in determining phytoplankton dynamics in wide-open coastal bays influenced by upwelling, even at short latitudinal distance.

Keywords: Upwelling; Chlorophyll *a* seasonality; Phytoplankton; HABs; *Ostreopsis*

RESUMO

Proliferações de algas nocivas (PANs), também conhecidas como florescimento de algas nocivas (FAN), é a denominação que se dá a qualquer proliferação de microalgas que, independentemente da sua concentração, resulte num impacto negativo ao meio ambiente, à exploração de recursos, à saúde pública ou às atividades económicas. As PANs são um fenómeno que se observa nas regiões costeiras de todo o mundo, e recentemente tem-se observado um aumento na variedade e na frequência de PANs a nível global. Os impactos das PANs na saúde dos humanos estão normalmente associados ao consumo de marisco e de peixes contaminados com toxinas provenientes das microalgas. Contudo, existem outras vias de transferência de toxinas para os seres humanos, tais como a libertação de aerossóis tóxicos que podem afetar o sistema respiratório, ou a transferência de toxinas por contato direto que pode causar irritação na pele, bem como outros problemas inflamatórios.

Atualmente aceita-se que as PANs se estão a expandir geograficamente, que estão a aumentar em frequência, e estão a aparecer novas espécies em novas áreas. A eutrofização, a descarga de águas de lastro e a translocação de mariscos, são agora reconhecidas como as principais causas da expansão global de PANs. Sabe-se ainda que as alterações climáticas também estão a afetar a frequência e a severidade das PANs. No entanto, ainda não é claro se parte da expansão que tem vindo a ser observada pode ser devido à melhoria das técnicas, da frequência e da capacidade de monitorização, ou se é unicamente pelo efeito combinado das causas antropogénicas e do aquecimento global.

Portugal situa-se na fronteira entre as regiões subtropical e temperada, e nesta região já se verificam registos da expansão dos limites biogeográficos de várias espécies, incluindo de espécies de fitoplâncton nocivo. A ocorrência desde 2008 de dinoflagelados bentónicos do género *Ostreopsis*, originário de regiões subtropicais/tropicais é um exemplo dessa expansão. As toxinas produzidas por algumas das espécies dentro do género *Ostreopsis* são consideradas das toxinas mais potentes de origem marinha. As proliferações de microalgas bentónicas constituem um novo desafio para os programas de monitorização, pela necessidade de passarem a incluir as comunidades bentónicas nos sistemas nacionais de monitorização.

A costa continental Portuguesa situa-se no limite nordeste do sistema de afloramento costeiro da Ibéria/Canárias, associado ao giro anticiclónico do Atlântico Norte. Na costa ocidental o afloramento costeiro está associado ao regime de nortada e tem uma frequência sazonal, sendo máximo no verão mas ocorrendo entre a primavera e o início do outono. Na costa sul

do Algarve o afloramento é ocasional e induzido por ventos de oeste. As regiões de afloramento costeiro são conhecidas por serem zonas ricas em nutrientes, altamente produtivas, onde se podem encontrar concentrações bastante elevadas de fitoplâncton marinho. Nas áreas costeiras de afloramento, a topografia e as irregularidades costeiras, como a existência de cabos proeminentes e de baías abrigadas, produzem alterações na intensidade e direção do vento e na direção das correntes costeiras locais. Nos cabos, pela elevada exposição ao vento, o afloramento e a advecção horizontal resultante são fortes. A sotavento dos cabos, na zona protegida do vento, quer os ventos quer o afloramento e a advecção horizontal são mais fracos. Nessas regiões abrigadas observam-se frequentemente elevados níveis de biomassa fitoplanctónica proporcionados pelas características locais que resultam em zonas naturais de retenção, susceptíveis a grandes proliferações de fitoplâncton, incluindo a ocorrência de PANs.

Esta tese teve como principal objetivo investigar, em duas baías abrigadas e influenciadas pelo afloramento costeiro, como é que as condições meteorológicas e oceanográficas (MetOc) podem influenciar as comunidades fitoplanctónicas. Deu-se especial ênfase à dinâmica das espécies de PANs, em particular à ocorrência do género bentónico *Ostreopsis*. Os locais de estudo foram a Baía de Lisboa (costa oeste) e a Baía de Lagos (costa sul), ambas localizadas a SE de dois cabos proeminentes, o Cabo da Roca e o Cabo de São Vicente, respetivamente. A Baía de Lisboa foi selecionada por nela existir uma estação costeira estudada há mais de 15 anos e onde, no início deste trabalho, não havia registos de problemas relacionados à presença de espécies bentónicas nocivas. A Baía de Lagos foi selecionada devido à ocorrência, em 2011, de *Ostreopsis* (numa praia local) com elevadas concentrações de células. Na Baía de Lagos selecionou-se uma estação adicional localizada a uma milha náutica da costa (denominada de *Offshore*), de modo a perceber se a estação costeira é representativa das condições oceanográficas circundantes e das comunidades fitoplanctónicas da plataforma interior.

De modo a alcançar o objetivo geral deste trabalho, utilizaram-se diferentes abordagens que são reportadas nos diferentes capítulos desta tese. No Capítulo 2 investigou-se em cada baía quais os ciclos sazonais típicos da clorofila *a* (Chl-*a*). Para tal, utilizaram-se dados de registo semanal (dados *in situ* em Lisboa e valores estimados por satélite para Lisboa e para Lagos) para um período de nove anos (2008-2016). Na Baía de Lisboa, as estimativas de satélite foram comparadas com os dados recolhidos *in situ* para avaliar a capacidade de diferentes produtos de satélite em reproduzirem os ciclos sazonais da Chl-*a* junto à costa. Desta análise

resultaram diferenças importantes entre as duas metodologias, tais como uma sobrestimação das concentrações de Chl-*a* e a antecipação do início e do fim do período produtivo nas estimativas de satélite. As diferentes séries temporais (*in situ* e satélite) mostraram a existência de uma elevada variabilidade inter-anual da biomassa fitoplanctónica. O modelo sinusoidal da Chl-*a*, utilizando as periodicidades anual (12 meses) e sua harmónica (6 meses), revelou padrões de variabilidade temporal da Chl-*a* diferentes em cada baía. Um padrão uni-modal, com um pico curto e com baixas concentrações de Chl-*a* caracterizaram a Baía de Lagos. A Baía de Lisboa apresentou um período longo de Chl-*a* máxima com concentrações mais elevadas e com um padrão a passar para uma tendência bi-modal. Analisou-se a contribuição de diferentes variáveis MetOc (SST, PAR, UI, MLD) para a biomassa fitoplanctónica em cada baía e em diferentes períodos do ano (inverno/início-primavera e fim-primavera/verão). Para tal, fez-se uma análise de correlações cruzadas do lag 0 ao lag 4 (i.e., entre 0 e 4 semanas atrás). A radiação fotossinteticamente ativa foi a variável que mais contribuiu para o aumento da Chl-*a* no inverno/início-primavera, enquanto o afloramento costeiro e a temperatura de superfície foram os principais fatores para os níveis de biomassa observados no final-primavera/verão.

A variabilidade dos principais grupos fitoplanctónicos observados nos anos 2014 e 2015 também foi estudada no Capítulo 2 de forma a compreender melhor os padrões de Chl-*a* observados. Os resultados indicaram uma elevada variabilidade espacial e inter-anual na estrutura da comunidade fitoplanctónica. A análise aos grupos (Capítulos 2 e 3) além de indicar que as diatomáceas foram as que mais contribuíram para a Chl-*a* em ambas as áreas, mostrou também que os cocolitóforos foram mais relevantes na Baía de Lisboa e os dinoflagelados na Baía de Lagos.

Para uma caracterização mais profunda das comunidades fitoplanctónicas estudou-se o ano 2015 com uma amostragem de periodicidade quinzenal (Capítulo 3). A análise multivariada efetuada revelou diferenças significativas nas comunidades fitoplanctónicas entre as baías (Lisboa *vs* Lagos), na Baía de Lagos (praia *vs offshore*) e no tempo (sazonalmente). Os resultados mostraram que diferentes comunidades fitoplanctónicas caracterizam as quatro estações do ano nas duas baías, apresentando particularidades próprias dentro de cada baía. Contudo, a estação costeira estudada na Baía de Lagos apresentou apenas três estações biológicas, uma vez que o verão e o outono não apresentaram diferenças significativas nas comunidades. Os resultados também sugerem que a Baía de Lagos tem uma maior

probabilidade de ocorrência de PANs, tanto de espécies planctónicas como bentónicas, quer em concentrações celulares mais elevadas como por períodos mais alargados.

A ecologia dos dinoflagelados bentónicos pertencentes ao género *Ostreopsis* foi estudada no Capítulo 4. Para tal, analisou-se uma série temporal de 7 anos (2011-2017) de amostras recolhidas na coluna de água com uma periodicidade semanal. A identificação das espécies foi realizada através de análises moleculares e revelou a presença de duas espécies: *Ostreopsis* cf. *ovata* presente apenas na costa sul, e *Ostreopsis* cf. *siamensis* que apresentou um intervalo de distribuição maior, aparecendo também na costa oeste. Nas duas baías, a concentração máxima de células observou-se entre o fim do verão e o início do outono. Na Baía de Lagos detetou-se *Ostreopsis* spp. com uma maior frequência de ocorrência, mas apenas em 2013 se registou um máximo (~17 x 10^3 cel L^{-1}) que atingiu concentrações celulares acima dos níveis de alerta reconhecidos em países afetados por estas PAN (>10 x 10^3 cel L^{-1}). Nesta baía observou-se uma relação significativa entre os máximos de *Ostreopsis* spp. e as anomalias positivas de temperatura da água. As densidades elevadas de *Ostreopsis* spp. observadas no plâncton foram frequentemente observadas após um período de mais de duas semanas de baixa agitação marítima, seguido de eventos curtos de ventos de levante e agitação marítima moderada. Na Baía de Lisboa, a presença de *O.* cf. *siamensis* foi sempre vestigial, com exceção do ano 2017 em que se registaram 620 cel L^{-1}. Como tal, não foi possível estabelecer uma relação clara entre a ocorrência desta espécie e as variáveis MetOc. De todo o modo, os registos de *Ostreopsis* na Baía de Lisboa parecem corresponder a uma fase inicial de colonização associada a um processo de invasão. O conhecimento adquirido sobre a dinâmica de *Ostreopsis* na costa Portuguesa pode contribuir para a melhoria das técnicas de monitorização de PANs, as quais devem ser adaptadas à ocorrência de espécies bentónicas.

O presente trabalho destacou como pecularidades meteorológicas e oceanográficas regionais podem ser relevantes na dinâmica fitoplanctónica em baías costeiras abertas influenciadas pelo efeito do afloramento costeiro, mesmo encontrando-se essas baías a uma curta distância latitudinal.

Palavras-chave: Afloramento costeiro; Sazonalidade da clorofila *a*; Fitoplâncton; Proliferações de algas nocivas; *Ostreopsis*

TABLE OF CONTENTS

LIST OF FIGURES

LIST OF TABLES

Chapter 1.

Introduction

1.1. General context

Harmful Algal Blooms, commonly denominated as HABs, is the name given to any proliferation of algae that, independently of its concentration, results in a negative impact in the environment, in the exploitation of resources, in public health or in economic activities. Coastal oceanic regions throughout the world are currently subject to frequent and diverse HAB events (Anderson, 2007; Hallegraef, 2010; Glibert et al., 2014; Gobler et al., 2017). HABs occur worldwide requiring an integrated and coordinated scientific understanding and demanding regional responses and solutions (Anderson et al., 2019). In humans, several serious illnesses are associated with the consumption of shellfish and fin-fish contaminated with microalgae toxins. The human syndromes are designated according to the symptoms that they produce, and in temperate areas these are predominantly the paralytic shellfish poisoning (PSP), diarrhetic shellfish poisoning (DSP), neurotoxic shellfish poisoning (NSP), amnesic shellfish poisoning (ASP) and azaspiracid poisoning (AZP) (Berdalet et al., 2016). There are however other routes of toxin transfer to humans, namely the release of toxic aerosols, which may affect the respiratory system, or toxin transfer by direct contact, which may cause skin irritation or other inflammatory responses (Anderson et al., 2012).

In Portugal, poisoning syndromes have been related mainly to the presence of diatoms of genus *Pseudo-nitzschia* (ASP producer) and to dinoflagellates of genus *Dinophysis* (DSP) and *Gymnodinium* (PSP) (Silva et al., 2016; Vale et al., 2008, Carvalho et al. 2019). The dinoflagellate *Lingulodinium polyedra* has also been associated with the production of toxins potentially harmful to humans, known as yessotoxins. Although so far it has never been associated with shellfish poisoning events, this species is frequently responsible for massive coastal blooms that cause water discoloration (red-tide) and impact tourism in the affected region (Amorim et al. 2001, 2004; Pinto, 1949). More recently, the potentially harmful genera *Karenia* and *Ostreopsis* have been recorded by the national HAB monitoring program, held by the Portuguese Institute for the Sea and Atmosphere (IPMA, I.P.) (Santos et al., 2019; Silva et al., 2016).

It is currently accepted that HABs are expanding globally, in frequency and extension, and new species are emerging in new areas (Glibert et al., 2014; Glibert and Burford, 2017; Gobler et al., 2017; Tester et al., 2020). The causes behind this expansion have been debated, with possible explanations ranging from natural mechanisms of species dispersal, through the ocean current systems, to several anthropogenic causes. Cultural eutrophication and other

human activities such as ballast water discharge and shellfish translocation are now recognized as major drivers of global HAB expansion (Anderson et al., 2012; Fu et al., 2012; Glibert and Burford, 2017; Hallegraeff, 2010). There is also an emerging evidence that climate change is already impacting the frequency and severity of HABs in marine, brackish and freshwater environments (Anderson et al., 2012; Fu et al., 2012; Gobler et al., 2017; Hallegraeff, 2010). Nevertheless, it is still not clear if part of this expansion is due to the improved detection and monitoring capacity or only due to the combined effect of global warming and anthropogenic forcing (Vila et al., 2016). As an example of HABs expansion, Figure 1.1 shows the cumulative global increase distribution recorded in 45 years of the species responsible for PSP. Paralytic shellfish poisoning is caused by saxitoxin and its derivatives, and can cause headaches, nausea, facial numbness and, in severe cases, respiratory failure and death (Berdalet et al., 2016).

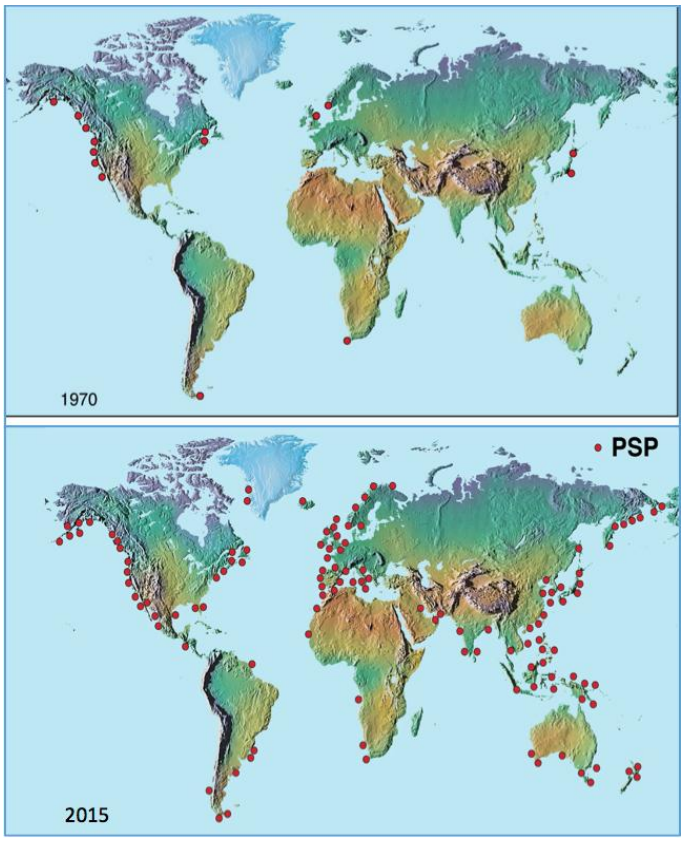

Fig. 1.1. The global expansion in the distribution of paralytic shellfish poisoning (PSP) toxins: 1970 versus 2015 (available at https://www.whoi.edu/website/redtide/regions/world-distribution/)

In the Mediterranean Sea, a recent threat has deserved attention: the proliferation of the benthic dinoflagellate of genus *Ostreopsis* Schmidt. Benthic HABs (BHABs) is the name given to proliferations of certain harmful species that have a dominant life cycle associated

with benthos (e.g macrophytes, algal turfs, rocks or sand substrates) to which they attach by synthesizing mucilaginous substances. Due to its physiology combined with water motion, the cells can be released from the benthos to the plankton communities as free-swimming cells or within floating aggregates (Wells et al., 2019). Species of *Ostreopsis* have been reported from the Mediterranean Sea since the 1970s but the first bloom was only detected in 1998 on coast of Toscany, Italy (Penna et al., 2005). After 2003, *Ostreopsis* blooms spread along the Tyrrhenian, Sicilian and Adriatic coasts where there were reports of people affected by toxins after swimming or when exposed to marine aerosols (Barone, 2007; Penna et al., 2007). In 2005 and 2006, high cell concentrations were reported from the west Mediterranean, Baleares and Murcia coasts (Spanish coast) (Gilabert et al., 2008; Penna et al., 2005). Following the outbreaks in the west Mediterranean, in 2004 a bloom of *Ostreopsis* was reported for the first time off the Moroccan upwelling coast (Bennouna et al., 2012). After that, in 2005 species of *Ostreopsis* were detected in Atlantic islands (Madeira and Canarias) (Fraga et al., 2005) and in 2008 on the upwelling coast of southwest Portugal (Sines) (Amorim et al., 2010). The first planktonic bloom, identified as *Ostreopsis* cf. *ovata*, in the south coast of Portugal (Lagos) was reported in 2011 (David et al., 2012). In Figure 1.2 is showed an illustrative map of the expansion of *Ostreopsis* in Mediterranean Sea and in upwelling Atlantic region (Santos et al., 2016).

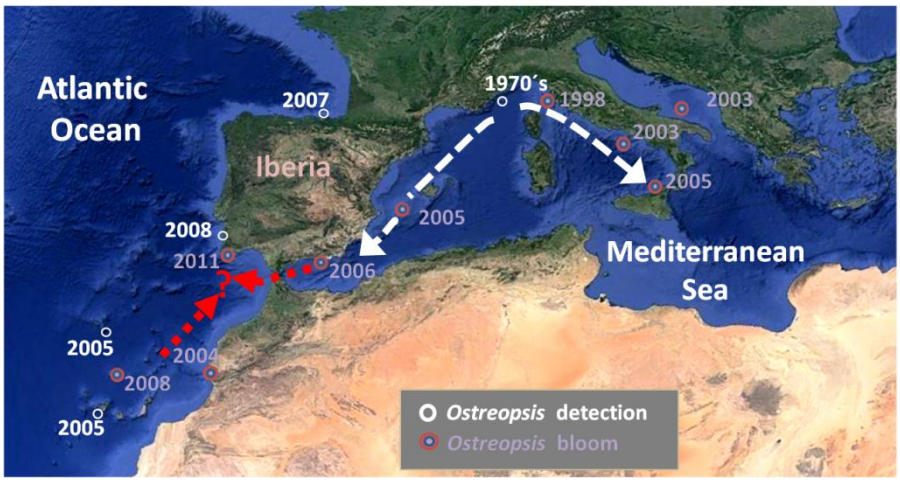

Fig. 1.2. Schematic map indicating the year when species of *Ostreopsis* were first detected (white circles) and the year of the first reported bloom (red circle). White arrows suggest the possible expansion route of the genus within the Mediterranean Sea, and the red arrows indicated the possible expansion routes of *Ostreopsis* to the SW Iberia. The information shown in this figure includes the occurrence of two species in some of the locations: *O.* cf. *ovata* and *O.* cf. *siamensis*.

Combining morphological data with phylogenetic analyses is a necessary approach to a correct identification of the different *Ostreopsis* species. In the Mediterranean Sea, only two

species have been recorded until now, *O.* cf. *ovata* and *O.* cf. *siamensis* (e.g. Battocchi et al., 2010; Mangialajo et al., 2011; Penna et al., 2005, 2010; Totti et al., 2010). Along the Mediterranean rocky coasts *O.* cf. *ovata* is the most abundant and widely distributed (Battocchi et al., 2010; Penna et al., 2010). *Ostreopsis* cf. *ovata* are widely dispersed from the western, Brazil (Nascimento et al., 2010, 2012), to the eastern Atlantic basin, being the south Portuguese coast the known northern limit of this species (David et al., 2012, 2013, Santos et al., 2019), and throughout the Mediterranean Sea (Penna et al., 2005, 2010). All these *O.* cf. *ovata* strains have a high degree of sequence homology (Penna et al., 2010). In the Mediterranean, *O.* cf. *siamensis* has a more restricted distribution occurring along the Catalan coast, in the Tyrrhenian Sea, and in Almería (Penna et al., 2005, 2010). This species is also observed in the NE Atlantic coast (Morocco, Portugal and northern Spain) (Amorim et al., 2010; Bennouna et al., 2012; David et al., 2013) and the studied strains shared the same sequence with the strains reported from the Mediterranean Sea.

Ostreopsis cf. *siamensis* strains of the Mediterranean and Atlantic seems to have irrelevant levels of toxicity, suggesting that this species has much lower risk to human health than *O.* cf. *ovata* (Ciminiello et al., 2013). *Ostreopsis* cf. *ovata* has been linked to massive mortalities of benthic fauna and mild respiratory irritations in people exposed to marine aerosols (Vila et al., 2016 and references therein). This genus also produces potent toxins that are among the most potent biotoxins of marine origin (palytoxins and analogues), which were associated with dramatic seafood poisonings in tropical latitudes (Randall, 2005). Today, emerging blooms associated with benthic *Ostreopsis,* which produce biotoxins that may cause respiratory irritation and cause potential seafood poisoning, constitute a new challenge that requires an adaptive monitoring design to include the benthos (Anderson et al., 2019).

Portugal is located in the temperate subtropical boundary and there is already evidence for the expansion of the biogeographical limits of several taxa, including HAB species (Ribeiro et al., 2012). The occurrence reported since 2008 of the sub-tropical/tropical benthic dinoflagellate *Ostreopsis* (Amorim et al., 2010; David et al., 2012, 2013) is an example of possible expansion, following the pattern already observed in other temperate regions (Cioccio, 2014; Rhodes, 2011; Fig. 1.3).

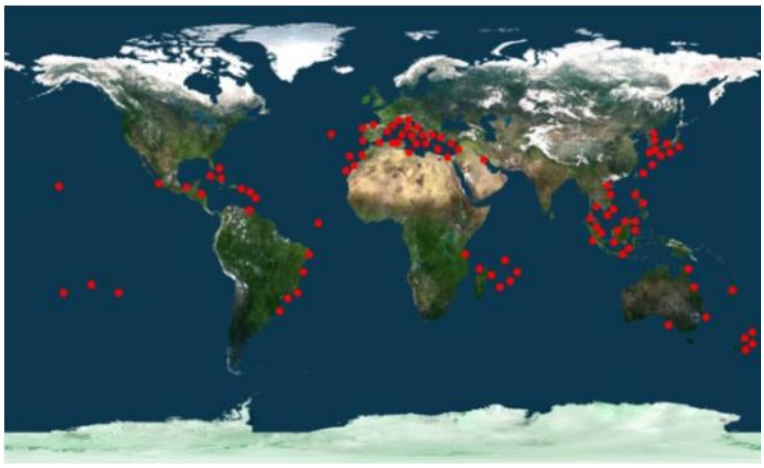

Fig. 1.3. *Ostreopsis* genus distribution, updated on March 2015 (from Cioccio, 2014).

1.2. Phytoplankton in the Portuguese coast

In nutrient-rich upwelling regions, generally denominated as Eastern Boundary Upwelling Ecosystems (EBUEs), phytoplankton shows some of the highest productivity levels in the world (Hill et al., 1998). The four main EBUEs (Fig. 1.4) are the Canary, California, Humboldt and Benguela Currents systems (see Fréon et al., 2009 for a review). EBUEs are narrow ocean strips, located on the western margin of the continents, which extend latitudinally for thousands of kilometers and longitudinally beyond the continental shelves (Fréon et al., 2009). In these regions, the combined effect of intense trade winds with the earth's rotation generates coastal upwelling that brings cold but nutrient-rich water from the deep to the surface (see Chavez and Messié, 2009, and Fréon et al., 2009 for a review).

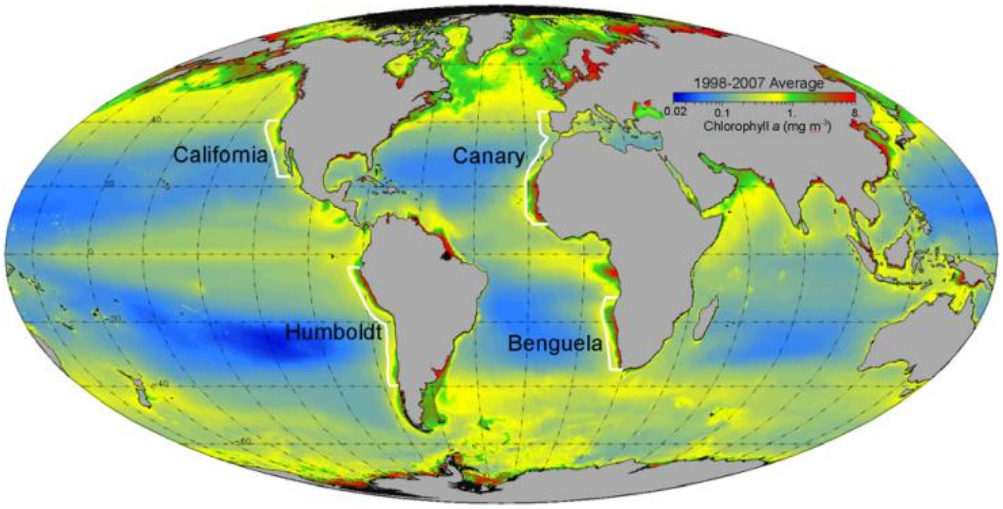

Fig. 1.4. Chlorophyll *a* concentration from SeaWiFS for the 1998–2007 period and EBUEs location (from Fréon et al., 2009).

The Portuguese continental coast is in the northeastern limit of the Iberia/Canary Current System (ICCS), one of the least studied or understood upwelling ecosystems in the world (Chavez and Messié, 2009), being located along the eastern rim of the North Atlantic anticyclonic gyre (Wooster et al., 1976). Some particular features of the ICCS are the high freshwater input, high variability in coastline configuration, complex topography, and retentive versus dispersive physical mechanisms (Fréon et al., 2009). Different tendencies on phytoplankton biomass have been reported in the Canary ecosystem. Bode et al. (2009) reported a continuous decrease in the upwelling intensity over the last 40 years on the northern region together with a warming trend of surface waters, but with no significant trends recorded in phytoplankton biomass. Arístegui et al. (2009), describe the ICCS as the EBUE that is warming faster and related this pattern with a slight decrease in productivity over the last decades. By contrast, Chavez and Messié (2009) did not find any phytoplankton biomass trend in NW Africa (Canary system, in the same NE Atlantic EBUE), but observed an increasing trend in the other three EBUEs.

In coastal upwelling regions, topography and coastline irregularities, such as capes and bays, produce variations in coastal wind, alongshore currents, as well as in chemical and biological responses (Chavez and Messié, 2009; Largier, 2020). Bays may act as upwelling shadow areas where weaker horizontal advection and retentive circulation patterns are frequently observed in association with higher nearshore phytoplankton biomass (see Largier, 2020 for a review). Strong gradients are formed between the new upwelled waters off a cape and these protected upwelling shadow waters (Chavez and Messié, 2009). Bays are usually stratified regions, maintain high light levels for phytoplankton growth, and the circulation patterns act as retention zones for plankton in the region (Largier et al., 2006). As a result, high levels of phytoplankton biomass are sustained in these upwelling shadows (e.g. Graham and Largier, 1997; Largier et al., 2006; Largier, 2020; Oliveira et al., 2009). These retention zones are thus more susceptible to phytoplankton bloom development, including the occurrence of HABs (Kudela et al., 2008; Moita et al., 2003; Pitcher et al., 2010, 2018). Although frequent and of high importance, these shallow coastal embayments are poorly studied (Walter et al., 2018).

The Portuguese continental coast is characterized by several prominent topographic features, like headlands and submarine canyons (Relvas et al., 2007), as well as by several mesoscale structures, such as fronts, jets, upwelling filaments and countercurrents (Haynes et al., 1993; Peliz et al., 2002; Relvas et al., 2007; Relvas and Barton, 2005). In this region, due to the prevailing northerly winds, upwelling has a seasonal periodicity occurring between spring and

early autumn, although stronger in summer (Fiúza et al., 1982; Goela et al., 2016; Relvas and Barton, 2002; Wooster et al., 1976). While some episodes of upwelling may occur in autumn and winter, there is a prevalence of downwelling induced by southerly winds during these seasons (Alvarez et al., 2008; Goela et al., 2016). At Cape S. Vicente, the Portuguese continental coastline changes from meridional to a zonal orientation. During summer, weak and intermittent westerlies along the coast produce weak local upwelling alternating with a recurrent warm coastal countercurrent along the southern coast (Relvas et al., 2007; Relvas and Barton, 2002, 2005). This counterflow can turn northward at the cape and extend along the west coast, inshore of the coastal upwelling jet that typically occupies the southwestern shelf. This equatorward coastal jet usually turns eastward at Cape S. Vicente along the southern shelf break, however, it can also continue southward or, rarely, turn westward to form a cold filament (Relvas and Barton, 2002, 2005) (Fig. 1.5).

Along the Portuguese coast, there are important shadow areas, with different circulation patterns downstream of prominent capes, which have been described associated with the separation of the coastal upwelling jet. This is the case of Lisbon and Setúbal Bays influenced by an upwelling jet rooted at Cape Roca (Oliveira et al., 2009). Lisbon and Setúbal Bays are considered as wide-open bays with a marked step (*i.e.* headland) at one end, where winds tend to separate from the coast (Largier, 2020). The main features of wide-open bays are the elevation of water level in the upwelling shadow and warm and stratified water at the surface (Largier, 2020). The circulation in the bay tends to be weakly cyclonic, and onshore advection is observed at mid-bay. In Lisbon Bay, an upwelling filament, rooted at Cape Roca, that extends southward or westward of the bay, is frequently observed (Moita et al., 2003; Oliveira et al., 2009). The patterns of chlorophyll *a*, as well as HABs distribution, associated with these features are asymmetric relative to the upwelling core (Moita et al., 2003; Oliveira et al., 2009). During the intense wind phase, the asymmetric chlorophyll *a* pattern relative to sea surface temperature (SST) was related to the shallower mixed layer depth and to the moderate horizontal advection (Oliveira et al., 2009). The highest phytoplankton abundances were observed at the leeward side of the filaments, where chain-forming dinoflagellates, including the harmful *Gymnodinium catenatum* dominated, whereas diatoms tended to dominate the core and the outer side of the filament (Moita et al., 2003). Setúbal Bay is characterized by a persistent stratified warmer water pool. In this bay, the development of a harmful dinoflagellate bloom was related to particular conditions, when the upwelling plumes rooted at Capes Roca and Cape Espichel were unusually displaced shoreward into Setúbal Bay

(Amorim et al., 2004). Cape S. Vicente being a major step break in shoreline orientation also exhibit comparable features with wide-open bays, such as a marked step at one end, an offshore band of wind curl, a tendency for poleward flow nearshore, and an upwelling-sheltered region (Largier, 2020). Lagos Bay, located in this region is an example of a sheltered bay where harmful blooms of benthic dinoflagellates genus *Ostreopsis*, observed since 2011, have been associated with warm sea surface temperatures and local sea state conditions (Santos et al., 2019).

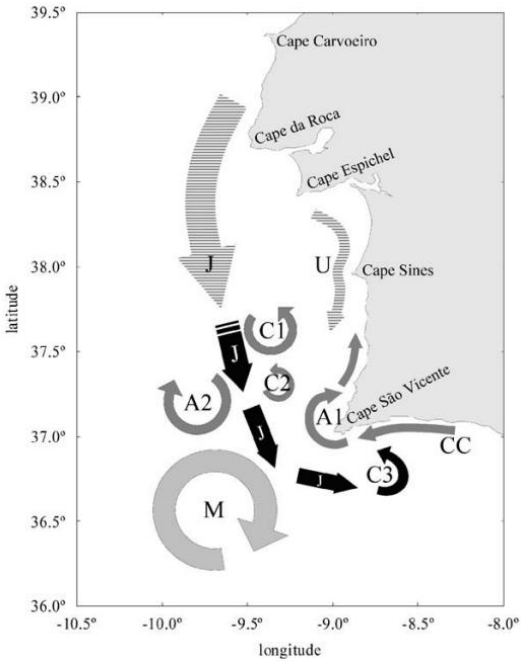

Fig. 1.5. Circulation scheme observed during upwelling relaxation off Cape S. Vicente (from Relvas and Barton, 2005). Upwelling jet (J), anticyclonic rotation (A), cyclonic rotation (C), coastal warm counterflow (CC), upwelling remnants off Cape Sines (U), and possible signature of a deeper meddy (M).

Several studies have been developed to better understand the phytoplankton patterns in the Atlantic Iberian coast. In the last 20 years, some of these studies were developed using *in situ* phytoplankton and/or chlorophyll *a* data (e.g. Cabrita et al., 2015; Cravo et al., 2010; Danchenko et al., 2019; Figueiras et al., 2002; Goela et al., 2014, 2015; Guerreiro et al., 2013; Loureiro et al., 2005, 2011; Mendes et al., 2011; Moita, 2001; Silva et al., 2008, 2009; Vidal et al., 2017), while others were performed using a remote sensing approach (e.g. Cristina et al., 2016; Ferreira et al., 2019; Goela et al., 2015; Krug et al., 2017, 2018; Navarro and Ruiz, 2006). Most of these studies addressed the zonal and meridional continental coasts separately. *In situ* studies allow for the taxonomical characterization of phytoplankton assemblages, however they have low sampling resolution and are time and space-limited. On the other hand, remote sensing based-studies have a high spatio-temporal resolution, but they lack the

discrimination of the phytoplankton communities. Different phytoplankton groups have different biogeochemical functions, allowing them to perform diverse functions in the marine ecosystem. Ecosystem processes are important determinants of the biogeochemistry of the ocean, thus may be affected by environmental changes such as climate warming (Machado et al, 2019). In the last decades, in addition to the more classical taxonomical approach, phytoplankton is incorporating the concept of functional types to better grasp the ecological relevance of the group. Phytoplankton functional types (PFTs) may be defined according to cell size (picophytoplankton (0.2–2 μm), nanophytoplankton (2–20 μm) and microphytoplankton (>20 μm)) or according to the biogeochemical functions, such as calcification (coccolithophores), silicification (e.g. diatoms), Dimethyl sulfide (DMS) production (e.g. autotrophic flagellates) or nitrogen fixation (e.g. cyanobacteria) (Nair et al., 2008). However, the classification in PFTs is not straightforward, since in the same taxonomic size class more than one biogeochemical functional type may occur (Nair et al., 2008). Only the combination of remote sensing data and the use of *in situ* phytoplankton data by different analysis techniques (e.g. microscopy, flow cytometry and HPLC-high performance liquid chromatography) allows the extraction of the maximum information on the distribution of PFTs at both regional (e.g. Brotas et al., 2013) and global scales (e.g. Quéré et al., 2005).

In the last years, the studies that analyzed the phytoplankton assemblages in the Atlantic Iberian coast focused mainly on microphytoplankton, such as diatoms and dinoflagellates, and on some species within nanophytoplankton, namely the coccolithophores and other small flagellates. Those studies allowed a better understanding of the seasonality of phytoplankton assemblages in this upwelling region.

The seasonal variation of phytoplankton assemblages observed along the Portuguese continental coast (see an example in Fig. 1.6) depends mainly on the seasonality of upwelling/downwelling dynamics, on the water column mixing/stratification patterns (Figueiras and Rios, 1993; Moita, 2001; Silva et al., 2009), and on the freshwater input especially observed to the North of Cape Roca (Moita, 2001). Strong water turbulence observed during spring and summer under active upwelling conditions favors the growth of diatoms, most of them of the chain-forming type, as for example *Chaetoceros* spp., *Guinardia* spp., *Pseudo-nitzschia* spp. *Leptocylindrus danicus*, *Cylindrotheca closterium*, *Thalassiosira* spp., *Detonula pumila* and *Thalassionema nitzschioides* (Figueiras and Rios, 1993; Moita, 2001; Silva et al., 2009). Water column stratification, maxima in summer and autumn, favor

both auto- and heterotrophic dinoflagellates (e.g. species of genus *Ceratium*, *Dinophysis*, *Protoperidinium*, *Prorocentrum* and *Gymnodinium*) (Figueiras and Rios, 1993; Moita, 2001; Silva et al., 2009). Unlike the other diatoms, *Proboscia alata* is also abundant in this community typical of stratification conditions (Moita, 2001).

The transition from upwelling to downwelling occurs in autumn. These conditions together with the decrease of stratification favor mainly the growth of chain-forming dinoflagellates, such as *Gymnodinium catenatum* and *Alexandrium affine* (Moita, 2001), as well as large forms of coccolithophores, like *Coronosphaera mediterranea* (Silva et al., 2008, 2009). In winter, phytoplankton concentration is minimal and the higher relative abundances belong to the coccolithophores, such as *Calcidiscus* species (Moita, 2001; Silva et al., 2008, 2009). In addition, due to the strong water column mixing, high resuspension and low stratification, winter community is also characterized by the presence of several benthic, and tycoplanktonic diatoms species (e.g. *Paralia sulcata*, *Navicula* spp., *Pleurosigma* spp. and *Diploneis* spp.) (Figueiras and Rios, 1993; Moita, 2001).

The differences observed in phytoplankton assemblages according to the latitude variation are usually regarded as being much less relevant than the seasonal differences (Moita, 2001). Nevertheless, the shelf to the north of Cape Roca is much wider and even, than to the south of this cape. In addition, there is a higher input of freshwater by rivers to the north of Cape Roca and the upwelling intensity is stronger to the south of the cape (Fiúza et al., 1982; Moita, 2001). These features promote different thermo-haline stratification patterns on the NW and SW Iberian coasts, and for instance, coccolithophores seem to be more abundant in the SW region. The diatom and dinoflagellate assemblages vary in response to the stratification/mixing conditions of the water column observed in each region (Moita, 2001).

Harmful algal species in the Portuguese continental coast, similarly to the non-harmful species, also have different growth patterns associated with the upwelling intensity and stratification conditions (e.g. Amorim et al., 2004; Danchenko et al., 2019; Loureiro et al., 2005, 2011, Moita et al., 2003, 2016; Palma et al., 2010; Vidal et al., 2017). The diatoms of genus *Pseudo-nitzschia* are highly representative in the phytoplankton assemblage during the upwelling season (Danchenko et al., 2019; Loureiro et al., 2005; Palma et al., 2010). However, either with microscopic identification (Danchenko et al., 2019; Loureiro et al., 2005; Palma et al., 2010) or using microarray probes (Danchenko et al., 2019), very little is known on the distribution and ecology of different *Pseudo-nitzschia* species.

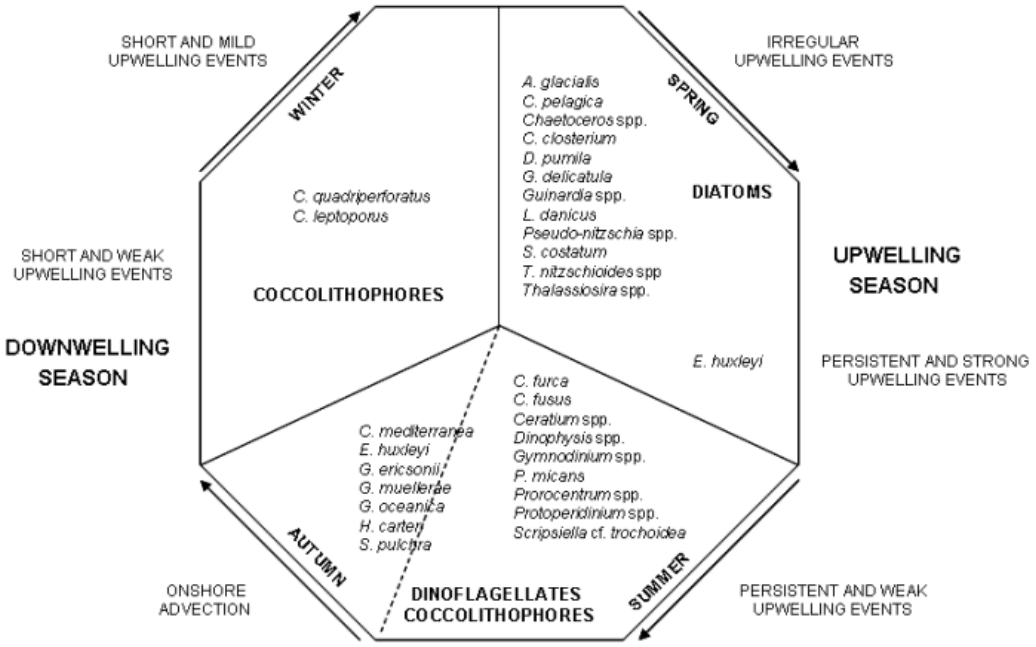

Fig. 1.6. Schematic representation of the seasonal distribution of phytoplankton groups and dominant species in Lisbon Bay (from Silva et al., 2009).

Dinophysis species (mixotrophic dinoflagellates) occur in a wide time-window, from spring to autumn, preferentially in a well-stratified water column, although also inshore of the upwelling fronts during summer (Moita, 2001). Different upwelling intensity, runoff and SST patterns were considered the main variables related to the location and timing of *Dinophysis* bloom initiation and intensity in NW Iberia (Moita et al., 2016). *Dinophysis acuminata* and *Dinophysis acuta* are the two most relevant species in W Iberia and show different behaviors in space and time (Moita et al., 2016; Díaz et al., 2019). Autotrophic dinoflagellates, such as *Gymnodinium catenatum* and *Lingulodinium polyedra* are usually observed in late summer/early-autumn, during the transition of upwelling to downwelling conditions (Amorim et al., 2004; Moita, 2001; Moita et al., 2003). About other HAB species observed in the Portuguese continental coast, there is only scattered information about *Karenia* spp., small dinoflagellates as *Karlodinium* spp. and *Azadinium* spp., and toxic flagellates as *Heterosigma akashiwo* (Danchenko et al., 2019; Loureiro et al., 2011).

A recent concern in the Portuguese coast, as mentioned in section 1.1, is the presence of the benthic dinoflagellate genus *Ostreopsis* in the SW region. These species were usually found in low concentrations, especially in summer and autumn (Amorim et al., 2010; Loureiro et al., 2011). Only in 2011 the first bloom of *Ostreopsis* cf. *ovata* was recorded in the water column, nearshore in Lagos Bay (south coast). No significant harmful effects were reported, but there

were negative impacts on tourism due to the closure of several beaches by the local authorities (David et al., 2012). After this first planktonic bloom, *Ostreopsis* spp. have been recurrently recorded in water samples in Lagos Bay, with a maximum cell concentration observed in 2013 (Santos et al., 2019). More recently, in 2017, a high planktonic density of *O.* cf. *siamensis* was recorded in Lisbon Bay (west coast) (Santos et al., 2019), concomitant with the first detection of a benthic bloom in the same area (David et al., 2018).

1.3. Thesis layout, objectives and proposed approach

The main objective of the present thesis was to investigate, in wide-open sheltered bays influenced by coastal upwelling, how the oceanographic setting may influence phytoplankton communities. Special emphasis was put on HAB species dynamics, in relation to the underlying meteorological and oceanographic conditions.

To achieve this goal, two wide-open coastal bays located at short latitudinal distances, but with different coastline orientations, were studied at high temporal resolution (weekly sampling) with different approaches. The sites chosen were Lisbon and Lagos Bays, located at SE of two prominent SW Iberia headlands. Lisbon Bay was selected because there is a long-term study station, at Cascais, monitored by IPMA for more than 15 years, and where, at the beginning of the current work, there were no known problems related to benthic HABs. Lagos Bay was selected due to the known occurrence of high cell concentrations of *Ostreopsis* in D. Ana beach, since 2011. In this location, a weekly time series was implemented since that event (late-2011). In the present work, an additional station, located offshore, was also studied in Lagos Bay. This study site was used to test if the nearshore station is representative of the offshore surrounding conditions and inner-shelf phytoplankton communities.

The different approaches are herein presented as separate chapters, and have already been submitted for publication in peer-reviewed journals:

- In Chapter 2, the relevance of small latitudinal distances and/or coastline orientation on chlorophyll *a* seasonal cycles were investigated using a weekly 9-years time series data (2008-2016). The role of several meteorological and oceanographic (MetOc) drivers to the spatio-temporal differences observed in the phytoplankton biomass were also investigated. In Lisbon Bay, satellite estimates were compared with *in situ* data to assess the ability of different L4 ocean color products to reproduce the near-coast chlorophyll *a*

seasonal cycle. Furthermore, main phytoplankton groups were studied during 2014 and 2015 to better understand the observed chlorophyll *a* patterns.

- In Chapter 3 phytoplankton assemblages were studied and compared for one year in the two bays. The main MetOc drivers responsible for shape the phytoplankton communities structure and dynamics were also investigated. The study also focused on the understanding of how the local environmental setting may influence different HAB species due to their potential impact on the regional economy. In this study, sampling was performed with a fortnightly scale.
- Chapter 4 addresses the ecology of benthic HABs of genus *Ostreopsis*. A weekly dataset of water samples collected over 7 years (2011-2017) was used in order to identify the different *Ostreopsis* species found in the studied bays and their spatial distribution. In this chapter, *Ostreopsis* temporal distribution patterns were also studied and different MetOc conditions investigated, in order to understand the main drivers that favor *Ostreopsis* blooms development and the favorable conditions to the resuspension of the benthic cells into the water column.

This work, making use of about a decade of different datasets, allows the characterization of the phytoplankton biomass and communities, from short-term to interannual scales of variability. The results and conclusions of this investigation are summarized in Chapter 5.

1.4. List of contributions

During the course of this thesis, the following scientific contributions were achieved:

1) Included in this dissertation for evaluation:

- **Santos, M.**, Moita, M.T., Oliveira, P.B., Amorim, A. Phytoplankton communities in two sheltered bays in the Iberian upwelling system. Journal of Sea Research (*under review*).
- **Santos, M.**, Mouriño, H., Moita, M.T., Silva, A., Amorim, A., Oliveira, P.B.. Characterizing phytoplankton biomass seasonal cycles in two NE Atlantic coastal bays. Continental Shelf Research (*under review*).
- **Santos, M.**, Oliveira, P.B., Moita, M.T., David, H., Caeiro, M.F., Zingone, A., Amorim, A., Silva, A. (2019). Ocurrence of *Ostreopsis* in two temperate coastal bays (SW Iberia): Insights from the plankton. Harmful Algae 86, 20–36. doi:10.1016/j.hal.2019.03.003

2) Within the scope of this thesis, but not included for evaluation:

- David, H., Laza-Martínez, A., **Santos, M.**, Caeiro, M.F., Tartaglione, L., Varriale, F., Dell'Aversano, C., Penna, A., Amorim, A. Morphological, molecular and toxicological data on *Ostreopsis* cf. *siamensis* (Dinophyceae): proposal of a new species *Ostreopsis rinoi* sp. nov. Proceedings of the 18th International Conference on Harmful Algae (*accepted*).
- Oliveira, P.B., **Santos, M.**, Moita, M.T., Amorim, A., 2018. Assessment of sea surface temperature estimates near the coast off SW Portugal. Actas das 5as Jornadas de Engenharia Hidrográfica, 19-21 Junho 2018, Lisboa, pp. 151-154. https://www.hidrografico.pt/recursos/files/jornadas_EH/JEH2018/Actas_5JEH.pdf
- Oliveira, P.B., **Santos, M.**, Moita, M.T., Amorim, A., 2016. Circulação costeira no barlavento Algarvio no verão e outono de 2015. Actas das 4as Jornadas de Engenharia Hidrográfica, 21-23 Junho 2016, Lisboa, pp. 199-202. https://www.hidrografico.pt/recursos/files/revistas_publicacoes/20160621_Atas_4jornadas_EH.pdf

3) Other contributions:

- Riou, V., Batista, D.F., Roukaerts, A., Biegala, I.C., Prakya, S.R., Loureiro, C.M., **Santos, M.**, MunizPiniella, A.E., Schmiing, M., Elskens, M., Brion, N., Martins, M.A. and Dehairs, F., 2016. Impact of contrasting conditions at the North-Western Azores Current on carbon- and N2- fixation rates and the abundance of diazotrophic unicellular cyanobacteria. PLoS ONE 11 (3): e0150827. doi:10.1371/journal.pone.0150827
- Silva, A., Pinto, L., Rodrigues, S.M., de Pablo, H., **Santos, M.**, Moita, T. and Mateus, M., 2016. A HAB warning system for shellfish harvesting in Portugal. Harmful Algae 53, 33-39. http://dx.doi.org/10.1016/j.hal.2015.11.017
- **Santos, M.**, P.R. Costa, F.M. Porteiro and M.T. Moita, 2014. First report of a massive bloom of *Alexandrium minutum* (Dinophyceae) in middle North Atlantic: a coastal lagoon in S. Jorge Island, Azores. Toxicon 90, 265-268. https://doi.org/10.1016/j.toxicon.2014.08.065

References

Alvarez, I., Gomez-gesteira, M., DeCastro, M., Dias, J.M., 2008. Spatio-temporal evolution of upwelling regime along the western coast of the Iberian Peninsula. J. Geophys. Res. 113, C07020. doi:10.1029/2008JC004744

Amorim, A., Palma, S., Sampayo, M.A., Moita, M.T., 2001. On a *Lingulodinium polyedrum* bloom in Setúbal Bay, Portugal, *in* Hallegraeff, G.M., Blackburn, S.I., Bolch, C.J., Lewis, R.J. (Eds.), Harmful Algal Blooms 2000, pp. 133-136

Amorim, A., Moita, M., Oliveira, P., 2004. Dinoflagellate blooms related to coastal upwelling plumes off Portugal, *in*: Steidinger, K.A., Landsberg, J.H., Tomas, C.R., Vargo, G.A. (Eds.), Harmful Algae 2002. Florida Fish and Wildlife Conservation Commission, Florida Institute of Oceanography, and Intergovernmental Oceanographic Commission of UNESCO, St. Petersburg, Florida, USA, pp. 89–91.

Amorim, A., Veloso, V., Penna, A., 2010. First detection of *Ostreopsis* cf . *siamensis* in Portuguese coastal waters. Harmful Algae News 42, 6–7.

Anderson, D.M., 2007. The Ecology and Oceanography of Harmful Algal Blooms: Multidisciplinary Approaches to Research and Management, IOC Technical Series 74. UNESCO. doi:IOC/2007/TS/74

Anderson, D.M., Cembella, A.D., Hallegraeff, G.M., 2012. Progress in Understanding Harmful Algal Blooms: Paradigm Shifts and New Technologies for Research, Monitoring, and Management. Ann. Rev. Mar. Sci. 4, 143–176. doi:10.1146/annurev-marine-120308-081121

Anderson, C.R., Berdalet, E., Kudela, R.M., Cusack, C.K., Silke, J., O'Rourke, E., Dugan, D., McCammon, M., Newton, J.A., Moore, S.K., Paige, K., Ruberg, S., Morrison, J.R., Kirkpatrick, B., Hubbard, K., Morell, J., 2019. Scaling Up From Regional Case Studies to a Global Harmful Algal Bloom. Front. Mar. Sci. 6, 250. doi:10.3389/fmars.2019.00250

Arístegui, J., Barton, E.D., Álvarez-salgado, X.A., Santos, A.M.P., Figueiras, F.G., Kifani, S., Hernández-león, S., Mason, E., Machú, E., Demarcq, H., 2009. Progress in Oceanography Sub-regional ecosystem variability in the Canary Current upwelling. Prog. Oceanogr. 83, 33–48. doi:10.1016/j.pocean.2009.07.031

Barone, R., 2007. Behavioural trait of *Ostreopsis ovata* (Dinophyceae) in Mediterranean rock

pools: The spider's strategy. Harmful Algae News 33, 1–3.

Battocchi, C., Totti, C., Vila, M., Masó, M., Capellacci, S., Accoroni, S., Reñé, A., Scardi, M., Penna, A., 2010. Monitoring toxic microalgae *Ostreopsis* (dinoflagellate) species in coastal waters of the Mediterranean Sea using molecular PCR-based assay combined with light microscopy. Mar. Pollut. Bull. 60, 1074–1084. doi:10.1016/j.marpolbul.2010.01.017

Bennouna, A., EL Attar, J., Abouabdellah, R., Chafik, A., Penna, A., Oliveira, P.B., Palma, S., Moita, M.T., 2012. *Ostreopsis* cf. *siamensis* blooms in Moroccan Atlantic Upwelling waters (2004-2009), *in*: Pagou, P., Hallegraeff, G. (Eds.), Proceedings of the 14th International Conference on Harmful Algae. International Society for the Study of Harmful Algae and IOC of UNESCO. pp. 19–22.

Berdalet, E., Fleming, L.E., Gowen, R., Davidson, K., Hess, P., Backer, L.C., Moore, S.K., Hoagland, P., Enevoldsen, H., 2016. Marine harmful algal blooms, human health and wellbeing: challenges and opportunities in the 21st century. J. Mar. Biol. Assoc. United Kingdom 96, 61–91.

Bode, A., Alvarez-ossorio, M.T., Cabanas, J.M., Miranda, A., Varela, M., 2009. Recent trends in plankton and upwelling intensity off Galicia (NW Spain). Prog. Oceanogr. 83, 342–350. doi:10.1016/j.pocean.2009.07.025

Brotas, V., Brewin, R.J., Sá, C., Brito, A.C., Silva, A., Mendes, C.R., Diniz, T., Kaufmann, M., Tarran, G., Groom, S.B., Platt, T., 2013. Deriving phytoplankton size classes from satellite data: Validation along a trophic gradient in the eastern Atlantic Ocean. Remote Sens. Environ. 134, 66-77.

Cabrita, M.T., Silva, A., Oliveira, P.B., Angélico, M.M., Nogueira, M., 2015. Assessing eutrophication in the Portuguese continental Exclusive Economic Zone within the European Marine Strategy Framework Directive. Ecol. Indic. 58, 286–299. doi:10.1016/j.ecolind.2015.05.044

Carvalho, I.L., Pelerito, A., Ribeiro, I., Cordeiro, R., Núncio, M.S., Vale, P., 2019. Paralytic Shellfish Poisoning Due to Ingestion of Contaminated Mussels: A 2018 Case Report in Caparica (Portugal). Toxicon: X 4, 100017. doi:10.1016/j.toxcx.2019.100017.

Chavez, F.P., Messié, M., 2009. A comparison of Eastern Boundary Upwelling Ecosystems. Prog. Oceanogr. 83, 80–96. doi:10.1016/j.pocean.2009.07.032

Ciminiello, P., Dell'Aversano, C., Iacovo, E.D., Fattorusso, E., Forino, M., Tartaglione, L., Yasumoto, T., Battocchi, C., Giacobbe, M., Amorim, A., Penna, A., 2013. Investigation of toxin profile of Mediterranean and Atlantic strains of *Ostreopsis* cf. *siamensis* (Dinophyceae) by liquid chromatography–high resolution mass spectrometry. Harmful Algae 23, 19-27.

Cioccio, D. Di, 2014. Ecology of the toxic dinoflagellate *Ostreopsis* cf. *ovata* along the coasts of the Campania region (Tyrrhenian Sea, Mediterranean Sea). Università degli Studi di Napoli "Federico II." PhD dissertation.

Cravo, A., Relvas, P., Cardeira, S., Rita, F., Madureira, M., Sa, R., 2010. An upwelling filament off southwest Iberia: Effect on the chlorophyll a and nutrient export. Cont. Shelf Res. 30, 1601–1613. doi:10.1016/j.csr.2010.06.007

Cristina, S., Cordeiro, C., Lavender, S., Goela, P.C., Icely, J., Newton, A., 2016. MERIS phytoplankton time series products from the SW Iberian Peninsula (Sagres) using seasonal-trend decomposition based on loess. Remote Sens. 8, 1–16. doi:10.3390/rs8060449

Danchenko, S., Fragoso, B., Guillebault, D., Icely, J., Berzano, M., Newton, A., 2019. Harmful phytoplankton diversity and dynamics in an upwelling region (Sagres, SW Portugal) revealed by ribosomal RNA microarray combined with microscopy. Harmful Algae 82, 52–71. doi:10.1016/J.HAL.2018.12.002

David, H., Moita, M.T., Laza-Martínez, A., Silva, A., Mateus, M., de Pablo, H., Orive, E., 2012. First bloom of *Ostreopsis* cf. *ovata* in the continental Portuguese coast. Harmful Algae News 45, 12–13.

David, H., Laza-Martínez, A., Miguel, I., Orive, E., 2013. *Ostreopsis* cf. *siamensis* and *Ostreopsis* cf. *ovata* from the Atlantic Iberian Peninsula: Morphological and phylogenetic characterization. Harmful Algae 30, 44–55. doi:10.1016/j.hal.2013.08.006

David, H., Nascimento, P., Melo, R., Amorim, A., 2018. Bloom of *Ostreopsis* cf. *siamensis* in Lisbon Bay. Harmful Algae News 60, 11–12.

Díaz, P.A., Reguera, B., Moita, T., Bravo, I., Ruiz-Villarreal, M., Fraga, S., 2019. Mesoscale dynamics and niche segregation of two *Dinophysis* species in Galician-Portuguese coastal waters. Toxins 11, 37.

Ferreira, A., Garrido-Amador, P., Brito, A.C., 2019. Disentangling Environmental Drivers of

Phytoplankton Biomass off Western Iberia. Front. Mar. Sci. 6, 1–17. doi:10.3389/fmars.2019.00044

Figueiras, F.G., Rios, A.F., 1993. Phytoplankton succession, red tides, and the hydrographic regime in the Rías Bajas of Galicia, *in*: Smayda, T.J., Shimizu, Y. (Eds.), Toxic Phytoplankton Blooms in the Sea. Elsevier Science Publishers B.V., pp. 239–244.

Figueiras, F.G., Labarta, U., Fernández Reiriz, M.J., 2002. Coastal upwelling, primary production and mussel growth in the Rías Baixas of Galicia. Hydrobiologia 484, 121–131.

Fiúza, A.F.D., de Macedo, M.E., Guerreiro, M.R., 1982. Climatological space and time variation of the Portuguese coastal upwelling. Oceanol. Acta 5, 31–40.

Fraga, S., Riobó, P., Diogène, J., Paz, B., Franco, J.M., 2005. Ciguatera related benthic dinoflagellates assemblage observed in Macaronesia (NE Atlantic Archipelagos), *in*: ASLO Summer Meeting. Santiago de Compostela (Spain). (Poster conference)

Fréon, P., Barange, M., Aristegui, J., 2009. Eastern Boundary Upwelling Ecosystems: Integrative and comparative approaches. Prog. Oceanogr. 83, 1–14. doi:10.1016/j.pocean.2009.08.001

Fu, F.X., Tatters, A.O., Hutchins, D.A., 2012. Global change and the future of harmful algal blooms in the ocean. Mar. Ecol. Prog. Ser. 470, 207–233. doi:10.3354/meps10047

Gilabert, J., Gómez, E., Hernández, A., Herrera, M.J., Tudela, J., García, M.J., Gutiérrez, C., 2008. Seguimiento y plan de vigilancia de fitoplancton tóxico en las costas de Águilas (Murcia) en verano de 2006, in: Gilabert, J. (Ed.), Avances y Tendencias En Fitoplancton Tóxico y Biotoxinas: Actas de La IX Reunión Ibérica Sobre Fitoplancton Tóxico y Biotoxinas. p. 47–58 (in Spanish).

Glibert, P.M., Allen, J.I., Artioli, Y., Beusen, A., Bouwman, L., Harle, J., Holmes, R., Holt, J., 2014. Vulnerability of coastal ecosystems to changes in harmful algal bloom distribution in response to climate change: projections based on model analysis. Glob. Chang. Biol. 20, 3845-3858.

Glibert, P.M., Burford, M.A., 2017. Globally Changing Nutrient Loads and Harmful Algal Blooms. Oceanography 30, 58–69. doi:10.5670/oceanog.2017.110.

Gobler, C.J., Doherty, O.M., Hattenrath-Lehmann, T.K., Griffith, A.W., Kang, Y., Litaker, R.W., 2017. Ocean warming since 1982 has expanded the niche of toxic algal blooms in

the North Atlantic and North Pacific oceans. Proc. Natl. Acad. Sci. 114, 4975–4980. doi:10.1073/pnas.1619575114

Goela, P.C., Danchenko, S., Icely, J.D., Lubian, L.M., Cristina, S., Newton, A., 2014. Estuarine, Coastal and Shelf Science Using CHEMTAX to evaluate seasonal and interannual dynamics of the phytoplankton community off the South-west coast of Portugal 151, 112–123.

Goela, P.C., Icely, J., Cristina, S., Danchenko, S., Angel DelValls, T., Newton, A., 2015. Using bio-optical parameters as a tool for detecting changes in the phytoplankton community (SW Portugal). Estuar. Coast. Shelf Sci. 167, 125–137. doi:10.1016/j.ecss.2015.07.037

Goela, P.C., Cordeiro, C., Danchenko, S., Icely, J., Cristina, S., Newton, A., 2016. Time series analysis of data for sea surface temperature and upwelling components from the southwest coast of Portugal. J. Mar. Syst. 163, 12–22. doi:10.1016/j.jmarsys.2016.06.002

Gouveia, N.N., Vale, P., Gouveia, N., Delgado, J., 2010. Primeiro Registo da Ocorrência de Episódios do Tipo Ciguatérico no Arquipélago da Madeira. *In*: Costa, P.R., Botelho, M.J., Rodrigues, S.M., Palma, A.S., Moita, M.T. (Eds.), Algas tóxicas e biotoxinas nas águas da Península Ibérica 2009. IPIMAR, Lisboa, Portugal, pp. 152–157.

Graham, W.M., Largier, J.L., 1997. Upwelling shadows as nearshore retention sites: The example of northern Monterey Bay. Cont. Shelf Res. 17, 509–532. doi:10.1016/S0278-4343(96)00045-3

Guerreiro, C., Oliveira, A., Stigter, H. De, Cachão, M., Sá, C., Borges, C., Santos, A., Fortuño, J., Rodrigues, A., 2013. Late winter coccolithophore bloom off central Portugal in response to river discharge and upwelling 59, 65–83. doi:10.1016/j.csr.2013.04.016

Hallegraeff, G.M., 2010. Ocean climate change, phytoplankton community responses, and harmful algal blooms: A formidable predictive challenge. J. Phycol. 46, 220–235. doi:10.1111/j.1529-8817.2010.00815.x

Haynes, R., Barton, E.D., Pilling, I., 1993. Development, persistence, and variability of upwelling filaments off the Atlantic coast of the Iberian Peninsula. J. Geophys. Res. 98, 22681. doi:10.1029/93JC02016

Hill, E.A., Hickey, B.M., Shillington, F.A., Strub, P.T., Brink, K.H., Barton, E.D., Thomas, A.C., 1998. Eastern ocean boundaries. Coastal segment (E), *in*: Robinson, A.R., Brink,

K.H. (Eds.), The Sea, the Global Coastal Ocean: Regional Studies and Syntheses. John Wiley and Sons, New York, pp. 29–67.

Krug, L.A., Platt, T., Sathyendranath, S., Barbosa, A.B., 2017. Unravelling region-specific environmental drivers of phytoplankton across a complex marine domain (off SW Iberia). Remote Sens. Environ. 203, 162–184. doi:10.1016/j.rse.2017.05.029

Krug, L.A., Platt, T., Sathyendranath, S., Barbosa, A.B., 2018. Patterns and drivers of phytoplankton phenology off SW Iberia: A phenoregion based perspective. Prog. Oceanogr. 165, 233–256. doi:10.1016/j.pocean.2018.06.010

Kudela, R.M., Barth, J.A., Frame, E.R., Jay, D.A., 2008. New insights into the controls and mechanisms of plankton productivity along the US West Coast. Oceanography 21, 46–59.

Largier, J.L., Lawrence, C.A., Roughan, M., Kaplan, D.M., Dever, E.P., Dorman, C.E., Kudela, R.M., Bollens, S.M., Wilkerson, F.P., Dugdale, R.C., Botsford, L.W., Garfield, N., Kuebel Cervantes, B., Koračin, D., 2006. WEST: A northern California study of the role of wind-driven transport in the productivity of coastal plankton communities. Deep. Res. Part II Top. Stud. Oceanogr. 53, 2833–2849. doi:10.1016/j.dsr2.2006.08.018

Largier, J.L., 2020. Upwelling Bays: How Coastal Upwelling Controls Circulation, Habitat, and Productivity in Bays. Ann. Rev. Mar. Sci. 12, 20.1-20.33.

Litaker, R.W., Vandersea, M.W., Faust, M.A., Kibler, S.R., Nau, A.W., Holland, W.C., Chinain, M., Holmes, M.J., Tester, P.A., 2010. Global distribution of ciguatera causing dinoflagellates in the genus *Gambierdiscus*. Toxicon, 56, 711-730. doi:10.1016/j.toxicon.2010.05.017

Loureiro, S., Newton, A., Icely, J.D., 2005. Microplankton composition, production and upwelling dynamics in Sagres (SW Portugal) during the summer of 2001. Sci. Mar. 69, 323–341. doi:10.3989/scimar.2005.69n3323

Loureiro, S., Reñé, A., Garcés, E., Camp, J., Vaqué, D., 2011. Harmful algal blooms (HABs), dissolved organic matter (DOM), and planktonic microbial community dynamics at a near-shore and a harbour station influenced by upwelling (SW Iberian Peninsula). J. Sea Res. 65, 401–413. doi:10.1016/j.seares.2011.03.004

Machado, K.B., Vieira, L.C.G., Nabout, J.C., 2019. Predicting the dynamics of taxonomic and functional phytoplankton compositions in different global warming scenarios.

Hydrobiologia 830, 115-134.

Mangialajo, L., Ganzin, N., Accoroni, S., Asnaghi, V., Blanfuné, A., Cabrini, M., Cattaneo-Vietti, R., Chavanon, F., Chiantore, M., Cohu, S., Costa, E., Fornasaro, D., Grossel, H., Marco-Miralles, F., Masó, M., Reñé, A., Rossi, A.M., Sala, M.M., Thibaut, T., Totti, C., Vila, M., Lemée, R., 2011. Trends in *Ostreopsis* proliferation along the Northern Mediterranean coasts. Toxicon 57, 408–420. doi:10.1016/j.toxicon.2010.11.019

Mendes, C.R., Sá, C., Vitorino, J., Borges, C., Tavano Garcia, V.M., Brotas, V., 2011. Spatial distribution of phytoplankton assemblages in the Nazaré submarine canyon region (Portugal): HPLC-CHEMTAX approach. J. Mar. Syst. 87, 90–101. doi:10.1016/j.jmarsys.2011.03.005

Moita, M.T., 2001. Estrutura , Variabilidade e Dinâmica do Fitoplâncton na Costa de Portugal Continental. Universidade de Lisboa. 209 pp. PhD dissertation (in Portuguese)

Moita, M.T., Oliveira, P.B., Mendes, J.C., Palma, A.S., 2003. Distribution of chlorophyll *a* and *Gymnodinium catenatum* associated with coastal upwelling plumes off central Portugal. Acta Oecologica 24, 125–132. doi:10.1016/S1146-609X(03)00011-0

Moita, M.T., Pazos, Y., Rocha, C., Nolasco, R., Oliveira, P.B., 2016. Toward predicting Dinophysis blooms off NW Iberia: A decade of events. Harmful Algae 53, 17–32. doi:10.1016/j.hal.2015.12.002

Nair, A., Sathyendranath, S., Platt, T., Morales, J., Stuart, V., Forget, M., Devred, E., Bouman, H., 2008. Remote sensing of phytoplankton functional types. Remote Sens. Environ. 112, 3366–3375.

Navarro, G., Ruiz, J., 2006. Spatial and temporal variability of phytoplankton in the Gulf of Cádiz through remote sensing images. Deep-sea Res Pt II 53, 1241–1260. doi:10.1016/j.dsr2.2006.04.014

Oliveira, P.B., Nolasco, R., Dubert, J., Moita, T., Peliz, Á., 2009. Surface temperature, chlorophyll and advection patterns during a summer upwelling event off central Portugal. Cont. Shelf Res. 29, 759–774. doi:10.1016/j.csr.2008.08.004

Otero, P.S., Pérez, A., Alfonso, C., Vale, C., Rodríguez, N.N., Gouveia, N., Gouveia, N., Delgado, J., Vale, P., Hirama, M., Ishihara, Y., Molgó, J., Botana, L.M., 2010. First Toxin Profile of Ciguateric Fish in Madeira Archipelago (Europe). Anal. Chem. 82, 6032-603.

Palma, S., Mouriño, H., Silva, A., Barão, M.I., Moita, M.T., 2010. Can *Pseudo-nitzschia* blooms be modeled by coastal upwelling in Lisbon Bay? Harmful Algae 9, 294–303. doi:10.1016/j.hal.2009.11.006

Peliz, A., Rosa, T.L., Santos, A.M.P., Pissarra, J.L., 2002. Fronts, jets, and counter-flows in the Western Iberian upwelling system. J. Mar. Syst. 35, 61–77. doi:10.1016/S0924-7963(02)00076-3

Penna, A., Vila, M., Fraga, S., Giacobbe, M.G., Francesco, A., Riobó, P., Vernesi, C., 2005. Characterization of *Ostreopsis* and *Coolia* (Dinophyceae) isolates in the western Mediterranean Sea based on morphology, toxicity and internal transcribed spacer 5.8s rDNA sequences. J. Phycol. 41, 212–225. doi:10.1111/J.1529-8817.2005.04011.x

Penna, A., Bertozzini, E., Battocchi, C., Galluzzi, L., Giacobbe, M.G., Vila, M., Garces, E., Lugliè, A., Magnani, M., 2007. Monitoring of HAB species in the Mediterranean Sea through molecular methods. J. Plankton Res. 29, 19–38. doi:10.1093/plankt/fbl053

Penna, A., Fraga, S., Battocchi, C., Casabianca, S., Giacobbe, M.G., Riobó, P., Vernesi, C., 2010. A phylogeographical study of the toxic benthic dinoflagellate genus *Ostreopsis* Schmidt. J. Biogeogr. 37, 830–841. doi:10.1111/j.1365-2699.2009.02265.x

Pérez-Arellano, J.-L., Luzardo, O.P., Brito, A.P., Cabrera, M.H., Zumbado, M., Carranza, C., AngelMoreno, A., Dickey, R.W., Boada, L.D., 2005. Ciguatera fish poisoning, Canary Islands. Emerg. Infect. Dis. 11, 1981–1982.

Pinto, J.S., 1949. Um caso de “red water” motivado por abundância anormal de *Gonyaulax polyedra* (Stein). Boletim da Sociedade Portuguesa de Ciências Naturais (Lisboa), II, Sér 2 (XVII), 94-97.

Pitcher, G.C., Figueiras, F.G., Hickey, B.M., Moita, M.T., 2010. The physical oceanography of upwelling systems and the development of harmful algal blooms. Prog. Oceanogr. 85, 5–32. doi:10.1016/j.pocean.2010.02.002

Quéré, C.L., Harrison, S.P., Colin Prentice, I., Buitenhuis, E.T., Aumont, O., Bopp, L., ... & Klaas, C., 2005. Ecosystem dynamics based on plankton functional types for global ocean biogeochemistry models. Glob. Chang. Biol. 11, 2016-2040.

Randall, J.E., 1958. A review of ciguatera, tropical fish poisoning, with a tentative explanation of its cause. Bull. Mar. Sci. Gulf Caribb. 8, 236–267.

Randall, J.E., 2005. Review of Clupeotoxism, an Often Fatal Illness from the Consumption of

Clupeoid Fishes. Pacific Sci. 59, 73–78.

Relvas, P., Barton, E.D., 2002. Mesoscale patterns in the Cape São Vicente (Iberian Peninsula) upwelling region. J. Geophys. Res. 107, 3164. doi:10.1029/2000JC000456

Relvas, P., Barton, E.D., 2005. A separated jet and coastal counterflow during upwelling relaxation off Cape São Vicente (Iberian Peninsula). Cont. Shelf Res. 25, 29–49. doi:10.1016/j.csr.2004.09.006

Relvas, P., Peliz, A., Oliveira, P.B., da Silva, J., Dubert, J., Barton, E.D., Santos, A.M.., 2007. Physical oceanography of the western Iberia ecosystem: latest views and challenges. Prog. Oceanogr. 74, 149–173.

Rhodes, L., 2011. World-wide occurrence of the toxic dinoflagellate genus *Ostreopsis* Schmidt. Toxicon 57, 400–407. doi:10.1016/j.toxicon.2010.05.010

Ribeiro, S., Amorim, A., Andersen, T.J., Abrantes, F., Ellegaard, M., 2012. Reconstructing the history of an invasion: The toxic phytoplankton species *Gymnodinium catenatum* in the Northeast Atlantic. Biol. Invasions 14, 969–985. doi:10.1007/s10530-011-0132-6

Santos, M., Oliveira, P.B., Moita, M.T., David, H., Caeiro, M.F., Zingone, A., Amorim, A., Silva, A. (2019). Ocurrence of *Ostreopsis* in two temperate coastal bays (SW Iberia): Insights from the plankton. Harmful Algae 86, 20–36. doi:10.1016/j.hal.2019.03.003

Silva, A., Palma, S., Moita, M.T., 2008. Coccolithophores in the upwelling waters of Portugal: Four years of weekly distribution in Lisbon bay. Cont. Shelf Res. 28, 2601–2613. doi:10.1016/j.csr.2008.07.009

Silva, A., Palma, S., Oliveira, P.B., Moita, M.T., 2009. Composition and interannual variability of phytoplankton in a coastal upwelling region (Lisbon Bay, Portugal). J. Sea Res. 62, 238–249. doi:10.1016/j.seares.2009.05.001

Silva, A., Pinto, L., Rodrigues, S.M., de Pablo, H., Santos, M., Moita, T., Mateus, M., 2016. A HAB warning system for shellfish harvesting in Portugal. Harmful Algae 53, 33–39.

Tester, P.A., Litaker, R.W., Berdalet, E., 2020. Climate change and harmful benthic microalgae. Harmful Algae 91, 101655. doi:10.1016/j.hal.2019.101655

Totti, C., Accoroni, S., Cerino, F., Cucchiari, E., Romagnoli, T., 2010. *Ostreopsis ovata* bloom along the Conero Riviera (northern Adriatic Sea): Relationships with environmental conditions and substrata. Harmful Algae 9, 233–239.

doi:10.1016/j.hal.2009.10.006

Vale, P., Botelho, M.J., Rodrigues, S.M., Gomes, S.S., Sampayo, M.A. de M., 2008. Two decades of marine biotoxin monitoring in bivalves from Portugal (1986 – 2006): A review of exposure assessment. Harmful Algae 7, 11–25. doi:10.1016/j.hal.2007.05.002

Vidal, T., Calado, A.J., Moita, M.T., Cunha, M.R., 2017. Phytoplankton dynamics in relation to seasonal variability and upwelling and relaxation patterns at the mouth of Ria de Aveiro (West Iberian Margin) over a four-year period. PLoS One 12, 1–25.

Vila, M., Abós-herràndiz, R., Isern-fontanet, J., Àlvarez, J., Berdalet, E., 2016. Establishing the link between *Ostreopsis* cf. *ovata* blooms and human health impacts using ecology and epidemiology. Sci Mar 80.S1, 107–115.

Walter, R.K., Armenta, K.J., Shearer, B., Robbins, I., Steinbeck, J., 2018. Coastal upwelling seasonality and variability of temperature and chlorophyll in a small coastal embayment. Cont. Shelf Res. 154, 9–18. doi:10.1016/j.csr.2018.01.002

Wooster, W.S., Baku, A., McLain, D.R., 1976. The seasonal upwelling cycle along the eastern boundary of the North Atlantic. J. Mar. Res. 34, 131–141.

Chapter 2.

Characterizing phytoplankton biomass seasonal cycles in two NE Atlantic coastal Bays

Under review as:

Santos, M., Mouriño, H., Moita, M.T., Silva, A., Amorim, A., Oliveira, P.B.. Characterizing phytoplankton biomass seasonal cycles in two NE Atlantic coastal Bays**.** Continental Shelf Research.

Abstract

The seasonal and interannual variability of chlorophyll *a* was studied between 2008 and 2016 in two coastal bays located in the northeastern limit of the Iberia/Canary upwelling ecosystem. The work aims (i) to understand if small latitudinal distances and/or coastline orientation can promote different chlorophyll *a* seasonal cycles; and (ii) to investigate if different meteorological and oceanographic variables can explain the differences observed on seasonal cycles. Results indicate three main periods where different patterns of chlorophyll *a* were identified for the two studied bays, of low latitudinal separation. A uni-modal pattern, with a short maximum peak and low concentrations of chlorophyll *a*, characterized the E-W oriented coastline, and a pattern changing to bi-modal, with a long period of high concentration, characterized the N-S oriented coastline. In addition, the phytoplankton biomass seasonal cycles showed high year-to-year variation of phase and amplitude, meaning that the seasonal cycle of some specific years may be different when compared with the global pattern. Comparisons made between satellite estimates of chlorophyll *a* and *in situ* data, in one of the bays, revealed some important differences, namely the overestimation of concentrations and the anticipation of the productive period's beginning and end time. Cross-correlation analyses were performed for phytoplankton biomass and different meteorological and oceanographic variables (SST, PAR, UI, MLD) using different time lags to identify the drivers of phytoplankton biomass seasonal cycles. Contrasting results were obtained across the different periods and locations. PAR contributed to higher phytoplankton biomass in winter/early-spring, while upwelling and SST were the main drivers in late-spring/summer. Upwelling along the West coast was the variable that contributed most to the phytoplankton biomass during late-spring/summer in Lisbon Bay, while the upwelling along the South coast combined with SST was more important in Lagos Bay. The spatial and interannual variability of the seasonal patterns was also reflected on the phytoplankton community structure. A two-year study (2014 and 2015) indicated that, diatoms contributed the most for chlorophyll *a* in both areas, while coccolithophores were more relevant in Lisbon Bay, and dinoflagellates had a greater contribution to the phytoplankton community in Lagos Bay.

Keywords

Chlorophyll *a* seasonality; Time series; *In situ* data; Ocean color; Phytoplankton; Iberian upwelling coast

2.1. Introduction

Chlorophyll *a* concentration is usually used as a proxy for phytoplankton biomass in aquatic ecosystems. The assessment of interannual variability of phytoplankton biomass requires the use of long time series, ideally spanning several decades. Long time series of *in situ* data are rare due to their high dependence on funding cycles and human resources. As a pigment, chlorophyll *a* can be estimated using satellite ocean color sensors. Since 1978, when the first satellite sensor to monitor ocean color (CZCS- Coastal Zone Color Scanner) was launched by NASA, satellite imagery has been used to routinely measure chlorophyll *a* variability in the ocean, and since then, sensors with better spectral resolution, improved calibration and new algorithms have been developed (IOCCG, 2000). The high spatial-temporal coverage of chlorophyll *a* provided by satellite observations revolutionized the understanding of the role of phytoplankton on global primary production (e.g. Field et al., 1998; Taboada et al., 2019; Tilstone et al., 2009). However, although remote sensing of ocean color is "relatively-simple" on waters where the optical properties can be described as a function of phytoplankton concentration (Case 1 waters), it has significant limitations in optically complex coastal areas where the optical properties not only depend on chlorophyll concentration (Case 2 waters). In Case 2 waters there is a significant contribution of other particulate matter and/or yellow substances to the optical properties (IOCCG, 2000). This increases the need for a wider grid of *in situ* observations to validate the data obtained by remote sensing (IOCCG, 2000).

Several studies have highlighted the influence of specific environmental drivers to the phytoplankton variability in space and time. Effects on phytoplankton growth have been associated with variables such as, the mixing and stratification of the water column, euphotic zone depth, wind forcing, coastal upwelling, surface irradiance and levels of nutrient concentrations (Krug et al., 2017, 2018; Lafuente and Ruiz, 2007; Navarro et al., 2012; Navarro and Ruiz, 2006). The analysis of chlorophyll *a* time series and correlated environmental variables can lead to the discrimination of the relative importance of phytoplankton variability drivers (Cloern et al., 2016). This is especially challenging in dynamic environments such as upwelling ecosystems (Lamont et al., 2014). An effective management of coastal ecosystems requires a multidisciplinary perspective to understand how processes operate together in biological changes (Cloern et al., 2016), and must take into account the spatial and temporal variability of the different phytoplankton drivers (Tweddle et al., 2018). In fact, there is a need to clearly understand the underlying mechanisms related to

changes in phytoplankton biomass, phenological patterns, primary production and community composition (Cloern et al., 2016).

In coastal upwelling regions, coastal topography and coastline irregularities, such as capes and bays produce variations in coastal wind, alongshore currents, chemistry and biology (Chavez and Messié, 2009; Largier, 2020). On wind-exposed capes, strong upwelling and horizontal advection occur, while on the lee side of such promontories, the winds, upwelling and horizontal advection are weaker (Chavez and Messié, 2009). As a result, high levels of phytoplankton biomass are sustained in these ‘‘upwelling shadows” (e.g., Graham and Largier, 1997; Largier et al., 2006, 2019; Oliveira et al., 2009b). Strong gradients are generated between the new upwelled waters off a cape and the protected shadow waters (Chavez and Messié, 2009), allowing the phytoplankton assemblage to maintain a consistent population in the region (Kudela et al., 2008; Largier, 2020). These features were observed in several upwelling regions, suggesting that these “upwelling shadows” may be characteristic features of these regions and play a significant role in the local biology (Graham and Largier, 1997 and references therein; Largier, 2020). Although frequent, these shallow coastal embayments are poorly studied (Walter et al., 2018) but of high importance since these regions promote conditions of higher stratification and less wind-driven mixing, increasing chlorophyll *a* levels, and potentially favoring the occurrence of Harmful Algal Blooms (HABs) (Kudela et al., 2005; Moita et al., 2003; Ryan et al., 2014).

The Portuguese continental coast, located on the western Iberian Peninsula, is in the northeastern limit of the Iberia/Canary upwelling ecosystem, associated with the North Atlantic anticyclonic gyre (Wooster et al., 1976). This region is characterized by several prominent topographic features, such as capes, promontories and submarine canyons (Relvas et al., 2007). It is also a complex area characterized by different mesoscale structures that are observed at a seasonal timescale, like fronts, jets, upwelling filaments and countercurrents (Haynes et al., 1993; Peliz et al., 2002; Relvas et al., 2007; Relvas and Barton, 2005). In Portugal, upwelling occurs between spring and early autumn, due to seasonally prevailing northerly winds, being stronger in summer (Fiúza et al., 1982; Goela et al., 2016; Relvas and Barton, 2002; Wooster et al., 1976). During autumn and winter, while some episodes of upwelling may occur, there is a prevalence of downwelling inducing, southerly winds (Alvarez et al., 2008; Goela et al., 2016).

Here we investigated, for the North Atlantic Iberian upwelling system, the relevance of small latitudinal distances and/or coastline orientation on chlorophyll *a* seasonal cycles, and which

meteorological and oceanographic variables can explain the observed temporal and spatial variability. To reach these goals, the present study focused on 9-years (2008-2016) of chlorophyll *a* data from two coastal bays located in the upwelling shadow of two prominent Iberian headlands, Cape Roca and Cape São Vicente. To one of the bays, satellite estimates were compared with *in situ* data to assess the ability of L4 ocean color products to reproduce the near-coast chlorophyll *a* seasonal cycles. Furthermore, phytoplankton communities were investigated during 2014 and 2015 to better understand the observed chlorophyll *a* patterns.

2.2. Material and methods

2.2.1. Study area

This work was conducted in two geographically distinct coastal bays located on the West and South Portuguese continental coast, respectively, Lisbon and Lagos Bays (Fig. 2.1). Lisbon Bay (LisB) is located SE of Cape Roca (CR) under the strong influence of seasonal upwelling and of the Tagus river flow. Between spring and early autumn, under steady northerly winds, upwelling occurs and a recurrent upwelling filament, rooted at CR, extends southward or westward of the bay (Moita et al., 2003; Oliveira et al., 2009b). Due to the coastline discontinuity, this bay was considered by previous studies an upwelling shadow area where phytoplankton can be accumulated through different retention mechanisms (Moita et al., 2003; Oliveira et al., 2009a). The Tagus river, with a mean annual flow of 10 km^3 (SNIRH, 2017), is the main source of freshwater into the bay (Valente and da Silva, 2009) and is an important source of nutrients, with higher concentrations observed during winter and early-spring (Cabrita et al., 2015). The conjunction of riverine and upwelling inputs sustains the availability of nutrients all year round in this region (Ferreira et al., 2019). The sampling site, referred to as LisB-IS, is a long-term monitoring station located about 12 km from CR (Fig. 2.1) at the entrance of a recreational marina in the north side of the Bay (38°41’36.82’’N, 9°24’52.93’’W).

Lagos Bay (LagB) is at the SW limit of Iberia and is located to the east of Cape São Vicente (CSV). CSV is a coastline discontinuity, which separates the West coast from the South coast. This Cape is a major upwelling center when north winds are predominant (Goela et al., 2016; Relvas and Barton, 2002), spreading the cold upwelled water along the southern coast’s shelf break and slope (Relvas et al., 2007). On the South coast, during summer, a westward warm

coastal countercurrent from the Gulf of Cádiz is recurrently observed and, under favorable conditions, can turn northward around CSV (Relvas and Barton, 2002, 2005; Relvas et al., 2007). Although irregular, upwelling events also occur in the South coast under westerly winds (Goela et al., 2016; Relvas and Barton, 2002), occasionally leading to the reversal of the above-mentioned summer alongshore flow (Relvas and Barton, 2002). Upwelling is the main source of nutrients in the region of CSV (Cravo et al., 2010). To the east of LagB is the Arade river, with a much lower mean annual flow, 0.05 km^3, than the Tagus river (SNIRH, 2017). The sampling site, referred to as LagB-IS, is at 1 nautical mile from the coast (Fig. 2.1) and 30 km to the east of CSV (37°4'12.31''N, 8°41'0.44''W).

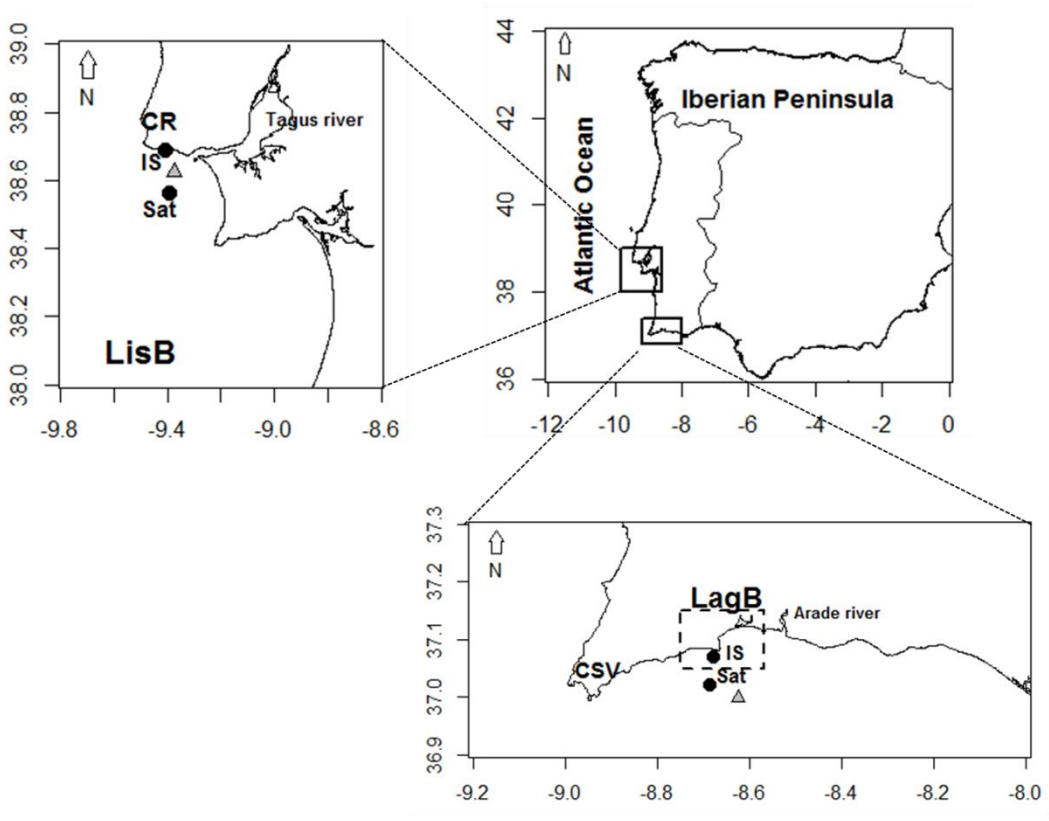

Fig. 2.1. Map of the study area. Circles identify the location of the time series datasets in Lisbon Bay (LisB) and in Lagos Bay (LagB), recorded *in situ* (IS) and estimated by satellite (Sat). Grey triangles indicate the location where meteorological parameters were extracted.

2.2.2. *In situ* data: chlorophyll *a* and phytoplankton assemblages

In situ chlorophyll *a* (Chl-*a*) data were gathered in Lisbon Bay using weekly water samples collected from 2008 to 2016 at the LisB coastal station (referred to as LisB-IS). The samples were collected under the National Monitoring Program of Harmful Algal Bloom species (HABs) led by IPMA, I.P. - Instituto Português do Mar e da Atmosfera (National Institute for

the Sea and Atmosphere). Integrated water samples (0-7 m depth) were collected with a hose, always one hour before high tide, to reduce the influence of the Tagus river and to optimize the direct influence of coastal waters on this near-shore station.

Water samples were stored in dark thermal bottles, for about half an hour, and analyzed in triplicate (250 mL each) in the laboratory. Each triplicate was vacuum filtered through 0.45 µm nitrate cellulose membranes. Pigments were extracted with 90 % acetone and Chl-*a* was determined according to the "Turner Fluorometer" method (Holm-Hansen et al., 1965) on a Fluorescence Spectrophotometer (Hitachi F-7000).

To analyze the phytoplankton community, water samples were collected every two weeks during 2014 and 2015 in LisB (same collection procedure mentioned above) and during 2015 in LagB at 10 m depth. LisB samples were field fixed with formaldehyde neutralized with hexamethylenetetramine to a final concentration of 0.4%, and LagB samples with Lugol's solution (Throndsen, 1978). Quantification of phytoplankton groups (diatoms, dinoflagellates, coccolithophores and "others") was carried out by settling 50 mL of water samples following the Utermöhl method (Utermöhl, 1958). Samples were analyzed with an inverted microscope equipped with phase contrast and bright field illumination (Zeiss IM35 and Leica DMi8) at a magnification of 160x or 200x, and 400 x with a detection limit of 20 cells L^{-1} and 2000 cells L^{-1}, respectively to the lower and higher magnifications. The group referred to as "others" was composed by small cryptophytes, chlorophytes, prasinophytes and other unidentified small algae. As this group account on average for less than 10 % of total phytoplankton it was not shown in the present work. A more detailed analysis of phytoplankton communities will be addressed specifically in a dedicated article.

2.2.3. Ocean color, meteorological, oceanographic and hydrographic data

Ocean color satellite data were extracted for the study period (2008 – 2016) for LisB, referred to as LisB-Sat, and for LagB, referred to as LagB-Sat (Fig. 2.1). The *in situ* Chl-*a* concentration in LisB was compared with several L4 satellite products available on CMEMS (Copernicus Marine Environment Monitoring Service, http://marine.copernicus.eu/), namely the datasets (CMEMS naming convention): *oc-glo-chl-multi_cci-l4-chl_4km_8days-rep-v02*, *oc-glo-chl-multi-l4-gsm_4km_8days-rep-v02* and *oc-glo-chl-multi-l4-oi_4km_daily-rep-v02*, herein referred to as Chl-blend, Chl-GSM and Chl-OI, respectively. L4 satellite products were

selected because mathematical analyses applied to the data do not allow for missing values in the series.

Several meteorological and oceanographic (MetOc) variables were obtained from remote sensing and model-derived products. In addition, some hydrological parameters were used, namely precipitation and river runoff. Daily data of Multi-scale Ultra-high Resolution (MUR) sea surface temperature (SST) products, with 0.01º spatial resolution (~1 km), were obtained from the PO.DAAC (Physical Oceanography Distributed Active Archive Center) of the Jet Propulsion Laboratory of NASA (National Aeronautics and Space Administration) (http://dx.doi.org/10.5067/GHGMR-4FJ04). This SST product showed in a previous study a strong correlation with *in situ* data ($r > 0.90$) in LisB and LagB (Santos et al., 2019). The 8-day Mixed Layer Depth (MLD) data were obtained from the Ocean Productivity group of the Oregon State University (http://www.science.oregonstate.edu/ocean.productivity/index.php). Maximum MLD values were limited to maximum bathymetry in the study area.

Daily surface Photosynthetically Available Radiation (PAR), total precipitation and sea surface wind stress components (U_{10} and V_{10}) were retrieved from the European Centre for Medium-Range Weather Forecasts (ECMWF, https://www.ecmwf.int/en/forecasts/datasets/). The sea surface wind stress and upwelling indices were computed according to Schwing et al. (1996). The wind stress components (τ) were computed using the quadratic drag law $\tau_{x,y} = \rho_a$ Cd $|v|$ U_{10},V_{10}, where $|v|$ is the wind speed (m s^{-1}), U_{10} and V_{10} are respectively the east-west and north-south 10 m wind components (m s^{-1}), ρ_a is the air density (1.22 kg m^{-3}) and Cd is the drag coefficient (0.0013). Upwelling indices were estimated from the components of the Ekman mass transport M_x and M_y, computed from the wind stress components as $M_x = \tau_y/f$ and $M_y = -\tau_x/f$. The upwelling indices are expressed as a volume transport in cubic meters per second per 100 meters of coastline (m^3 s^{-1} /100 m), which is equivalent to metric tons/s/100 m coastline (Schwing et al., 1996). With this definition, the indices preserve the same sign convention as the wind components, therefore, negative values indicate upwelling conditions along the western (M_x) and southern coasts (M_y). From now on, the terms zonal and meridional transport will be used to highlight the upwelling conditions along the west coast (M_x) and along the south coast (M_y), respectively.

In order to reduce the coastal uncertainties provided by satellite data, the grid-point selected to extract the oceanographic parameters time series (Chl-*a*, SST, and MLD) was selected at 4 nautical miles from the coast in LagB. In LisB, to reduce the Tagus river turbid plume influence the grid-point was selected meridionally aligned with the *in situ* station but at 8.5

nautical miles from the coast (Fig. 2.1). The meteorological parameters time series (PAR, wind components and precipitation) were extracted from the nearest grid point to the coast (grey triangles, Fig. 2.1).

River runoff data were obtained from the SNIRH ("Sistema Nacional de Informação de Recursos Hídricos") database (https://snirh.apambiente.pt/). For the Tagus river daily runoff data was obtained from the hydrometric station at "Albufeira do Fratel", and for the Arade river monthly runoff data was obtained from the hydrometric station at "Albufeira do Funcho". For the latter, daily outflow was estimated assuming that the monthly hydrometric measurements resulted from equal daily contributions.

2.2.4. Data analyses

The *in situ* 9-year time series contains some gaps, representing approximately 9 % of the total samples. As the following mathematical analyses applied to the data do not allow for missing values in the series, the gaps were filled with the average between the Chl-*a* values of the immediately preceding and subsequent weeks. In order to study the periodic structure of each Chl-*a* time series (LisB-IS, LisB-Sat and LagB-Sat), some analyses in the frequency domain were carried out. Emphasis was given to the estimation of the spectral density functions by the periodograms (Chatfield, 2004; Priestley, 1981; Wei, 1990). The relevant periodic components of each time series were evaluated by the Hartley Test (Hartley, 1949). This test addresses the significance of each periodic component in the context of the analysis of variance. Thus, it provides information about the statistical significance of each Fourier frequency on the overall variance of the process. Although being an inconsistent estimator of the spectral density function, the periodogram is a useful tool to unveil hidden periodicities mainly due to the possibility of evaluating the statistical significance of its ordinates.

The need for keeping a balance between the percentage of variance explained by the ordinates of the periodograms and the consistency issues related to the comparison of the seasonal cycles of the three-phytoplankton biomass time series led to the procedure described as follows. The fundamental frequency (12-month periodicity), which accounts for the larger proportion of the total variation, and its first harmonic (6-month periodicity) were used to estimate each sine-cosine wave. The parameters of the sinusoidal curves were estimated by the Ordinary Least Squares (OLS). The independent variables were the Fourier frequencies associated to the 12- and 6-month periodicities. When the residuals exhibited an

autoregressive structure of order one, the respective model was re-estimated after adding the dependent variable (Chl-*a*) lagged by one-time unit to the set of the covariates (that is, to the sine-cosine wave based on the 12 and 6-months periodicities). The OLS was then applied to obtain the estimated regression coefficients for the Fourier frequencies under consideration. This procedure produced reliable estimates for the parameters of the sinusoidal curve (Mouriño and Barão, 2010).

To study the correlation between Chl-*a* and each MetOc variable (SST, PAR, UI and MLD), three different periods were defined based on oceanographic conditions: winter/early-spring (from 1 January to 30 April), corresponding to the beginning of water column stratification; late-spring/summer (from 1 May to 30 September), matching with the upwelling season; and autumn/winter (from 1 October to 31 December), corresponding to the period of MLD increase. Cross-correlation analyses were performed between Chl-*a* and each MetOc variable to the winter/early-spring and late-spring/summer periods. This methodology allows us to measure the correlation structure (strength and direction) between two time series at different distances apart (Box et al., 2016; Chatfield, 2004; Tsay, 2010; Wei, 1990).

Suppose that $\{(X_t, Y_t)\}_{t\in\mathbf{Z}}$ is a stationary bivariate process. The Cross-Correlation Function (CCF), denoted by $\rho_{XY}(k)$, is defined as

$$\rho_{XY}(k) = \frac{\gamma_{XY}(k)}{\sigma_X \sigma_Y} = \frac{E\left[(X_t - \mu_X)(Y_{t+k} - \mu_Y)\right]}{\sqrt{E(X_t - \mu_X)^2}\sqrt{E(Y_t - \mu_Y)^2}}, \quad k = 0, \pm 1, \pm 2, \ldots \tag{1}$$

where $\gamma_{XY}(k)$ is the covariance function; $\{X_t\}_{t\in\mathbf{Z}}$ represents each MetOc variable measured every week (with mean value μ_X); and $\{Y_t\}_{t\in\mathbf{Z}}$ corresponds to the weekly values of Chl-*a* concentration (with mean value μ_Y).

In this context, there is only one direction of interest for computing the CCF - equation (1) - because only the MetOc variables can influence Chl-*a* concentration (the reverse situation cannot happen). This means that the lag parameter, *k*, can only assume natural values and, of course, the zero value.

For a given realization of the bivariate stochastic process, $(x_t, y_t), t = 1, \mathrm{K}, n$, the CCF is estimated by the sample CCF:

$$\hat{\rho}_{XY}(k)=\frac{\hat{\gamma}_{XY}(k)}{s_X s_Y},\ k=0,1,\ldots,n-1. \tag{2}$$

where

$$\hat{\gamma}_{XY}(k)=\frac{1}{n}\sum_{t=1}^{n-k}\left(x_t-\bar{x}\right)\left(y_{t+k}-\bar{y}\right),\ s_X=\sqrt{\hat{\gamma}_{XX}(0)},\ s_Y=\sqrt{\hat{\gamma}_{YY}(0)},$$

and $\bar{x}, \bar{y}$ are the sample means of the x_t and y_t time series, respectively.

It can be shown that these estimators (equation 2) are consistent (Chatfield, 2004; Tsay, 2010). Under the Gaussian assumption, the approximate variance of the sample CCF at lag *k* is given by (Box et al., 2016; Wei, 1990)

$$\begin{aligned} &Var\left(\hat{\rho}_{XY}(k)\right)\approx \\ &\approx\frac{1}{n-k}\left\{\sum_{i=-\infty}^{+\infty}\left[\rho_{XX}(i)\rho_{YY}(i)+\rho_{XY}(k+i)\rho_{XY}(k-i)+\rho_{XY}^2(k)\left(\rho_{XY}^2(i)+\frac{1}{2}\rho_{XX}^2(i)+\frac{1}{2}\rho_{YY}^2(i)\right)\right]\right. \\ &\qquad\left.-2\rho_{XY}(k)\sum_{i=-\infty}^{+\infty}\left(\rho_{XX}(i)\rho_{XY}(i+k)+\rho_{XY}(-i)\rho_{YY}(i+k)\right)\right\}. \end{aligned} \tag{3}$$

To estimate the approximate variance of the sample CCF, some issues were taken into account. Namely, the autocorrelations and cross-correlations involved in the expression (3) were replaced by the respective estimates. Also, the terms of the summation (3) were set equal to zero for all *i* such that $|i|>s$ (i.e., the system has limited memory as expected). To obtain reliable estimates of the autocorrelations and cross-correlations (equation 3) in the present study, it was considered that *s* = 15. Above this value, there is no guarantee for the accuracy of the estimates cited in this paragraph.

To compute Confidence Intervals (CI) for the CCF simultaneously at different lags, it must be taken into consideration that the estimators of the CCF at neighboring lags are themselves correlated (Chatfield, 2004). The Bonferroni inequality was used to construct the simultaneous confidence intervals. Thus, the large-sample simultaneous confidence intervals for $\rho_{XY}(k)$ take the form

$$\rho_{XY}(k)\in\left(\hat{\rho}_{XY}(k)\pm\Phi^{-1}(1-\alpha/(2m+2))\,S_{\hat{\rho}_{XY}(k)}\right),\ k=0,1,\ldots,m \tag{4}$$

where *m* is the maximum number of lags under study, and $\Phi^{-1}(\alpha)$ is the α-quantile of the standard Gaussian distribution. This procedure ensures that the joint confidence coefficient

for all (m+1) CCF's is at least 1-α. The nature of the time series under study, collected on a weekly basis, determined m=4, that is, the CCF's were estimated from zero lag to the maximum of 4 weeks lag. It is worth mentioning that if the CI for the CCF at a certain lag k contains the zero value, the null hypothesis of no correlation between the time series under consideration is not rejected; but if the zero value is not included in the interval, the null hypothesis is rejected.

Straightforward adaptation of the expression (2) and the estimation version of the expression (3) led to the determination of the CI for the CCF's based on a dataset split by season. As mentioned above, in this study emphasis was given to winter/early-spring and late-spring/summer.

Due to the high number of missing values in precipitation and river runoff time series, it was not possible to perform cross-correlation analyses with these hydrological variables.

The statistical analyses referred to above were performed using the R 3.5.0 software (R Core Team, 2018) and Microsoft Excel.

2.3. Results

2.3.1. Characterization of environmental conditions

2.3.1.1. Hydrological parameters

The precipitation regime in both Bays was characterized by high interannual variability (Fig. 2.2A and B). The driest months, and with less variation, were recorded from June to August in LisB and from May to September in LagB. The remaining months were rainier, with high variability. The non-outlier limits and the 75th percentile, indicate that precipitation was more intense in LisB (Fig. 2.2A) than in LagB (Fig. 2.2B) during the study period.

Concerning the runoff of the Tagus and Arade rivers (Fig. 2.2C and 2.2D), the order of magnitude was 100 times higher in the former. In LisB, the highest variation was recorded between November and April, with the maximum inter-quartile range in March and the most extreme values in April, > 3000 $m^3 s^{-1} day^{-1}$ (Fig. 2.2C). Minimum river outflow was recorded in September (Fig. 2.2C). In LagB, runoff of the Arade river was low all year-round, with higher values recorded between November and February, December being the month with higher variation (from 0 to 12 $m^3 s^{-1} day^{-1}$) (Fig. 2.2D).

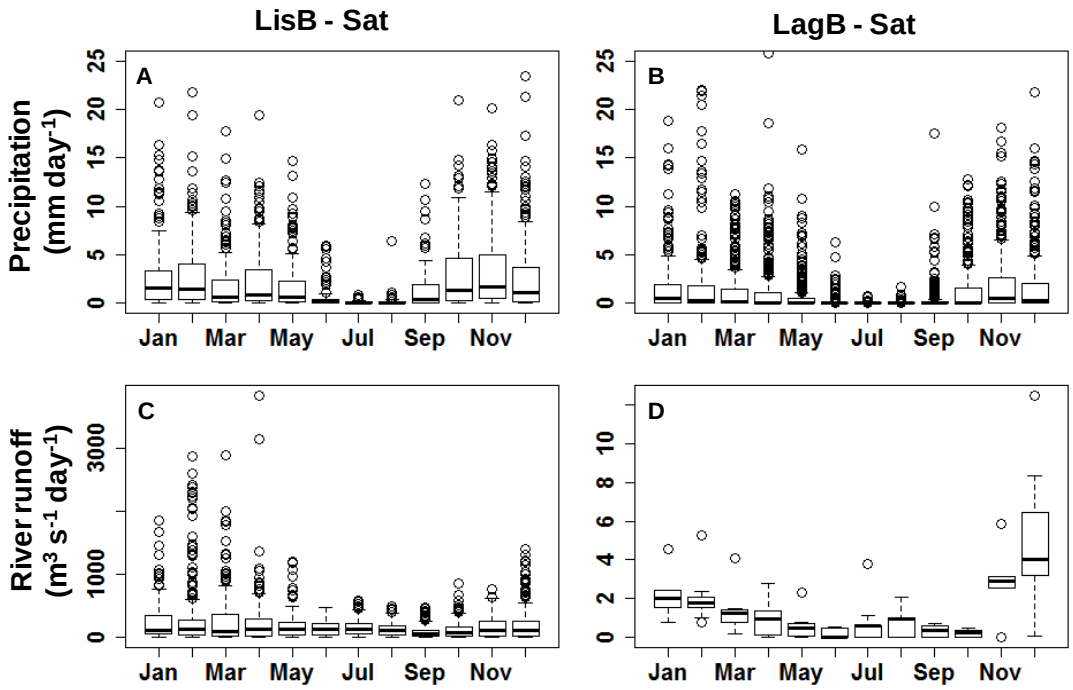

Fig. 2.2. Monthly variability of hydrological variables in LisB (left panel) and in LagB (right panel) during the period 2008-2016. A/B – Precipitation (mm day^{-1}); and C/D – River runoff (m^3 s^{-1} day^{-1}). Note the different scale in river runoff graphs. The lines within the boxes represent median values, 25th to 75th percentiles are denoted by box edges, and whiskers denote non-outlier limits and circles represent outliers' values.

2.3.1.2. Meteorological and Oceanographic parameters

Figure 2.3 shows the seasonal variation of the different meteorological (PAR, M_x and M_y) and oceanographic (SST and MLD) parameters of both studied bays. PAR and SST showed similar patterns in both bays (Fig. 2.3A to 2.3D). PAR reached minimum values in winter (December/January) and maxima in summer (June/July) (Fig. 2.3A and 2.3B). SST reached minima in February and March and maxima from August to October (Fig. 2.3C and 2.3D). The median of the minima and maxima temperature values were around 1 ºC cooler in LisB (~14 ºC and 19 ºC, respectively, Fig. 2.3C) than in LagB (~15 ºC and 20 ºC, respectively, Fig. 2.3D). A SST range of ~7 ºC was found during August in LagB, when the 24 ºC maximum occurred (Fig. 2.3D), while in LisB the highest variability was ~5 ºC in June with the maximum of 21 ºC recorded in September (Fig. 2.3C). The zonal mass transport (M_x) was similar in both bays with conditions favorable to upwelling prevailing along the west coast all year round (negative values), although it intensified in summer, from June to August (Fig. 2.3E and 2.3F). The monthly variability of the zonal transport was consistently higher in LagB (Fig. 2.3F). The meridional transport (M_y) was stronger and with higher variation in LagB (Fig. 2.3H) than in LisB (Fig. 2.3G). In both bays, the two transport components had

smaller variation during summer. Concerning MLD, it should be noted that the values were set to be equal to local depth in LagB whenever the model estimates were unrealistically above that limit (Fig. 2.3J). In both bays, the deepening period started in October. Median values showed that, in LisB, the maximum MLD was reached in January and shoaling started in February. MLD reached minimum median values (*ca*. 20m) from June to September. In LagB, MLD reached local depth in December and spring shoaling was only evident from April onwards. As for LisB, minimum median values (*ca*. 20m) were recorded between June and September. Higher winter/spring variability was observed in LisB (Fig. 2.3I) than in LagB (Fig. 2.3J).

2.3.2. Characterization of phytoplankton biomass

2.1.1.1. Comparison between *in situ* data and ocean color products

The comparison between *in situ* Chl-*a* concentration and the three L4 satellite products available on CMEMS (Chl-blend, Chl-GSM and Chl-OI), between 2008 and 2016 in LisB, showed that Chl-OI correlated the most with the *in situ* data (N=470, r = 0.42, p < 0.001, Table 2.1). Therefore, the following chapters were drawn based on Chl-OI product.

Table 2.1. Statistical results of the comparison between in situ Chl-a and several ocean color (OC) products. "N" indicated the number of observations and "r" the Pearson correlation.

OC Product	*N*	*r*	*p*-value
Chl-OI	470	0.42	< 0.001
Chl-Blend	470	0.09	0.04
Chl-GSM	470	0.22	< 0.001

2.1.1.1. Temporal variability

Phytoplankton biomass showed a high interannual variability both in LisB and in LagB with minimum values recorded in winter and maxima varying from early-spring to late-summer (Fig. 2.4). In LisB (Fig. 2.4A), *in situ* and satellite Chl-*a* varied between below 0.5 mg m^{-3} during winter to approximately 6 mg m^{-3} in spring and summer. Values above 6 mg m^{-3} were

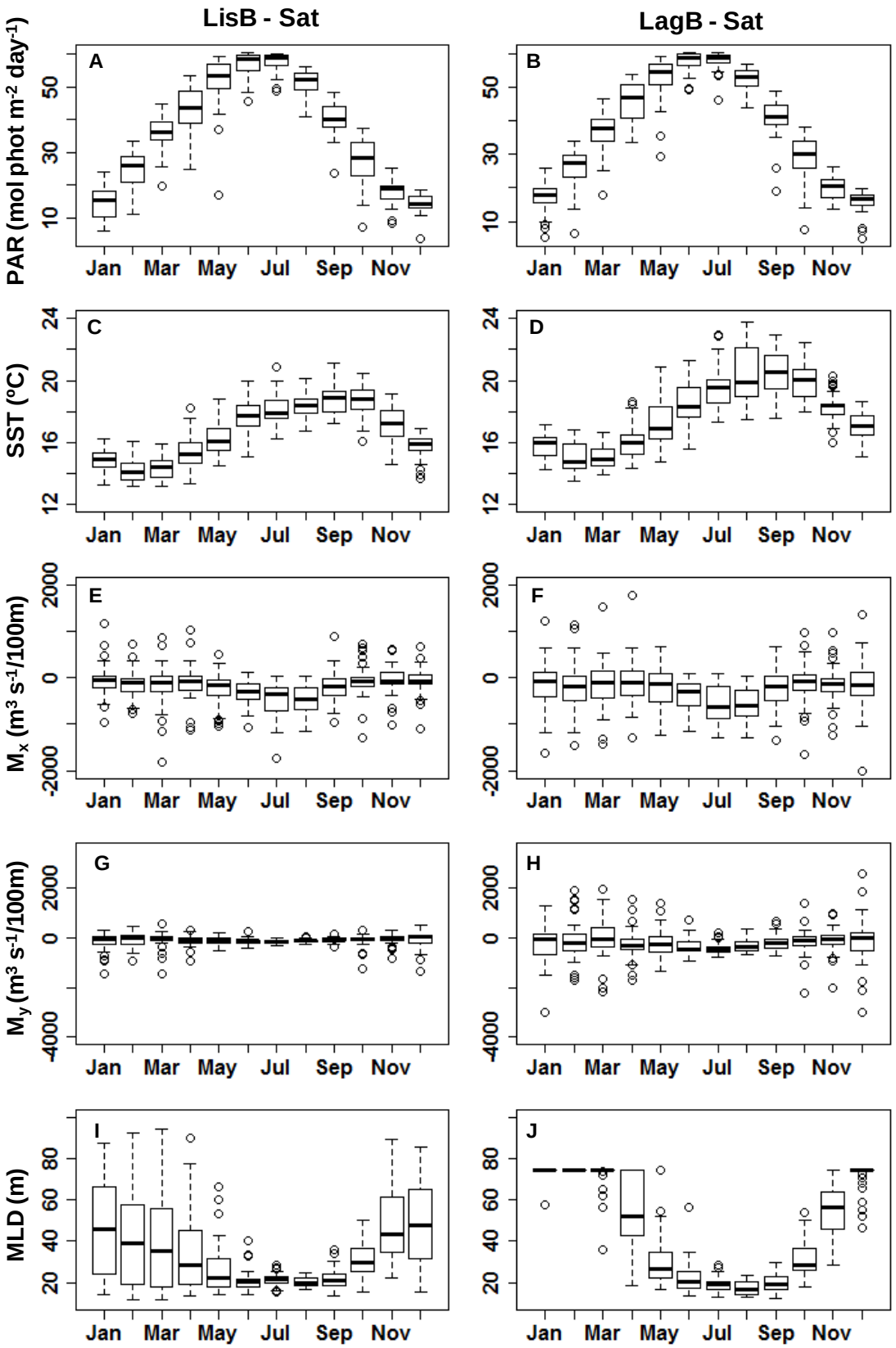

Fig. 2.3. Monthly variability of meteorological and oceanographic variables in LisB (left panel) and in LagB (right panel) during the period 2008-2016. A/B - Photosynthetically available radiation (PAR, mol phot m^{-2} day); C/D – Sea surface temperature (SST, ºC); E/F - Zonal mass transport (M_x, $m^3 s^{-1}$/100 m); G/H - Meridional mass transport (M_y, $m^3 s^{-1}$/100 m); and I/J – Mixed layer depth (MLD, m). The lines within the boxes represent median values, 25th to 75th percentiles are denoted by box edges, and whiskers denote non-outlier limits and circles represent outliers' values.

recorded episodically both *in situ* (in 2009, 2010 and 2014) and from satellite estimates (in 2012 and 2013). The maximum-recorded value was observed *in situ* in April 2014 (10.7 mg m^{-3}) (Fig. 2.4A). In LagB, where only satellite information is available, Chl-*a* varied between below 0.5 mg m^{-3} during winter to around 4 mg m^{-3} in spring and summer, with the exception being 2012, where 8 mg m^{-3} was reached in June (Fig. 2.4B).

The comparison between *in situ* measurements and satellite data for LisB indicated that satellite data, in general, overestimated Chl-*a* values (Fig. 2.5 and 2.6) with a global mean difference of 0.77 mg m^{-3} (Fig. 2.5). Nevertheless, in 17 events satellite data underestimated by more than 1 mg m^{-3} *in situ* Chl-*a*, which included the maximum *in situ* value recorded in April 2014 (Fig. 2.5). The difference between the two datasets by month indicated that median values above 0.77 mg m^{-3} were observed from January to May and in July and August (Fig. 2.6).

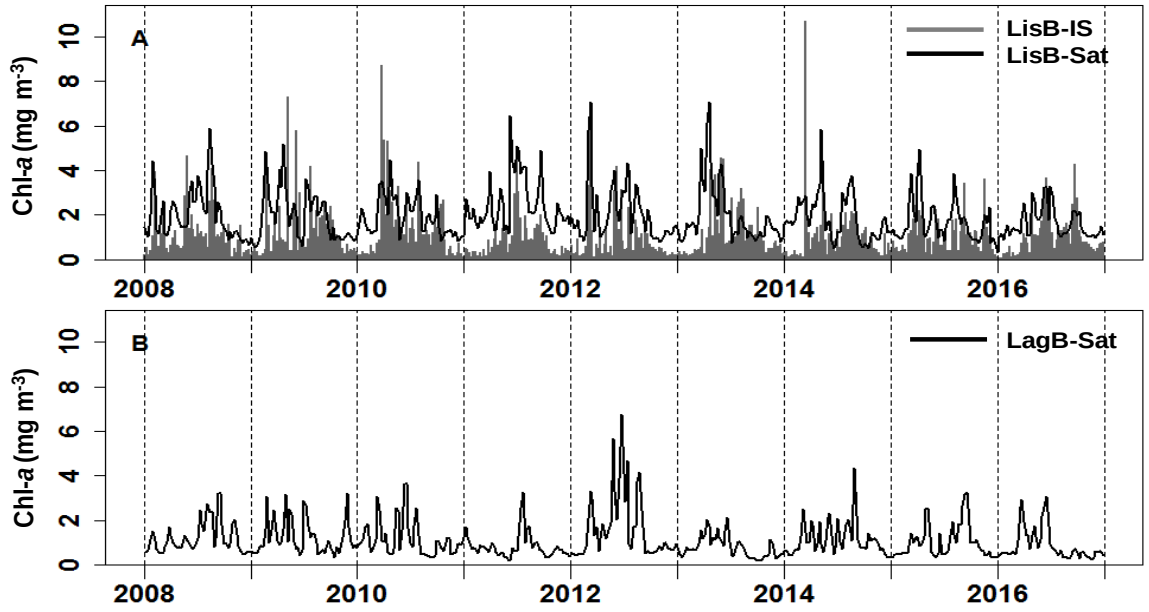

Fig. 2.4. Time series of weekly Chl-a measured in situ (IS) and by satellite (Sat), mg m-3, in LisB (A) and in LagB (B).

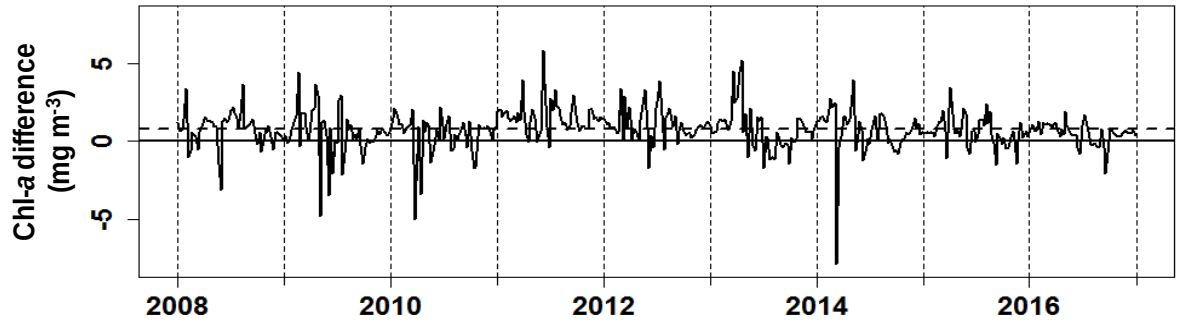

Fig. 2.5. Difference between satellite and *in situ* Chl-*a* data, mg m^{-3}, in LisB. Horizontal dashed line indicates Chl-*a* global mean difference.

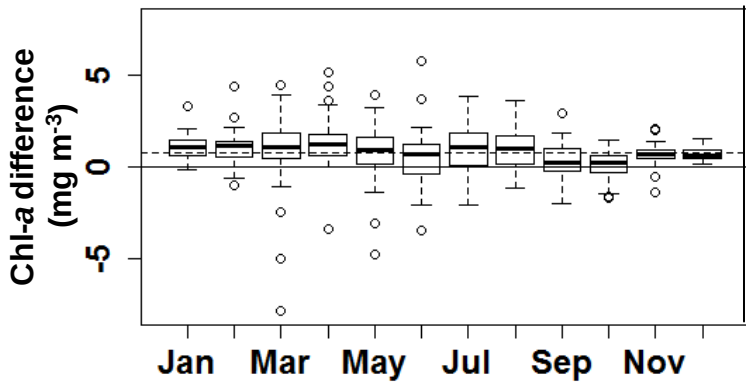

Fig. 2.6. Monthly boxplots of Chl-*a* difference, mg m^{-3}, between satellite and *in situ* data in LisB during the period 2008-2016. The lines within the boxes represent median values, 25th to 75th percentiles are denoted by box edges, and whiskers denote non-outlier limits and circles represent outliers' values. Horizontal dashed line indicates Chl-*a* global mean difference.

2.1.1.2. Intra-annual variability and sinusoidal curve

Figure 2.7 displays the periodograms for LisB-IS, LisB-Sat and LagB-Sat. For better visualization of the graphs, the ordinates of the periodograms at timescales shorter than one month were not displayed here. Results showed pronounced seasonal variations with the dominant peak at the 12-month periodicity. Its first harmonic, 6-month periodicity, was also included in the estimation of the sinusoidal curve. The significance of these peaks was confirmed by performing the Hartley test on the three time series (simultaneously testing 12-month and 6-month periodicities, *p*-value = 0.00 for each one of them). At timescales longer than one month, the percentage of variance explained by the annual cycle and its first harmonic accounted for 24.5 %, 25.8 % and 15.4 % of the total variance for LisB-IS, LisB-Sat and LagB-Sat, respectively. The addition of the remaining harmonics of the 12-month periodicity did not enhance the seasonal structure of each time series under consideration. The other periodicities that make up the total variance of each time series corresponded to periodicities that were not directly related with the annual cycles, and so they were not incorporated in the components aforementioned. Therefore, the comparison of the seasonal structures at the different locations studied was based on the 12-month and 6-month periodicities.

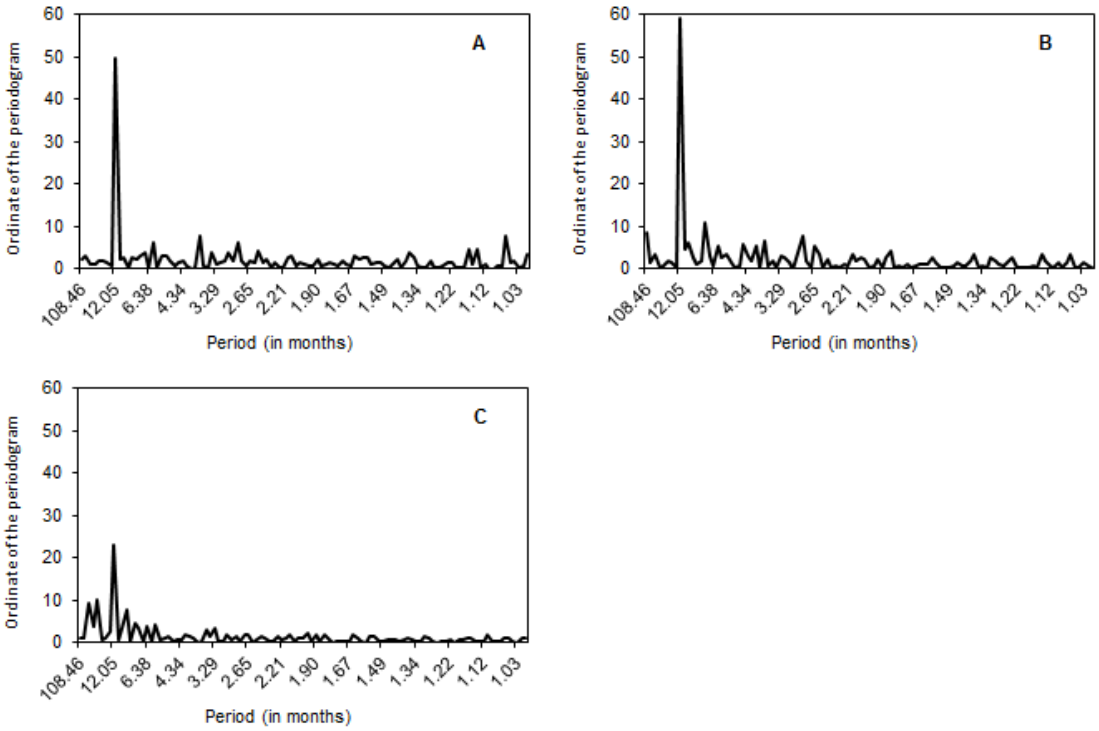

Fig. 2.7. Periodograms of the Chl-*a* time series: LisB-IS (A), LisB-Sat (B) and LagB-Sat (C). The graphs only show the results at timescales longer than one month.

Figure 2.8 shows the intra-annual variability of Chl-*a* for LisB (*in situ* and satellite) and for LagB. Relative to LisB-IS (Fig. 2.8A), the less productive periods and with less variation were the late-autumn and winter months (from November to February). Median values suggest the presence of an almost uni-modal pattern, with a long period with high phytoplankton biomass between March and October (median maximum in June). The highest values were recorded during spring (outliers above 6 mg m^{-3} in March and May). Some differences were observed between *in situ* and satellite estimations (Fig. 2.8B): the period with higher phytoplankton biomass also started in March, but ended in September, one month earlier than the *in situ* record. Two median maxima were recorded, in April and July, showing an annual cycle similar to a bi-modal pattern. The extreme values were also recorded in spring, although this time in March and April (Fig. 2.8B). The satellite data showed higher variability of Chl-*a* in winter months, especially in January and February (Fig. 2.8B), compared to *in situ* data (Fig. 2.8A). Phytoplankton biomass in LagB-Sat (Fig. 2.8C) was higher between March and September with a bi-modal pattern (median maxima in March and June/July). The higher values in this bay were registered during late-spring and summer (outliers above 4 mg m^{-3} from May to August).

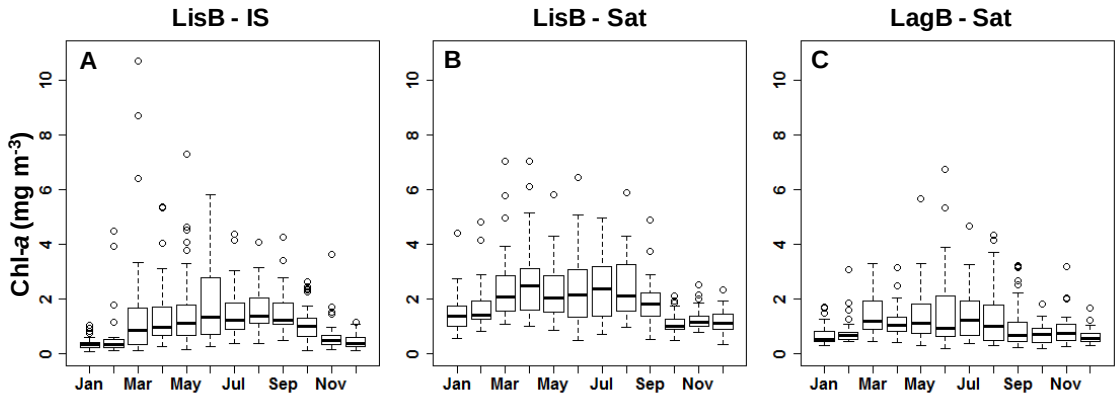

Fig. 2.8. Monthly Chl-*a* boxplots (mg m^{-3}) for LisB-IS (A), LisB-Sat (B) and LagB-Sat (C) during the period 2008-2016. The lines within the boxes represent median values, 25th to 75th percentiles are denoted by box edges, and whiskers denote non-outlier limits and circles represent outliers' values.

The global Chl-*a* sinusoidal curve for the 9-year time series showed a similar pattern between both LisB time series, i.e. using *in situ* and satellite data, but a different pattern between LisB and LagB time series (Fig. 2.9). In LisB, the sinusoidal model showed a sharp Chl-*a* increase during early-winter/early-spring months, indicating the early onset of the spring bloom, a sharp decrease starting in late-summer with minima in late-autumn/early-winter months, and a period of five months characterized by Chl-*a* above the 60th percentile, slightly higher in spring than in summer. The latter period occurred from April to early-September using *in situ* data (Chl-*a* above 1.55 mg m^{-3}) and from early-March to early-August using satellite data (Chl-*a* above 2.32 mg m^{-3}). Lower Chl-*a* values characterized the remaining months, reaching a minimum in December/January (~0.30 mg m^{-3}) based on *in situ* data, and in November (~1.03 mg m^{-3}) based on satellite data. The main differences observed between both LisB time series were the anticipation of the beginning and end of the Chl-*a* maxima by 15 days and one month, respectively, and a global mean overestimation of 0.77 mg m^{-3} when using satellite data, as already referred to above in 3.2.2.

The adjusted Chl-*a* sinusoidal curve in LagB (Fig. 2.9) was almost symmetrical with a peak Chl-*a* value centered in June. Similar to LisB, the onset of the spring bloom occurred in early-winter, but showed a slower rate of increase, reaching a maximum value in June. It was followed by a slow decrease rate from July to November. Despite this, a period characterized by Chl-*a* above the 60th percentile (1.24 mg m^{-3}) of almost five months, from early-April to late-August, was also recorded. The Chl-*a* minima were observed in November/December (~0.60 mg m^{-3}). Overall, the comparison of the two satellite time series showed that the phytoplankton biomass was persistently higher in LisB than in LagB.

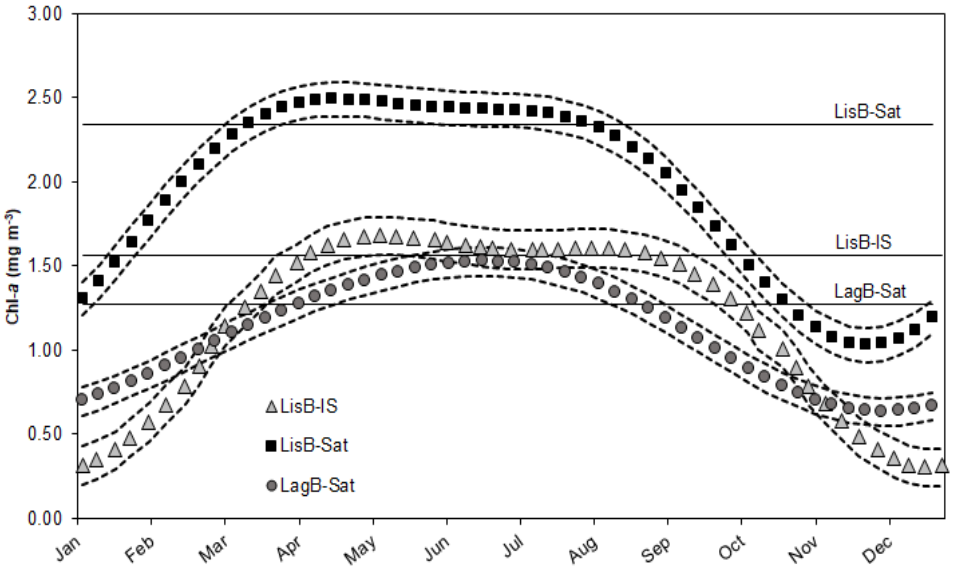

Fig. 2.9. Chl-*a* sinusoidal curves adjusted to the time series of LisB-IS, LisB-Sat and LagB-Sat for the period 2008-2016. Horizontal lines indicate the 60th percentile of each Chl-*a* data set. The dashed lines correspond to the standard errors of each sinusoidal curve.

2.3.3. Cross-correlation structure between Chl-*a* and MetOc data

Figure 2.10 shows the results of cross-correlation analyses between Chl-*a* and each MetOc variable, from lag 0 to lag 4 (0 - 4 weeks), during the winter/early-spring period (Jan–Apr) in LisB and in LagB. During winter/early-spring a significant positive correlation between Chl-*a* and PAR was observed in both bays at lag 0 and 1, although stronger at lag 0 (Fig. 2.10A and 2.10B, Table A.2.1 in appendix). Cross-correlation analyses did not show any other significant correlation between Chl-*a* and the remaining MetOc variables (SST, M_x, M_y and MLD) during the winter/early-spring period (Fig. 2.10, Table A.2.1 in appendix).

The cross-correlation analyses, during the late-spring/summer period (May-Sep) in LisB and in LagB (Fig. 2.11, Table A.2.2 in appendix), showed a negative correlation between Chl-*a* and SST at lag 0 in both bays (Fig. 2.11C and 11D), but also at lag 1 in LagB, although this was weaker than at lag 0 (Fig. 2.11D). However, this correlation was only significant in LagB (Table A.2.2 in appendix). Relative to the zonal transport (M_x), a significant negative correlation with Chl-*a* was found, which was stronger in LisB than in LagB (Fig. 2.11E and 2.11F, Table A.2.2 in appendix). In both bays, this relationship was much more significant at lag 0, although in LisB it was also significant at lag 1. A significant negative correlation with Chl-*a* and the meridional transport (M_y) at lag 0 and 1 in LagB was also identified, stronger at lag 1 (Fig. 2.11H, Table A.2.2 in appendix). No other significant correlations were found between Chl-*a* and the remaining MetOc variables (PAR and MLD in both bays, and M_y in LisB) during the late-spring/summer period (Fig. 2.11H, Table A.2.2 in appendix).

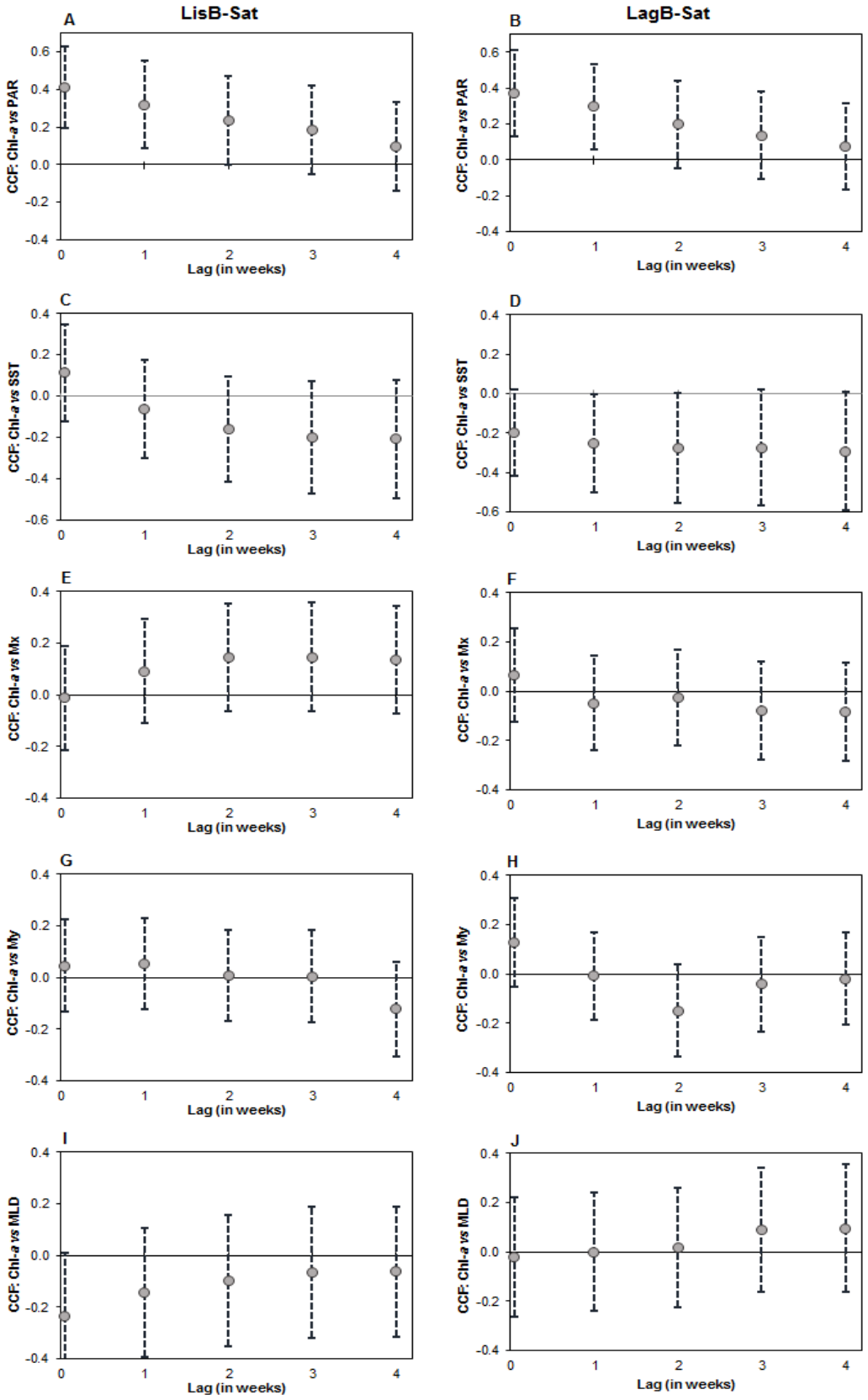

Fig. 2.10. Cross-correlations functions (CCF) between Chl-*a* and MetOc variables using satellite data for winter/early-spring in LisB (left panel) and in LagB (right panel): Chl-*a versus* PAR (A and B); Chl-*a versus* SST (C and D); Chl-*a versus* M_x (E and F); Chl-*a versus* M_y (G and H); Chl-*a versus* MLD (I and J). The dots represent the point estimates and the dashed lines show the lower and upper limits of the 90% CI (confidence interval) for the CCF's. For each lag, if the dashed line crosses the *x*-axis, the null hypothesis of no correlation between the time series is not rejected at the significance level $\alpha \leq 0.10$.

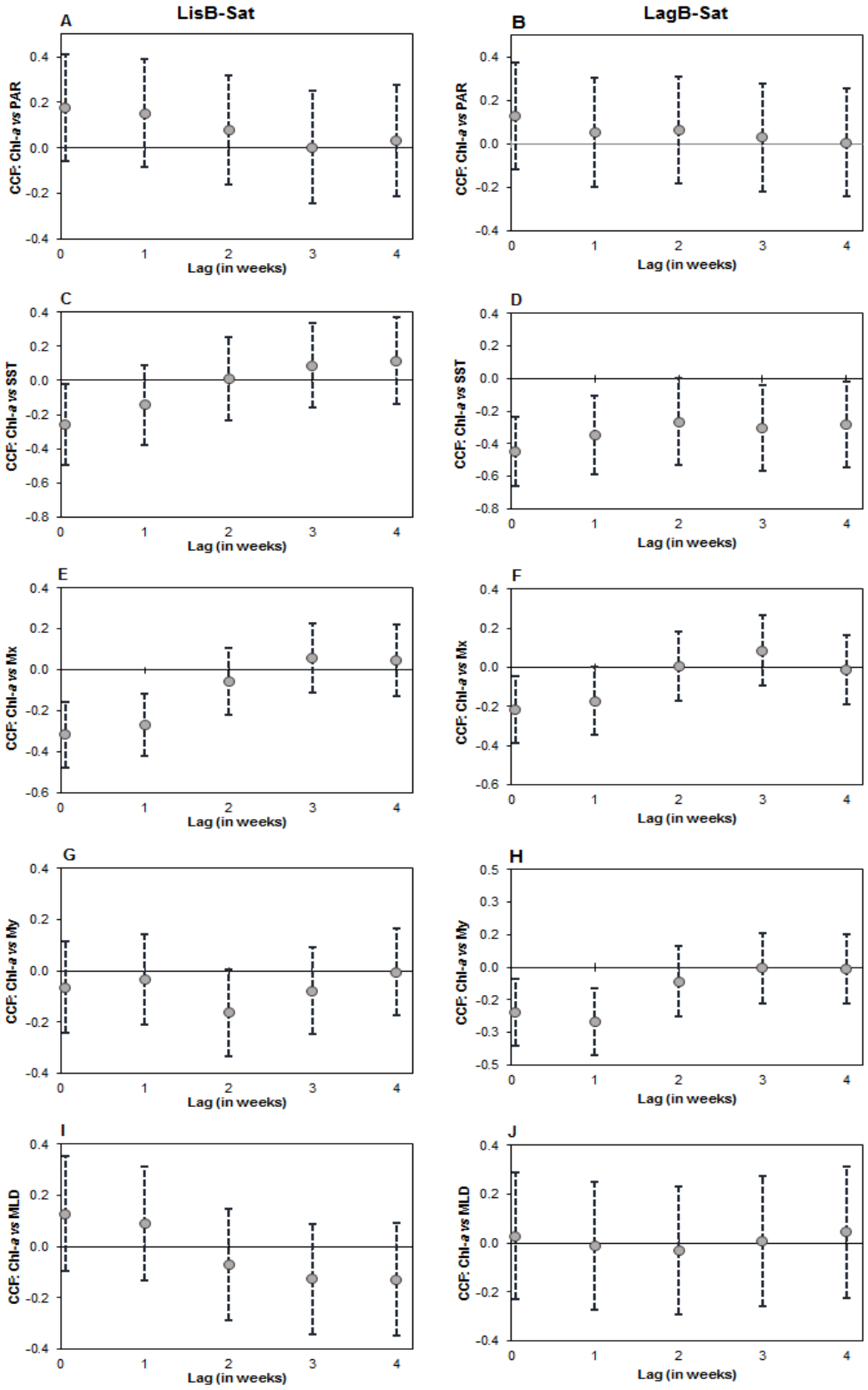

Fig. 2.11. Cross-correlation functions (CCF) between Chl-*a* and MetOc variables using satellite data for late-spring/summer in LisB (left panel) and in LagB (right panel): Chl-*a versus* PAR (A and B); Chl-*a versus* SST (C and D); Chl-*a versus* M_x (E and F); Chl-*a versus* M_y (G and H); Chl-*a versus* MLD (I and J). The dots represent the point estimates, and the dashed lines show the lower and upper limits of the 90% CI (confidence interval) for the CCF's. For each lag, if the dashed line crosses the *x*-axis, the null hypothesis of no correlation between the time series is not rejected at the significance level $\alpha \leq 0.10$.

2.3.4. Phytoplankton biomass, adjusted sinusoidal curve and main phytoplankton groups for 2014 and 2015

Figure 2.12 represents the weekly Chl-*a* data, the global sinusoidal curve for the 9-year (hereafter named global model - solid lines), and the sinusoidal curves adjusted separately for 2014 and 2015 in LisB and in LagB (hereafter named subset model – dash-dotted lines). Concerning LisB, the main differences observed between the subset model and the global model were the earlier observation of the Chl-*a* maximum in 2014 and the occurrence of a summer decline in 2014 and 2015, suggesting a clear bi-modal pattern, and contrasting with the 5-months long high Chl-*a* values on the global model (Fig. 2.12A and 2.12B). In 2015, both for LisB-IS and for LisB-Sat, the summer decline was more pronounced (Fig. 2.12A and 2.12B). Furthermore, for 2015, the *in situ* data showed a delay in the decreasing autumn/winter trend. In these two years in LisB, the early-spring bloom was higher than that observed in late-summer (Fig. 2.12A and 2.12B).

In LagB the subset model showed marked differences compared with the global model in both years (Fig. 2.12C). Although much more accentuated in 2015, two Chl-*a* peaks were recorded in both years with the maximum in late-summer (Fig. 2.12C). The LagB subset model indicated a decrease in June in both years, although more accentuated in 2015, in contrast with the uni-modal global model that peaks in that month (Fig. 2.12C).

To understand the contribution of the different phytoplankton groups to Chl-*a* concentration, figures 2.13 and 2.14 show Chl-*a* and total phytoplankton concentrations (Fig. 2.13A and 2.14A), and the relative abundance of the main phytoplankton groups (diatoms, dinoflagellates and coccolithophores) (Fig. 2.13B and 2.14B). In LisB, despite the similar pattern observed between both *in situ* and satellite Chl-*a* datasets in 2014 and 2015, the satellite Chl-*a* maxima did not always match with *in situ* phytoplankton biomass, nor with phytoplankton abundance (Fig. 2.13A). This was particularly evident in February and December of 2014 and in April and June of 2015. February and December 2014, were characterized by higher precipitation levels, and February also recorded maximum river runoff (data not shown), in agreement with the general pattern for the whole study period (2008-2016) (cf. Fig. 2.2.2). In May 2014, the maximum Chl-*a* recorded by satellite agreed with the increase in phytoplankton abundance and *in situ* Chl-*a*, however it was three times higher in satellite records (Fig. 2.13A).

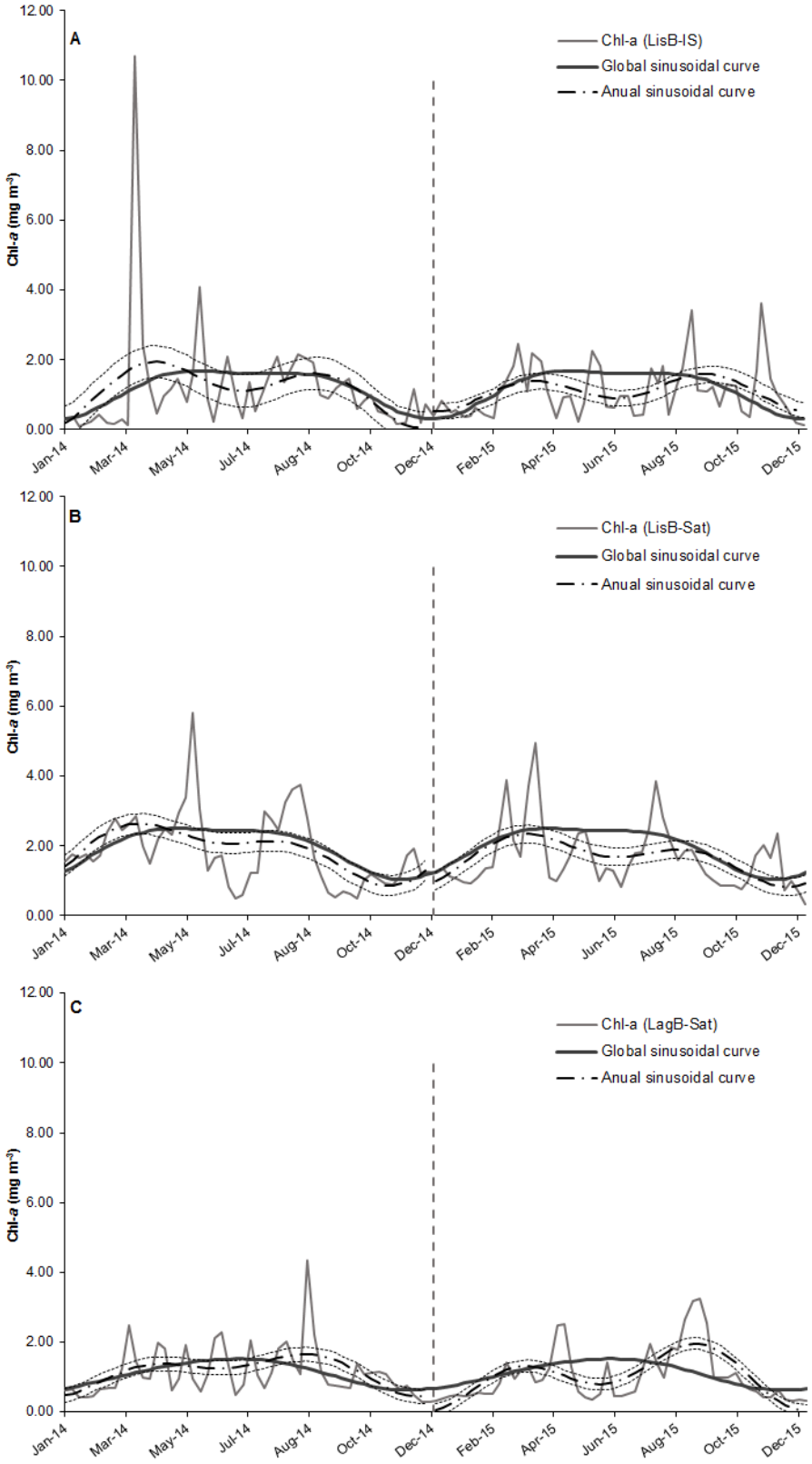

Fig. 2.12. Comparison between weekly Chl-*a* data, global sinusoidal model by using the entire 9-years study period (solid line) and the subset models (dash-dotted lines) resulting from fitting sinusoidal curves for each year, 2014 and 2015: LisB-IS (A), LisB-Sat (B) and LagB-Sat (C). The dashed lines correspond to the standard errors of each sinusoidal curve.

In 2014, maximum phytoplankton abundance was observed in August (1.0 x 10^6 cells L^{-1}) and in 2015 maxima were recorded in March, July and August (above 2.5 x 10^5 cells L^{-1}) (Fig. 2.13A). Diatoms were the phytoplankton group that showed higher relative abundance (around 80 %) in all Chl-*a* maxima observed both *in situ* and by satellite (Fig. 2.13B), and with a few exceptions were always the dominant group. The only Chl-*a* maximum that was dominated by a mixed phytoplankton community was observed in November of 2015 (Fig. 2.13B). Coccolithophores, although with higher relative abundances (> 50 %) during late-winter (February of 2014 and 2015) and late-autumn (at the beginning of December in 2014 and at the end of October in 2015), were never abundant (Fig. 2.13B). Dinoflagellates occasionally dominated the assemblages, namely in late-spring/early-summer 2014 and August 2015 when water stratification is higher (cf. Fig. 2.3I), but were never abundant.

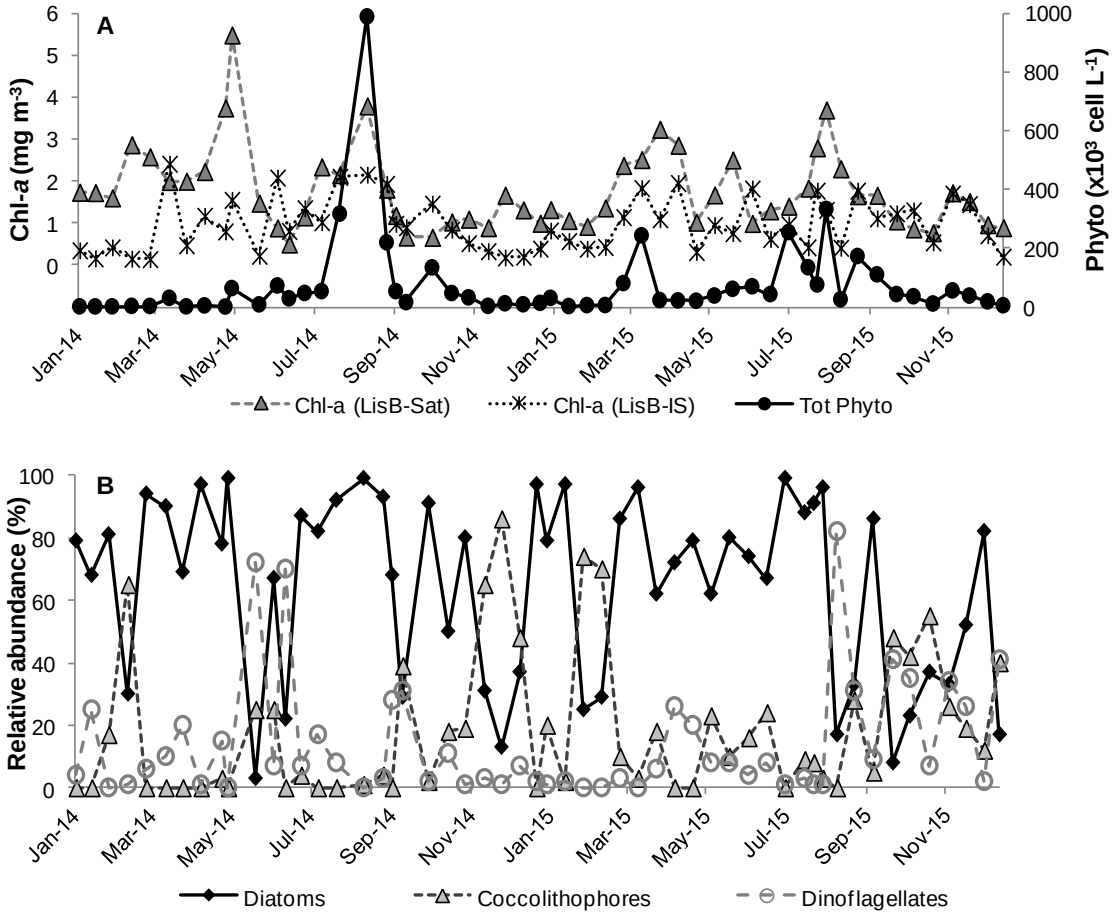

Fig. 2.13. Fortnightly data for 2014 and 2015 in LisB. (A) Chl-*a* (Satellite and *in situ* data) (mg m^{-3}) and phytoplankton abundance (Phyto) (cells L^{-1}); (B) relative abundance of main phytoplankton groups (Diatoms, Dinoflagellates and Coccolithophores).

During 2015 in LagB there were four Chl-*a* maxima estimated by satellite (two during spring and another two during late-summer/early-autumn) (Fig. 2.14A). With a few exceptions, diatoms were the dominant group and all Chl-*a* maxima matched with higher relative abundances of diatoms (Fig. 2.14B). Maximum phytoplankton abundance (1.5 x 10^6 cells L^{-1}) was observed in March, but it did not match with the Chl-*a* maximum (Fig. 2.14A). Rather, that sample was dominated by a small flagellate identified as a coccolithophore holococcolith life-stage (data not shown), which did not contribute much to Chl-*a* (Fig. 2.14A). Coccolithophores were present all year round, but except for the March bloom, their presence was residual (Fig. 2.14B). At the end of April and at the beginning of September, the high values of Chl-*a* observed did not coincide with higher values of phytoplankton abundance (Fig. 2.14A). In September, the decrease in phytoplankton abundance coincided with a change in the dominant group from dinoflagellates to diatoms (Fig. 2.14B). Dinoflagellates had relative abundances between 20 and 60 % from the early-summer to the early-winter, reaching the maximum (90 %) in August (Fig. 2.14B), coinciding with the stratification season (cf. Fig. 2.3D).

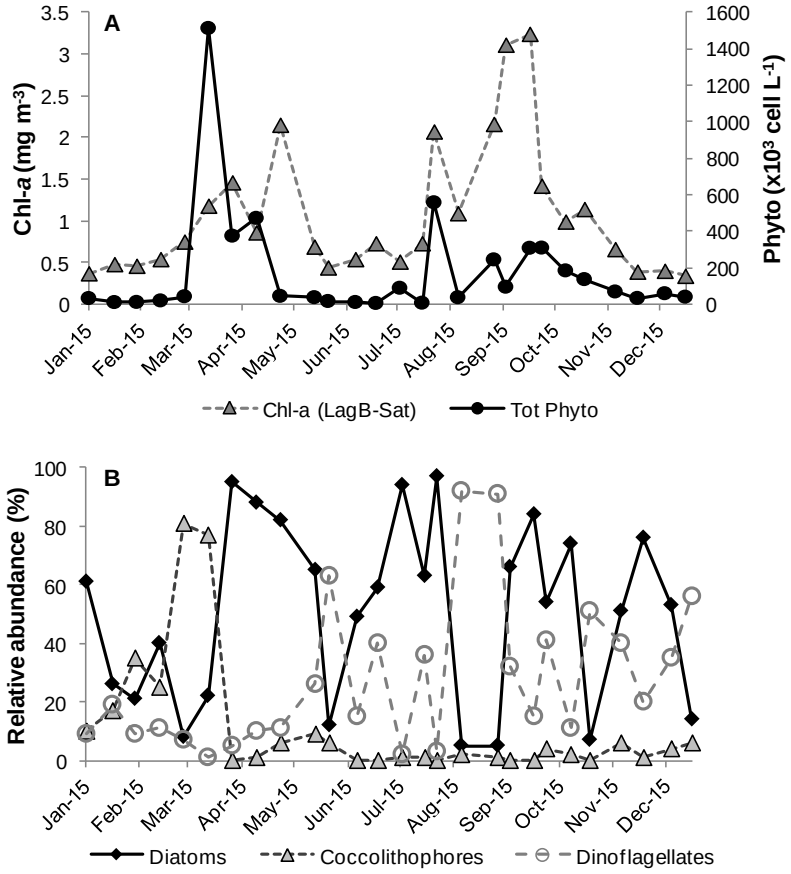

Fig. 2.14. Fortnightly data for 2015 in LagB. (A) Chl-*a* (Satellite) (mg m^{-3}) and phytoplankton abundance (Phyto) (cells L^{-1}); (B) relative abundance of main phytoplankton groups (Diatoms, Dinoflagellates and Coccolithophores).

2.4. Discussion

2.4.1. Comparison between *in situ* and satellite Chl-*a* data sets

Nowadays, satellite Ocean Color (OC) datasets are routinely used to estimate the temporal and spatial Chl-*a* variability in the ocean. Recent remote sensing validation studies were performed on the West (Sá et al., 2015) and on the Southwest coast of Portugal (Cristina et al., 2014, 2015, 2016b). These studies focused on different standard products produced for the MERIS (Cristina et al., 2014, 2015, 2016b; Sá et al., 2015), MODIS and on data products generated within the Ocean Color Climate Change Initiative (Sá et al., 2015). The above validation studies showed that these OC products produce acceptable estimates of *in situ* phytoplankton biomass, albeit with higher uncertainties in near-coast stations.

The present study was not performed with such validation purposes. Here, the aim was to identify the L4 ocean color product (which merge the results from the several satellite products available to the region), currently available on the Copernicus Marine Environment Monitoring Service, that presents the most similar temporal variability pattern with the *in situ* data collected on a weekly sampling frequency. From the different analyzed products (Chl-blend, Chl-GSM, Chl-OI), the one that showed the highest correlation with the Lisbon Bay near-coast *in situ* station and the most similar Chl-*a* seasonal cycle model was the Chl-OI product (level 4, daily, at 4 km resolution). This product has a higher temporal resolution, which may be a reason for the higher correlation. As mentioned by Caballero et al. (2014) smaller spatial scale and a shorter temporal separation window between remote sensing and *in situ* Chl-*a* improve the correlations. Still, the resulting correlation coefficient (r = 0.42) was weak compared to the one obtained in the aforementioned studies in the region. However, for the several study sites located on the central and north Portuguese coast, analyzed in Sá et al. (2015), the lower quality scores were found in exactly the same sampling station as the present study, namely Lisbon Bay. According to these authors, the high temporal variability and the poor atmospheric correction in near-coast stations are factors that affect the satellite estimations.

Similar to previous studies on the Atlantic Iberian coast (Cristina et al., 2014, 2015, 2016b; Sá et al., 2015), the Chl-OI product overestimated Chl-*a* concentrations when compared with *in situ* Chl-*a* data, especially in winter and spring months. This period coincided with the rainier months, and subsequently with the increase in river runoff (this work, Fig. 2.2). An increase in river turbid plume during winter/spring months is frequent, as previously observed in the

Tagus and Guadalquivir rivers for example (Caballero et al., 2014; Fernández-Nóvoa et al., 2017). Besides precipitation and river discharge, other factors such as winds and the fortnightly spring–neap tidal cycle can increase a rivers' turbid zone (Valente and da Silva, 2009). The high concentration of suspended material present in a river plume will induce a strong signal detected by the satellite, overestimating the Chl-*a* (e.g. Fernandez-Novoa et al., 2017 and references therein). Areas such as Lisbon Bay, where optical variability throughout the year is high due to the near-coast location, the presence of a river plume and the frequent occurrence of upwelling filaments, are among the most challenging regions for the performance of satellite Chl-*a* estimates. The present work reinforces the need for further work to continue the search for better ocean color algorithms in these complex waters.

2.4.2. Phytoplankton biomass seasonality

Recent studies were performed on the Portuguese continental coast using satellite Chl-*a* data to model the temporal and spatial variability of phytoplankton biomass (Reboreda et al., 2014), assess the eutrophication areas (Cabrita et al., 2015) and evaluate the region-specific phytoplankton temporal variability patterns (Krug et al., 2017, 2018a). In agreement with these studies, the satellite Chl-*a* variability in the two bays studied in this work showed a productive period from March/April to September and exhibited a bi-modal pattern (cf. Fig. 2.8B and 2.8C). However, the current *in situ* data revealed a different result in Lisbon Bay, with a productive period lasting one month longer than the satellite data (from March to October) and exhibiting an almost uni-modal pattern (c.f. Fig. 2.8A).

To the authors' knowledge, the identification of the characteristic high phytoplankton biomass periods, based on the analyses of Chl-*a* sinusoidal curve to a decade-long time series, has not yet been performed for the selected study area. The closest geographical studies on this subject were developed using *in situ* and satellite data in NW Iberia (Bode et al., 2011, 2019; Nogueira et al., 1997) and in the open ocean using satellite derived-products in the NE Atlantic (Bashmachnikov et al., 2013). The present 9-year time series analysis in the two Portuguese coastal bays reveals a dominant 12-month cycle and a significant 6-month periodic component, similar to the results obtained in the NE Atlantic (Bashmachnikov et al., 2013; Bode et al., 2019). Also Winder and Cloern (2010) in a study that considered 125 estuarine, coastal, lake and oceanic sites in the temperate and subtropical region, observed that the 12-month periodicity, which corresponds to one single phytoplankton peak per year

(spring bloom), was the most common pattern. According to those authors, the bi-modal pattern (6-month periodicity), which corresponds to spring and autumn blooms, was highly variable, but also frequently observed.

From the above 12- and 6-month periodicities a similar seasonal cycle in Lisbon Bay using *in situ* and the selected satellite product data was observed. The main difference between these two datasets was the anticipation of the beginning and end of maximum Chl-*a* concentrations by satellite estimates. Three main periods were identified relative to phytoplankton biomass dynamics in this bay. These periods based on satellite data were: (1) the spring bloom period (December/early-March) characterized by a rapid increase in phytoplankton biomass, reaching maximum values in early-spring; (2) early-spring/summer period (early-March/early-August), marked by sustained high phytoplankton biomass; and (3) late-summer/autumn period (mid-August-November), with a steep decline in phytoplankton biomass. Palma et al. (2010), described for Lisbon Bay three 4-month seasons based on the upwelling characteristics, that roughly correspond to the biomass periods identified in the present work. These were, the spring transition period, from downwelling to upwelling (February-May), the upwelling season (June-September) and the downwelling season (October-January). However, there are differences that should be stressed. In the seasons herein identified, the start of each period is anticipated (delayed) at least one month relative to the proposed upwelling seasons, and the different periods are not equal in length.

In Lagos Bay, the sinusoidal model, indicated a uni-modal seasonal cycle reaching the maximum in June (cf. Fig. 2.9), instead of showing a bi-modal pattern with maxima in March and June/July as suggested by the analysis of Chl-*a* variability (cf. Fig. 2.8C). These results contrast with previous studies on Chl-*a* that showed two annual Chl-*a* maxima in the CSV region, namely, the spring bloom and a late-summer maximum (e.g. Navarro and Ruiz, 2006; Krug et al., 2017, 2018). According to the present study, the phytoplankton biomass seasonal cycle in Lagos Bay can be characterized also by three main periods: (1) the spring bloom period (December/March), marked by a slow steady increase in phytoplankton biomass; (2) the mid-spring/summer period (April/August) with a maximum centered in June; and (3) the late-summer/autumn period (September/November), characterized by a slow decrease in biomass. These three periods contrast with the four oceanographic seasons previously defined for the CSV region based on upwelling forcing which coincide with the astronomical seasons (Goela et al., 2016). Summer was characterized by strong persistent upwelling, autumn by upwelling relaxation, and spring and winter by intermittent periods of upwelling (Goela et al.,

2016). The mismatch between phytoplankton biomass seasons for Lisbon and Lagos Bays and those identified based on upwelling cycles highlights the need for explanatory drivers other than upwelling dynamics, to understand the phytoplankton biomass seasonal cycle on the West and South coasts of Iberia (see 4.3. below).

The differences observed between both bays, specifically a long period with high Chl-*a* concentrations in Lisbon Bay *versus* a unique short maximum of low concentration in Lagos Bay, probably reflect distinct nutrient cycles and sources in each bay. The Tagus estuary drains into Lisbon Bay nutrient-rich waters, particularly in winter/early-spring (Cabrita et al. 2015). This, combined with strong persistent upwelling in the summer months (this study (Fig. 2.3E), Moita et al. 2003, Oliveira et al. 2009b), allows for a long nutrient-rich period in this bay. In addition, the river plume induces haline stratification, which may also contribute to the increase in phytoplankton biomass due to increased water stratification and reduction of physical flushing losses (Bode et al. 2019). Ferreira et al. (2019), based on Chl-*a* climatology, described the area off the Tagus estuary as a major coastal hotspot for phytoplankton biomass. By contrast, the absence of major rivers in the westernmost sector of the South coast of Iberia renders seasonal upwelling as the single primary nutrient source in Lagos Bay.

Bode et al. (2011) analyzed long-term trends in phytoplankton biomass in the NW Iberian coast and found a high spatial variability in Chl-*a* seasonal cycles at a relatively small regional scale, related to upwelling prevalence and amplification, by remineralization processes in the Galician rias. The West coastal site, under the strong influence of seasonal upwelling and nutrient remineralization, showed a uni-modal Chl-*a* seasonal cycle, which peaked in July/August, and was characterized by high concentration values (3-4 mg m^{-3}). Relative to Lisbon and Lagos Bays, the onset of the spring phytoplankton bloom was delayed 2-months and only initiated in late-February/March. Further north, coastal sites beyond Cape Finisterre and in Mar Cantabrico, less influenced by coastal upwelling and remineralization processes, were characterized by lower maximum Chl-*a* concentrations and a bi-modal pattern with a spring and autumn bloom.

Given the above, and keeping in mind the non-stationary feature of a time series (Winder and Cloern, 2010), it is possible to observe a latitudinal trend on Chl-*a* seasonal patterns along the upwelling influenced Atlantic Iberian coast. The westernmost South Iberian coast presents a uni-modal pattern, characterized by low Chl-*a* concentrations (maximum of 1.5 mg m^{-3}, this study, Fig. 2.9) and a short maximum in June; on the central West coast, in the vicinity of a major river, a uni-modal pattern (changing to bi-modal) is observed, characterized by an

extended high biomass period from March to August (maximum of 2.5 mg m^{-3}, this study, Fig. 2.9); on the Northwest coast under the influence of the Galician rias, a uni-modal pattern is observed with a long high biomass period from April to November, but with a short maximum peak centered in July/August (4 mg m^{-3}, Bode et al., 2011); and lastly a bi-modal pattern on the North Iberian coast characterized by low biomass spring and autumn blooms (0.5-2.5 mg m^{-3}, Bode et al., 2011). Although a latitudinal increase of Chl-*a* on the Western Iberian coast was observed (this study; Bode et al., 2011; Ferreira et al., 2019), typical for the Iberia/Canary Upwelling Ecosystem at latitudes between 35º and 45º (e.g. Carr, 2002; Chavez and Messié, 2009), the same did not occur when the coastline changed to a West-East orientation. The main reason for that is the smaller influence of upwelling and river input on the Northern coast, which is much stronger on the W coast.

2.4.3. Relationship between Chl-*a* seasonal cycle and underlying Meteorological and Oceanographic drivers

Understanding the patterns and linkages between environmental drivers and phytoplankton biomass is a rather difficult task. The time scale used in this analysis might be an important feature for explaining these dynamics. Unlike other recent studies (e.g. Ferreira et al., 2019; Krug et al., 2017), in this work the data was analyzed at a weekly time scale, which introduced an additional source of complexity in data analysis due to the time series nature of the datasets. Here, cross-correlation analyses were used because it is a suitable tool to study the relationship between two time series. This technique is of particular interest since it allows one to quantify the strength of the correlation between two time series k, $k \in \mathbf{Z}$, units apart. Moreover, the significance of each correlation coefficient can be evaluated by means of the Bartlett's formula (expression (3)). In this study, cross-correlation analyses were performed to understand the relationship between phytoplankton biomass and meteorological and oceanographic (MetOc) variables in different periods (winter/early-spring and late-spring/summer) within a maximum 1-month time period, i.e., from 0 up to 4 weeks apart (k = 0, …, k = 4). The lagged correlations of the MetOc drivers on Chl-*a* concentration allowed one to quantify the extent to which (in terms of weeks) the effect of these environmental variables remains significant on Chl-*a*.

The winter/early-spring period was characterized by the increase of PAR, low SST values and shoaling of MLD. The increase of Chl-*a* was significantly associated with the increase of

PAR in both of the studied bays, which indicates light limitation in winter/early-spring. The late-spring/summer period was characterized by the highest values of PAR, and by the increase and highest values of SST. It was also the most favorable upwelling period with shallower MLD. The increase of Chl-*a* during this period was significantly related to the increase in upwelling and to the associated decrease of SST in the two bays. Light levels, combined with higher nutrient availability from winter mixing (Moita, 2001) and the decrease of MLD were previously considered as favorable conditions for the occurrence of the spring phytoplankton bloom on the West Portuguese coast (Moita, 2001; Palma et al., 2010). Furthermore, Oliveira et al. (2009b), after studying a summer upwelling event, found that MLD had played an important role in defining the physical conditions for phytoplankton growth. More recently, negative correlations between MLD and Chl-*a* anomalies were reported for the western Iberian coast (Ferreira et al., 2019). Other studies on temporal and spatial patterns of phytoplankton in Southwest Iberia, reported that the timing of the spring bloom onset occurred during the MLD deepening phase and not during the MLD shoaling phase (Krug et al., 2017, 2018; Navarro et al., 2012). Other studies on the West Iberian coast reported a Chl-*a* increase matching with the deepening of MLD, south of 43 ºN (Reboreda et al., 2014). By contrast, in the present study, no significant correlation was found between MLD and the annual Chl-*a* patterns. Despite this, both the interannual variability of Chl-*a* (cf. Fig. 2.8) and the global sinusoidal curve (cf. Fig. 2.9) show the onset of the spring bloom, in both bays, coinciding with the deep MLD phase (cf. Fig. 2.3 I, J). On the other hand, the high biomass spring/summer season described above (4.2) agrees with the MLD shoaling phase and high stratification conditions. Reports of the onset of the spring bloom and increases in Chl-*a* concentration during the deepening phase of the MLD have questioned the long-standing interpretation of the critical depth hypothesis, proposed by Sverdrup (1953) for the development of the phytoplankton spring bloom in the middle and high latitudes of the North Atlantic. This has stimulated the search for other drivers that better explain the onset of phytoplankton blooms (Behrenfeld, 2010; Fisher et al. 2014 for a review). A key aspect is to consider that phytoplankton standing stocks are not only dependent on the specific growth rate of phytoplankton but also on a variable specific loss rate, dependent on several abiotic (e.g. sinking, dilution, advection) and biotic (e.g. grazing, parasitism, viral infections) components. The absence of a significant correlation between MLD and Chl-*a* concentrations, in the present study, suggests that other drivers are responsible for the onset of phytoplankton blooms in Lisbon and Lagos Bays. The ecological disturbance-recovery hypothesis recently proposed by Behrenfeld (2010) is one possibility. According to this view, blooms are initiated

by physical processes that disrupt the predator-prey balanced interactions, such as deep winter mixing and low light, freshwater input or upwelling (Behrenfeld et al., 2013; Behrenfeld and Boss, 2014). Further research designed to test this hypothesis, and other phytoplankton top-down controls, in coastal areas affected by seasonal upwelling will certainly contribute to a better understanding of marine ecosystem functioning.

Regarding the upwelling indices and SST, both variables showed a higher correlation with Chl-*a* during late-spring/summer. Nevertheless, there were some differences between the two studied bays regarding the correlation between Chl-*a* and the two upwelling indices. In Lisbon Bay, zonal transport (M_x) showed a significant negative correlation at both lag 0 and lag 1-week. This highlights the relevance of intensity and persistence of seasonal upwelling, induced by northerly winds, on phytoplankton biomass in this bay. Lagos Bay also showed a significant negative correlation with zonal transport, albeit weaker and only at lag 0. Meridional transport (M_y) was only significant in Lagos Bay (at both lag 0 and lag 1) where it showed a more significant correlation than M_x. Lisbon Bay is located close to the meridionally oriented Iberian West coast near the Cape Roca upwelling center (~12 Km). Several studies covering this region have shown the influence of the coastal discontinuity, which characterizes Lisbon Bay, on the generation of upwelling coastal jets with associated recirculation cells that concentrate phytoplankton, stimulate growth or reduce losses, thus allowing for high phytoplankton biomass in the bay in response to coastal upwelling (Moita et al., 2003, Oliveira et al., 2009a, b). Lagos Bay is located on the most western sector of the South coast of Iberia, close to the CSV upwelling center (~30 Km), where the West coast meets the South coast. This geographical setting, explains the influence of upwelling generated by both the N-S and W-E wind component in this bay. Although considered occasional, our results show that the intensity and persistence of upwelling that occur under westerly winds have a stronger influence on phytoplankton biomass in Lagos Bay than the upwelling filaments generated near CSV under northerly winds. Previous studies on the West and South Atlantic Iberian waters, based on long time series satellite data, also found a correlation between upwelling indices and Chl-*a* concentrations (Ferreira et al., 2019; Krug et al., 2017, 2018). However, on the South coast they only found positive effects of the M_y, and not of the M_x, over Chl-*a*. Both studies used Generalized Additive Models (GAMs), and in some cases Generalized Additive Mixed Models (GAMMs), to identify the most important environmental drivers of Chl-*a* variability. The datasets were analyzed at longer time scales (e.g. monthly) than the one used in the present work (weekly), which largely reduced the time

dependence between observations. Furthermore, these studies did not analyzed the lagged effects of each environmental driver on Chl-*a* concentration, but rather fitted multiple regression models (in their cases, additive models) to describe Chl-*a*. These two methodological approaches contrast with the present one and might represent the origin of the differences found in the results. It is also important to stress that Ferreira et al. (2019) analyzed the correlation between each environmental variable and Chl-*a*, but only at the same time point (at lag 0). In this case, looking particularly at the studied areas comparable with the current work, the authors found, similarly to us, a strong correlation with the North-South water flow (M_y) on the South coast. However, the East-West component of water flow (M_x) was not related with the increase of phytoplankton biomass on the South coast, neither in Lisbon Bay. In this case, it is important to note that the authors analyzed the data as a whole, losing the temporal structure of the data. Our work highlights the need to consider the variability of temporal scales when investigating the patterns of phytoplankton biomass and their relation to oceanographic processes, namely high variability processes such as upwelling. The treatment of the 4-seasons data together, especially in winter and summer, masks, along with other oceanographic processes the true importance of upwelling to phytoplankton dynamics.

In upwelling ecosystems, a direct decrease in SST is usually observed when associated with the occurrence of upwelling. In the present work, that relationship was observed to be stronger in Lagos Bay, where two different wind components are contributing to that result. The relationship between those variables was weaker in the sheltered Lisbon Bay, which is affected by the presence of an estuary that seems to keep the waters warmer during summer. In agreement with this result, a previous study in Lisbon Bay (Palma et al., 2010) found that SST showed better the annual variation in air temperature than the upwelling pulses. With these observations in mind, it seems reasonable to say that SST cannot be used as a proxy of upwelling in Lisbon Bay.

2.4.4. Contribution of the main phytoplankton groups

The determination of dominant phytoplankton groups provides additional insight into the understanding of the phytoplankton biomass peaks. In 2014 and 2015 in Lisbon Bay, and in 2015 in Lagos Bay, diatoms were the group that contributed most towards the total phytoplankton biomass. These results are in good agreement with previous works developed

for both West and South Portuguese coasts (e.g. Danchenko et al., 2019; Goela et al., 2014, 2015; Loureiro et al., 2005; Mendes et al., 2011; Silva et al., 2009; Vidal et al., 2017). In the present study there were a few Chl-*a* peaks that matched a decrease in phytoplankton total abundance, most of which were recorded in winter and spring. Moreover, those situations were associated with a higher relative abundance of diatoms. However, it is important to enhance that description of phytoplankton communities using light microscopy only reliably detects well-preserved specimens of the microphytoplankton component (>20 µm). Species belonging to the nanoplankton fraction (2-20µm) tend to be overlooked or unidentified, and picoplankton (< 2 µm) is below the microscope resolution power. Studies, using phytoplankton marker pigments developed on the West and South Iberian Atlantic waters indicate that, in general, microphytoplankton is the dominant group, but in some periods pico- and nanoplankton may attain more than a 50% contribution to Chl-*a* (Brito et al., 2015; Goela et al., 2014, 2013; Sañé et al., 2019). In fact, in the Northeast Atlantic these small groups usually dominate the community in autumn/winter (Goela et al., 2014, 2013) and in some cases until early-spring (Cadier et al., 2017). This could explain the few inconsistencies found between Chl-*a* biomass and phytoplankton abundance peaks.

In the current work, dinoflagellates and coccolithophores were the groups that contributed most to the differences observed between the two studied bays. Dinoflagellates had a more relevant contribution to the phytoplankton community in Lagos Bay, while coccolithophores were more relevant in Lisbon Bay, which is in agreement with previous studies (Danchenko et al., 2019; Loureiro et al., 2005; Silva et al., 2009). Dinoflagellates are associated with warmer summer stratified conditions. The presence of warmer waters on the South coast (e.g. this study) and of a warm coastal countercurrent near CSV (e.g. Relvas and Barton, 2002; Santos et al., 2019) may explain the higher relative abundance of this group in Lagos Bay.

Coccolithophores, although with a smaller contribution to the global community on the South coast, can also reach high cell concentrations, as observed in late-winter during this study or in summer near CSV region in a previous study (Moita, 2001, chapter 2.2). This group occurs under several oceanographic conditions, such as weak upwelling, upwelling relaxation and convergence conditions (Silva et al., 2008). In the present work, the higher contribution of coccolithophores occurred in late-winter and autumn, which can be related to the presence of tropical and subtropical oligotrophic waters that reach near-coast locations during convergence periods (Moita, 2001; Silva et al., 2008).

In addition, high short-time variability was observed in phytoplankton biomass and community on a weekly scale. For example, Danchenko et al. (2019) also mentioned a high variability on a timescale of several days. This highlights the importance of acquiring fine sampling scales in long-term stations when studying phytoplankton variability. The continuous development of sensitive satellite sensors and the possibility of using new *in situ* sensors, such as the Imaging FlowCytobot (Olson and Sosik, 2007), are key strategies to obtain high temporal resolution of phytoplankton community data to understand bloom phenology and phytoplankton species succession patterns.

2.5. Conclusions

In this study, the phytoplankton biomass seasonal cycle obtained through a sinusoidal model was analyzed using 9 years of data in two Portuguese coastal bays. Comparisons between *in situ* and satellite datasets performed in Lisbon Bay revealed that even when using the OC product that best fitted with *in situ* Chl-*a*, there were still substantial differences when adjusting the sinusoidal model to the data. This highlights the importance of a critical use of satellite estimates in near-coast upwelling centers.

Despite the small latitudinal distance between the two studied sites, differences in the seasonal dynamics of phytoplankton biomass were observed for the two bays. Coastal areas affected by both upwelling and river discharge, like West Atlantic Iberian coast, may sustain high phytoplankton biomass for longer periods.

Analyses of the linear correlations between different meteorological and oceanographic variables and Chl-*a* showed clear differences in the role of the different wind components and SST in phytoplankton biomass dynamics in each bay. In Lagos Bay, the role of each wind component and the differences in the weight of those components at different lags should be further investigated to better understand their implications in phytoplankton bloom phenology. The SST correlations showed that SST anomalies should be used with caution as a proxy for upwelling in sheltered bays influenced by large rivers, such as Lisbon Bay. The non-significant correlation between MLD shoaling and Chl-*a* increase suggests that this was not a main driver of bloom onset in the studied bays. Other hypotheses, such as the recent ecological disturbance-recovery hypothesis, should be investigated in future studies.

This study reconfirmed that a high spatial and interannual variability can be observed in phytoplankton biomass seasonal curves. This variability of the seasonal patterns was also reflected on the phytoplankton community structure.

Acknowledgments

Financial support of M. Santos was provided by a Portuguese PhD grant from FCT - Fundação para a Ciência e a Tecnologia (SFRH/BD/52560/2014). This work was financially supported by IPMA, I.P. (MAR2020/SNMB-MONITOR) and by FCT Funding of RD Units (UID/MAR/04292/2019, UID/Multi/04326/2019 and UID/MAT/04561/2019). The work was co-financed by the Regional Operational Program of Lisbon, Portugal 2020 and the European Union through FEDER, and by National Funds through FCT under the project PTDC/CTA-AMB/31265/2017.

A. Silva acknowledges former FCT funding (SFRH/BPD/63106/2009) and current IPMA funding (IPMA-BCC-2016-35). The authors would like to express a special thanks to "Testa & Cunhas, SA" for sample collection in LagB-IS and to all the colleagues at IPMA who helped with sample collection, fieldwork and laboratory support. This study has been conducted using E.U. Copernicus Marine Service Information for the Chl-*a* L4 Reprocessed datasets (http://marine.copernicus.eu/).

References

Alvarez, I., Gomez-gesteira, M., DeCastro, M., Dias, J.M., 2008. Spatio temporal evolution of upwelling regime along the western coast of the Iberian Peninsula. J. Geophys. Res. 113, C07020. doi:10.1029/2008JC004744

Amorim, A., Moita, M., Oliveira, P., 2004. Dinoflagellate blooms related to coastal upwelling plumes off Portugal, *in*: Steidinger, K.A., Landsberg, J.H., Tomas, C.R., Vargo, G.A. (Eds.), Harmful Algae 2002. Florida Fish and Wildlife Conservation Commission, Florida Institute of Oceanography, and Intergovernmental Oceanographic Commission of UNESCO, St. Petersburg, Florida, USA, pp. 89–91.

Bashmachnikov, I., Belonenko, T. V., Koldunov, A. V., 2013. Intra-annual and interannual non-stationary cycles of chlorophyll concentration in the Northeast Atlantic. Remote

Sens. Environ. 137, 55–68. doi:10.1016/j.rse.2013.05.025

Behrenfeld, MJ., 2010. Abandoning Sverdrup's Critical Depth Hypothesis on phytoplankton blooms. Ecology 91, 977–89. doi:10.1890/09-1207.1

Behrenfeld, M.J., Doney, S.C., Lima, I., Boss, E.S., Siegel, D.A., 2013. Annual cycles of ecological disturbance and recovery underlying the subarctic Atlantic spring plankton bloom. Global 27, 526–540. doi:10.1002/gbc.20050

Behrenfeld, M.J., Boss, E.S., 2014. Resurrecting the Ecological Underpinnings of Ocean Plankton Blooms. Annu. Rev. Mar. Sci. 6, 167–194. doi:10.1146/annurev-marine-052913-021325

Bode, A., Anadón, R., Morán, X.A.G., Nogueira, E., Teira, E., Varela, M., 2011. Decadal variability in chlorophyll and primary production off NW Spain. Clim Res 48, 293-305. doi:10.3354/cr00935

Bode, A., Álvarez, M., Ruíz-Villarreal, M., Varela, M. M., 2019. Changes in phytoplankton production and upwelling intensity off A Coruña (NW Spain) for the last 28 years. Ocean Dyn. 69, 861-873. doi:10.1007/s10236-019-01278-y

Box, G.E.P., Jenkins, G.M., Reinsel, G.C., Ljung, G.M., 2016. Time Series Analysis: Forecasting and Control, 5th ed. John Wiley & Sons, New Jersey.

Brito, A.C., Sá, C., Brotas, V., Brewin, R.J.W., Silva, T., Vitorino, J., Platt, T., Sathyendranath, S., 2015. Effect of phytoplankton size classes on bio-optical properties of phytoplankton in the Western Iberian coast: Application of models. Remote Sens. Environ. 156, 537–550. doi:10.1016/j.rse.2014.10.020

Caballero, I., Morris, E.P., Prieto, L., Navarro, G., 2014. The influence of the Guadalquivir River on the spatio-temporal variability of suspended solids and chlorophyll in the Eastern Gulf of Cadiz. Mediterr. Mar. Sci. 15, 721–738. doi: 10.12681/mms.844

Cabrita, M.T., Silva, A., Oliveira, P.B., Angélico, M.M., Nogueira, M., 2015. Assessing eutrophication in the Portuguese continental Exclusive Economic Zone within the European Marine Strategy Framework Directive. Ecol. Indic. 58, 286–299. doi:10.1016/j.ecolind.2015.05.044

Cadier, M., Gorgues, T., Sourisseau, M., Edwards, C.A., Aumont, O., Marié, L., Memery, L., 2017. Assessing spatial and temporal variability of phytoplankton communities' composition in the Iroise Sea ecosystem (Brittany, France): A 3D modeling approach.

Part 1: Biophysical control over plankton functional types succession and distribution. J. Mar. Syst. 165, 47–68. doi:10.1016/j.jmarsys.2016.09.009

Carr, M.E., 2002. Estimation of potential productivity in Eastern Boundary Currents using remote sensing. Deep. Res. Part II Top. Stud. Oceanogr. 49, 59–80. doi:10.1016/S0967-0645(01)00094-7

Chatfield, C., 2004. The Analysis of Time Series: An Introduction, 6th ed., Chapman & Hall/CRC.

Chavez, F.P., Messié, M., 2009. A comparison of Eastern Boundary Upwelling Ecosystems. Prog. Oceanogr. 83, 80–96. doi:10.1016/j.pocean.2009.07.032

Cloern, J.E., Abreu, P.C., Carstensen, J., Chauvaud, L., Elmgren, R., Grall, J., Greening, H., Roger, J.O., 2016. Human activities and climate variability drive fast-paced change across the world's estuarine – coastal ecosystems. Glob. Chang. Biol. 22, 513–529. doi:10.1111/gcb.13059

Cravo, A., Relvas, P., Cardeira, S., Rita, F., Madureira, M., Sa, R., 2010. An upwelling filament off southwest Iberia: Effect on the chlorophyll *a* and nutrient export. Cont. Shelf Res. 30, 1601–1613. doi:10.1016/j.csr.2010.06.007

Cristina, S.C.V., Moore, G.F., Goela, P.R.F.C., Icely, J.D., Newton, A., 2014. *In situ* validation of MERIS marine reflectance off the southwest Iberian Peninsula: assessment of vicarious adjustment and corrections for near-land adjacency. Int. J. Remote Sens. 35, 2347–2377. doi:10.1080/01431161.2014.894657.

Cristina, S., Icely, J., Goela, P.C., DelValls, T.A., Newton, A., 2015. Using remote sensing as a support to the implementation of the European Marine Strategy Framework Directive in SW Portugal. Cont. Shelf Res. 108, 169–177. doi:10.1016/j.csr.2015.03.011.

Cristina, S., Cordeiro, C., Lavender, S., Goela, P.C., Icely, J., Newton, A., 2016a. MERIS phytoplankton time series products from the SW Iberian Peninsula (Sagres) using seasonal-trend decomposition based on loess. Remote Sens. 8, 1–16. doi:10.3390/rs8060449

Cristina, S., D'Alimonte, D., Goela, P.C., Kajiyama, T., Icely, J., Moore, G., Fragoso, B., Newton, A., 2016b. Standard and Regional Bio-Optical Algorithms for Chlorophyll *a* Estimates in the Atlantic off the Southwestern Iberian Peninsula. IEEE Geosci. Remote Sens. Lett. 13, 757–761. doi:10.1109/LGRS.2016.2529182

Danchenko, S., Fragoso, B., Guillebault, D., Icely, J., Berzano, M., Newton, A., 2019. Harmful phytoplankton diversity and dynamics in an upwelling region (Sagres, SW Portugal) revealed by ribosomal RNA microarray combined with microscopy. Harmful Algae 82, 52–71. doi:10.1016/J.HAL.2018.12.002

Fernández-Nóvoa, D., Gómez-Gesteira, M., Mendes, R., DeCastro, M., Vaz, N., Dias, J.M., 2017. Influence of main forcing affecting the Tagus turbid plume under high river discharges using MODIS imagery. PLoS One 12, 1–27. doi:10.1371/journal.pone.0187036

Ferreira, A., Brito, A.C., Harvey, E.T., 2019. Disentangling Environmental Drivers of Phytoplankton Biomass off Western Iberia. Front. Mar. Sci. 6, 1–17. doi:10.3389/fmars.2019.00044

Field, C.B., Behrenfeld, M.J., Randerson, J.T., Falkowski, P., 1998. Primary production of the biosphere: Integrating terrestrial and oceanic components. Science 281, 237–240. doi:10.1126/science.281.5374.237

Fischer, A.D., Moberg, E.A., Alexander, H., Brownlee, E.F., Hunter-Cevera, K.R., Pitz, K.J., Rosengard, S.Z., Sosik, H.M., 2014. Sixty years of Sverdrup: a retrospective of progress in the study of phytoplankton blooms. Oceanography 27, 222–235. doi:10.5670/oceanog.2014.26.

Fiúza, A.F. de G., de Macedo, M.E., Guerreiro, M.R., 1982. Climatological space and time variation of the Portuguese coastal upwelling. Oceanol. Acta 5, 31–40.

Goela, P.C., Icely, J., Cristina, S., Newton, A., Moore, G., Cordeiro, C., 2013. Specific absorption coefficient of phytoplankton off the Southwest coast of the Iberian Peninsula: A contribution to algorithm development for ocean colour remote sensing. Cont. Shelf Res. 52, 119–132. doi:10.1016/j.csr.2012.11.009

Goela, P.C., Danchenko, S., Icely, J.D., Lubian, L.M., Cristina, S., Newton, A., 2014. Using CHEMTAX to evaluate seasonal and interannual dynamics of the phytoplankton community off the South-west coast of Portugal. Estuar. Coast. Shelf Sci. 151, 112–123. doi:10.1016/j.ecss.2014.10.001.

Goela, P.C., Icely, J., Cristina, S., Danchenko, S., DelValls, T.A., Newton, A., 2015. Using bio-optical parameters as a tool for detecting changes in the phytoplankton community (SW Portugal). Estuar. Coast. Shelf Sci. 167, 125–137. doi:10.1016/j.ecss.2015.07.037.

Goela, P.C., Cordeiro, C., Danchenko, S., Icely, J., Cristina, S., Newton, A., 2016. Time series analysis of data for sea surface temperature and upwelling components from the southwest coast of Portugal. J. Mar. Syst. 163, 12–22. doi:10.1016/j.jmarsys.2016.06.002

Graham, W.M., Largier, J.L., 1997. Upwelling shadows as nearshore retention sites: The example of northern Monterey Bay. Cont. Shelf Res. 17, 509–532. doi:10.1016/S0278-4343(96)00045-3

Hartley, A.H.O., 1949. Tests of Significance in Harmonic Analysis. Biometrika 36, 194–201. doi:10.1093/biomet/36.1-2.194

Haynes, R., Barton, E.D., Pilling, I., 1993. Development, persistence, and variability of upwelling filaments off the Atlantic coast of the Iberian Peninsula. J. Geophys. Res. 98, 22681-22692. doi:10.1029/93JC02016

Holm-Hansen, O., Lorenzen, C.J., Holmes, R.W., Strickland, J.D.H., 1965. Fluorometric determination of Chlorophyll. J Cons Perm Int Explor Mer 30, 3–15. doi: 10.1093/icesjms/30.1.3

IOCCG, 2000. Remote Sensing of Ocean Colour in Coastal, and Other Optically-Complex,Waters, (ed. S. Sathyendranath). Dartmouth, NS, Canada, International Ocean-Colour Coordinating Group (IOCCG), 140pp. (Reports of the International Ocean-Colour Coordinating Group, No. 3) doi:10.25607/OBP-95

Krug, L.A., Platt, T., Sathyendranath, S., Barbosa, A.B., 2017. Unravelling region-specific environmental drivers of phytoplankton across a complex marine domain (off SW Iberia). Remote Sens. Environ. 203, 162–184. doi:10.1016/j.rse.2017.05.029

Krug, L.A., Platt, T., Sathyendranath, S., Barbosa, A.B., 2018. Patterns and drivers of phytoplankton phenology off SW Iberia: A phenoregion based perspective. Prog. Oceanogr. 165, 233–256. doi:10.1016/j.pocean.2018.06.010

Kudela, R.M., Cruz, S., Pitcher, G.C., Figueiras, F.G., National, S., 2005. Harmful Algal Blooms in Coastal Upwelling Systems. Oceanography 18, 184–197. doi:10.5670/oceanog.2005.53

Kudela, R.M., Banas, N.S., Barth, J.A., Frame, E.R., Jay, D.A., Largier, J.L., Lessard, E.J., Peterson, T.D., Woude, A.J.V., 2008. New insights into the Controls and Mechanisms of Plankton Productivity in Coastal Upwelling Waters of the Northern California Current System. Oceanography 21, 46–59. doi:10.5670/oceanog.2008.04

Lafuente, J.G., Ruiz, J., 2007. The Gulf of Cádiz pelagic ecosystem: A review. Prog. Oceanogr. 74, 228–251. doi:10.1016/j.pocean.2007.04.001

Lamont, T., Barlow, R.G., Kyewalyanga, M.S., 2014. Physical drivers of phytoplankton production in the southern Benguela upwelling system. Deep. Sea Res. Part I: Oceanographic Res Papers 90, 1–16. doi:10.1016/j.dsr.2014.03.003

Largier, J.L., Lawrence, C.A., Roughan, M., Kaplan, D.M., Dever, E.P., Dorman, C.E., Kudela, R.M., Bollens, S.M., Wilkerson, F.P., Dugdale, R.C., Botsford, L.W., Garfield, N., Kuebel Cervantes, B., Koračin, D., 2006. WEST: A northern California study of the role of wind-driven transport in the productivity of coastal plankton communities. Deep. Res. Part II Top. Stud. Oceanogr. 53, 2833–2849. doi:10.1016/j.dsr2.2006.08.018

Largier, J.L., 2020. Upwelling Bays: How Coastal Upwelling Controls Circulation, Habitat, and Productivity in Bays. Ann. Rev. Mar. Sci. 12, 20.1-20.33.

Loureiro, S., Newton, A., Icely, J.D., 2005. Microplankton composition, production and upwelling dynamics in Sagres (SW Portugal) during the summer of 2001. Sci. Mar. 69, 323–341. doi:10.3989/scimar.2005.69n3323

Mendes, C.R., Sá, C., Vitorino, J., Borges, C., Garcia, V.M.T., Brotas, V., 2011. Spatial distribution of phytoplankton assemblages in the Nazaré submarine canyon region (Portugal): HPLC-CHEMTAX approach. J. Mar. Syst. 87, 90–101 doi:10.1016/j.jmarsys.2011.03.005.

Moita, M.T., 2001. Estrutura, Variabilidade e Dinâmica do Fitoplâncton na Costa de Portugal Continental. Universidade de Lisboa. (PhD Thesis, in Portuguese). https://www.ipma.pt/pt/publicacoes/pescas/index.jsp?page=teses.xml

Moita, M.T., Oliveira, P.B., Mendes, J.C., Palma, A.S., 2003. Distribution of chlorophyll *a* and *Gymnodinium catenatum* associated with coastal upwelling plumes off central Portugal. Acta Oecologica 24, S125–S132. doi:10.1016/S1146-609X(03)00011-0

Mouriño, H., Barão, M.I., 2010. A comparison between the Linear Regression Model with autocorrelated errors and the Partial Adjustment Model. Stoch. Environ. Res. Risk Assess. 24, 499–511. doi:10.1007/s00477-009-0340-0

Navarro, G., Ruiz, J., 2006. Spatial and temporal variability of phytoplankton in the Golf of Cadiz through remote sensing images. Deep. Sea Res. Part II: Top. Stud. Oceanogr. 53, 1241–1260. doi:10.1016/j.dsr2.2006.04.014

Navarro, G., Caballero, I., Prieto, L., Vázques, A., Flecha, S., Huertas, I.E., Ruiz, J., 2012. Seasonal-to-interannual variability of chlorophyll-*a* bloom timing associated with physical forcing in the Gulf of Cádiz. Adv. Sp. Res. 50, 1164–1172. doi:10.1016/j.asr.2011.11.034

Nogueira, E., Pérez, F.F., Ríos, A.F., 1997. Seasonal Patterns and Long-term Trends in an Estuarine Upwelling Ecosystem (Ría de Vigo, NW Spain). Estuar. Coast. Shelf Sci. 44, 285–300. doi:10.1006/ecss.1996.0119

Oliveira, P.B., Moita, T., Silva, A., Monteiro, I.T., Palma, S., 2009a. Summer diatom and dinoflagellate blooms in Lisbon Bay from 2002 to 2005: Pre-conditions inferred from wind and satellite data. Prog. Oceanogr. 83, 270–277. doi:10.1016/j.pocean.2009.07.030

Oliveira, P.B., Nolasco, R., Dubert, J., Moita, T., Peliz, Á., 2009b. Surface temperature, chlorophyll and advection patterns during a summer upwelling event off central Portugal. Cont. Shelf Res. 29, 759–774. doi:10.1016/j.csr.2008.08.004

Olson, R.J., Sosik, H.M., 2007. A submersible imaging-in-flow instrument to analyze nano- and microplankton: Imaging FlowCytobot. Limnol. Oceanogr. Methods 5, 195–203. doi:10.4319/lom.2007.5.195

Palma, S., Mouriño, H., Silva, A., Barão, M.I., Moita, M.T., 2010. Can *Pseudo-nitzschia* blooms be modeled by coastal upwelling in Lisbon Bay? Harmful Algae 9, 294–303. doi:10.1016/j.hal.2009.11.006

Peliz, A.J., Fiúza, A.F.G., 1999. Temporal and spatial variability of CZCS-derived phytoplankton pigment concentrations off the western Iberian Peninsula. Int. J. Remote Sens. 20, 1363–1403. doi:10.1080/014311699212786.

Peliz, A., Rosa, T.L., Santos, A.M.P., Pissarra, J.L., 2002. Fronts, jets, and counter-flows in the Western Iberian upwelling system. J. Mar. Syst. 35, 61–77. doi:10.1016/S0924-7963(02)00076-3.

Priestley, M.B., 1981. Spectral analysis and time series. New York: Academic Press, London.

R Core Team, 2018. R: A language and environment for statistical computing. R Foundation for Statistical Computing, Vienna, Austria. https://www.R-project.org

Reboreda, R., Cordeiro, N.G.F., Nolasco, R., Castro, C.G., Álvarez-Salgado, X.A., Queiroga, H., Dubert, J., 2014. Modeling the seasonal and interannual variability (2001-2010) of chlorophyll-*a* in the Iberian margin. J. Sea Res. 93, 133–149.

doi:10.1016/j.seares.2014.04.003

Relvas, P., Barton, E.D., 2002. Mesoscale patterns in the Cape São Vicente (Iberian Peninsula) upwelling region. J. Geophys. Res. 107, 3164. doi:10.1029/2000JC000456.

Relvas, P., Barton, E.D., 2005. A separated jet and coastal counterflow during upwelling relaxation off Cape São Vicente (Iberian Peninsula). Cont. Shelf Res. 25, 29–49. doi:10.1016/j.csr.2004.09.006.

Relvas, P., Barton, E.D., Dubert, J., Oliveira, P.B., Peliz, Á., da Silva, J.C.B., Santos, A.M.P., 2007. Physical oceanography of the western Iberia ecosystem: Latest views and challenges. Prog. Oceanogr. 74, 149–173. doi:10.1016/j.pocean.2007.04.021.

Ryan, J.P., Mcmanus, M.A., Kudela, R.M., Artigas, M.L., Chavez, F.P., Doucette, G., Foley, D., Godin, M., Harvey, J.B.J., Marin III, R., Messié, M., Bellingham, J.G., Mikulski, C., Pennington, T., Py, F., Rajan, K., Shulman, I., Wang, Z., Zhang, Y., 2014. Boundary influences on HAB phytoplankton ecology in a stratification-enhanced upwelling shadow. Deep. Sea Res. II 101, 63–79. doi:10.1016/j.dsr2.2013.01.017

Sá, C., D'Alimonte, D., Brito, A.C., Kajiyama, T., Mendes, C.R., Vitorino, J., Oliveira, P.B., Silva, J.C.B., Brotas, V., 2015. Validation of standard and alternative satellite ocean-color chlorophyll products off Western Iberia. Remote Sens. Environ. 168, 403–419. doi:10.1016/j.rse.2015.07.018

Sañé, E., Valente, A., Fatela, F., Cabral, M.C., Beltrán, C., Drago, T., 2019. Assessment of sedimentary pigments and phytoplankton determined by CHEMTAX analysis as biomarkers of unusual upwelling conditions in summer 2014 off the SE coast of Algarve. J. Sea Res. 146, 33–45. doi:10.1016/j.seares.2019.01.007

Santos, M., Oliveira, P.B., Moita, M.T., David, H., Caeiro, M.F., Zingone, A., Amorim, A., Silva, A., 2019. Ocurrence of *Ostreopsis* in two temperate coastal bays (SW iberia): Insights from the plankton. Harmful Algae 86, 20–36. doi:10.1016/j.hal.2019.03.003

Schwing, F.B., O'Farrel, M., Steger, J.M., Baltz, K., 1996. Coastal Upwelling Indices, West Coast of North America, 1946-1995, NOAA Tech. Mem., NMFS-SWFSC-231, 144pp.

Silva, A., Palma, S., Moita, M.T., 2008. Coccolithophores in the upwelling waters of Portugal: Four years of weekly distribution in Lisbon bay. Cont. Shelf Res. 28, 2601–2613. doi:10.1016/j.csr.2008.07.009.

Silva, A., Palma, S., Oliveira, P.B., Moita, M.T., 2009. Composition and interannual

variability of phytoplankton in a coastal upwelling region (Lisbon Bay, Portugal). J. Sea Res. 62, 238–249. doi:10.1016/j.seares.2009.05.001.

SNIRH, 2017. Sistema Nacional de Informação de Recursos Hídricos. Boletim de escoamento. http://snirh.apambiente.pt (accessed 03.11.2017).

Sverdrup, H.U., 1953. On Conditions for the Vernal Blooming of Phytoplankton. J. Cons. Int. Explor. Mer 18, 287–295. doi:10.1093/icesjms/18.3.287

Taboada, F.G., Barton, A.D., Stock, C.A., Dunne, J., John, J.G., 2019. Seasonal to interannual predictability of oceanic net primary production inferred from satellite observations. Prog. Oceanogr. 170, 28–39. doi:10.1016/j.pocean.2018.10.010

Throndsen, J., 1978. Preservation and storage, in: Sournia, A. (Ed.), Phytoplankton Manual: Monographs on Oceanographic Methodology 6. UNESCO, Paris, pp. 69–74.

Tilstone, G., Smyth, T., Poulton, A., Hutson, R., 2009. Measured and remotely sensed estimates of primary production in the Atlantic Ocean from 1998 to 2005. Deep Sea Res. Part II: Top. Stud. Oceanogr. 56, 918–930. doi:10.1016/j.dsr2.2008.10.034

Tsay, R.S., 2010. Analysis of Financial Time Series, 3rd Ed. John Wiley & Sons, New Jersey.

Tweddle, J.F., Gubbins, M., Scott, B.E., 2018. Should phytoplankton be a key consideration for marine management? Mar. Policy 97, 1–9. doi:10.1016/j.marpol.2018.08.026

Utermöhl, H., 1958. Zur Ver vollkommung der quantitativen phytoplankton-methodik. Mitteilung Internationale Vereinigung Fuer Theoretische unde Amgewandte Limnol. 9, 1–38. doi:10.1080/05384680.1958.11904091

Valente, A.S., da Silva, J.C.B., 2009. On the observability of the fortnightly cycle of the Tagus estuary turbid plume using MODIS ocean colour images. J. Mar. Syst. 75, 131–137. doi:10.1016/j.jmarsys.2008.08.008

Vidal, T., Calado, A.J., Moita, M.T., Cunha, M.R., 2017. Phytoplankton dynamics in relation to seasonal variability and upwelling and relaxation patterns at the mouth of Ria de Aveiro (West Iberian Margin) over a four-year period. PLoS One 12, 1–25. doi:10.1371/journal.pone.0177237

Walter, R.K., Armenta, K.J., Shearer, B., Robbins, I., Steinbeck, J., 2018. Coastal upwelling seasonality and variability of temperature and chlorophyll in a small coastal embayment. Cont. Shelf Res. 154, 9–18. doi:10.1016/j.csr.2018.01.002

Wei, W.W.S., 1990. Time Series Analysis - Univariate and Multivariate Methods. Addison-Wesley Publishing Company, Redwood City, California.

Winder, M., Cloern, J.E., 2010. The annual cycles of phytoplankton biomass. Philos. Trans. R. Soc. B Biol. Sci. 365, 3215–3226. doi:10.1098/rstb.2010.0125

Wooster, W.S., Baku, A., McLain, D.R., 1976. The seasonal upwelling cycle along the eastern boundary of the North Atlantic. J. Mar. Res. 34, 131–141.

Chapter 3.

Phytoplankton communities in two sheltered bays in the Iberian upwelling system

Under review as:

Santos, M., Moita, M.T., Oliveira, P.B., Amorim, A.. Phytoplankton communities in two sheltered bays in the Iberian upwelling system. Journal of Sea Research.

Abstract

Several studies have suggested that phytoplankton can accumulate in upwelling shadow areas, where offshore advection is weaker. This study aims to characterize the phytoplankton assemblages and their relationships with key meteorological and oceanographic processes in two Portuguese sheltered bays. The study also aimed to understand how harmful algal blooms (HABs) may be influenced by the local processes. The current work was developed during one year in Lisbon Bay (central-west coast) and in Lagos Bay (south coast), which are located on the upwelling shadow of two prominent headlands. Fortnightly water samples were collected to analyze the phytoplankton community. Several meteorological and oceanographic data were collected *in situ* or extracted from satellite and model-derived products, and multivariate analyses of phytoplankton community structure were performed using PRIMER-E with PERMANOVA add-on software. In both bays, the results indicate a bi-modal pattern in phytoplankton biomass, as well as phytoplankton concentration maxima associated with high diatom abundances between spring and late-summer. In Lagos Bay, higher dinoflagellate abundances were observed from spring to autumn, while in Lisbon Bay higher concentrations were only recorded from late-summer to autumn. Coccolithophores were a frequent group in Lisbon Bay all year round, but in Lagos Bay it was the least dominant group. The phytoplankton community structure showed significant spatial and seasonal differences. The community succession, although with differences between the bays, indicates the existence of four "biological seasons" in Lisbon Bay and in the offshore site studied in Lagos Bay. However, the beach station in Lagos Bay is a particular environment with only three "biological seasons", with summer and autumn merged as only one season. Differences in HAB species/groups were also observed between the bays. Higher HAB species concentration and a longer period of occurrence characterized Lagos Bay. *Dinophysis acuta* was the only species that causes greater concern in Lisbon Bay, and the benthic HABs group is particularly relevant at the nearshore station in Lagos Bay.

Keywords: Phytoplankton assemblage; Harmful species; Upwelling region; Oceanographic conditions; SW Iberia

3.1. Introduction

Marine phytoplankton is responsible for almost half of global net primary production (Field et al., 1998), and has an important role in sustaining the aquatic food webs, supporting the production of higher trophic levels. Phytoplankton community structure and abundance in temperate coastal areas are characterized by high spatial and temporal variability. A variety of complex and dynamic environmental drivers work as limiting factors or forcing mechanisms of phytoplankton growth and species selection, namely nutrients, light, temperature, salinity and turbulence (Margalef, 1978; Smayda et al., 2004; Tweddle et al., 2018).

Phytoplankton shows some of the highly productivity levels of the world in nutrient-rich upwelling regions (Hill et al., 1998). These regions are denominated as Eastern Boundary Upwelling Ecosystems (EBUEs). In upwelling regions, there is an apparent paradox of productivity (Largier et al., 2006). Alongside with the favorable conditions for phytoplankton growth provided by nutrient enrichment, the developing populations are subjected to reduced light through vertical mixing and offshore export of near-surface phytoplankton due to strong winds (Largier et al., 2006). In coastal upwelling regions, topography and coastline irregularities, such as capes and bays, produce variations in coastal wind, alongshore currents, as well as on chemical and biological responses (Chavez and Messié, 2009; Largier, 2020). The bays may act as upwelling shadow areas where weaker horizontal advection and retentive circulation patterns are frequently observed in association with higher nearshore phytoplankton biomass (see Largier et al., 2020 for a review). Strong gradients are formed between the new upwelled waters off a cape and these protected upwelling shadow waters (Chavez and Messié, 2009). The "upwelling paradox" mentioned-above seems to be partially resolved in bays (Largier et al., 2006). As bays are stratified regions, maintain high light levels for phytoplankton growth, and the circulation patterns here observed act as retention zones for plankton in the region (Largier et al., 2006). These features were observed in several upwelling regions, worldwide (Largier, 2020). These retention areas are more susceptible to phytoplankton bloom development, including the occurrence of harmful algal blooms (HABs) (Kudela et al., 2008; Moita et al., 2003; Pitcher et al., 2010, 2018), which may affect human health and marine resources, and result in important economic losses for aquaculture and tourism (Kudela et al., 2005; Pitcher et al., 2010, 2018).

Among the world's EBUEs, the Iberia/Canary Current System (ICCS) is one of the least studied (Chavez and Messié, 2009). Off west Iberia (between 37º N and 41º N) the upwelling

is seasonal with maxima recorded in summer (e.g. Fiúza et al., 1982), and is weaker than the observed further south, off west Africa (between 10º N and 25º N) (Chavez and Messié, 2009). The Portuguese continental coast is located in the northeastern limit of the ICCS and is influenced by seasonal upwelling. It is characterized by several prominent topographic features, like headlands and submarine canyons (Relvas et al., 2007), as well as by several mesoscale structures, such as fronts, jets, upwelling filaments and countercurrents (Haynes et al., 1993; Peliz et al., 2002; Relvas et al., 2007; Relvas and Barton, 2005). In this region, important shadow areas, with different circulation patterns downstream of prominent capes, have already been described associated with the separation of the coastal upwelling jet rooted at Cape Roca, namely in Lisbon and Setúbal Bays (Oliveira et al., 2009a). In Lisbon Bay, the patterns of chlorophyll a, as well as HABs distribution, were asymmetric about the upwelling center, with the highest phytoplankton abundances observed at the leeward side of the filaments (Moita et al., 2003; Oliveira et al., 2009a). Setúbal Bay is characterized by a persistent stratified warmer water pool. In this bay, the development of a harmful dinoflagellate bloom was related to particular conditions, when the upwelling plumes rooted at Capes Roca and Cape Espichel were unusually displaced shoreward into Setúbal Bay (Amorim et al., 2004). These bays are considered as wide-open bays with a marked step (*i.e.* headland) at one end, where winds tend to separate from the coast (Largier, 2020). According to this author, the main features of this type of bays are the elevation of water level in the upwelling shadow and warm and stratified water at the surface. The circulation in the bay tends to be weakly cyclonic, being possible to observe onshore advection at mid-bay. Cape S. Vicente is a major coastline discontinuity, which separates the West coast from the Southern Portuguese coast. This Cape is a major upwelling center when north winds are predominant (Relvas and Barton, 2002), spreading the cold upwelled water along the southern coast shelf break and slope (Relvas et al., 2007). Here, similar features of wide-open bays with a marked step at one end are observed, including an offshore band of wind curl, a tendency for poleward flow nearshore, and an upwelling-sheltered region (Largier, 2020). Lagos Bay, located in this region is an example of a sheltered bay where harmful blooms of benthic dinoflagellates genus *Ostreopsis*, observed since 2011, have been associated with particular oceanographic features. In this bay, *Ostreopsis* concentrations were related to sea surface temperatures and occurred after a period of more than two weeks of low sea state, followed by short-time events of onshore wind and moderate waves (Santos et al., 2019).

Lisbon Bay is relatively well studied in terms of phytoplankton communities. It has been studied since 1948 (e.g. Silva, 1949; Moita, 2001), and in 2001 a long-term time series was initiated to better understand phytoplankton dynamics (Silva et al, 2008, 2009; Palma et al. 2010). Phytoplankton communities in Lagos Bay are much less known, having been studied only in the 80s (Moita, 2001). In the last 20 years, studies of phytoplankton community structure have been performed from 5 Km east from Cape S. Vicente and about 20 Km west from Lagos Bay (Danchenko et al., 2019; Goela et al., 2014, 2015; Loureiro et al., 2005 2011). Most of these studies addressed the zonal and meridional continental coasts separately.

The main objective of the present work is to understand, at short latitudinal scales, which are the main meteorological and oceanographic drivers shaping phytoplankton community structure and dynamics in wide-open bays under the influence of coastal upwelling. To achieve this goal, phytoplankton communities from Lisbon and Lagos Bays, located in the shadow of prominent capes off West Iberia, were studied during 2015 using a comparative approach. Due to the regional economic importance of HABs in both bays, and due to the recent recurrent occurrence of *Ostreopsis* in Lagos Bay, the study also focused on understanding how HABs may be influenced by the local environmental settings.

3.2. Material and methods

3.2.1. Study area

The study was conducted in two geographically distinct coastal bays, located on the West and South Portuguese continental coast, respectively, Lisbon and Lagos Bays (Fig. 3.1). Lisbon Bay (LisB) is located SE of Cape Roca (CR), under the strong influence of seasonal upwelling and of the Tagus river flow. Between spring and early autumn, under steady northerly winds, upwelling occurs and a recurrent upwelling filament, rooted at CR, extends southward or westward of the Bay (Moita et al., 2003; Oliveira et al., 2009b). The Tagus river, with a mean annual flow of 10 km^3 (SNIRH, 2017), is the main source of freshwater into the bay (Valente and da Silva, 2009) and is an important source of nutrients, with higher concentrations observed during winter (Cabrita et al., 2015). The sampling site, Cascais, is located about 15 km from CR (Fig. 3.1), at the entrance of a recreational marina in the north side of Lisbon Bay (38°41’36.82’’N, 9°24’52.93’’W), and about 10 km west of Tagus mouth.

Lagos Bay (LagB) is at the SW limit of Iberia and is located to the east of a major upwelling center under the influence of north winds, Cape S. Vicente (CSV). On the South coast, during the summer, a westward warm coastal countercurrent episodically flows from the Gulf of Cádiz to Lagos Bay (Oliveira et al., 2016) and under favorable conditions can turn northward around CSV (Relvas and Barton, 2002, 2005; Relvas et al., 2007). Although weaker, occasional upwelling events may occur in the S coast throughout the year under prevailing westerly winds. Strong episodes of westerly winds may reverse the above-mentioned summer alongshore flow (Relvas and Barton, 2002). Upwelling is the main source of nutrients in the region of CSV (Cravo et al., 2010). The Arade river, located eastern of LagB, has a mean annual flow of three orders of magnitude lower than Tagus river, 0.05 km^3 (SNIRH, 2017). In LagB there were two sampling sites, both located 35 km to the east of CSV, Beach and Offshore (Fig. 3.1). The site referred to as Beach (37°5'28.54" N, 8°40'8.48" W) is located in D. Ana beach, a sheltered sandy beach with rock formations, and the referred to as Offshore (37°4'12.31''N, 8°41'0.44''W) is located in Porto de Mós at 1 nautical mile from the coast.

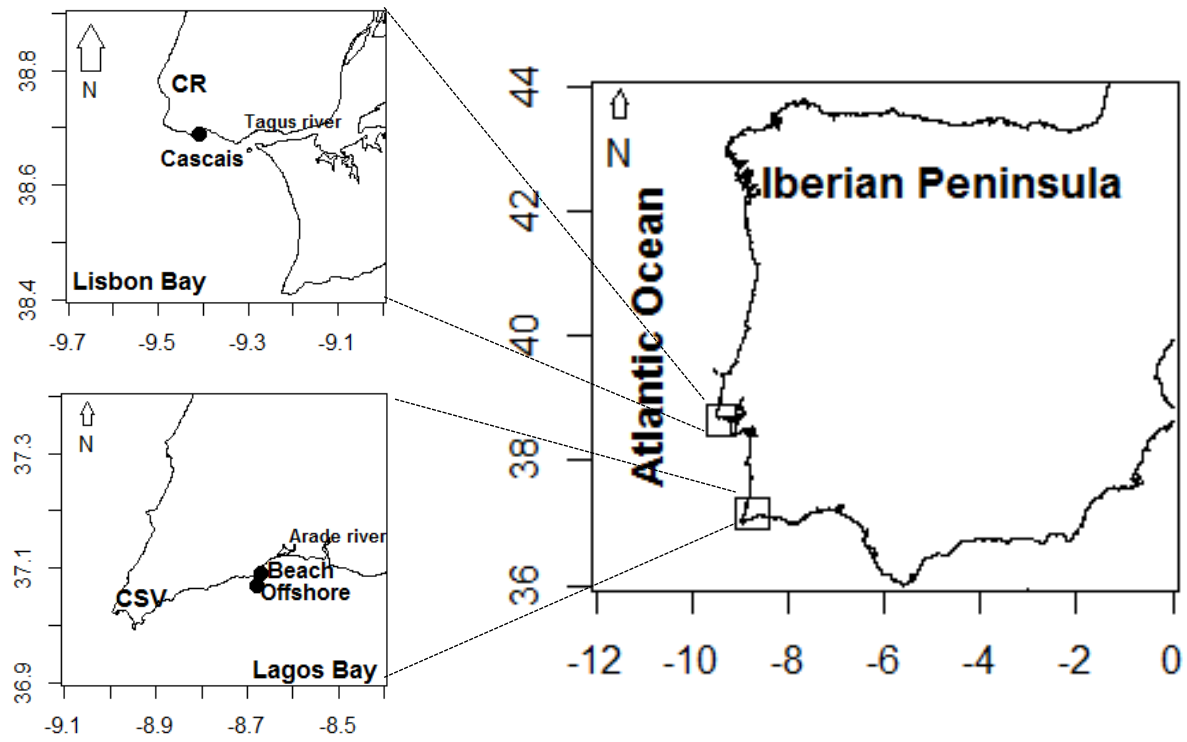

Fig. 3.1. Map of the study area. Circles identify the location of the sampling stations, Cascais in Lisbon Bay, and Beach and Offshore in Lagos Bay.

3.2.2. Sampling strategy and laboratory procedures

To analyze the phytoplankton community, fortnightly water samples were collected in 2015, under the National Monitoring Program of Harmful Algal Bloom species (HABs) led by IPMA, I.P. - Instituto Português do Mar e da Atmosfera (National Institute for the Sea and Atmosphere). In LisB, integrated samples of the total water column (0-7 m depth) were collected with a hose, always one hour before high tide to reduce the influence of Tagus river and to optimize the direct influence of coastal waters on this nearshore station. In LagB-Beach, water samples were collected at the surface in the naturally mixed surf zone, and in LagB-Offshore, where the bottom depth is around 30 m, the samples were collected at 10 m depth. LisB samples were field fixed with formaldehyde neutralized with hexamethylenetetramine to a final concentration of 0.4%, as part of a long-term monitoring site. In LagB, samples were collected within the national HABs monitoring program and preserved with Lugol's solution (Throndsen, 1978). Phytoplankton identification and quantification, in cells L^{-1} (or in colonies L^{-1} in the case of *Chaetoceros socialis*, cf. *Delphineis surirella*, *Thalassiosira subtilis* and *Phaeocystis* spp.), were carried out by settling 50 mL of water samples following the Utermöhl method (Utermöhl, 1958). In the case of uncertainty in the identification of some phytoplankton species or genus, it was decided to group different species/genus in taxonomic entities (e.g. *Amphora/Halamphora, Amphidinium/Oxytoxum, Coronosphaera/Syracosphaera*, see Table B.3.1 in appendix for more examples). Samples were analyzed with an inverted microscope equipped with phase contrast and bright field illumination (Leica DMi8) at a magnification of 200x and 400 x. Phytoplankton were divided in diatoms, dinoflagellates, coccolithophores and "others". The group named as "others" is composed by euglenophytes, cryptophytes, prasinophytes, *Dictyocha fibula*, *Octactis octonaria*, *Octactis speculum*, cf. *Heterosigma akashiwo* and *Phaeocystis* spp.. The taxonomic composition of phytoplankton was identified using the descriptions in Dodge (1982), Hoppenrath et al. (2009), Peragallo & Peragallo (1908), Schiller (1937) and Tomas (1997). Some of the names used in these references have been changed. In the present work was made an effort to use the currently accepted taxonomic names available on the AlgaeBase database (Guiry and Guiry, 2020) (https://www.algaebase.org/).

3.2.3. Ocean color, meteorological and oceanographic (MetOc) data

Weekly-mean Ocean Color data provided by Copernicus-GlobColour (level 4, at 4 km resolution) were extracted from CMEMS (Copernicus Marine Environment Monitoring Service) to both studied Bays. *In situ* surface temperature data were collected weekly using a multi-parameter probe (YSI Model 30) in LisB and LagB-Beach. In LagB-Offshore, the temperature was recorded daily at 3 m depth, using a Temperature Data Logger (TidbiT v2/Pro v2, Onset). Daily estimates from the Multi-scale Ultra-high Resolution (MUR) sea surface temperature (SST) product, with 0.01º spatial resolution (~1 km), were also obtained on PODAAC (Physical Oceanography Distributed Active Archive Center) of Jet Propulsion Laboratory of NASA (National Aeronautics and Space Administration). The 8-day Mixed Layer Depth (MLD) data were obtained from the Ocean Productivity group of Oregon State University. Maximum MLD values were limited to maximum bathymetry in the study area. Due to problems detected in river runoff estimates available on SNIRH ("Sistema Nacional de Informação de Recursos Hídricos") database (https://snirh.apambiente.pt/) for the year 2015 in Tagus river, runoff data was not considered in the present study.

Daily surface Photosynthetically Available Radiation (PAR), total precipitation, surface wind components (U_{10} and V_{10}) and significant wave height (SWH) were retrieved from the European Centre for Medium-Range Weather Forecasts (ECMWF). The wind stress components were computed using the quadratic drag law $\tau_{x,y} = \rho_a\ Cd\ |v|\ U_{10},V_{10}$; where $|v|$ is the wind speed (m s^{-1}), U_{10} and V_{10} are respectively the east-west and north-south 10 m wind components (m s^{-1}), ρ_a is the air density (1.22 kg m^{-3}) and Cd is the drag coefficient (0.0013). Upwelling indices were estimated by the components of the Ekman mass transport M_x and M_y, computed from the wind stress components as $M_x = \tau_y/f$ and $M_y = -\tau_x/f$. The upwelling indices are expressed as a volume transport in cubic meters per second per 100 meters of coastline ($m^3\ s^{-1}$ /100 m), which is equivalent to metric tons/s/100 m coastline (Schwing et al., 1996). With this definition, the indices preserve the same sign convention as the wind components, therefore, negative values indicate upwelling conditions along the western (M_x) and southern coasts (M_y). The terms zonal and meridional transport will be used in this study when considering, respectively, M_x and M_y. Wind intensity as $(U_{10}^2 + V_{10}^2)^{0.5}$ was calculated from the wind components to obtain the wind turbulent entrainment (W), or turbulence, which is proportional to the cube of wind velocity (Kato and Phillips, 1969).

The grid-point selected to extract Chl-*a*, SST and MLD time series was at 4 nautical miles from the coast in LagB and at 8.5 nautical miles from the coast in LisB. Wind stress components, PAR, precipitation, and SWH time series were extracted from the nearest grid point to the coast. See Santos et al. (submitted) (Chapter 2, this thesis) for more details about the point selected to each dataset.

3.2.4. Data processing and statistical analysis

To analyze the intra-annual variation in phytoplankton community structure in space and time (composition and abundance), and the associated meteorological and oceanographic variables, multivariate analyses were performed using PRIMER-E (version 6.1.13) with PERMANOVA (version 1.0.3) add-on software (Anderson et al., 2008; Clarke and Gorley, 2006). Phytoplankton community and MetOc data were considered according to each site (LisB, LagB-Offshore and LagB-Beach) and according to the meteorological seasons (winter, spring, summer and autumn). Unidentified species of diatoms, dinoflagellates and coccolithophores, which accounted for 6 % of overall abundance, were not considered in the multivariate analyses. In addition, all taxa that occurred in less than 5 % of the 80 samples were also excluded. Only 60 % of the 228 identified taxonomic entities were considered in these analyses. To reduce the disproportionate influence of highly abundant taxa, phytoplankton abundances were log (x+1) transformed. In the environmental matrix, the following variables were considered: PAR, SST (*in situ*), turbulence, M_x, M_y, SWH, MLD and precipitation. To study the spatial and temporal variability of phytoplankton community, based on a Bray-Curtis resemblance matrix, a permutational analysis of variance (PERMANOVA) was performed with 999 permutations and the two fixed factors (site and season) were evaluated separately. A Principal Coordinates Analysis (PCO) was used to visualize the multivariate patterns of the phytoplankton composition (Anderson et al., 2008), as well as to explore the relationship between environmental variables and phytoplankton community structure. A significant level of $\alpha = 0.05$ was considered in the analyses.

3.3. Results

3.3.1. Meteorological and oceanographic characterization of Lisbon and Lagos Bays

Figure 3.2 presents meteorological (PAR, W, M_x, M_y and Precipitation) and oceanographic (SST, MLD and SWH) data recorded in 2015 for Lisbon and Lagos Bays. The PAR showed the same pattern in both Bays (Fig. 3.2 A and B), with minima in winter and maxima recorded from May to September. SST pattern showed differences between the bays. In LisB, SST begins to increase in April, reaching and maintaining temperatures around 17 ºC from June to the end of November, when it starts to decrease (Fig. 3.2 C). In LagB, temperature values were 1 ºC warmer (around 18 ºC) and were recorded from one month earlier (May), although also until November (Fig. 3.2 D). *In situ* SST data showed a high similarity between the weekly data recorded in LisB and satellite estimates (r = 0.94) (Fig. 3.2 C). In LagB the daily data collected offshore match better with satellite estimates (r = 0.91) than with the data recorded weekly in the beach (r = 0.86), where frequently higher temperature values were observed (Fig. 3.2 D). In this bay, important differences were observed during summer between SST measured offshore and estimated by satellite (Fig. 3.2 D), often coinciding with some upwelling events (c.f. Fig. 3.2 F).

The wind turbulence (W) was higher (above 1000 $m^3 s^{-3}$) in both Bays from January to March and in May (Fig. 3.2 E and F). In the remaining period, turbulence was estimated below 1000 $m^3 s^{-3}$. Two marked events (above 2500 $m^3 s^{-3}$) were observed in LisB at the end of March and in May. Zonal transport data (M_x), which indicates upwelling conditions along the N-S oriented coastline, showed that 2015 was dominated by upwelling favorable conditions in both bays from January until October, except in April. From October to December dominated the downwelling favorable conditions (Fig. 3.2 G and H). During the downwelling favorable period, a strong upwelling event was observed in the second half of November. A difference observed between the bays was the occurrence of several stronger upwelling and downwelling events in LagB than in LisB (Fig. 3.2 G and H). Highly contrasting results were observed in meridional transport (M_y), which indicates upwelling conditions along the E-W oriented coastline. This variable was not relevant in LisB (Fig. 3.2 I), with transport around 1000 $m^3 s^{-1}$/100 m recorded only a few days in winter (January and late-December). In LagB an upwelling dominant period was observed from mid-April to end-September (Fig. 3.2 J). In the remaining period, conditions alternated between downwelling and upwelling favorable conditions.

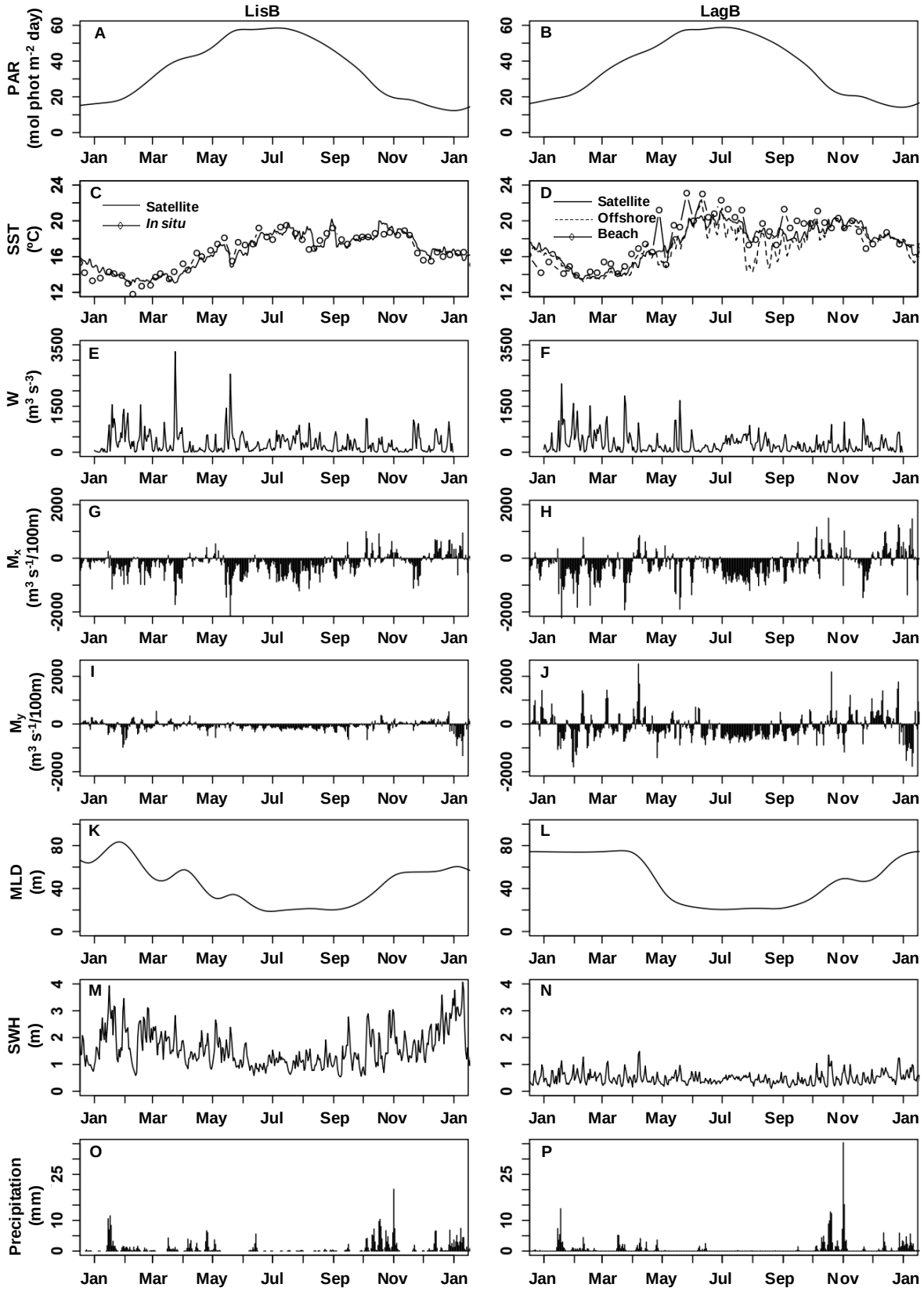

Fig. 3.2. Meteorological and oceanographic variables time series in LisB (left panel) and in LagB (right panel) during 2015. A/B - Photosynthetically available radiation (PAR, mol phot m^{-2} day); C/D – Sea surface temperature (SST, ºC); E/F – Turbulence (W, m^3 s^{-3}); G/H - Zonal mass transport (M_x, m^3 s^{-1} /100 m); I/J - Meridional mass transport (M_y, m^3 s^{-1} /100 m); K/L – Mixed layer depth (MLD, m), M/N – Significant wave height (SWH, m) and O/P – Precipitation (mm).

Mixed layer depth showed a different pattern in the two bays. In LisB, MLD showed a steady decrease from January to the end of May (Fig. 3.2 K). In LagB a fully mixed water column was observed until March, and a sharp decrease of MLD occurred from March to the end of April, 1-month earlier than in LisB (Fig. 3.2 L). In both bays, the period with shallow MLD values ended in October (Fig. 3.2 K and L). Regarding sea wave height, Lag B was characterized by SWH generally below 1 m, contrasting with LisB where SWH was only occasionally below 1 m (Fig. 3.2 M and N). In LisB, with the exception of summer months, SWH was frequently above 2 m, reaching 4 m in winter. The studied year was characterized generally by low precipitation levels in both bays (Fig. 3.2 O and P). In both bays, the months with higher precipitation were January and especially October.

3.3.2. Intra-annual variation of phytoplankton

During 2015 two main periods of high phytoplankton biomass were observed in both bays, one in spring and the other in summer (Fig. 3.3 A and B). The spring bloom, although showing a decrease during April in both bays, occurred for a longer period in LisB (from March to late-May) than in LagB (from March to late-April). The summer bloom contrasted with the spring bloom and was 1-month longer in LagB (from July to September) than in LisB (from July to August). While in LisB maxima Chl-*a* was almost the same in both blooms (3.0-3.5 mg m^{-3}), in LagB higher Chl-*a* concentration was recorded in summer (3.5 mg m^{-3}) than in spring (2.0 mg m^{-3}).

Phytoplankton abundance showed that, similarly to Chl-*a*, two main periods of high concentration (spring and summer) were observed in LisB and in LagB (Fig. 3.3 C, D and E). During the studied period, LagB reached maxima values of phytoplankton concentration six times greater than LisB. These maxima were about 1.5 x 10^6 cell L^{-1} in March (LagB-Offshore) and in July (LagB-Beach) and corresponded, respectively, to a bloom of a small flagellate identified as a coccolithophore holococcolith life-stage (cf. *Coccolithus pelagicus* var *braarudii*) and a bloom of the diatom *Skeletonema marinoi* (Fig. 3.3 D and E).

The three main phytoplankton groups (diatoms, dinoflagellates and coccolithophores), accounted on average for more than 90 % of total identified phytoplankton. Diatoms were the most abundant group of the total phytoplankton concentration at the three sampling sites (Fig. 3.3 F, G and H). This group showed higher abundances in LagB than in LisB. The maxima diatom concentrations were 1.4 x 10^6 cell L^{-1} in LagB-Beach, 5.5 x 10^5 cell L^{-1} in LagB-

Offshore and 3.0 x 10^5 cell L^{-1} in LisB. Dinoflagellates, with a much lower concentration than diatoms, showed high concentration levels in summer and autumn in the three sites, starting in August at LisB, in July at LagB-Offshore and earlier, mid-June, at LagB-Beach (Fig. 3.3 I, J and K). An earlier dinoflagellates peak was recorded in spring (April) in LagB-Offshore, together with diatoms, which was not observed in the other stations. In August, this group exceptionally dominated 90 % of the total community in LagB-Offshore, being composed mainly by species of *Scrippsiella*, *Gymnodinium*, *Gonyaulax* and other unidentified species of small size (< 15 µm), while diatoms dominated in LagB-Beach and in LisB. Coccolithophores were more frequent in LisB but more abundant in LagB. In LisB, this group reached concentrations around and above 1.0 x 10^4 cell L^{-1} during most of the year and the maximum was recorded at the end of August (5.0 x 10^4 cell L^{-1}) (Fig. 3.3 L). In LagB, at both stations, main peaks were observed in March and in September/October (Fig. 3.3 M and N). However, the winter/spring coccolithophores bloom was much higher in LagB-Offshore than in LagB-Beach, reaching 1.2 x 10^6 cell L^{-1} in the former (Fig. 3.3 M). This very high peak recorded in LagB-Offshore corresponded to 99.5 % of total coccolithophores abundance and was due to a bloom of the holococcolith life-stage of *Coccolithus pelagicus* var *braarudii*, which was not observed in LagB-Beach. The group named as "others" resulted in small abundances recorded frequently in LisB (Fig. 3.3 O) and in LagB-Offshore (Fig. 3.3 P). While in LagB-Beach, this group reached higher concentrations during all summer, reaching a maximum of 9.0 x 10^4 cell L^{-1} in August (Fig. 3.3 Q), in Lag-B-Offshore cell concentrations were lower and the maximum was observed in October (6.0 x 10^4 cell L^{-1}). The lowest concentrations were recorded in LisB, reaching only 1.0 x 10^4 cell L^{-1} in August.

3.3.3. Characterization of phytoplankton assemblages

Overall, Lagos Bay showed a higher taxonomic diversity than Lisbon Bay, with 167 taxonomic entities identified at LagB-Offshore *versus* 160 in LisB (Table B.3.1 in appendix). Diatoms were the only group that had a higher diversity in Lisbon than in Lagos Bay. There were some common features between the bays (Table B.3.1 in appendix). The most common diatoms recorded during the sampling period (in frequency of occurrence) were the pennate *Cylindrotheca closterium,* the chain-forming centric species *Chaetoceros* spp., the chain-forming pennate species *Pseudo-nitzschia delicatissima* group, and also several pennate species of genus *Pleurosigma/Gyrosigma*, *Navicula* and *Nitzschia*. The most recorded

dinoflagellates in the three studied sites were species of *Scrippsiella*, *Gyrodinium*, *Protoperidinium*, *Gymnodinium* and *Ceratium*. Coccolithophores were dominated by the group *Emiliania huxleyi/Gephyrocapsa* spp., followed by *Coronosphaera*/*Syracosphaera* group. Within the group "others", the assemblage was composed mainly by small cryptophytes and by euglenophytes in LagB-Beach and in LagB-Offshore, while only euglenophytes dominated in LisB.

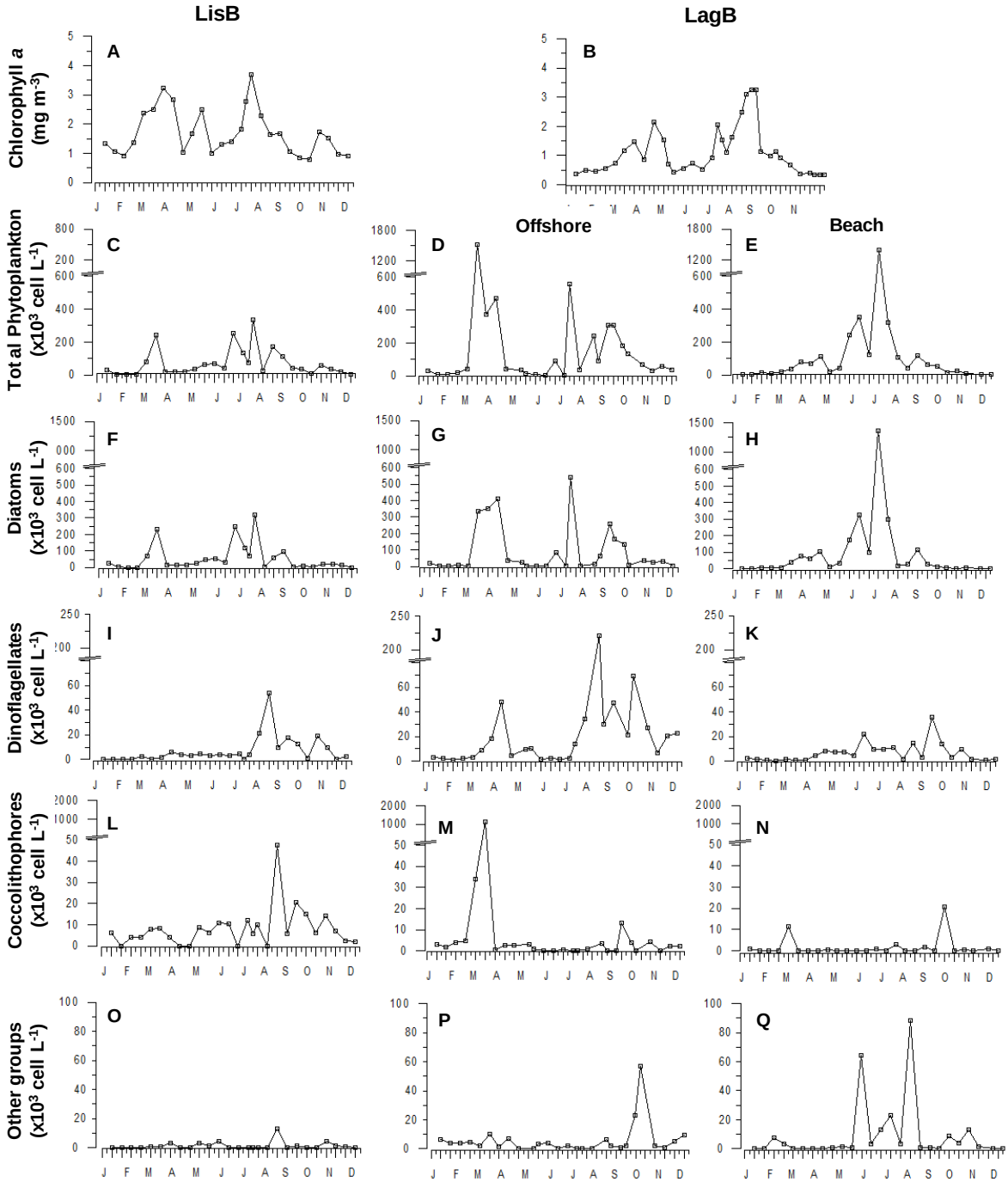

Fig. 3.3. Fortnightly data during 2015 in LisB, LagB-Offshore and LagB-Beach. A/B - Chlorophyll *a* concentration (mg m^{-3}); C/D/E - total phytoplankton concentration (cells L^{-1}), F/G/H - total diatom concentrations (cells L^{-1}), I/J/K - total dinoflagellate concentrations (cells L^{-1}); L/M/N - total coccolithophore concentrations (cells L^{-1}), and O/P/Q – total concentration of other phytoplankton groups (cells L^{-1}).

3.3.3.1. Spatial differences

To analyze the statistical differences of phytoplankton assemblage between the three studied sites, a PERMANOVA analysis was performed. The differences between the bays were analyzed by comparing Lisbon Bay with the offshore station in Lagos Bay (*i.e.* LisB *vs* LagB-Offshore in Table 3.1 and Fig. 3.4). To better understand phytoplankton assemblages within Lagos Bay, the two studied sites within this bay were also analyzed (*i.e.* LagB-Offshore *vs* LagB-Beach in Table 3.1 and Fig. 3.5).

Lisbon Bay *versus* Lagos Bay

The PERMANOVA analysis of the phytoplankton assemblages revealed highly significant differences between Lisbon and Lagos Bays ($p < 0.01$, Table 3.1). The spatial differences in phytoplankton community structure were better observed when considering the axis 1 and axis 3 of the PCO analysis (Fig. 3.4), which together explained around 30 % of total phytoplankton variability. Lisbon Bay was clearly separated from LagB-Offshore by axis 3, with LisB on the positive side and LagB on the negative side (Fig. 3.4 A and B). The species *Leptocylindrus minimus*, *Chaetoceros* spp. and *Chaetoceros curvisetus* were more correlated with LisB assemblages (Fig. 3.4 A). Besides these species, *Dinophysis acuta*, *A. glacialis*, *Ceratium tripos*, *D. pumila* and euglenophytes also contribute more to LisB community than to LagB (not shown). The taxa that contributed more to LagB-Offshore phytoplankton structure were the small cryptophytes and several dinoflagellates, such as *Amphidinium* spp., *Karenia mikimotoi* and *Gyrodinium fusiforme* (Fig. 3.4 A), and *Cochlodinium* spp., *Diplopsalis* group, *Karenia* spp. and *Gymnodinium* spp. (not shown). In terms of meteorological and oceanographic variables, the ones that better explained the differences observed in the phytoplankton community between the studied bays were the SWH and MLD (Fig. 3.4 B).

Lagos Bay: Offshore *versus* Beach

The PERMANOVA analysis also revealed significant differences between the offshore and the nearshore stations within Lagos Bays ($p < 0.01$, Table 3.1). The PCO axes 1 and 3, together, explained around 30 % of total phytoplankton variability in this bay (Fig. 3.5), and

the communities of LagB-Offshore were separated from LagB-Beach assemblages by axis 3 (Fig. 3.5). Many dinoflagellates (e.g., *Amphidinium* spp., *Gymnodinium* spp., *Prorocentrum dentatum*, *Karenia mikimotoi*) and coccolithophores (e.g *E. huxleyi/Gephyrocapsa* spp. and *Ophiaster* spp.) highly contributed to the LagB-Offshore community structure. In turn, benthic, epiphytic and/or tycoplanktonic species were the ones that characterized LagB-Beach assemblages (e.g., *Nitzschia longissima*, *Protoperidinium quinquecorne*, *Coolia* spp., *Prorocentrum lima* and *Climacosphenia* spp.). In terms of MetOc drivers, it was not possible to test the different correlations observed between LagB-Offshore and LagB-Beach since the spatial resolution of the available data cannot distinguish these two sites.

Table. 3.1. Summary of results of permutational univariate analysis of variance (PERMANOVA) of the phytoplankton assemblages between Lisbon and Lagos Bays (LisB *vs* LagB-Offshore) and between the two studied sites in Lagos Bay (Offshore *vs* Beach). PERMANOVA significant results are presented in bold ($p < 0.05$).

Study site (Global test)	**df**	**SS**	**MS**	**F**	***p***	**Unique perms**
LisB vs LagB (Offshore)	1	12571	12571	8.400	<**0.01**	998
LagB (Offshore vs Beach)	1	6373	6373	4.098	<**0.01**	999

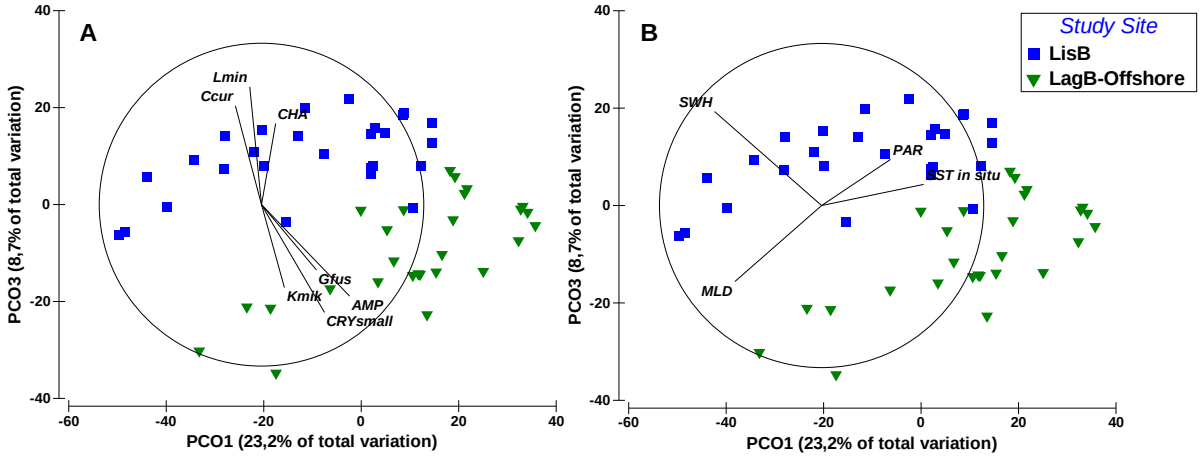

Fig. 3.4. Principal coordinates analysis (PCO) plots of phytoplankton community structure between Lisbon (LisB) and Lagos (LagB-Offshore) Bays, based on Bray-Curtis resemblance matrix. A shows the most significant taxa (abbreviated according to Table B.3.1 in appendix), and B shows the meteorological and oceanographic drivers with correlations above 0.4.

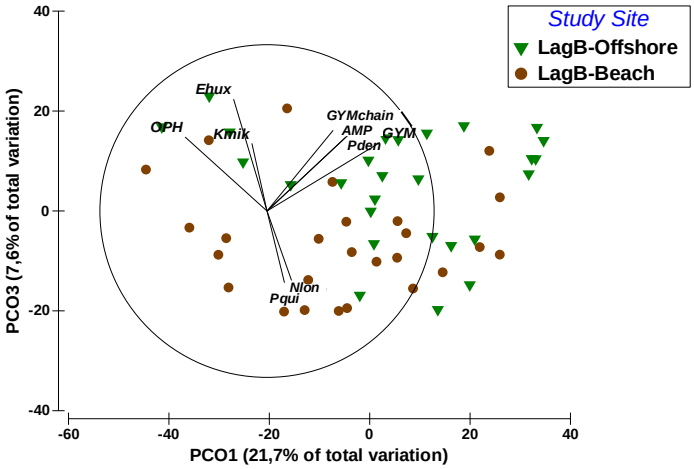

Fig. 3.5. Principal coordinates analysis (PCO) plots of phytoplankton community structure between the two sampling sites analyzed in Lagos Bay (LagB-Offshore and LagB-Beach), based on Bray-Curtis resemblance matrix. The most significant taxa are shown according to the abbreviations in Table B.3.1 in appendix.

3.3.3.2. Temporal differences

To investigate the temporal variation in the different studied sites, a PERMANOVA analysis was performed considering the four meteorological seasons: winter, spring, summer and autumn. The analyses revealed highly significant seasonal differences in the three studied sites (p < 0.01, Table 3.2). The seasonal pair-wise comparisons showed that, with the exception of summer/autumn in LagB-Beach, all the other pairs had significant differences between each other (p < 0.05, Table 3.3). This result indicated the existence of four biological seasons in LisB and in LagB-Offshore, but only three seasons in LagB-Beach (*i.e.* winter, spring and summer/autumn).

Table. 3.2. Summary of results of PERMANOVA of the phytoplankton abundance to each studied site when considering the factor Season. PERMANOVA significant results are presented in bold (p < 0.05).

Season (Global test)	**df**	**SS**	**MS**	**F**	***p***	**Unique perms**
LisB	3	15577	5192	3.254	<**0.01**	998
LagB-Offshore	3	14152	4717	3.375	<**0.01**	996
LagB-Beach	3	14180	4727	2.748	<**0.01**	999

Table. 3.3. Summary of results of pair-wise comparisons considering the factor Season for each studied site. Significant results are presented in bold ($p \leq 0.05$) and non-significant results in italics.

Season (Pair-wise tests)	**LisB**	**LagB Offshore**	**LagB Beach**
Winter, Spring	<**0.01**	**0.03**	<**0.01**
Winter, Summer	<**0.01**	<**0.01**	<**0.01**
Winter, Autumn	<**0.01**	<**0.01**	<**0.01**
Spring, Summer	**0.01**	<**0.01**	<**0.01**
Spring, Autumn	**0.01**	<**0.01**	**0.01**
Summer, Autumn	**0.04**	<**0.01**	*0.09*

The first two axes of PCO analysis explained between 35 % (LagB-Beach) and 42 % (LisB and LagB-Offshore) of the phytoplankton communities' temporal variability (Fig. 3.6). In LisB (Fig. 3.6 A and B), the different 4-seasons were separated mainly by axis 1, with winter in the negative values of the axis, summer in the positive values, and spring and autumn in an intermediate location. In this bay, the winter community was mainly composed by the coccolithophore *Coccolithus pelagicus* and by benthic or tycoplanktonic diatoms (e.g., *Amphora* spp., *Coscinodiscus* spp., *Grammatophora serpentine*, *Trieres mobiliensis*, *Actinoptychus senarius*, *Licmophora* spp. and *Surirella* spp., Fig. 3.6 A). This is in good agreement with the identified main MetOc drivers associated with water column mixing (SWH and MLD, Fig. 3.6 B). The summer and autumn seasons were characterized by a diverse dinoflagellate assemblage (e.g., *Torodinium robustum*, *Protoperidinium* spp., *Gyrodinium* spp., *D. acuta*, *Ceratium fusus* and *Scrippsiella* spp.) and by the diatom genus *Rhizosolenia* (Fig. 3.6 A). The MetOc drivers that better explain the summer/autumn communities were SST and PAR (Fig. 3.6 B), which presented the highest values during this period (cf. Fig. 3.2). In this bay, the spring showed a weak correlation with both upwelling indexes (< 0.4), but the phytoplankton community was dominated by several chain-forming diatoms (e.g. *Detonula pumila*, *Guinardia striata* and *Chaetoceros* spp.) (Fig. 3.6 A). The same was also observed in a few autumn samples.

In LagB-Offshore (Fig. 3.6 C and D), the PCO axis 1 separated winter and spring from summer and autumn communities. Several coccolithophores (e.g., *Ophiaster* spp., *C. pelagicus* and *E. huxleyi/Gephyrocapsa* spp.), centric and pennate diatoms (e.g., *Thalassiosira* spp., *Ditylum brightwellii*, *Licmophora* spp., *Thalassionema nitzschioides* and *Navicula* spp.) and euglenophytes characterized the winter community (Fig. 3.6 C). The summer and autumn,

both located on the positive side of axis 1, were associated with several dinoflagellate species (e.g., *Ceratium fusus*, *Ceratium furca*, *Gonyaulax* spp. and *Prorocentrum micans*). Winter was related to water column mixing (MLD) and other drivers typical of winter (turbulence and precipitation), while summer and autumn were associated with thermal stratification (SST and PAR) (Fig. 3.6 D). The PCO 2 clearly separated summer from autumn, as well as several spring sampling dates, with both upwelling indexes (M_x and M_y) more related to the autumn and spring communities (Fig. 3.6 D). This community was composed by several diatoms, most of them chain-forming species (e.g., *Rhizosolenia* spp., *Hemiaulus hauckii*, *Dactyliosolen phuketensis*, *Guinardia striata* and *Guinardia flaccida*) (Fig. 3.6 C).

In LagB-Beach (Fig. 3.6 E and F), where only 3-seasons were highlighted by the PERMANOVA analysis, PCO 1 separated the winter from the remaining seasons, and PCO 2 distinguished the spring from the summer/autumn season. Turbulence, MLD and precipitation were the main drivers that contributed to the winter community (Fig. 3.6 F), which was characterized by several pennate diatom species (e.g., *Asteromphalus flabellatus*, *Nitzschia* spp., *D. brightwelli* and *Biddulphia biddulphiana*) (Fig. 3.6 E). The summer/autumn season was highly correlated with SST and PAR (Fig. 3.6 F). This season, although with a high contribution of the diatom *S. marinoi*, was mainly composed by dinoflagellates (e.g., *P. quinquecorne*, *Gonyaulax* spp., *Protoperidinium curtipes/Protoperidinium crassipes* and *Protoperidinium* spp.) (Fig. 3.6 E). The spring was correlated with both upwelling indexes, Mx and My (Fig. 3.6 F), and was characterized by several chain-forming diatom species (e.g., *D. phuketensis*, *H. hauckii*, *Rhisosolenia* spp., *Pseudo-nitzschia* spp., *D. pumila* and *Leptocylindrus* cf. *danicus*) (Fig. 3.6 E).

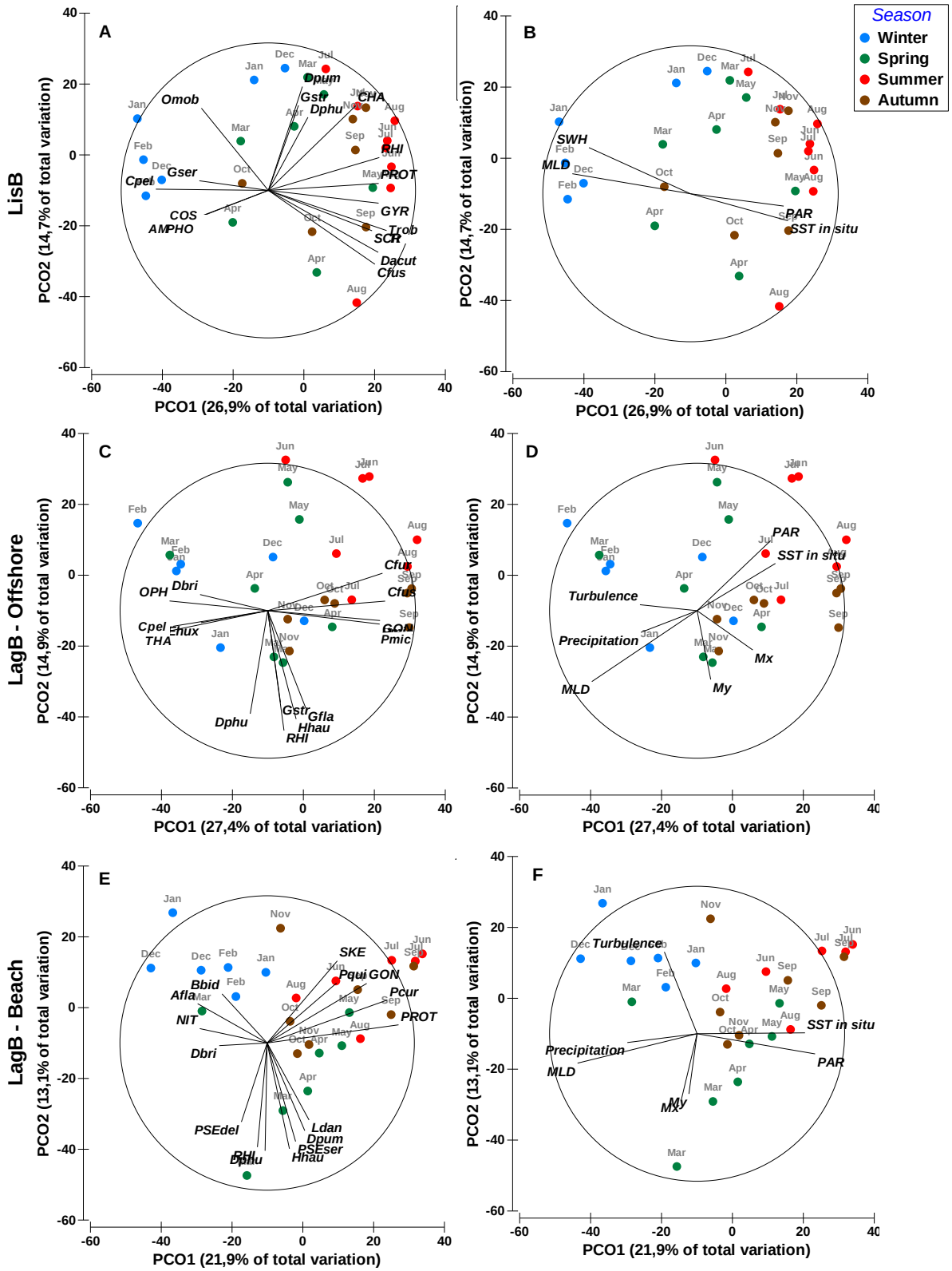

Fig. 3.6. Principal coordinates analysis (PCO) plots of phytoplankton community structure in each studied site by season, based on Bray-Curtis resemblance matrix: A/B – LisB; C/D – LagB-Offshore; and E/F – LagB-Beach. The left panel shows the most significant taxa (abbreviated according to Table B.3.1 in appendix), and the right panel shows the meteorological and oceanographic drivers with correlations higher than 0.4.

3.3.4. Harmful algal species (HABs)

Figure 3.7 shows a representation of maxima cell concentrations of the main HAB species or groups in each month recorded in the two bays. Table B.3.2 in appendix shows the summary of minima, maxima and average cell concentrations recorded by month. The highest concentrations of most HAB species/groups were recorded in Lagos Bay. The only exception was *D. acuta*, which occurred sporadically and at negligible concentrations in Lagos Bay, but reached high concentrations in Lisbon Bay from late-spring to summer. In Lagos Bay, the highest concentrations of planktonic HABs were always recorded in LagB-Offshore, being the only exception the *Pseudo-nitzschia seriata* group that showed higher cell concentration in LagB-Beach in September.

The diatom genus *Pseudo-nitzschia* was present in both studied bays all year round, although most of the situations at low concentrations. Nevertheless, *Pseudo-nitzschia* reached much higher concentrations during summer in Lagos Bay than in Lisbon Bay (Fig. 3.7 A and B. Table B.3.2 in appendix). The seasonality of *Pseudo-nitzschia* differed between the two groups and from station to station. In LagB-Offshore, the *delicatissima*-group (Fig. 3.7 A) had the annual maximum recorded in summer (July), and presented two secondary peaks of lower magnitude, in spring and autumn (April and October, respectively). In LagB-Beach the spring bloom co-occurred with the bloom offshore but the annual maximum was only recorded in August and no peak was recorded in autumn. In Lisbon Bay, the group occurred almost year-round but at low concentrations, and the annual maximum was shifted to September. Species of the *seriata*-group (Fig. 3.7 B) did not show a marked seasonality in Lisbon Bay, and the group was present all year round in low numbers. In Lagos Bay, the group showed a clear seasonality with annual maxima recorded in September in both stations, reaching maximum cell concentration above the alert reference level in LagB-Beach (Table B.3.2 in appendix). In addition, in LagB-Offshore, a low magnitude peak was recorded in March. The highest cell concentrations of *P. seriata*-group observed in LagB were always associated with few or no cells belonging to *P. delicatissima*-group.

Species of the genus *Dinophysis* (Fig. 3.7 C, D and E) showed a temporal pattern characterized by being almost absent during the winter months, with the exception of *D. ovum* with records in December in LagB-Offshore. In both bays, *Dinophysis* spp. started to occur in spring (from March to May). *D. acuminata* (Fig. 3.7 C) were recorded until early-autumn in both bays. However, differences in the seasonality of this species can be observed. In Lisbon

Bay, *D. acuminata* showed higher concentrations during late-summer/early-autumn, while in Lagos Bay maxima were recorded in spring (April) (Fig. 3.7 C, Table B.3.2 in appendix). *D. acuminata* concentrations above the interdiction reference level were recorded only in Lisbon Bay in August and September (Table B.3.2 in appendix). *D. ovum* was seldom recorded in Lisbon Bay (Fig. 3.7 D). In Lagos Bay, this species had the longest period of occurrence, being observed until December and reaching values above the alert and the interdiction reference levels several times from spring to early-winter (Table B.3.2 in appendix). The seasonality of *D. ovum* in LagB-Offshore indicated higher cell concentrations during late-summer and autumn, although with a first peak of low concentration recorded in April. *D. acuta* was the one that had the shortest period of occurrence (six months) ending in late-summer (Fig. 3.7 E). This species was seldom recorded in Lagos Bay and only reached high cell concentrations in Lisbon Bay. The maxima values were recorded in summer in LisB (Fig. 3.7 E, Table B.3.2 in appendix), reaching concentrations above the interdiction reference level in June, and above the alert reference level in August (Table B.3.2 in appendix).

The genus *Karenia* was only observed in a few records in Lisbon Bay, and always in trace concentrations (Fig. 3.7 F, Table B.3.2 in appendix). In Lagos Bay, the seasonality of *Karenia* indicated a bloom in spring (Fig. 3.7 F), although with low concentrations (Table B.3.2 in appendix). This genus was present in Lagos Bay almost all year round, except in June, July and October (Fig. 3.7 F). *Gonyaulax* cf. *spinifera* was detected in very low concentrations in Lisbon Bay (Fig. 3.7 G; Table B.3.2 in appendix). In Lagos Bay, this species occurred from late-spring to early-winter, reaching a maximum in August, above the alert reference level (Fig. 3.7 G, Table B.3.2 in appendix). *Lingulodinium polyedra* was not detected in Lisbon Bay all year round (Fig. 3.7 H). In Lagos Bay, *L. polyedra* occurred sporadically, reaching a maximum above the alert reference level in August (Fig. 3.7 H, Table B.3.2 in appendix). *Protoceratium reticulatum* was always observed in low concentrations but showed two periods of maxima occurrence in both bays, in spring and in summer, peaking in April and in August, respectively (Fig. 3.7 I, Table B.3.2 in appendix). Compared to LagB-Offshore, *P. reticulatum* was seldom recorded in LagB-Beach.

During the study period, benthic HABs, represented by *Ostreopsis* spp. and *Prorocentrum lima*, were always recorded in very low numbers (Table B.3.2 in appendix) at the two most coastal stations of Lisbon and Lagos Bays. This group was never detected in the LagB-Offshore station (Fig. 3.7 J). Despite the low concentrations, in LagB-Beach this group

consistently occurred for several months, from spring to summer, while in Lisbon Bay it was only recorded in September.

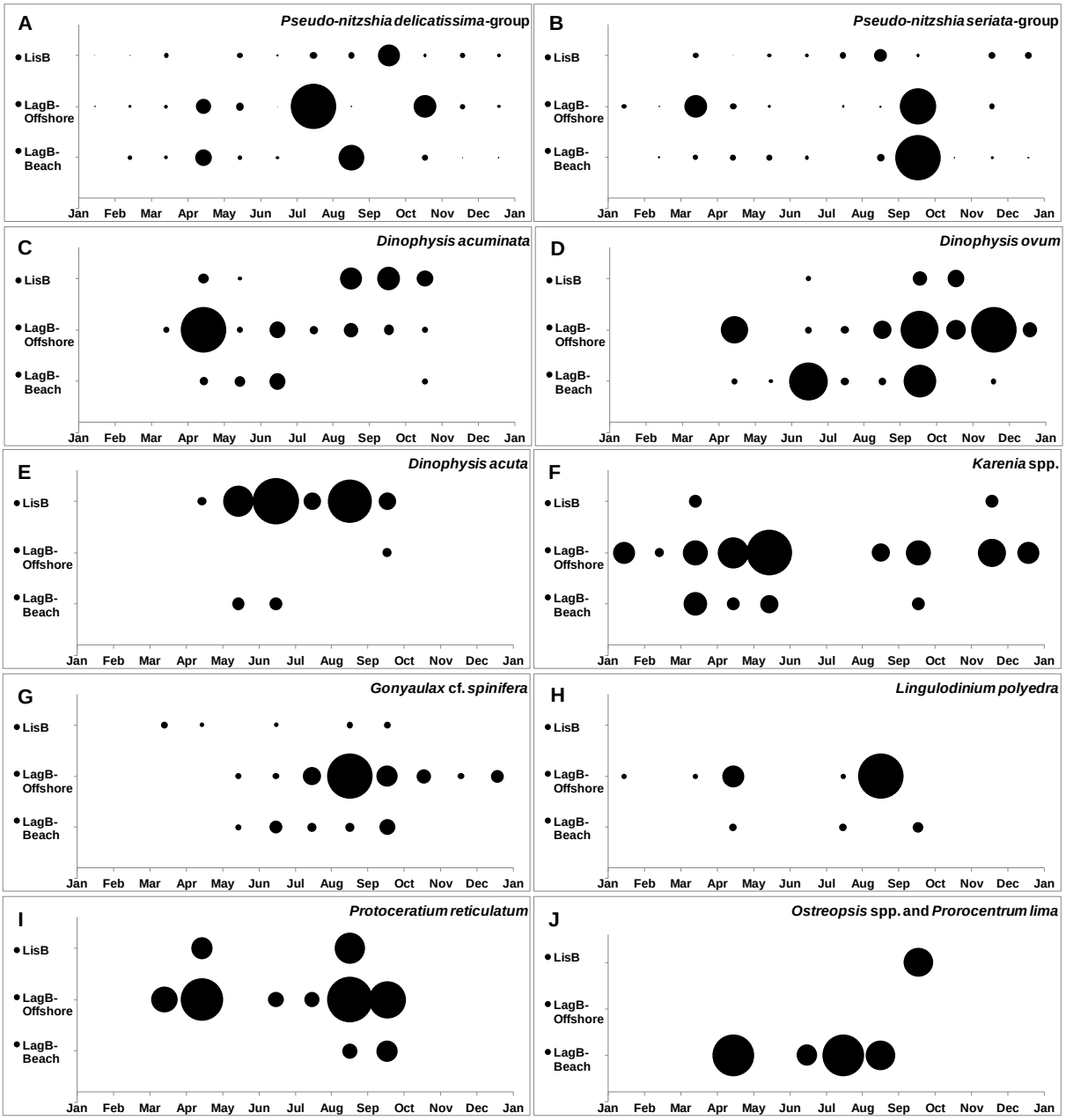

Fig. 3.7. Maxima cell concentrations recorded by month of main HAB species/groups identified in 2015: species of the *Pseudo-nitzschia delicatissima*-group, species of the *Pseudo-nitzschia seriata*-group, *Dinophysis acuminata*, *Dinophysis ovum*, *Dinophysis acuta*, *Karenia* spp., *Gonyaulax* cf. *spinifera*, *Lingulodinium polyedra*, *Protoceratium reticulatum* and the sum of potentially harmful benthic dinoflagellate species (*Ostreopsis* spp and *Prorocentrum lima*). For the actual cell concentrations please check the maximum values shown in Table B.3.2 in appendix.

3.4. Discussion

In the present study, the dynamics of phytoplankton communities were investigated during one year (2015), simultaneously in two wide-open coastal bays off West Iberia influenced by seasonal upwelling and sheltered by prominent capes. Lisbon Bay was studied within a long-

term studied site. Lagos Bay started to be studied recently, due to the occurrence of *Ostreopsis* blooms, a benthic HAB species. To better characterize phytoplankton dynamics in Lagos Bay, a nearshore and an offshore station were investigated.

In both bays, the studied year was characterized by persistent upwelling conditions almost all year round, being the exceptions a month in spring and the last three months of the year, and by SST maxima seldom reaching 20 ºC in summer (Fig. 3.2). In Lagos Bay, the studied year was characterized by negative SST anomalies observed almost all year round, except in late-spring/early-summer (Santos et al., 2019). In Lisbon Bay, SST anomalies were also mostly negative, although slightly positive during summer and late-autumn (Santos et al., 2019).

The two bays showed a similar bi-modal phytoplankton seasonal pattern, with the annual concentration maxima observed in spring and summer (Fig. 3.3). However, the magnitude of the phytoplankton blooms in both bays was quite different, reaching much higher cell concentrations in Lagos Bay (Fig. 3.3). This suggests that, during 2015, meteorological and oceanographic conditions were more favorable to phytoplankton development in Lagos Bay. Despite the similar Chl-*a* pattern observed between the bays in 2015, it is important to consider that phytoplankton has a high interannual variability (Santos et al., submitted - Chapter 2 of this thesis). In a previous study that analyzed a decade long time series of Chl-*a* in Lisbon and Lagos Bays, the authors identified Chl-*a* seasonal patterns that contrast with the observed in 2015, fact also mentioned in that work (Santos et al., submitted). According to these authors, the typical pattern of phytoplankton biomass in Lisbon Bay is characterized by a long period (~5 months) of high biomass from spring to summer, and in Lagos Bay by a uni-modal seasonal cycle reaching the maximum in the early-summer. These Chl-*a* patterns are different from the bi-modal observed here.

3.4.1. Spatio-temporal variability of phytoplankton

3.4.1.1. Features of main phytoplankton groups

Diatoms were the dominant group and were the main contributors to total phytoplankton biomass maxima in both studied bays. Diatoms showed several maxima from spring to late-summer (Fig. 3.3) in response to upwelling events (Fig. 3.2). This is in accordance with what is known for upwelling regions (eg. Anabalón et al., 2016; Kudela et al., 2005; Lassiter et al., 2006; Margalef, 1978) and in particular for the Iberian upwelling system, including the

Galician Rias (Figueiras et al., 2002), central Iberia (Vidal et al., 2017), Lisbon Bay (Palma et al., 2010, Silva et al., 2009) and the south coast of Portugal in the vicinity of Lagos Bay (Danchenko et al., 2019; Goela et al., 2014, 2015; Loureiro et al., 2005).

Previous work close to CSV, using other methods than microscopy (pigment and molecular markers), indicated nanoflagellates as the most abundant group, with diatoms ranking in second (Danchenko et al., 2019; Loureiro et al., 2011). Within the nanoflagellates group, cryptophytes were suggested as an important contributor to the CSV community, although not always dominant (Danchenko et al., 2019; Goela et al., 2014). Cryptophytes were not dominant in the present study, nevertheless, this group stood out as a key taxon distinguishing phytoplankton assemblages from Lagos Bay (highest correlation), located near CSV, and Lisbon Bay (lowest correlation) (Fig. 3.4). Recently Cabrita et al. (2015) analyzed, for the period of 1995-2008, the published and grey literature to assess eutrophication in the Portuguese continental exclusive economic zone (EEZ). Results indicated that in coastal areas there were no significant differences in nutrient levels between the areas (NW, SW and S coast). However, higher nutrient values were recorded in areas adjacent to river plumes, including the Tagus river, and the south coast presented the lowest mean values of dissolved inorganic nitrogen, phosphate and silica (Cabrita et al., 2015). Cryptophytes are small size and motile phytoplankton cells, which are more efficient in nutrient uptake than large non-motile cells such as diatoms (Marañón and Fernández, 1995). This may give them a competitive advantage to other groups in low nutrient waters, and could justify the high importance of this group in Lagos when compared to Lisbon Bay.

Coccolithophores have been described along the Portuguese coast associated with relaxation or convergence periods (Moita, 2001; Silva et al., 2008; Vidal et al., 2017). This was also observed for the study period in both bays albeit with some notorious differences. Similarly to Silva et al. (2009), in Lisbon Bay coccolithophores were the second most abundant group, being regularly present throughout the year. The higher cell concentrations were observed between late-summer and autumn (Fig. 3.3), associated with the transition from upwelling to downwelling favorable conditions (Fig. 3.2). In Lagos Bay, coccolithophores occurred at a much lower frequency. This group was present in high cell concentrations only in March and in September/October, months characterized mainly by weak upwelling and by the occurrence of several downwelling events. However, it is important to notice that, despite the lower contribution of this group in Lagos, the magnitude of coccolithophores blooms seems to be able to reach significant higher concentrations in the CSV vicinity (this study; Moita, 2001).

In the present work, a bloom of a holococcolith stage, tentatively identified as *Coccolithus pelagicus* var. *braarudii*, was recorded in March in Lagos Bay. *Coccolithus pelagicus* var *braarudii* is known as being the temperate form of *C. pelagicus* (Young et al., 2003). This species has an haplodiplontic life cycle with two morphologically distinct phases, a motile holococcolith- (HOL) and a non-motile heterococcolith- (HET) bearing phases (Parke and Adams, 1960). *Coccolithus pelagicus* var *braarudii* (HET) is a frequent species in the Portuguese upwelling system occurring throughout the upwelling season (from spring to early autumn), with maximum densities mainly during spring and minima during winter (Cachão and Moita, 2000). Evidence suggests that *C. pelagicus* var *braarudii* (HET) along the western Iberian coast occupies a niche of moderate turbulence between the coastal areas of enhanced productivity and the offshore stratified warmer and saltier waters (Cachão & Moita, 2000). Little is known about the ecology of the holococcolith stage of coccolithophores. Holococcolithophores degrade easily in water samples and cannot be reliably identified with standard optical microscopy. Probably for that reason, in the Portuguese coast there are only a couple of records of *C. pelagicus* var *braarudii* (HOL), both recorded in studies performed in Lisbon Bay (Cabeçadas and Oliveira, 2005; Silva, 2008). Cabeçadas and Oliveira (2005) performed a study during late-spring of 2002 and recorded a bloom of *C. pelagicus* var *braarudii* (HET) offshore of Lisbon Bay in a region characterized by higher thermal stratification, when colder and mixed upwelled waters were observed inshore, agreeing with what was previously described by Cachão and Moita (2000). On the other hand, in Lisbon Bay, *C. pelagicus* var *braarudii* (HOL) was related to the colder and mixed waters found inshore (Cabeçadas and Oliveira, 2005). In the present work, a bloom of *C. pelagicus* var *braarudii* (HOL) (1.1×10^6 cell L^{-1}) was recorded at 1 nautical mile from the coast at 10 m depth, and occurred after a strong downwelling event caused by easterly favorable winds, which slightly increased the water temperature. This ecological niche contrasts with the observed in Lisbon Bay (Cabeçadas and Oliveira, 2005), being more similar to what has been described for *C. pelagicus* var *braarudii* (HOL) in the Mediterranean Sea, where it has been described from oligotrophic, warm, stratified waters, and appeared to prefer shallow waters (Cros and Estrada, 2013; D'Amario et al., 2017).

Dinoflagellates were less abundant in Lisbon Bay, with higher concentrations recorded from late-summer to autumn (Fig. 3.3.). In this bay, favorable conditions to dinoflagellates occurrence were observed right after maximum PAR, during the period of maxima thermal stratification and during the reduction of upwelling to downwelling favorable conditions. In

Lagos Bay, dinoflagellates were the second most abundant group, especially in the offshore station. In this bay, higher dinoflagellate abundances were recorded for a longer period, from spring to autumn, and appear also more related to higher PAR levels and thermal stratification. Dinoflagellates have been frequently associated with warm and stratified conditions in Iberia (e.g. Figueiras et al., 2002; Moita, 2001; Silva et al., 2009). The higher contribution of this group in Lagos than in Lisbon Bay seems to be associated with the higher temperatures and stable conditions (as the lower SWH) observed in this bay. These conditions of warmer waters and low turbulence are known as favoring dinoflagellates development (Gilbert, 2016; Margalef, 1978). The presence of a recurrent warm coastal countercurrent near CSV also favors the growth of dinoflagellates in this region (Loureiro et al., 2005; Santos et al., 2019). Notwithstanding, there is a component of variability linked to this kind of circulation structure near capes, which can change this seasonal pattern observed in 2015. Oliveira and co-workers (2009a) observed that the stability and the full establishment of the main upwelling circulation structures associated with CR (i.e. the setup of strong coastal jets) favored a diatom bloom during July of 2002. However, two years later, an earlier setup of the offshore stratification conditions and the shedding of a slope eddy favored a bloom of dinoflagellates during the same month (July). According to these authors, the earlier and faster onset of summer stratification observed in 2004 favored the development of dinoflagellates in the offshore side of the upwelled waters. When the cyclone moves westward leaving the slope, dinoflagellates were transported to the shelf and the inshore poleward flow favors the cells accumulation in Lisbon Bay.

3.4.1.2. Phytoplankton communities

Coastal upwelling areas are characterized by high environmental variability on most spatio-temporal scales (Kudela et al., 2005; Pitcher et al., 2010), and this was also observed in the present study in the phytoplankton assemblages between Lisbon and Lagos Bays. Phytoplankton communities were also significantly different even when considering near locations, as observed between the nearshore and the offshore stations at Lagos Bay, located only one nautical mile apart. This shows how phytoplankton can be spatially patchy. This feature is particularly important in the scope of Marine Strategy Framework Directives since in some locations each station is considered to be representative of a larger area without having into account the phytoplankton patchiness within that area (Tweddle et al., 2018).

Some particular features of the ICCS are the local continental freshwater outflows, the variability in coastline configuration, complex topography, and retentive versus dispersive physical mechanisms (Fréon et al., 2009). All these features influence phytoplankton spatial and temporal dynamics. Previous studies, based on chlorophyll *a* variability, distinguished distinct phytoplankton regions in Iberia that are driven by different environmental drivers (e.g. Ferreira et al., 2019; Krug et al., 2017, 2018; Navarro and Ruiz, 2006). Lisbon and Lagos Bays, which are within regions characterized by having different patterns of chlorophyll *a* variability (Ferreira et al., 2019; Santos et al., under review), were also characterized here by having different phytoplankton assemblages (this study). Lisbon Bay was characterized by a higher contribution of several diatom species, particularly *L. minimus* and *C. curvisetus*, both almost absent in Lagos Bay, a high contribution of particular dinoflagellate species, namely the harmful species *D. acuta*, and euglenophytes. Lagos Bay was largely characterized by the high concentration and persistence of cryptophytes and the presence of several dinoflagellate species of which *Amphidinium* spp, *Karenia* spp. and *Gyrodinium fusiforme* are worth mentioning.

In Lagos Bay, phytoplankton communities in the nearshore and offshore sites, reflected local features. The general pattern indicated that the phytoplankton observed on the nearshore site did not reflect the phytoplankton present offshore. Some examples were the bloom of *C. pelagicus* var *braarudii* (HOL) that occurred in March at the offshore site, but no cells were recorded nearshore, and a bloom of the diatom *Skeletonema marinoi* (1.3×10^6 cell L^{-1}) developed locally nearshore in July, under strong northerly winds, while very few cells were observed offshore. Another example was observed in August. While dinoflagellates dominated 90 % of the total community offshore, in particular due to the high abundance of *Scrippsiella*, *Gymnodinium*, *Gonyaulax* and other unidentified species of small size, diatoms dominated nearshore (again due to the high concentration of *S. marinoi*). Nevertheless, especially under convergence conditions the phytoplankton community could be characterized by the same species in both sites. The coccolithophores bloom of the group *Emiliania huxleyii*/*Gephyrocapsa* spp. recorded under downwelling conditions in October was observed first offshore, accumulating and reaching higher cell concentrations later in the nearshore station.

The above-mentioned spatial differences in the phytoplankton assemblages can also vary with time. Multivariate analyses indicated that phytoplankton communities respond to the four meteorological seasons (winter, spring, summer and autumn) in Lisbon and in Lagos Bay (at

the offshore site). However, while in Lisbon Bay, winter and spring appear as completely separated stations, in Lagos Bay some mixing can be observed within these seasons (Fig. 3.6). Nevertheless, it is important to point out that the significant differences observed in Lagos Bay (offshore) between winter and spring (p = 0.03), as well as in Lisbon Bay between summer and autumn (p = 0.04), are close to the adopted cut off significance level (α < 0.05). This indicates some similarities between these communities. Nearshore in Lagos Bay, summer and autumn phytoplankton assemblages showed high similarities, suggesting the occurrence of only three main biological seasons (winter, spring and summer/autumn).

Our results indicate great seasonal similarities with previous studies performed on the Iberian coast based on phytoplankton assemblages (Figueiras et al., 2002; Moita, 2001; Silva et al., 2009). All these studies highlighted that chain-forming diatoms are the dominant species during spring, while dinoflagellates were the typical community observed during summer. While in Lagos Bay the spring community was associated with upwelling, in Lisbon Bay this was not a significant variable, suggesting that there are other relevant drivers in this bay during spring (Fig. 3.6). It can be that the river input in Lisbon Bay, which allows a great supply of nutrients mainly during winter and spring (Cabrita et al., 2015), could be an important driver to spring phytoplankton assemblages. In Lisbon Bay and in Lagos Bay (offshore), autumn was characterized by the transition from upwelling to downwelling conditions and, associated with this reversal circulation patterns, a mixed population of dinoflagellates and chain-forming diatoms was observed. A mixed population of these features during autumn is also a typical feature in NW Iberia (Figueiras et al., 2002), but coccolithophores can also be highly representative during this season in the Portuguese coast (Moita, 2001; Silva et al., 2009). During winter, coccolithophores (this study; Moita, 2001; Silva et al., 2009) and benthic diatoms (this study; Figueiras et al., 2002; Moita, 2001) were the typical communities observed in the Iberian coast. The meteorological and oceanographic drivers related to mixing processes were identified as the driving variables for the winter communities in both bays (MLD, SWH and turbulence). In addition, precipitation was also identified as a significant variable in Lagos Bay (Fig. 3.6). In Lagos Bay, precipitation is the main source of freshwater, while in Lisbon Bay the Tagus river is highly important during winter (Cabrita et al., 2015). Precipitation can be an important supply of nutrients in Lagos Bay, either by increasing the Arade river runoff or by increasing local land flows, which may justify its relationship with the winter community.

The comparison between the present study and the previous studies mentioned above (Figueiras et al., 2002; Moita, 2001; Silva et al., 2009), indicated that in 2015 Lisbon and Lagos Bays followed the same successional pattern. The biggest difference observed between both bays was found during winter. The Lisbon Bay site, being shallower than the offshore station in Lagos Bay, has a much higher contribution of benthic diatoms (similarly to nearshore in Lagos), in addition to the coccolithophores. The nearshore of Lagos Bay proved to be a very particular environment. Here, coccolithophores were not significant in any season, and the summer community that was dominated mainly by dinoflagellates extended until the autumn, which resulted in only three biological seasons.

3.4.2. Harmful Algal Bloom species (HABs)

Recurrent outbreaks of HAB species occur in Portuguese coastal and estuarine regions (IPMA, 2019). Frequently, it results in economic losses due to shellfish harvesting bans (Vale et al., 2008) or to beach closure to baths (David et al., 2012). Due to the regional economic importance, the present study also focused on understanding the role of HABs in the SW Iberian region. Our study showed that Lagos Bay had a higher frequency and abundance of several HAB species than Lisbon Bay. Of the overall identified species, *Pseudo-nitzschia* spp. were the most frequent in both bays, present all year round, but with maxima concentration constantly below the reference levels considered by the National Monitoring Program of HABs (IPMA, 2019, Table B.3.2 in appendix). The alert level was exceeded only once in the nearshore station of Lagos Bay in September. Fehling et al. (2006) suggested photoperiod as the most significant variable favoring the *Pseudo-nitzschia* summer blooms (Fehling et al., 2006). The present results also suggest dependence between *Pseudo-nitzschia* and daylength, being the maxima recorded between March and October, precisely between the beginning of PAR increase, during its maximum and until PAR decreasing. Nevertheless, the higher *Pseudo-nitzschia* spp. concentrations occurred during summer/autumn, which also showed a strong relationship with the several upwelling events observed during this period.

It was interesting to observe that, in Lagos Bay, *P. seriata*-group had the higher concentrations when *P. delicatissima*-group was scarce (March) or absent (September). Previous studies suggested that there were differences in seasonality within *Pseudo-nitzschia* genus, as well as there were differences observed between nearside locations and a great interannual variability (Bresnan et al., 2015). Different temporal distributions were frequently

observed between both *Pseudo-nitzschia* studied groups. A previous study in Lisbon Bay suggested that *P. seriata*-group dominated in spring, while *P. delicatissima*-group was more abundant in summer (Palma et al., 2010). Another study performed at higher latitudes (in Scottish waters) indicated that *P. delicatissima*-group was persistent in spring and then again in summer, while *P. seriata*-group dominated in summer/early-autumn (Fehling et al., 2006). In the present work, based on Lagos Bay observations, *P. delicatissima*-group appears as maxima in spring, summer and autumn, while *P. seriata* group is maxima in early-spring and early-autumn. The comparison of our results in Lagos Bay with another study performed near CSV during the summer/autumn of 2015 (Danchenko et al., 2019) indicate that, although *P. delicatissima*-group reached similar cell concentrations on both sites, *P. seriata*-group has the double of cell concentrations near CSV. It can be that *P. seriata*-group was favored by the proximity of the upwelling center of CSV.

In the current work, *Dinophysis* cell concentrations reached the alert and the interdiction reference levels several times during the year (Table B.3.2 in appendix). Different patterns were observed between the most commonly identified species in each studied location. *Dinophysis acuta* had the shortest period of occurrence and seems to be spatially restricted to Lisbon Bay; *D. acuminata* showed a longer period of occurrence than the previous species and was frequent in both bays; and *D. ovum* had the longest period of occurrence and was much more frequent and abundant in Lagos Bay. These results indicate some temporal restriction, mainly of *D. acuta,* and differences in the spatial distribution of those three species, with preferable conditions to *D. acuta* occurrence in Lisbon Bay and of *D. ovum* in Lagos Bay. *Dinophysis* species are favored by well-stratified water columns in upwelling shadows but are also tolerant to upwelling turbulence (e.g. GEOHAB, 2005). In addition, species occurring earlier in the year seem to show some relationship with the annual cycle of PAR and not only with the average annual SST cycle (Moita et al., 2016). A previous study performed in NW Iberia indicated that *D. acuta* blooms were characterized by a larger interannual variability, than the observed in this one-year study, occurring in variable periods from February/March to October (Moita et al., 2016). Nevertheless, it is common to both studies that *D. acuminata* starts earlier than *D. acuta* (this study; Moita et al., 2016). For what is known in NW Iberia, *D. acuta* bloom epicenter is located in the Aveiro-F.Foz coast and can propagate to north, while *D. acuminata* blooms start further north (epicenter at the Galician Rías Bajas) and can propagate southwards (Moita et al., 2016). The northward expansion of *D. acuta* can explain the high frequency of occurrence and cell concentrations of that species

in Lisbon Bay (central-west coast) than in Lagos Bay (south coast). On the south coast, *D. ovum* was more frequent and abundant than *D. acuminata.* This is in accordance with the observed near CSV in a previous study (Danchenko et al., 2019). However, in particular *D. ovum* reached the double of cell concentrations in the sheltered Lagos Bay (this study) than near the upwelling center of CSV (Danchenko et al., 2019). Although with no certainty of the reason, there is a clear preference for the occurrence of *D. ovum* on the south coast than on the west coast. This fact was already highlighted by Moita (1993) based on 7 cruises covering the entire coast of Portugal during the '80s and '90s. It is interesting to observe similar spatial distribution patterns of *D. ovum* after 40 years, suggesting a steady population of the species on the south coast of Portugal.

Within harmful dinoflagellates, *Karenia* showed a high frequency of occurrence in Lagos Bay, in particular at the offshore station, reaching maxima cell concentrations during spring and almost no cells during summer and autumn. The study of Danchenko et al. (2019) near CSV also revealed low cell concentrations of *Karenia* by microarray analysis during the summer/autumn of 2015. This pattern was the opposite of what would be expected from these efficient swimmers, which are frequently found in late-summer/early-autumn when upwelling conditions change to downwelling (GEOHAB, 2005 and references therein). The temporal pattern showed by *Karenia* spp. in this work in Lagos Bay may be explained by the SST pattern that characterized 2015, a warm spring/early-summer followed by a cold summer/autumn period (Santos et al., 2019).

Gonyaulax spinifera has a widespread distribution, from polar to subtropical waters, in the NE Atlantic (Dodge and Harland, 1991). The *Gonyaulax spinifera* group includes at least three species with similar morphological features, which can easily be confused: *G. spinifera*, *G. digitale* and *G. diegensis* (Dodge, 1989; Lewis et al., 1999). The information available on the seasonality of this group of species is very limited. In the Iberian coast there are no reports of harmful effects caused by species of the *Gonyaulax spinifera* group. During the present study, *Gonyaulax* cf. *spinifera* showed very low concentrations in Lisbon Bay, from early-spring to summer. By contrast, in Lagos Bay it had a long period of occurrence, from late-spring to early-winter, and reached cell concentrations above the alert reference level in August, although well below the interdiction reference level.

Protoceratium reticulatum showed two periods of occurrence in both bays (in spring and in late-summer) but was always recorded in low concentrations. *Protoceratium reticulatum* is known to be a cosmopolitan species (Dale, 1996) but little is known about the ecology of this

species in Portugal. Currently, three main ribotypes of *P. reticulatum* are recognized and all can be found in the northern hemisphere (Wang et al., 2019). These are termed cold, moderate and warm ribotypes according to their presence in different geographic areas (Wang et al., 2019). So far, there are no studies correlating the seasonal and peak occurrence of *P. reticulatum* in the water column and each specific ribotype (Wang et al., 2019). In laboratory experiments, the moderate and warm ribotypes show high growth rates at temperatures above 20 ºC (Wang et al., 2019). During 2015, water temperature above 20 ºC (the value suggested as optimum growth temperature to the moderate and warm ribotypes (Wang et al., 2019)) was never recorded in Lisbon Bay and rarely observed in Lagos Bay. This can explain the low concentration of *P. reticulatum* in this study.

Blooms of *Lingulodinium polyedra* leading to water discoloration (red tide) have been reported along the coast of Portugal since 1944 (Amorim et al. 2001, 2004; Pinto, 1949). In Iberian shelf waters, the ecological niche for the development of *L. polyedra* blooms was described based on observations made on the south coast, in the vicinity of Lagos Bay (Amorim et al., 2004). These blooms have been described as occurring in warm stratified waters adjacent to upwelling nutrient-rich plumes, or in warm along-shore countercurrents that flow between upwelling plumes and the coast (Amorim et al., 2004). Lagos Bay is characterized by the presence of a recurrent warm countercurrent observed nearshore that develop during the upwelling season (e.g. Relvas et al., 2007; Santos et al., 2019). This can explain the several records of this species in this bay, reaching cell concentrations above the alert reference level during the peak of summer.

The benthic HABs group (BHABs), which in the present study included *Ostreopsis* spp. and *Prorocentrum lima,* was also investigated. BHABs have been an important cause of concern in warm-temperate and tropical waters. In particular, the frequency and geographic spread of *Ostreopsis* have been increasing in temperate areas, which includes the Atlantic Iberian coast (Amorim et al., 2012; David et al., 2012, 2013, 2018; Santos et al., 2019). The presence of BHABs during 2015 was recorded in extremely low cell concentrations and were only detected in the nearshore stations of both bays, although much more frequent in Lagos Bay. Although with only one year of data, these results agree with the observations made in a previous study performed in Lisbon and Lagos Bays, which covered 7-years of weekly data (Santos et al., 2019). According to these authors, *Ostreopsis* were found in both bays, but with higher abundances and frequency of occurrence in Lagos Bay. In Lisbon Bay, the first bloom of *Ostreopsis* was found only in 2017 (David et al., 2018; Santos et al., 2019). In Lagos Bay,

strong and significant correlations were found between high *Ostreopsis* concentrations and positive SST anomalies (Santos et al., 2019). Santos and co-workers (2019) highlighted that 2015 was characterized by a gross change performed in beach morphology, as well as by an atypical SST pattern, with a warm spring/early-summer and cold summer/autumn, the latter period characterized by negative SST anomalies. These features that characterized 2015 can be an explanation for the low BHABs concentrations found in Lagos Bay during that year.

3.5. Conclusions

This study compares the phytoplankton communities of two wide-open sheltered bays, located at short latitudinal distances but with different coastline orientations. Significant spatial and temporal differences were observed in phytoplankton assemblages. Lisbon Bay, located on the west coast and near the Tagus estuary influence had a higher contribution of diatoms and euglenophytes, as well as of the harmful dinoflagellate *D. acuta*. The phytoplankton communities that most characterized Lagos Bay, located on the south coast, were the dinoflagellates and cryptophytes. Lagos Bay nearshore is a very particular environment that, in most of the situations, did not reflect the phytoplankton communities that developed offshore. An important feature observed nearshore is the high contribution of benthic species, both of diatoms and dinoflagellates. This study highlights the relevance of considering the phytoplankton spatial patchiness in regional studies, in particular when dealing with harmful algae detection. In addition, the data analyzed here suggests that Lagos Bay had a higher probability for the occurrence of HABs, both in higher cell concentrations and persistence.

On a temporal scale in Lisbon and in Lagos Bays (offshore), different phytoplankton assemblages were observed in response to the four meteorological seasons (winter, spring, summer and autumn). In nearshore waters in Lagos Bay, no differences were recorded between summer and autumn phytoplankton assemblages, and only three biological seasons could be identified (winter, spring and summer/autumn). In general, winter assemblages in both bays were dependent on the water column mixing processes, as well as on precipitation in Lagos Bay. Coccolithophores were the dominant community during this season in Lisbon and in Lagos Bay (offshore), but the benthic diatoms were also relevant in the shallower stations, in Lisbon and in Lagos Bay (nearshore). The spring phytoplankton community, mostly composed by chain-forming diatoms, was dependent on upwelling in Lagos Bay,

while in Lisbon Bay other factors seem to have a higher contribution. Lastly, both summer and autumn communities, mostly composed by dinoflagellates, were influenced by the SST and PAR conditions. During autumn, due to the reversal circulation patterns observed, a mixed population of diatoms with dinoflagellates characterized Lisbon and Lagos (offshore) Bays.

Acknowledgments

Financial support of M. Santos was provided by a Portuguese PhD grant from FCT - Fundação para a Ciência e a Tecnologia (SFRH/BD/52560/2014). This work was financially supported by IPMA, I.P. (MAR2020/SNMB-MONITOR), by FCT through UID/MAR/04292/2019, UIDB/04326/2020, and project LISBOA-01-0145-FEDER-031265 co-funded by EU ERDF funds, within the PT2020 Partnership Agreement and Compete 2020. The authors would like to express a special thanks to "Testa & Cunhas, SA", "SOPROMAR" and "Marina de Lagos" for logistic support, and Luciano Júnior for his support during LagB fieldwork. The authors also acknowledge all the technicians and colleagues from IPMA for sample collection and fieldwork support. M. Santos would like to express a special thanks to José Lino Costa for statistical guidance.

This study was conducted using E.U. Copernicus Marine Service Information for the Chl-a L4 Reprocessed datasets (http://marine.copernicus.eu/). The Group for High Resolution Sea Surface Temperature (GHRSST) Multi-scale Ultra-high Resolution (MUR) SST data were obtained from the NASA EOSDIS Physical Oceanography Distributed Active Archive Center (PO.DAAC) at the Jet Propulsion Laboratory, Pasadena, CA (http://dx.doi.org/10.5067/GHGMR-4FJ04). MLD data were obtained from the Ocean Productivity group of the Oregon State University (http://www.science.oregonstate.edu/ocean.productivity/index.php). PAR, SWH, total precipitation and wind stress components were obtained from European Centre for Medium-Range Weather Forecasts (https://www.ecmwf.int/en/forecasts/datasets/).

References

Amorim, A., Palma, S., Sampayo, M.A., Moita, M.T., 2001. On a *Lingulodinium polyedrum* bloom in Setúbal Bay, Portugal, *in* Hallegraeff, G.M., Blackburn, S.I., Bolch, C.J., Lewis, R.J. (Eds.), Harmful Algal Blooms 2000, pp. 133-136

Amorim, A., Moita, M., Oliveira, P., 2004. Dinoflagellate blooms related to coastal upwelling plumes off Portugal, *in*: Steidinger, K.A., Landsberg, J.H., Tomas, C.R., Vargo, G.A. (Eds.), Harmful Algae 2002. Florida Fish and Wildlife Conservation Commission, Florida Institute of Oceanography, and Intergovernmental Oceanographic Commission of UNESCO, St. Petersburg, Florida, USA, pp. 89–91.

Amorim, A., Veloso, V., Battocchi, C., Penna, A., 2012. Occurrence of *Ostreopsis* cf. *siamensis* along the upwelling coast of Portugual (NE Atlantic), *in*: Pagou, K.A., Hallegraeff, G.M. (Eds.), Proceedings of the 14th International Conference on Harmful Algae. International Society for the Study of Harmful Algae and Intergovernmental Oceanographic Commission of Unesco, pp. 10–12.

Anabalón, V., Morales, C. E., González, H. E., Menschel, E., Schneider, W., Hormazabal, S., Valencia, L., Escribano, R., 2016. Micro-phytoplankton community structure in the coastal upwelling zone off Concepción (central Chile): Annual and interannual fluctuations in a highly dynamic environment. Prog. Oceanogr. 149, 174-188.

Anderson, M.J., Gorley, R.N., Clarke, K.R., 2008. PERMANOVA + for PRIMER: Guide to Software and Statistical Methods. Prim. Plymouth. 214 pp.

Bresnan, E., Kraberg, A., Fraser, S., Brown, L., Hughes, S., Wiltshire, K.H., 2015. Diversity and seasonality of *Pseudo-nitzschia* (Peragallo) at two North Sea time series monitoring sites. Helgol. Mar. Res. 193–204. doi:10.1007/s10152-015-0428-5

Cabeçadas, L., Oliveira, A. P., 2005. Impact of a *Coccolithus braarudii* bloom on the carbonate system of Portuguese coastal waters. J. Nannoplankton Res. 27, 141-147.

Cabrita, M.T., Silva, A., Oliveira, P.B., Angélico, M.M., Nogueira, M., 2015. Assessing eutrophication in the Portuguese continental Exclusive Economic Zone within the European Marine Strategy Framework Directive. Ecol. Indic. 58, 286–299. doi:10.1016/j.ecolind.2015.05.044

Cachao, M., Moita, M. T., 2000. *Coccolithus pelagicus*, a productivity proxy related to moderate fronts off Western Iberia. Mar. Micropaleontol. 39, 131-155.

Chavez, F.P., Messié, M., 2009. A comparison of Eastern Boundary Upwelling Ecosystems. Prog. Oceanogr. 83, 80–96. doi:10.1016/j.pocean.2009.07.032

Clarke, K.R., Gorley, R.N., 2006. PRIMER v6: User Manual/Tutorial (Plymouth Routines in Multivariate Ecological Research). Prim. Plymouth UK. 192 pp. doi:10.1111/j.1442-9993.1993.tb00438.x

Cravo, A., Relvas, P., Cardeira, S., Rita, F., Madureira, M., Sa, R., 2010. An upwelling filament off southwest Iberia: Effect on the chlorophyll *a* and nutrient export 30, 1601–1613. doi:10.1016/j.csr.2010.06.007

Cros, L., Estrada, M., 2013. Holo-heterococcolithophore life cycles: ecological implications. Mar Ecol Prog Ser 492, 57-68.

Dale, B., 1996. Dinoflagellate cyst ecology: modeling and geological applications. *In* Jansonius, J. and McGregor, D.C. (Eds.), Palynology: principles and applications, Dallas, American Association of Stratigraphic Palynologists Foundation 3, 1249–1275.

D'Amario, B., Ziveri, P., Grelaud, M., Oviedo, A., Kralj, M., 2017. Coccolithophore haploid and diploid distribution patterns in the Mediterranean Sea: can a haplo-diploid life cycle be advantageous under climate change? J. Plankton Res. 39, 781-794.

Danchenko, S., Fragoso, B., Guillebault, D., Icely, J., Berzano, M., Newton, A., 2019. Harmful phytoplankton diversity and dynamics in an upwelling region (Sagres, SW Portugal) revealed by ribosomal RNA microarray combined with microscopy. Harmful Algae 82, 52–71. doi:10.1016/j.hal.2018.12.002

David, H., Moita, M.T., Laza-Martínez, A., Silva, A., Mateus, M., de Pablo, H., Orive, E., 2012. First bloom of *Ostreopsis* cf. *ovata* in the continental Portuguese coast. Harmful Algae News 45, 12–13.

David, H., Laza-Martínez, A., Miguel, I., Orive, E., 2013. *Ostreopsis* cf. *siamensis* and *Ostreopsis* cf. *ovata* from the Atlantic Iberian Peninsula: Morphological and phylogenetic characterization. Harmful Algae 30, 44–55. http://dx.doi.org/10.1016/j.hal.2013.08.006

David, H., Nascimento, P., Caeiro, M.F., Melo, R., Amorim, A., 2018. Bloom of *Ostreopsis* cf. *siamensis* in the Bay of Lisbon. Harmful Algae News 60, 11–12.

DiTullio, G. R., Geesey, M. E., Maucher, J. M., Alm, M. B., Riseman, S. F., Bruland, K. W., 2005. Influence of iron on algal community composition and physiological status in the Peru upwelling system. Limnol. Oceanogr. 50, 1887-1907.

Dodge, J.D., 1982. Marine Dinoflagellates of the British Isles. H.M. Stationery Office, London. 303 pp.

Dodge, J.D., 1989. Some Revisions of the Family Gonyaulacaceae (Dinophyceae) Based on a Scanning Electron Microscope Study. Botanica Marina 32, 275-298.

Fehling, J., Davidson, K., Bolch, C., Tett, P., 2006. Seasonality of *Pseudo-nitzschia* spp. (Bacillariophyceae) in western Scottish waters. Mar Ecol Prog Ser 323, 91–105.

Ferreira, A., Brito, A.C., Harvey, E.T., 2019. Disentangling Environmental Drivers of Phytoplankton Biomass off Western Iberia. Front. Mar. Sci. 6, 1–17. doi:10.3389/fmars.2019.00044

Field, C.B., Behrenfeld, M.J., Randerson, J.T., Falkowski, P., 1998. Primary production of the biosphere: Integrating terrestrial and oceanic components. Science 281, 237–240. doi:10.1126/science.281.5374.237

Figueiras, F.G., Labarta, U., Fernández Reiriz, M.J., 2002. Coastal upwelling, primary production and mussel growth in the Rías Baixas of Galicia. Hydrobiologia 484, 121–131.

Fiúza, A.F.G., de Macedo, M.E., Guerreiro, M.R., 1982. Climatological space and time variation of the Portuguese coastal upwelling. Oceanol. Acta 5, 31–40.

Fréon, P., Barange, M., Aristegui, J., 2009. Eastern Boundary Upwelling Ecosystems: Integrative and comparative approaches. Prog. Oceanogr. 83, 1–14. doi:10.1016/j.pocean.2009.08.001

GEOHAB, 2005. Global Ecology and Oceanography of Harmful Algal Blooms, *in*: Pitcher, G., Moita, T., Trainer, V., Kudela, R., Figueiras, P., Probyn, T. (Eds.), GEOHAB Core Research Project: HABs in Upwelling Systems. IOC and SCOR, Paris and Baltimore, 82 pp.

Glibert, P. M., 2016. Margalef revisited: a new phytoplankton mandala incorporating twelve dimensions, including nutritional physiology. Harmful Algae 55, 25-30.

Goela, P.C., Danchenko, S., Icely, J.D., Lubian, L.M., Cristina, S., Newton, A., 2014. Using CHEMTAX to evaluate seasonal and interannual dynamics of the phytoplankton community off the South-west coast of Portugal. Estuar. Coast. Shelf Sci. 151, 112–123. doi:10.1016/j.ecss.2014.10.001

Goela, P.C., Icely, J., Cristina, S., Danchenko, S., Angel DelValls, T., Newton, A., 2015. Using bio-optical parameters as a tool for detecting changes in the phytoplankton community (SW Portugal). Estuar. Coast. Shelf Sci. 167, 125–137. doi:10.1016/j.ecss.2015.07.037

Guiry, M.D. & Guiry, G.M., 2020. AlgaeBase. World-wide electronic publication, National University of Ireland, Galway. https://www.algaebase.org; searched on 28 January 2020.

Hill, E.A., Hickey, B.M., Shillington, F.A., Strub, P.T., Brink, K.H., Barton, E.D., Thomas, A.C., 1998. Eastern ocean boundaries. Coastal segment (E), *in*: Robinson, A.R., Brink, K.H. (Eds.). The Sea, the Global Coastal Ocean: Regional Studies and Syntheses. John Wiley and Sons, New York, pp. 29–67.

Hoppenrath, M., Elbrächter, M., Drebes, G., 2009 Marine phytoplankton. Selected microphytoplankton species from the North Sea around Helgoland and Sylt. E. Schweizerbart'sche Verlagsbuchhandlung, Stuttgart. 264 pp.

IPMA, I.P., 2019. Instituto Português do Mar e de Atmosfera, I.P. http://www.ipma.pt/pt/bivalves, accessed on 06 December 2019.

Kato, H., Phillips, O.M., 1969. On the penetration of a turbulent layer into stratified fluid. J. Fluid Mech. 37, 643–655.

Krug, L.A., Platt, T., Sathyendranath, S., Barbosa, A.B., 2017. Unravelling region-specific environmental drivers of phytoplankton across a complex marine domain (off SW Iberia). Remote Sens. Environ. 203, 162–184. doi:10.1016/j.rse.2017.05.029

Krug, L.A., Platt, T., Sathyendranath, S., Barbosa, A.B., 2018. Patterns and drivers of phytoplankton phenology off SW Iberia: A phenoregion based perspective. Prog. Oceanogr. 165, 233–256. doi:10.1016/j.pocean.2018.06.010

Kudela, R.M., Cruz, S., Pitcher, G.C., Figueiras, F.G., National, S., 2005. Harmful Algal Blooms in Coastal Upwelling Systems. Oceanography 18, 184–197. doi:10.5670/oceanog.2005.53

Kudela, R.M., Barth, J.A., Frame, E.R., Jay, D.A., 2008. New insights into the controls and mechanisms of plankton productivity along the US West Coast. Oceanography 21, 46–59.

Largier, J.L., Lawrence, C.A., Roughan, M., Kaplan, D.M., Dever, E.P., Dorman, C.E., Kudela, R.M., Bollens, S.M., Wilkerson, F.P., Dugdale, R.C., Botsford, L.W., Garfield,

N., Kuebel Cervantes, B., Koračin, D., 2006. WEST: A northern California study of the role of wind-driven transport in the productivity of coastal plankton communities. Deep. Res. Part II Top. Stud. Oceanogr. 53, 2833–2849. doi:10.1016/j.dsr2.2006.08.018

Largier, J.L., 2020. Upwelling Bays: How Coastal Upwelling Controls Circulation, Habitat, and Productivity in Bays. Ann. Rev. Mar. Sci. 12, 20.1-20.33.

Lassiter, A. M., Wilkerson, F. P., Dugdale, R. C., & Hogue, V. E., 2006. Phytoplankton assemblages in the CoOP-WEST coastal upwelling area. Deep Sea Res. Part II: Topical Studies in Oceanography, 5, 3063-3077.

Lewis, J., Rochon, A., Harding, I., 1999. Preliminary observations of cyst-theca relationships in *Spiniferites ramosus* and *Spiniferites membranaceus* (Dinophyceae). Grana 38, 113-124. 10.1080/00173139908559220

Loureiro, S., Newton, A., Icely, J.D., 2005. Microplankton composition, production and upwelling dynamics in Sagres (SW Portugal) during the summer of 2001. Sci. Mar. 69, 323–341. doi:10.3989/scimar.2005.69n3323

Loureiro, S., Reñé, A., Garcés, E., Camp, J., Vaqué, D., 2011. Harmful algal blooms (HABs), dissolved organic matter (DOM), and planktonic microbial community dynamics at a near-shore and a harbour station influenced by upwelling (SW Iberian Peninsula). J. Sea Res. 65, 401–413. doi:10.1016/j.seares.2011.03.004

Maranón, E., & Fernandez, E., 1995. Changes in phytoplankton ecophysiology across a coastal upwelling front. J. Plankton Res. 17, 1999-2008.

Margalef, R., 1978. Life-forms of phytoplankton as survival alternatives in an unstable environment. Oceanol. Acta 1, 493–509. doi:10.1007/BF00202661

Moita, M.T., 1993. Development of toxic dinoflagellates in relation to upwelling patterns off Portugal. *In*: T.J. Smayda e Y.Shimizu (Eds.) Toxic Phytoplankton Blooms in the Sea, Elsevier, Amsterdam, pp. 299-304

Moita, M.T., 2001. Estrutura, Variabilidade e Dinâmica do Fitoplâncton na Costa de Portugal Continental. Universidade de Lisboa. Tese de doutoramento.

Moita, M.T., Oliveira, P.B., Mendes, J.C., Palma, A.S., 2003. Distribution of chlorophyll a and *Gymnodinium catenatum* associated with coastal upwelling plumes off central Portugal. Acta Oecologica 24, 125–132. doi:10.1016/S1146-609X(03)00011-0

Moita, M.T., Pazos, Y., Rocha, C., Nolasco, R., Oliveira, P.B., 2016. Toward predicting *Dinophysis* blooms off NW Iberia: A decade of events. Harmful Algae 53, 17–32. doi:10.1016/j.hal.2015.12.002

Navarro, G., Ruiz, J., 2006. Spatial and temporal variability of phytoplankton in the Golf of Cadiz through remote sensing images. Deep. Sea Res. Part II: Top. Stud. Oceanogr. 53, 1241–1260. doi:10.1016/j.dsr2.2006.04.014

Oliveira, P.B., Moita, T., Silva, A., Monteiro, I.T., Palma, S., 2009a. Summer diatom and dinoflagellate blooms in Lisbon Bay from 2002 to 2005: Pre-conditions inferred from wind and satellite data. Prog. Oceanogr. 83, 270–277. doi:10.1016/j.pocean.2009.07.030

Oliveira, P.B., Nolasco, R., Dubert, J., Moita, T., Peliz, Á., 2009b. Surface temperature, chlorophyll and advection patterns during a summer upwelling event off central Portugal. Cont. Shelf Res. 29, 759–774. doi:10.1016/j.csr.2008.08.004

Oliveira, P.B., Santos, M., Moita, M.T., Amorim, A., 2016. Circulação costeira no barlavento Algarvio no verão e outono de 2015, *in*: Actas Das 4as Jornadas de Engenharia Hidrográfica. Lisbon, pp. 199–202.

Palma, S., Mouriño, H., Silva, A., Barão, M.I., Moita, M.T., 2010. Can *Pseudo-nitzschia* blooms be modeled by coastal upwelling in Lisbon Bay? Harmful Algae 9, 294–303. doi:10.1016/j.hal.2009.11.006

Parke, M., Adams, I., 1960. The motile (Crystallolithus hyalinus Gaarder & Markali) and non-motile phases in the life history of Coccolithus pelagicus (Wallich) Schiller. J. Mar. Biolog. Assoc. U.K. 39, 263-274.

Peragallo, H. & Peragallo, M., 1908. Diatomées marines de France. Tempère, H.J. (Ed.), Grez-surLoing, 491 pp.

Pinto, J.S., 1949. Um caso de “red water” motivado por abundância anormal de *Gonyaulax polyedra* (Stein). Boletim da Sociedade Portuguesa de Ciências Naturais (Lisboa), II, Sér 2 (XVII), 94-97.

Pitcher, G.C., Figueiras, F.G., Hickey, B.M., Moita, M.T., 2010. The physical oceanography of upwelling systems and the development of harmful algal blooms. Prog. Oceanogr. 85, 5–32. doi:10.1016/j.pocean.2010.02.002

Relvas, P., Barton, E.D., 2002. Mesoscale patterns in the Cape São Vicente (Iberian Peninsula) upwelling region. J. Geophys. Res. 107 (C10), 3164. doi:10.1029/2000JC000456

Relvas, P., Barton, E.D., 2005. A separated jet and coastal counterflow during upwelling relaxation off Cape São Vicente (Iberian Peninsula). Cont. Shelf Res. 25, 29–49. doi:10.1016/j.csr.2004.09.006

Relvas, P., Peliz, A., Oliveira, P.B., da Silva, J., Dubert, J., Barton, E.D., Santos, A.M.., 2007. Physical oceanography of the western Iberia ecosystem: latest views and challenges. Prog. Oceanogr. 74, 149–173. doi:10.1016/j.pocean.2007.04.021

Santos, M., Oliveira, P.B., Moita, M.T., David, H., Caeiro, M.F., Zingone, A., Amorim, A., Silva, A., 2019. Ocurrence of *Ostreopsis* in two temperate coastal bays (SW iberia): Insights from the plankton. Harmful Algae 86, 20–36. doi:10.1016/j.hal.2019.03.003

Schiller, J., 1937. Dinoflagellatae. Akad. Verlagsgeselleschaft M.B.H., Leipzig, Vol. I, 617 pp.; Vol. II, 589 pp.

Schwing, F.B., O'Farrel, M., Steger, J.M., Baltz, K., 1996. Coastal Upwelling Indices, West Coast of North America, 1946-1995, NOAA Tech. Rep., NMFS SWFSC, 231, 144p.

Silva, A., Palma, S., Moita, M.T., 2008. Coccolithophores in the upwelling waters of Portugal: Four years of weekly distribution in Lisbon bay. Cont. Shelf Res. 28, 2601–2613. doi:10.1016/j.csr.2008.07.009

Silva, A., Palma, S., Oliveira, P.B., Moita, M.T., 2009. Composition and interannual variability of phytoplankton in a coastal upwelling region (Lisbon Bay, Portugal). J. Sea Res. 62, 238–249. doi:10.1016/j.seares.2009.05.001

Silva, A. M. A. D., 2009. Coccolithophores in coastal waters: Lisbon bay, Portugal. Doctoral dissertation, Universidade de Lisboa, Portugal.

Silva, E.S., 1949. Diatomáceas e dinoflagelados da Baía de Cascais. Portugaliae Acta Biológica (B), Vol. "Júlio Henriques": 300-383.

Smayda, T.J., Borkman, D.G., Beaugrand, G., Belgrano, A., 2004. Responses of marine phytoplankton populations to fluctuations in marine climate. *in*: Marine Ecosystems and Climate Variation: The North Atlantic: A Comparative Perspective. Oxford University Press, Oxford, pp. 49–58.

SNIRH, 2017. Sistema Nacional de Informação de Recursos Hídricos. Boletim de escoamento. http://snirh.apambiente.pt accessed on 03 November 2017.

Throndsen, J., 1978. Preservation and storage, *in*: A., S. (Ed.), Phytoplankton Manual: Monographs on Oceanographic Methodology 6. UNESCO, Paris, pp. 69–74.

Thomas, C.R., 1997. Identifying Marine Phytoplankton. Academic Press, New York. 858 pp.

Tweddle, J.F., Gubbins, M., Scott, B.E., 2018. Should phytoplankton be a key consideration for marine management? Mar. Policy 97, 1–9. doi:10.1016/j.marpol.2018.08.026

Utermöhl, H., 1958. Zur Ver vollkommung der quantitativen phytoplankton-methodik. Mitteilung Internationale Vereinigung Fuer Theoretische unde Amgewandte Limnol. 9, 1–38. doi:10.1080/05384680.1958.11904091

Vale, P., Botelho, M.J., Rodrigues, S.M., Gomes, S.S., Sampayo, M.A. de M., 2008. Two decades of marine biotoxin monitoring in bivalves from Portugal (1986 – 2006): A review of exposure assessment. Harmful Algae 7, 11–25. doi:10.1016/j.hal.2007.05.002

Valente, A.S., da Silva, J.C.B., 2009. On the observability of the fortnightly cycle of the Tagus estuary turbid plume using MODIS ocean colour images. J. Mar. Syst. 75, 131–137. doi:10.1016/j.jmarsys.2008.08.008

Vidal, T., Calado, A.J., Moita, M.T., Cunha, M.R., 2017. Phytoplankton dynamics in relation to seasonal variability and upwelling and relaxation patterns at the mouth of Ria de Aveiro (West Iberian Margin) over a four-year period. PLoS One 12, 1–25. doi:10.1371/journal.pone.0177237

Wang, N., Mertens, K. N., Krock, B., Luo, Z., Derrien, A., Pospelova, V Liange, Y., Bilienb, G., Smithf, K.F., Schepperg, S.D., Wietkampc, S., Tillmannc, U., Gu, H., 2019. Cryptic speciation in Protoceratium reticulatum (Dinophyceae): Evidence from morphological, molecular and ecophysiological data. Harmful Algae, 88, 101610.

Young, J. R., Geisen, M., Cros, L., Kleijne, A., Sprengel, C., Probert, I., Østergaard, J., 2003. A guide to extant coccolithophore taxonomy. Journal of nannoplankton research 1, 1-125.

Chapter 4.

Occurrence of *Ostreopsis* in two temperate coastal bays (SW Iberia): Insights from the plankton

Published as:

Santos, M., Oliveira, P.B., Moita, M.T., David, H., Caeiro, M.F., Zingone, A., Amorim, A., Silva, A. (2019). Ocurrence of *Ostreopsis* in two temperate coastal bays (SW Iberia): Insights from the plankton. Harmful Algae 86, 20–36. https://doi.org/10.1016/j.hal.2019.03.003

Abstract

The benthic genus *Ostreopsis* contains toxic-bloom forming species and is an important cause of concern in warm-temperate and tropical waters. On the coast of Portugal, NE Atlantic, the occurrence of *Ostreopsis* cf. *siamensis* and *Ostreopsis* cf. *ovata* has been reported since 2008 and 2011, respectively. This work aims to understand the favorable conditions for high concentrations of *Ostreopsis* cells in the plankton at two sites, Lagos and Lisbon Bays, located in the South and West coast of Portugal, respectively. This study is based on weekly *Ostreopsis* abundance data in the plankton, from 2011 to 2017, daily satellite and *in situ* sea surface temperature (SST), and meteorological and sea state parameters, namely wind stress and significant wave height. The molecular identification of local *Ostreopsis* spp. is also presented. The maximum cell densities occur between late-summer and autumn. The distribution range of *Ostreopsis* cf. *ovata* is restricted to the South coast, while *Ostreopsis* cf. *siamensis* has a wider distribution range, being also present on the West coast. In the study period, there was only one occurrence of *Ostreopsis* spp., in Lagos Bay, with concentrations within the alert phase of monitoring. In Lagos Bay, high *Ostreopsis* spp. concentrations were related with positive SST anomalies. These high concentrations were often recorded after a period of almost 2-weeks to more than 4-weeks of low sea state (< 0.6 m), followed by short time events of onshore wind and moderate waves (0.6 – 1 m). The former conditions are interpreted as favoring bloom development on the substrate and the latter as causing the re-suspension of *Ostreopsis* cells in the water column. In Lisbon Bay, *O.* cf. *siamensis* occurred in the plankton in few occasions and no clear relation could be established with the studied environmental variables. It is here hypothesized that the recent records of *O.* cf. *siamensis* in Lisbon Bay may correspond to an early colonization stage of an invasion process. Knowledge gained on *Ostreopsis* dynamics along the Portuguese coast can be used for both the improvement of benthic harmful algal blooms (BHABs) monitoring in the region and as a basis to design forecasting models.

Keywords: *Ostreopsis* cf. *ovata*; *Ostreopsis* cf. *siamensis*; Benthic harmful algae; Environmental conditions; Molecular identification; Portuguese coast

4.1. Introduction

Until recently, problems with Harmful Algal Blooms (HABs) in temperate regions were mainly related to planktonic species of several microalgae groups. These blooms can seriously threaten public health and cause high economic losses to fisheries, aquaculture and tourism (Berdalet et al., 2014). In the last two decades, the frequency and geographic spread of benthic HABs (BHABs), in particular of the dinoflagellate *Ostreopsis* Schmidt, have been increasing in temperate areas (Amorim et al., 2012; Bennouna et al., 2012; Parsons et al., 2012; David et al., 2013). Species of this genus are known to produce several analogs of palytoxins, which are the most potent biotoxins reported so far in dinoflagellates (Ciminiello et al., 2010; Ramos and Vasconcelos, 2010; Rossi et al., 2010). The Mediterranean coast has been particularly affected by blooms of *Ostreopsis* species, which have caused several outbreaks leading to human respiratory problems and fever after the inhalation of marine aerosols, skin irritation due to contact with seawater, and economic losses due to beach closures during the summer (Tichadou et al., 2010; Mangialajo et al., 2011). These events have raised new sanitary concerns to environmental and health authorities and have stimulated new research programs (e.g., Zingone et al., 2012).

The genus *Ostreopsis*, with *Ostreopsis siamensis* Schmidt as the type species, includes 11 currently accepted nominal species, which sometimes show subtle morphological differences and are reliably identified only using molecular information (Penna et al., 2005; Sato et al., 2011; David et al., 2013). Species of *Ostreopsis* have been reported from the Mediterranean Sea since 1972 in Villefranche sur Mer, France (Taylor, 1979), but the first bloom was only detected in 1998 on the coast of Tuscany, Italy (Sansoni et al., 2003; Simoni et al., 2003). After that time, *Ostreopsis* blooms have been spreading along the Mediterranean coast, where mainly *Ostreopsis* cf. *ovata* Fukuyo and in some cases *Ostreopsis* cf. *siamensis* have been reported (see Parsons et al., 2012 and Accoroni and Totti, 2016 for a review). Blooms of *Ostreopsis* were also reported from the Moroccan coast (Bennouna et al., 2012) followed by reports of *Ostreopsis* species in NE Atlantic Islands, such as Madeira and the Canary Islands (Penna et al., 2010) and in the mid-Atlantic Azores Archipelago (Silva et al., 2010). At the Portuguese mainland coast, *O.* cf. *siamensis* was identified in 2008 on the Southwest upwelling coast, in Sines (Amorim et al., 2010), and *O.* cf. *ovata* in 2011 on the South coast, in Lagos, the latter corresponding to the first record of an event of high concentration of species of this genus in Portugal (David et al., 2012). As a precautionary measure, local authorities interdicted bathing in 11 beaches of a highly touristic area (Mateus et al., 2012).

The possibility of the existence of a third species in Portugal, *Ostreopsis fattorussoi* Accoroni, Romagnoli & Totti, has recently been suggested (Accoroni et al., 2016).

The dynamics of *Ostreopsis* blooms is still not well understood. Several environmental variables have been proposed to influence the growth of *Ostreopsis* spp. in the benthos (see Parsons et al., 2012; Accoroni and Totti, 2016; Berdalet et al., 2017 for a review). Results of laboratory experiments indicate that temperature and day-length are key factors for bloom development (Granéli et al., 2011; Scalco et al., 2012). The information on the influence of salinity and nutrients on *Ostreopsis* blooms is scarce and based on contrasting results (Accoroni and Totti, 2016). Even so, a recent study reported that the growth of *O.* cf. *ovata* is limited under river influence (Carnicer et al., 2015) and others found that phosphate seems to be the most important nutrient to this species occurrence (Cohu et al., 2013; Accoroni et al., 2015). Hydrodynamism is considered as having a major role in the development of *Ostreopsis* blooms, with higher abundances observed in sheltered areas compared with exposed ones (Totti et al., 2010).

Benthic HABs spreading all over the world have generated new challenges for monitoring programs since they require distinct sampling strategies and methodologies compared with planktonic HABs (GEOHAB, 2012; Berdalet et al., 2017). In the benthic compartment, the method most widely used consists of the collection of natural substrates, such as macroalgae, followed by detachment and quantification of the epibenthic community (Litaker et al., 2010 and references therein). This approach has several problems, including those deriving from different substrate preferences of the dinoflagellates (GEOHAB, 2012), hindering the comparisons among samples, the need of a large number of samples (Lobel et al., 1988) and the high amount of detritus making sample analysis difficult (Tester et al., 2014). Alternative sampling approaches have been proposed (e.g. Tester et al., 2014; Jauzein et al., 2016; Mangialajo et al., 2017; Vassalli et al., 2018), but no consensus has been reached, yet. A further disadvantage in BHABs sampling is the access to samples and, in the case of artificial substrates, two visits to the site are needed to deploy and retrieve them (Tester et al., 2014).

Cells of *Ostreopsis* normally proliferate within mucous sheets forming a thin pellicle, which seem to play an important role in cell aggregation and attachment to substrates (Barone, 2007), but increased hydrodynamism is suggested to favor the release of the benthic cell aggregates into the water column (Totti et al., 2010; Accoroni and Totti, 2016). Several authors have reported a strong positive correlation between the abundance of *Ostreopsis* spp. in the benthic and planktonic compartments (Aligizaki and Nikolaidis, 2006; Mangialajo et

al., 2011; Giussani et al., 2017; Hachani et al., 2018; Jauzein et al., 2018). From the perspective of human exposure to toxins, the highest impact occurs when high cell concentrations in the benthos are accompanied by cells in the plankton, leading to skin irritation and respiratory disorders (Vila et al., 2016). This raises questions regarding the possibility of using planktonic samples as part of an alert system for health risks associated with *Ostreopsis* spp. proliferations. In a recent article, Jauzein and co-workers (2018) discussed several methods used for the estimation of *Ostreopsis* spp. abundance, including the advantages and drawbacks of planktonic surveys, and concluded that the latter may represent a valuable option for the evaluation of the toxic risk to humans, although not the best alternative for monitoring benthic blooms.

In the present study, weekly water samples collected over 7 years, within the National Monitoring Program of HABs, in Lisbon (central West coast) and Lagos (South coast) Bays, were analyzed for the presence of *Ostreopsis* spp. in the plankton. This work aims to: (i) identify the species of *Ostreopsis* present in Portuguese coastal waters; (ii) characterize their spatial and temporal distribution; (iii) understand the meteorological and oceanographic variables that may be associated with the presence of *Ostreopsis* in the water column; and (iv) test the detection of planktonic *Ostreopsis* spp. at concentrations below those currently considered of high risk to human health, *i.e.* 3.0×10^4 cells L^{-1} (Funari et al., 2015; Asnaghi et al., 2017).

4.2. Material and methods

4.2.1. Study area

This work was conducted in two geographically distinct upwelling sheltered bays, on the Atlantic coast of Iberia, both characterized by a maximum tidal range of ~4 m. Lagos Bay (LagB) is located on the South coast of Portugal and Lisbon Bay (LisB) on the West coast (Fig. 4.1).

Lagos Bay is at the SW limit of the Iberian Peninsula and at the NW side of the Gulf of Cadiz. It is located in the northern part of the Canary Current Upwelling System. This Bay is close to Cape São Vicente (CSV), a major coastline discontinuity, which separates the meridionally aligned W coast from the zonal S coast. This Cape is a major upwelling center, mainly between spring and early autumn when north winds are predominant (Relvas and

Barton, 2002). Summer average of Sea Surface Temperature (SST) maps shows that the preferred direction for the spreading of cold water, upwelled north of the cape, is along the southern shelf break and slope (Relvas et al., 2007). This circulation pattern leads to a distinctive wedge-like shape of the SST distribution over the shelf, with warm water close to the coast, bordered by cold water at the shelf break. Satellite image sequence analysis and current measurements show the recurrent development, during the upwelling season, of a warm countercurrent over the inner shelf, progressing from the Gulf of Cadiz, often turning poleward around CSV (Relvas and Barton, 2002, 2005; Relvas et al., 2007). The LagB sampling site is located in D. Ana beach (37°5'28.54" N, 8°40'8.48" W, 35 km to the East of CSV, Fig. 4.1), a sheltered sandy beach with rock formations and macroalgae communities. Between mid-April to the end of June of 2015, the beach was artificially closed on its east side and was filled with offshore dredged sand, which significantly changed the beach morphology and presumably affected the epibenthic communities.

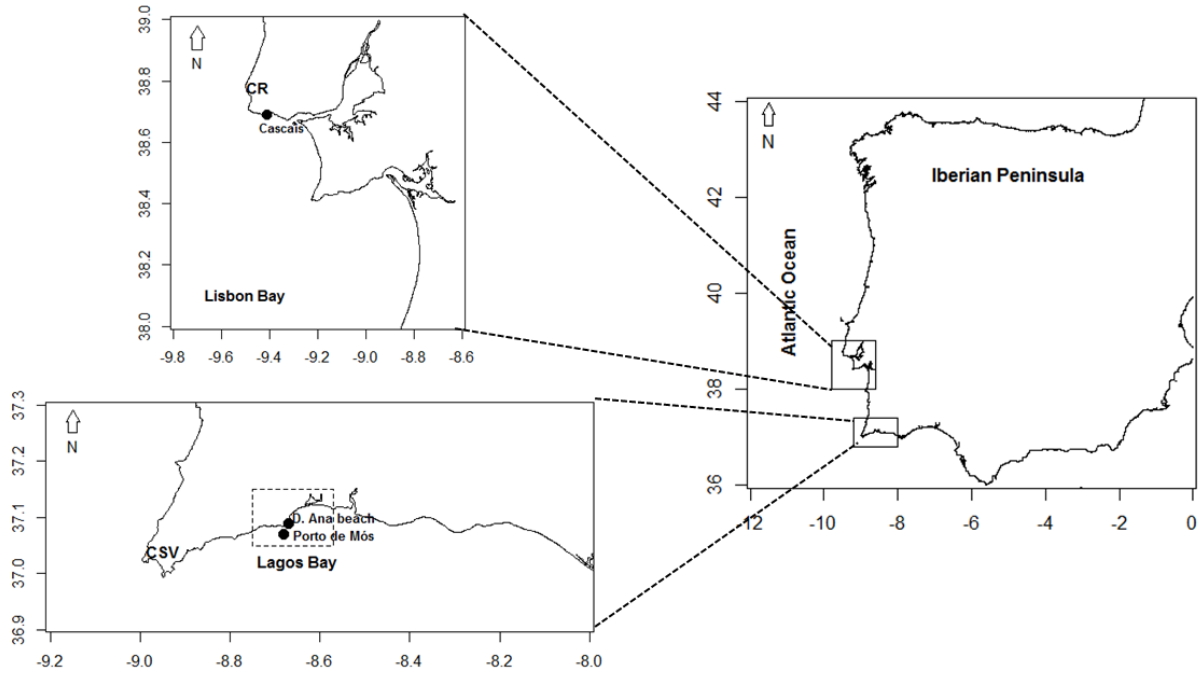

Fig. 4.1. Map of the study area with the location of the sampling stations (Cascais – Lisbon Bay and D. Ana beach – Lagos Bay) and of the sites where the *in situ* temperature data were recorded (Porto de Mós – Lagos Bay).

Lisbon Bay is located in the W coast of Portugal and SE of a major cape, Cape Roca (CR). Along this stretch of coast, seasonal upwelling occurs from spring to early autumn due to steady northerly winds (Wooster et al., 1976; Fiúza et al., 1982; Relvas and Barton, 2002). The sampling station is located on the north side of LisB, where a recurrent upwelling filament occurs, rooted at CR and that extends westward or southward (Moita et al., 2003; Oliveira et al., 2009b). This Bay represents an important coastline discontinuity and is

considered an upwelling shadow area where phytoplankton can be accumulated through different retention mechanisms (Moita et al., 2003; Oliveira et al., 2009a). The sampling site, located in Cascais (38°41'36.82" N, 9°24'52.93" W, about 15 km distant from CR, Fig. 4.1) is at the entrance of a marina, with a rocky bottom and around 7 m depth.

4.2.2. Sampling strategy

Samples were collected under the National Monitoring Program of Harmful Algal Bloom species (HABs) led by IPMA, I.P. - Instituto Português do Mar e da Atmosfera (National Institute for the Sea and Atmosphere). The planktonic data comprised weekly water samples collected from September 2011 to December 2017 in LagB, and from January 2011 to December 2017 in LisB. In LagB samples were collected at surface in the surf zone, and in LisB the water column (0-7 m depth) was integrated with a hose, one hour before high tide. The collected samples were field fixed with 1% neutral Lugol's iodine solution (Utermöhl, 1958). In order to verify the correlation of *Ostreopsis* spp. cell density between the plankton and the benthos, samples of representative macroalgae with the surrounding water were collected by hand with plastic bags during low-tide, from tide pools or by snorkeling to a maximum of 2 m depth, on nine summer/autumn dates between 2013 and 2016 in LagB. The macroalgae assemblages were characterized by cespitose species, although occasionally with the presence of larger specimens of *Plocamium* sp., *Cystoseira* sp. and *Dictyota* sp.. Due to that, the concentration of *Ostreopsis* spp. seldom could be referred to one particular macroalgae species. To detach the epiphytic community, macroalgae samples were vigorously shaken for 1 min and the resulting water was sieved through a 100 µm mesh. The filtrate was collected and stored in plastic bottles. The macroalgae were kept in the plastic bags for fresh weight (FW) determination. In the laboratory, the water samples were measured to a known volume with filter-sterilized seawater and sub-samples fixed with neutral Lugol solution.

4.2.3. Cell abundances

Determination of *Ostreopsis* spp. cell abundances were carried out by settling 50 mL of planktonic samples and 5 mL of benthic samples using the Utermöhl (1958) method (Hasle, 1978). Samples were analyzed with an inverted microscope equipped with phase contrast and bright field illumination (Zeiss IM35 or Leica DMi8), at a magnification of 160, 200 or 400 x.

Abundances of epiphytic *Ostreopsis* were expressed in cells g^{-1} FW of macroalgae and planktonic concentrations in cells L^{-1}.

4.2.4. Culture conditions and molecular analysis

Cell isolation was carried out by capillarity using a Pasteur pipette under an inverted microscope (ZEISS IM35). Isolates were maintained in microwell plates (Thermo Scientific™ Nunc™) or petri-dishes in f/20 medium prepared with seawater from the isolation site, without the addition of silicates. Salinity was adjusted to 33-34 and cells were incubated at 20 ºC under a 14L:10D or 12L:12D photo-cycle. In addition to the strains isolated during the study period, a strain isolated in 2010 (IO 96-05) was also used for the phylogenetic studies (Table 4.1).

For the genomic DNA extraction from *Ostreopsis* cultures and environmental samples, 15-50 mL of each sample were centrifuged for 30 min at 2410 g, the supernatant partially removed, and the sample centrifuged again for 10 min at 17700 g. Some samples were treated with 2 mM NaEDTA before DNA extraction, to dissolve the abundant mucilage produced by *Ostreopsis* spp..

For the amplifications targeting the LSU region, the genomic DNA was extracted by using the CTAB method adapted from Doyle (1991), with addition of Proteinase K at 0.2 mg mL^{-1} and RNaseA at 0.1 mg mL^{-1}. Each DNA sample was stored at -20 °C. PCR amplification was performed using *D1R* and *D3Ca* universal primer pairs (Scholin et al., 1994; Lim et al., 2012) in a C1000 Touch™ Thermal Cycler (Bio-Rad), using the Taq DNA Polymerase (Roche, Germany), in the following PCR conditions: an initial denaturation step of 3 min at 94 ºC, 40 cycles of 35 s at 94 ºC, 35 s at 51 ºC and 1 min 30 s at 72 ºC, and a final extension step of 15 min at 72 ºC. The PCR products were purified with the DNA Isolation Spin-Kit Agarose (PanReac AppliChem). Sequencing was performed at the Molecular Biology Service of the Stazione Zoologica Anton Dohrn in Naples (Italy).

Amplifications targeting the ITS region were performed with genomic DNA of monoclonal *Ostreopsis* strains or environmental samples, extracted according to David et al. (2013) or using a protocol adapted from Silva et al. (2015), by adding to each pellet 250 µL of extraction buffer without KCL and with 100 µg mL^{-1} RNaseA. Each DNA sample was stored at 4 °C. PCR amplification of the 5.8S rDNA-ITS1 regions was performed using the species-

specific primer sets *ovataF/OstreopsisR* and *siamensisF/OstreopsisR* (Battocchi et al., 2010), already confirmed as reliable with environmental samples from the Portuguese coast (Ramos et al., 2015). Amplifications were carried out in a T100™ Thermal Cycler (Applied Biosystems) using the MyTaq™ Red Mix (Bioline, London, UK) in the following PCR conditions: an initial denaturation step of 3 min at 95 ºC, 35 cycles of 15 s at 95 ºC, 15 s at 44.6 ºC and 10 s at 72 ºC, and a final extension step of 5 min at 72 ºC. The PCR products were purified with the DNA Clean and Concentrator™-5 Kit (Zymo Research). Sanger sequencing was performed by STAB VIDA (Portugal), using the same sets of primers.

Table 4.1. *Ostreopsis* species from Lagos (LagB) and Lisbon (LisB) Bays identified in this study. "Env Sp" means environmental sample.

Species	Code	Location	Geographic coordinates	Date of Collection	Type of Sampling	Amplified region	GenBank ID
O. cf. *siamensis*	IO 96-05	Cascais, LisB	38°41'36.82" N, 9°24'52.93' W	2010-09-28	Plankton net	LSU	MH520096
O. cf. *siamensis*	IO 96-06	Cascais, LisB	38°41'36.82" N, 9°24'52.93' W	2011-06-14	Plankton net	LSU	MH520097
O. cf. *siamensis*	IPMA 01	Cascais, LisB	38°41'36.82" N, 9°24'52.93' W	2011-09-07	Plankton net	ITS1-5.8S - ITS2	MH478526
O. cf. *siamensis*	IO 96-07	D. Ana beach, LagB	37°5'28.54" N, 8°40'8.48" W	2015-05-13	Plankton net	ITS1-5.8S rDNA	MH478556
O. cf. *siamensis*	IO 96-08	D. Ana beach, LagB	37°5'28.54" N, 8°40'8.48" W	2015-05-13	Plankton net	ITS1-5.8S rDNA	MH478557
O. cf. *ovata*	Env Sp 1	D. Ana beach, LagB	37°5'28.54" N, 8°40'8.48" W	2016-09-27	Macroalgae	ITS1-5.8S rDNA	MH478554
O. cf. *ovata*	Env Sp 2	D. Ana beach, LagB	37°5'28.54" N, 8°40'8.48" W	2016-09-27	Macroalgae	ITS1-5.8S rDNA	MH478555
O. cf. *ovata*	IO 124-03*	D. Ana beach, LagB	37°5'28.54" N, 8°40'8.48" W	2016-09-27	Macroalgae	ITS1-5.8S rDNA	——
O. cf. *siamensis*	Env Sp 3*	D. Ana beach, LagB	37°5'28.54" N, 8°40'8.48" W	2016-09-27	Macroalgae	ITS1-5.8S rDNA	——
O. cf. *siamensis*	Env Sp 4*	D. Ana beach, LagB	37°5'28.54" N, 8°40'8.48" W	2016-09-27	Macroalgae	ITS1-5.8S rDNA	——
O. cf. *siamensis*	IO 96-09*	D. Ana beach, LagB	37°5'28.54" N, 8°40'8.48" W	2016-09-27	Macroalgae	ITS1-5.8S rDNA	——
O. cf. *siamensis*	IO 96-10*	D. Ana beach, LagB	37°5'28.54" N, 8°40'8.48" W	2016-09-27	Macroalgae	ITS1-5.8S rDNA	——
O. cf. *siamensis*	IO 96-11*	D. Ana beach, LagB	37°5'28.54" N, 8°40'8.48" W	2016-09-27	Macroalgae	ITS1-5.8S rDNA	——
O. cf. *siamensis*	IO 96-12*	D. Ana beach, LagB	37°5'28.54" N, 8°40'8.48" W	2016-09-27	Macroalgae	ITS1-5.8S rDNA	——

*****Amplicons not sequenced. Identification made by PCR with the species-specific primer pairs *ovataF/OstreopsisR* and *siamensisF/OstreopsisR* (Battocchi et al., 2010).

All the above-mentioned kits were used according to the manufacturer's instructions. The LSU and ITS sequences (Table 4.1) were aligned using BioEdit v7.0.9 (Hall, 1999) and MUSCLE (www.ebi.ac.uk) software. The alignment was manually verified. Resulting sequences were deposited in GenBank (National Center for Biotechnology Information, NCBI) with the accession numbers provided in Table 4.1.

4.2.5. Phylogenetic analysis

Phylogenetic analyses were performed on ITS1-5.8S rDNA sequences (Table 4.1). The final dataset comprised 52 sequences, 5 from this study and 47 from GenBank. Two sequences of *Coolia monotis*, which is a close relative of *Ostreopsis*, were used to root the tree. Phylogenetic relationships were inferred by Maximum Likelihood (ML), Maximum Parsimony (MP) and Neighbor Joining (NJ) methods using MEGA7 (Kumar et al., 2016). Bootstrap confidence values were calculated from 3000 replications in all analyses (NJ, MP and ML). Prior to ML analyses, a test to find the best fitting model of DNA substitution was performed with the Akaike information criterion corrected in MEGA7. The model used was the one with the lowest BIC (Bayesian Information Criterion) scores. Maximum Likelihood analyses were conducted using the Tamura 3-parameter model (T92, Tamura, 1992) + gamma (5 categories (+G = 0.3914)) + invariable sites proportion (+I = 23.79% sites). The MP tree was obtained using the Subtree-Pruning-Regrafting (SPR) algorithm (Nei and Kumar, 2000) with a search level of 1 in which the initial trees were obtained by the random addition of sequences (10 replicates). Neighbor Joining was computed using the Tamura 3-parameter method (Tamura, 1992). All positions containing gaps and missing data were eliminated. There was a total of 124 positions in the final dataset.

4.2.6. Meteorological and oceanographic data

Temperature in LagB was recorded daily at 3 m depth in station "Porto de Mós" (Fig. 4.1), at 1 nautical mile from the coast, between June 2014 and October 2017, using a Temperature Data Logger (TidbiT v2/Pro v2, Onset). Daily *in situ* temperature data were also recorded at D. Ana beach during summer/autumn of 2013 and 2016. In LisB, at the sampling site, weekly surface temperature data were collected between 2011 and 2016, using a multi-parameter probe (YSI Model 30).

Daily data from the Multi-scale Ultra-high Resolution (MUR) sea surface temperature (SST) product starting on 1 June 2002, with 0.01º spatial resolution (~1 km), were obtained on PODAAC (Physical Oceanography Distributed Active Archive Center, http://podaac.jpl.nasa.gov/) of Jet Propulsion Laboratory of NASA (National Aeronautics and Space Administration). Synoptic SST distributions off SW Iberia were obtained from the EUMETSAT's OSI-SAF (Ocean and Sea Ice Satellite Application Facility) single-sensor NAR SST product.

As a proxy for the quantification of hydrodynamics, meteorological and sea state parameters (surface wind components – U_{10}/V_{10} and significant wave height – SWH) were obtained from the ECMWF HRES-SAW (European Centre for Medium-Range Weather Forecasts - High RESolution Stand Alone Wave model, https://www.ecmwf.int/en/forecasts/datasets/set-ii) with a spatial resolution of 0.1º (~10 km) (Janssen, 2004). The sea surface wind stress (WSTR) components were computed using the quadratic drag law $\tau_{x,y} = \rho_a C_D |v| U_{10},V_{10}$; where $|v|$ is the wind speed (m s^{-1}), U_{10}/V_{10} are respectively the east-west and north-south, 10 m wind components (m s^{-1}), ρ_a is the air density (1.22 kg m^{-3}) and C_D is the drag coefficient (0.0013) (e.g. Schwing et al., 1996). Significant wave height was considered as weak (wave height < 0.6 m) or moderate (0.6-1 m).

Time series parameters (SST, SWH, and WSTR) in LagB were extracted from the grid-point coincident with the offshore site used for *in situ* daily temperature acquisition ("Porto de Mós") and in LisB from the grid-point closest to the location where the phytoplankton samples were collected. The data were treated using the R 3.1.2 software (R Core Team, 2016) and Ferret, an interactive computer visualization and analysis environment developed and maintained at NOAA/PMEL (Pacific Marine Environmental Laboratory) (Hankin et al., 1996).

4.2.7. Statistical analyses

Generalized linear mixed-effects models (GLMMs) were fitted to assess the relative importance of meteorological and oceanographic variables (explanatory variables) in explaining high *Ostreopsis* spp. concentrations (dependent variable) in plankton. GLMMs combine the properties of linear mixed models and of generalized linear models, both widely used in ecology (Bolker et al., 2009). This method provides a more flexible approach for

analyzing non-normal data, such as count or proportion, when comparing with classical statistical procedures (Bolker et al., 2009).

Skewness-kurtosis graph (Cullen and Frey, 1999) was used to choose, among a family of distributions candidates, the one that best fitted the dependent variable based on the Akaike's information criterion (AIC) (Akaike, 1973). After that, it was considered to use a Negative Binomial distribution.

Considering that population growth and other biological processes are not instantaneous responses to environmental changes, the explanatory variables were calculated for different time periods relative to the sampling date, consistent with the processes that they are hypothesized to reflect. To account for the effects of temperature, sea state, wind and solar radiation conditions to the high *Ostreopsis* spp. concentrations in plankton, the variables considered were: average SST one month prior to sampling; average SST anomaly 3-months prior to sampling; average of SWH in the second and third weeks before sampling (low SWH on Tables 4.4 and 4.5); third-quartile of SWH in the week before sampling (high SWH on Tables 4.4 and 4.5); most frequent wind direction in the week before sampling (considered as a categorical variable); average WSTR one week before sampling; and average Photosynthetically Active Radiation (PAR) 3-months prior to sampling. Potential correlations among these variables ($r \geq 0.90$) were analyzed by computing a heterogeneous correlation matrix, Pearson correlation coefficients and *p*-value (Crawley, 2007; Hafdahl, 2008). Multicollinearity between covariates was checked using the generalized variance inflation factors (GVIF) (Fox and Monette, 1992) and any variable that were linearly dependent on others were removed from the fitting GLMMs (e.g., Zuur et al., 2010). Here, a threshold of $GVIF < 5$ was used as an indicator to the presence of collinear structure, and so, PAR was removed from the analysis in Lisbon Bay.

Final model diagnostic test was assessed based on the normal Q-Q plot (Wu, 2010).The Negative Binomial GLMMs were fitted using the package "glmmADMB" in R (Fournier et al., 2012; Skaug et al., 2013). All analyses were performed using the R 3.1.2 software (R Core Team, 2016) and considering a significance level of $\alpha < 0.05$.

4.3. Results

4.3.1. Molecular identification and phylogeny

Concerning *Ostreopsis* strains isolated in LisB, during and before the study period (three samples), the amplicons of the ITS and LSU regions only showed the presence of *O.* cf. *siamensis* (Table 4.1). Amplifications targeting the ITS1-5.8S rDNA region of the 11 *Ostreopsis* cultures and environmental samples from LagB showed the presence of two species, namely *O.* cf. *ovata* (three samples) and *O.* cf. *siamensis* (eight samples) (Table 4.1). From the seven sequenced amplicons, five were confirmed as *O.* cf. *siamensis* and two as *O.* cf. *ovata* (Table 4.1).

The tree topologies from NJ, ML and MP based on ITS1-5.8S rDNA were identical, therefore only the ML tree is shown here (Fig. 4.2). Strong bootstrap values allowed the identification of six main clades in the phylogenetic tree.

One of these comprised all sequences of *O.* cf. *ovata* and could be separated into four subgroups. The first subgroup included sequences of the Atlantic Ocean, Mediterranean Sea and one from the Pacific Ocean, and the two sequences obtained in the present study from environmental samples (MH478554 and MH478555). The second and third subgroups included sequences from South China Sea and Gulf of Thailand, respectively. The last subgroup of this clade had sequences from the Celebes Sea and Malacca Strait.

A second major clade included all sequences of *O.* cf. *siamensis* from the Atlantic Ocean, Mediterranean Sea and Pacific Ocean. The three sequences from the present study (MH478526, MH478556 and MH478557) were also included in this clade. Other two well-defined clades included sequences of the recently described species *Ostreopsis rhodesiae* Verma, Hoppenrath & S.A.Murray and *Ostreopsis fattorussoi* Accoroni, Romagnoli & Totti. The *O. rhodesiae* clade had all sequences originated from the Pacific, while the clade of *O. fattorussoi* included sequences from the Atlantic Ocean and Mediterranean Sea. The last two clades were named as *Ostreopsis* sp. 1 and *Ostreopsis* sp. 2 (Sato et al., 2011), both including sequences from the Pacific Ocean.

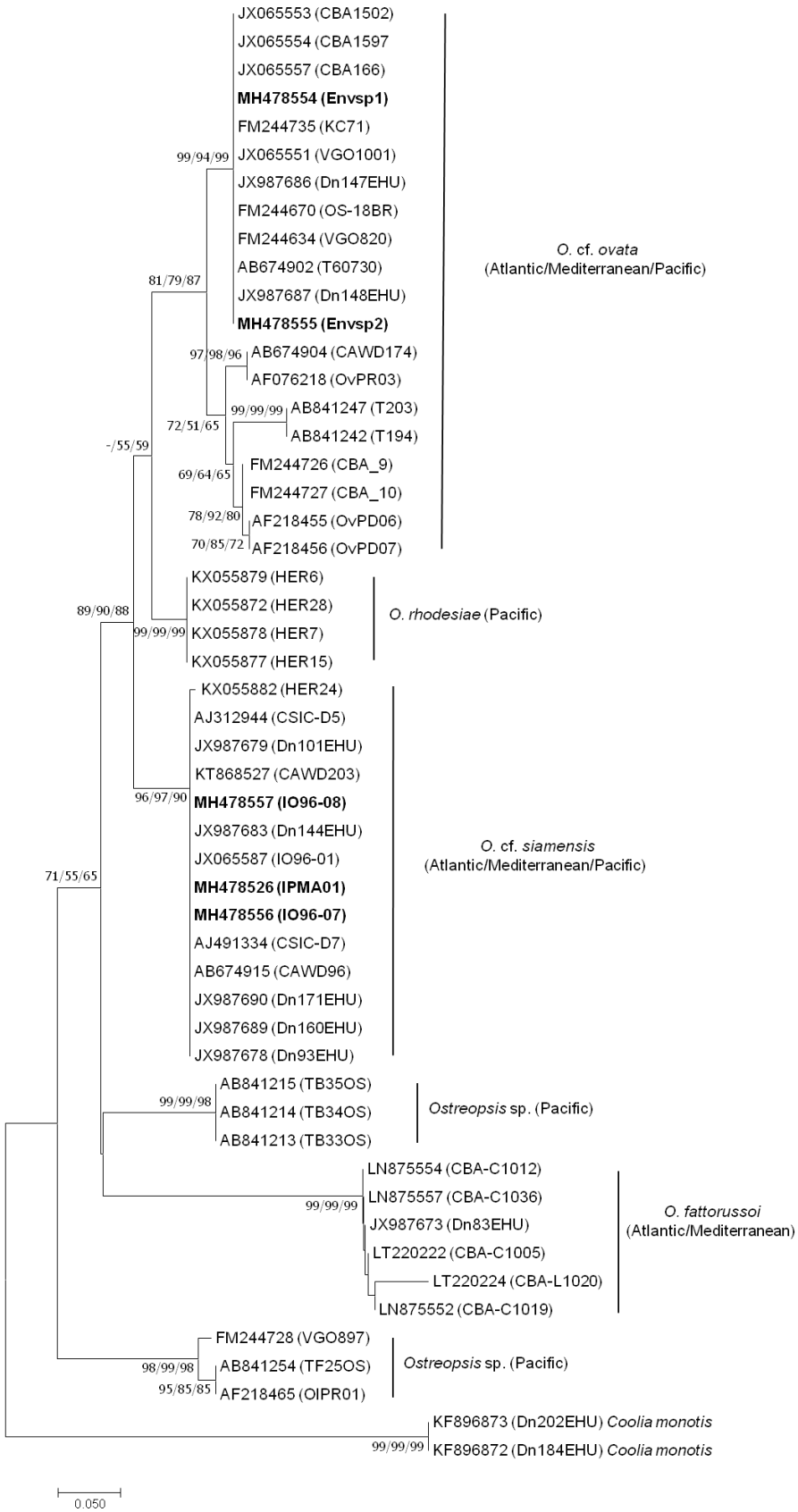

Fig. 4.2. Maximum Likelihood phylogenetic tree of *Ostreopsis* strains based on the ITS1-5.8S rDNA sequences. Numbers on the major nodes represent NJ (3000 pseudoreplicates, before slash), MP (3000 pseudoreplicates, between slashes) and ML (after slash) bootstrap values. The tree was rooted using *Coolia monotis* (strains Dn202EHU and Dn184EHU) as outgroup. Strains from this study are in bold.

4.3.2. Relation between benthic and planktonic *Ostreopsis* abundances

A total of 31 macroalgae samples, collected in Lagos Bay on nine different summer/autumn dates between 2013 and 2016, were analyzed to assess the relation between epiphytic *Ostreopsis* spp. abundances and planktonic cell concentrations (Table 4.2). In all samples analyzed, the epiphytic assemblage was dominated by pennate diatoms (data not shown). The most abundant dinoflagellates, other than *Ostreopsis* spp., were *Prorocentrum lima*, *Prorocentrum* cf. *rhathymum* and *Coolia* spp.. The cell density of *Ostreopsis* spp. showed high variability between replicates (up to three orders of magnitude) (Table 4.2). The highest concentration of epiphytic *Ostreopsis* spp. (1.16×10^5 cells g^{-1} FW of macroalgae) was recorded in September 2013, three days after the maximum concentration was recorded in the plankton (1.68×10^4 cells L^{-1}) (Table 4.2). In 2014, several macroalgae samples were collected in June, September and October and the epiphytic *Ostreopsis* spp. was recorded at low concentrations and only in a few samples. This coincided with the lack of cell records in the water column samples. Whenever cells of *Ostreopsis* spp. were detected in the plankton, these were also recorded in the epiphytic community. Figure 4.3 shows the correlation, in a base-10 logarithmic scale, between average *Ostreopsis* spp. concentrations on macroalgae and water column concentrations. Results showed a significant positive correlation ($n = 9$, $r = 0.87$, $p = 0.001$), explaining a high percentage of variation between both type of samples ($R^2 = 0.76$, Fig. 4.3).

Table 4.2. Epiphytic and planktonic *Ostreopsis* spp. abundances between 2013 and 2016 in Lagos Bay. Min: minimum, Max: maximum.

Date	Number of macroalgae samples	*Ostreopsis* Cells g^{-1} FW of macroalgae (Min-Max)	*Ostreopsis* Cells g^{-1} FW of macroalgae (Average)	*Ostreopsis* Cells L^{-1} of seawater
2013-09-16	7	1647-29600	9420	16840
2013-09-19	5	1255-115831	28162	8660
2013-09-20	2	4820-21641	13230	7360
2014-06-16	3	0	0	0
2014-09-09	3	0-4	1	0
2014-10-11	3	0-20	7	0
2015-06-29	2	1438-2145	1791	100
2016-07-26	2	0-35	17	0
2016-09-27	4	75-45251	15378	20

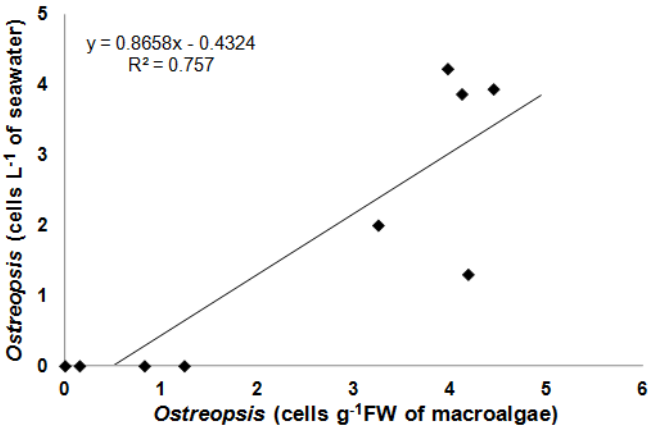

Fig. 4.3. Correlation between average epiphytic *Ostreopsis* spp. abundance (cells g^{-1} FW of macroalgae) and concentration in the water column (cells L^{-1}), on a base-10 logarithmic scale.

4.3.3. Planktonic *Ostreopsis* time series

4.3.3.1. Lagos Bay

A high interannual variability was recorded in planktonic *Ostreopsis* cell abundances in LagB, with higher concentrations always recorded in late-summer/early-autumn and cells never recorded between late November and mid-April (Fig 4.4A).

On 18 September 2011, mucilaginous filaments were observed at the sea surface and a seawater sample collected two days after showed a concentration of 5.4 x 10^3 cells L^{-1} of *Ostreopsis* spp. (Fig. 4.4A). In mid-September 2013, the highest concentration for the area was reported with values reaching around 1.7 x 10^4 cells L^{-1}. In the beginning of October 2016 and mid-November 2017, two lower peaks were recorded, reaching 640 cells L^{-1} and 1.1 x 10^3 cells L^{-1}, respectively. By contrast, in 2012 no cells were detected, and in 2014 and 2015 cells were detected sporadically and in low numbers (maximum of 100 cells L^{-1} in July 2015) (Fig. 4.4A).

4.3.3.2. Lisbon Bay

In LisB *Ostreopsis* cf. *siamensis* was rarely recorded in the plankton (Fig. 4.4B). The first detection was in September 2011 (40 cells L^{-1}), followed by a record in May 2015 (20 cells L^{-1}). In late September 2017, a few cells started to be detected in the water column and in mid-October concentrations of *O.* cf. *siamensis* reached the maximum value for the whole study period (620 cells L^{-1}). The Bay of Lisbon has been weekly monitored for HABs since

2001 and *Ostreopsis* species were not detected in planktonic samples prior to the present report (IPMA, I.P., data not shown).

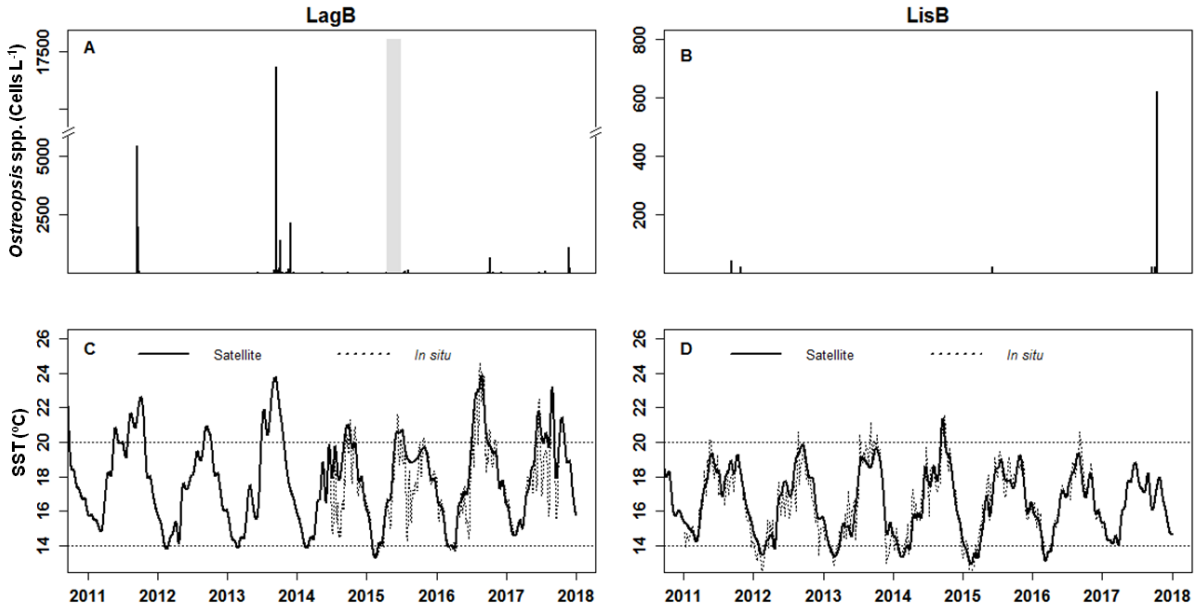

Fig. 4.4. Time series of *Ostreopsis* cell concentration in the plankton, cells L^{-1} (A and B) and satellite (solid line) *vs* offshore *in situ* (dotted line) SST, ºC (C and D) in LagB (left panel) and LisB (right panel). Grey rectangle in A: period when the beach was artificially filled with sand. Horizontal dotted lines in C and D indicate temperature values of 14 ºC and 20 ºC.

4.3.4. Relationship between planktonic *Ostreopsis* and environmental conditions

4.3.4.1. Lagos Bay

Water temperature

Satellite-derived SST data were validated against *in situ* temperature data recorded offshore (Fig. 4.4C). Both series showed strong correlations (r = 0.91), although satellite data did not reproduce summer surface cooling events when it overestimated SST in more than 3 ºC (2014, 2015 and 2017 in Fig. 4.4C). As this *in situ* data series only covered 2014 onwards, satellite SST data were used to cover the whole study period.

The seasonal pattern of SST in LagB showed a high interannual variability, although with some similarities among years (Fig. 4.4C). Temperature values varied between 14 ºC in winter and 24 ºC in summer. In general, summer SST always reached values above 20 ºC. The years 2011 and 2017 were characterized by winters with a minimum SST about 1 ºC warmer (~ 15 ºC) than the remaining study winters (Fig. 4.4C). Summers in 2013 and 2016 showed the highest SST (~ 24 ºC). At the sampling site, measured SST exceeded 25 ºC in

2013 (July and September/mid-October) and in 2016 (July and mid-August/September) (Fig. 4.5).

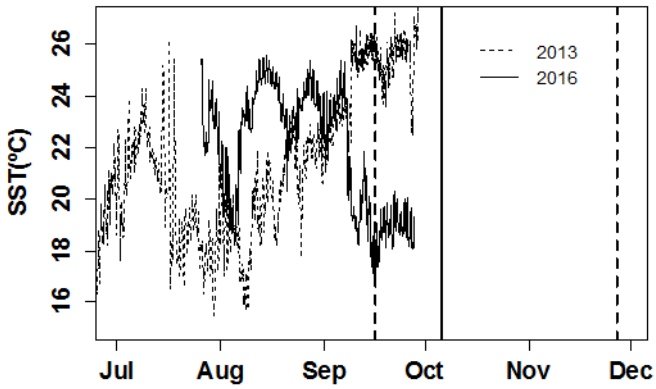

Fig. 4.5. *In situ* SST (ºC) from D. Ana beach (LagB) during summer/autumn. Dashed line: 2013; Solid line: 2016.

The years with higher *Ostreopsis* concentration in the water column were characterized by positive SST anomalies (with periods reaching more than 3 ºC relative to the 2003-2017 average) almost all year round (2011 and 2017, Fig. 4.6A and 4.6G, respectively), or at least during the summer period (2013 and 2016, Fig. 4.6C and 4.6F, respectively). In 2011, *Ostreopsis* spp. was detected in the plankton in late September in two consecutive (7 days) samples with temperature above 20 ºC (Fig. 4.6A).

In 2013 and 2016 (Fig. 4.6C and 4.6F), summer/autumn temperatures were always above 20°C, and above 22 ºC for over one month. It was within this period, mid-September of 2013, that the highest concentrations of *Ostreopsis* spp. were recorded. A second peak of lower magnitude was recorded later in 2013 (November), at lower temperatures (17 ºC), following a steady decrease from 24 °C. In both 2013 episodes, cells were recorded in the water column for 42 days (Table 4.3). In October 2016, *Ostreopsis* spp. was detected for 9 days with temperatures above 20 ºC (Fig. 4.6F) and in November 2017 for 6 days, when temperatures were close to 20 ºC, following a one-month period of positive SST anomalies and a short period of negative anomalies (Fig. 4.6G). The years 2012 and 2014 stand out as very cold years, dominated by negative anomalies even in summer, rarely reaching temperature values above 20 ºC (Fig. 4.6B and 4.6D). In 2012, *Ostreopsis* spp. was not detected in the plankton and in 2014 it was recorded at quite low concentrations. The year 2015 was atypical, with a warm spring/early-summer followed by a cold summer/autumn and, as referred above, characterized by a major change in beach morphology. In that year, cells of *Ostreopsis* spp. could occasionally be detected in the water column but at low concentrations (Fig. 4.6E).

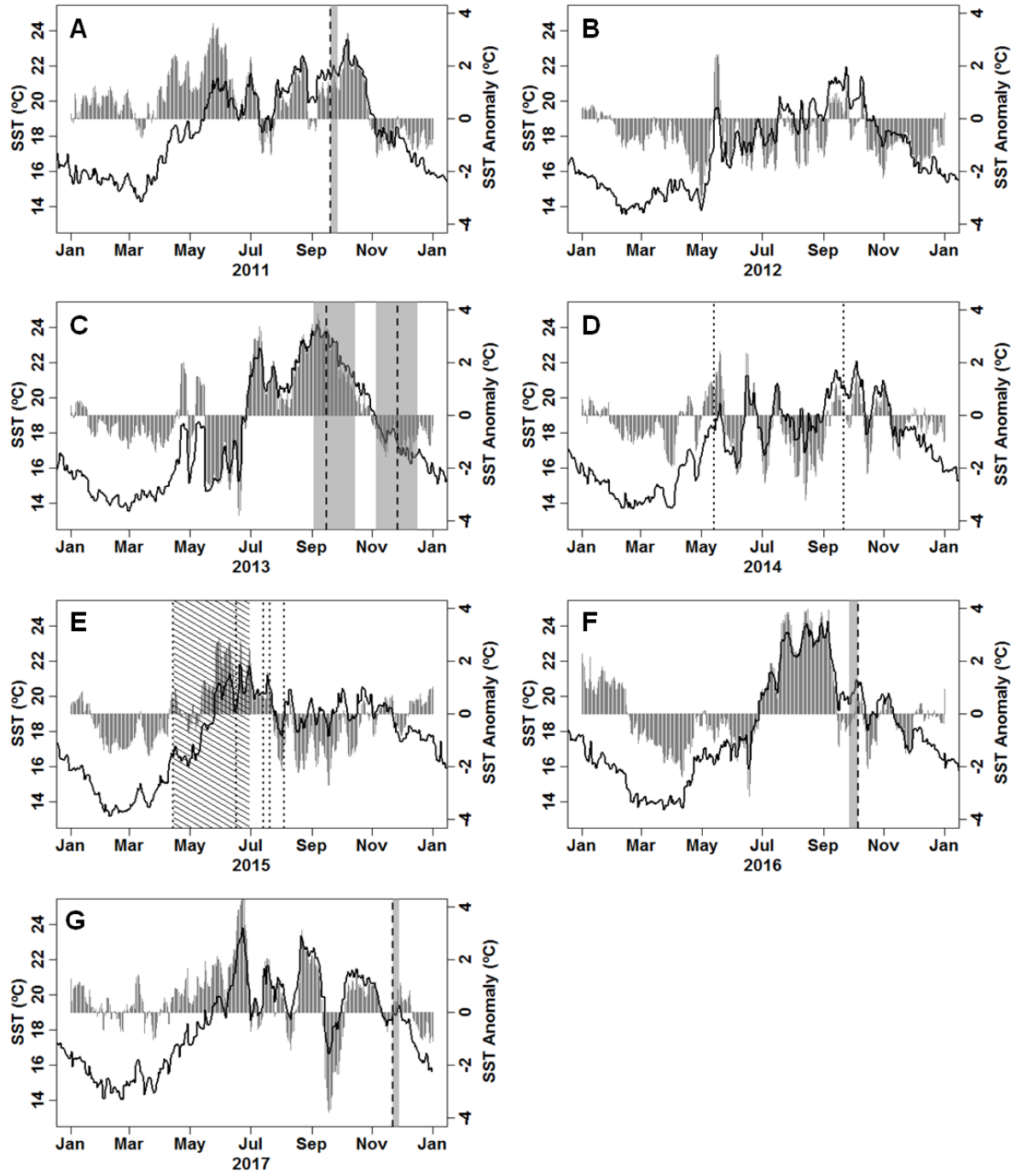

Fig. 4.6. Annual satellite SST and SST anomaly (ºC) of 15-years data (2003-2017) from LagB. Solid line: SST; Grey vertical bars: SST anomaly; Grey area: period of *Ostreopsis* spp. in the plankton; Dashed line: maximum cell concentration; Dotted line: presence of cells in water; Dashed area in 2015: period when the beach was artificially filled with sand.

Wind and waves

Figure 4.7 shows, for the years 2011, 2013, 2016 and 2017, the wind stress (WSTR) and the significant wave height (SWH) conditions one month before the record of the first event of

moderate SWH (0.6-1 m) and during the maximum cell concentration of *Ostreopsis* spp.. These conditions are summarized in Table 4.3, together with the number of cells in the water column, SST and the number of days with weak SWH (< 0.6 m). Except for 2017, the highest concentrations of *Ostreopsis* in the water column were recorded within a week after two short events (1-2 days each) of increased SWH (> 0.6 m) (Fig. 4.7, right panel). In 2017, these events occurred three weeks before the *Ostreopsis* spp. peak. These events of moderate sea state were induced by changes in the direction of the predominant winds (Fig. 4.7, left panel), generally from N/NW (weak upwelling favorable winds, < 0.1 N m^{-2}) to SE (weak downwelling favorable winds). Before the increase of SWH, the conditions were dominated by weak SWH for a period of almost 2-weeks to more than 4-weeks (Fig. 4.7, right panel).

4.3.4.2. Lisbon Bay

Water temperature

As for LagB, in LisB *in situ* temperature data recorded were used to validate the SST satellite data (Fig. 4.4D). The two dataset showed strong correlations (r = 0.92) and the satellite data were used to provide a continuous daily SST record. During the study period, SST ranged between winter values always below 14 ºC and summer values seldom above 20 ºC (Fig. 4.4D). The maximum SST (21.5 ºC) was recorded in mid-September 2014.

Considering the SST anomalies relative to the 15-year mean (Fig. 4.8), 2011 and 2017 were dominated by positive anomalies from January until July, reaching more than 2 ºC above the mean in spring and summer, respectively (Fig. 4.8A and 4.8G). This contrasts with the period from 2012 to 2016, when the first half of the year was dominated by negative SST anomalies (Fig. 4.8B to 4.8F).

In LisB the first records of cells of *O.* cf. *siamensis* occurred in 2011 (Fig. 4.8A) and the maximum concentration was recorded in 2017, in early-autumn (Fig. 4.8G). In both cases, the observations followed winters about 1 ºC warmer (~14 ºC) than the other studied winters (Fig. 4.4D). In 2017, *O.* cf. *siamensis* was observed in the water over almost one month (Table 4.3) and the maximum concentration coincided with a period of increased temperature (18 ºC), about one month after a sharp temperature decrease (Fig. 4.8G).

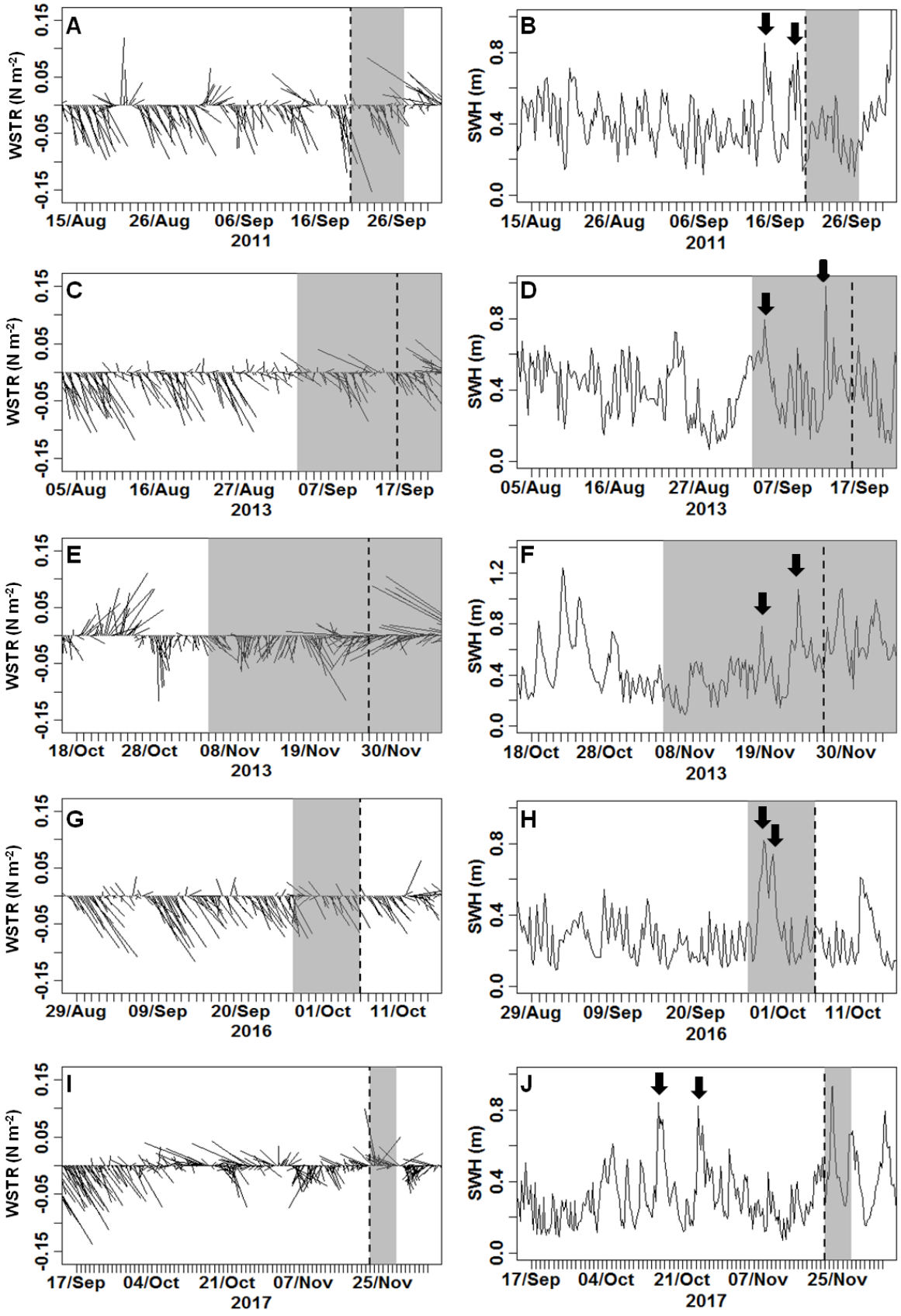

Fig. 4.7. Wind stress (WSTR, N m^{-2}), left panel, and significant wave height (SWH, m), right panel, during the maximum cell concentrations and one month before the first event of moderate SWH, to the years presenting *Ostreopsis* spp. peaks in LagB. Grey rectangle: period of *Ostreopsis* spp. in the plankton; Dashed line: maximum cell concentration; Arrows: events of increasing SWH.

Table 4.3. Summary of oceanographic and meteorological conditions during planktonic *Ostreopsis* peaks in Lagos and Lisbon Bays. Range: temperature variation in the month before the peak, indicating the temperature tendency (*i.e.*, increasing or decreasing); Avg: average; Peak: temperature recorded at the maximum *Ostreopsis* concentration.

Site	Year	Month	Maximum cell concentration (Cells L^{-1}) and date of occurrence	Presence of cells in the plankton (days)	Temperature (ºC)		Significant Wave Height (SWH)		Wind Stress (N m^{-2})
					Previous month (Range and Avg)	Peak	Weak (days)	Moderate (days)	
LAGOS BAY	2011	Sep	5420 on 20-Sep	7 (20/27-Sep)	[20-22.5] ($\overline{x}$ = 21.0)	21.5	24	2 events of 2 days	1st SE 2nd NW
	2013	Sep/Oct	16840 on 16-Sep	42 (3-Set/15-Oct)	[20-24] ($\overline{x}$ = 21.0)	23.5	11	2 events of 1 day	SE
		Nov/Dec	2120 on 27-Nov	42 (5-Nov/17-Dec)	[20-17] ($\overline{x}$ = 19.0)	17.0	18	2 events of 1 day	1st NW 2nd SE
	2016	Oct	640 on 6-Oct	9 (27-Sep/6-Oct)	[24-19] ($\overline{x}$ = 21.5)	20.5	> 30	2 events of 1 day	SE
	2017	Nov/Dec	1100 on 22-Nov	6 (22/28-Nov)	[21-18] ($\overline{x}$ = 19.5)	19.0	> 30	2 events of 2 days	SE
LISBON BAY	2017	Sep/Oct	620 on 17-Oct	29 (18-Sep/17-Oct)	[15.5-19] ($\overline{x}$ = 17.2)	18.0	0	0 events *	S

* No events of moderate SWH, but 1 day with increasing SWH from around 1 m to 2.5 m.

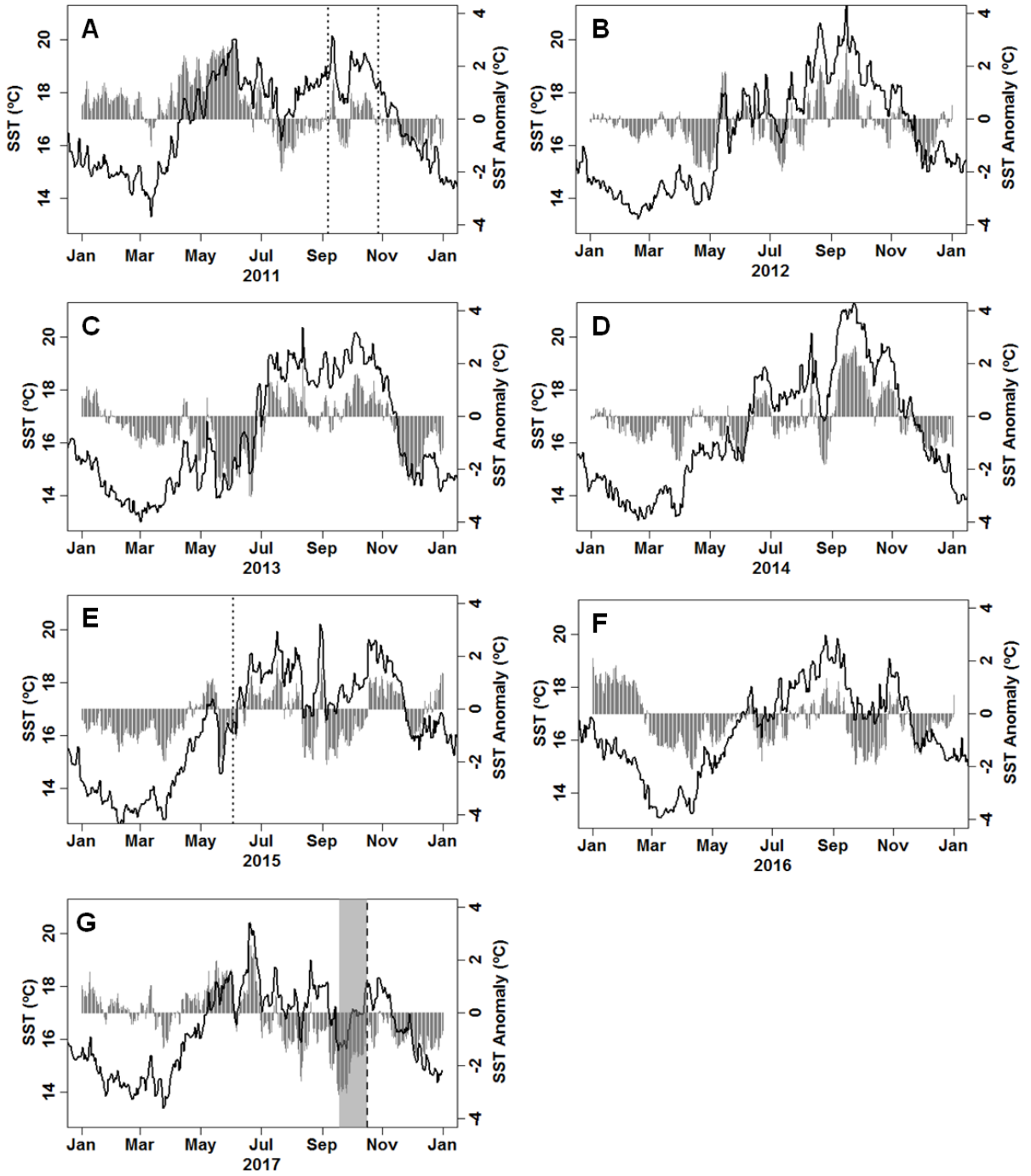

Fig. 4.8. Annual satellite SST and SST anomaly (ºC) of 15-years data (2003-2017) from LisB. Solid line: SST; Grey area: SST anomaly; Grey rectangle: period of *O.* cf. *siamensis* in the plankton; Dashed line: maximum cell concentration; Dotted line: presence of cells.

Wind and waves

In LisB**,** SWH values were considerably higher than the ones observed in LagB, frequently above 1 m height. In 2017, in the month prior to the detection of the *O.* cf. *siamensis* peak, N upwelling favorable winds predominated (Fig. 4.9A) and SWH ranged between 0.5 and 2 m (Fig. 4.9B). Under these conditions *Ostreopsis* spp. cells were detected in the water column, but only reached the peak 5 days after a shift from N to S winds, with maximum intensity of 0.1 N m^{-2} (Fig. 4.9A), which caused an increase of SWH from around 1 m to 2.5 m (Fig. 4.9B).

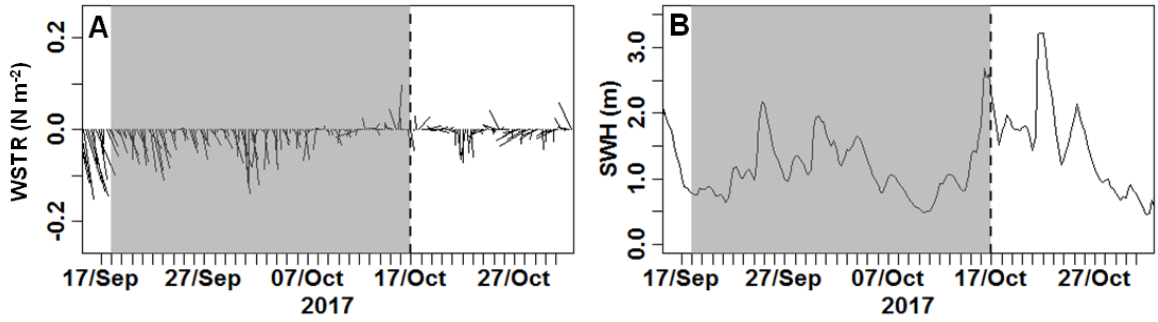

Fig. 4.9. Wind stress (WSTR, N m^{-2}), A, and significant wave height (SWH, m), B, one month before the maximum cell concentrations, during 2017 in LisB. Grey rectangle: period of *O.* cf. *siamensis* in the plankton; Dashed line: maximum cell concentration.

4.3.5. Oceanographic characterization of SW Iberia during late-summer

Figure 4.10 shows the satellite SST for the SW Iberia in September of 2011 and 2013, when the two most intense peaks of planktonic *Ostreopsis* spp. were recorded in LagB. Under northerly winds on the W coast, upwelling favorable conditions predominated and the SST was lower over the shelf and along the W coast, with a much stronger SST gradient between cold upwelled waters (Fig. 4.10A and 4.10C) and warmer stratified waters (Fig. 4.10B and 4.10D) in LagB than LisB. Depending on the duration and intensity of N winds, the SST decrease in the S coast was more or less intense. When the wind changed its direction to SE, SST increased along the S coast (Fig. 4.10B and 4.10D). In 2011, the separation between the warmer waters coming from the east, along the S coast, and the cold waters upwelled along the W coast and turning eastward around CSV was clearly observed (Fig. 4.10B). In 2013, the S coast was characterized by warm waters near the coast and offshore, turning northwards

around CSV under SE winds (Fig. 4.10D). During that period along the W coast, warmer waters were observed from CSV to Lisbon Bay. Nevertheless, a cold filament turning eastward around the CSV could still be observed along the shelf break (Fig. 4.10C).

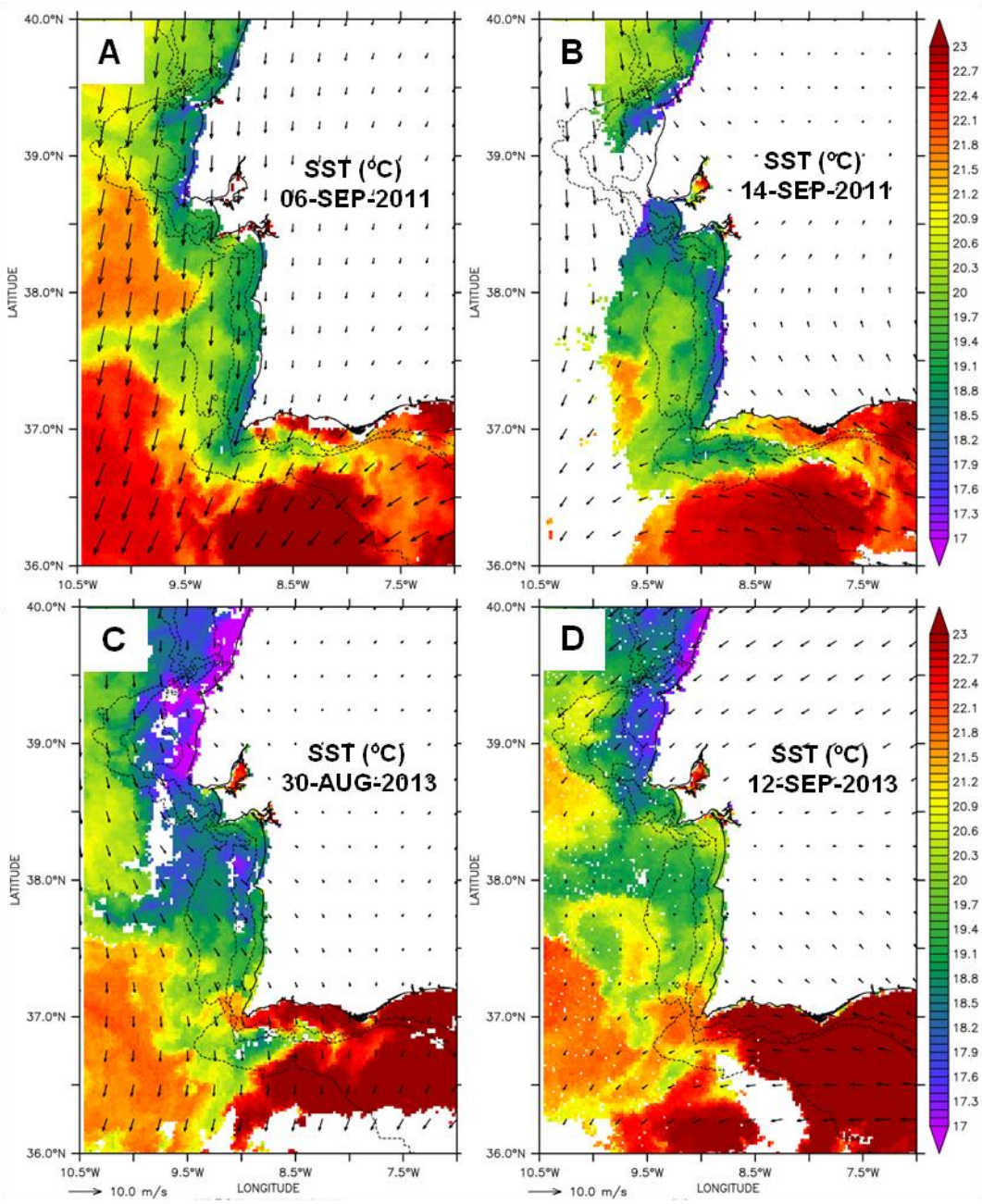

Fig. 4.10. SST (ºC) and surface winds (arrows, scale in 10 m s^{-1}) in SW Iberia during late-summers of 2011 (upper panel) and 2013 (bottom panel).

4.3.6. Statistical analyses

The results of GLMM indicate that *Ostreopsis* spp. concentrations in Lagos Bay increase significantly with the increase in the average SST anomaly 3-months prior to sampling ($p < 0.001$, Table 4.4). A significant positive correlation was also found between *Ostreopsis* cells and the averaged PAR 3-months prior to sampling ($p < 0.01$, Table 4.4). A strong negative significant correlation was found between *Ostreopsis* spp. and low SWH ($p < 0.01$, Table 4.4), meaning that cell concentrations were favored by weaker SWH in the second and third weeks before sampling. Higher *Ostreopsis* cell concentrations were also related to the decrease in NW and W winds ($p < 0.01$, Table 4.4), and N and SW winds ($p < 0.05$, Table 4.4). Although not significant, GLMM indicated as potentially important the relationship between *Ostreopsis* cells and the higher SWH values observed in the week before sampling ($p = 0.08$, Table 4.4). In Lisbon Bay, GLMM only showed a weak negative significant relationship between *Ostreopsis* spp. abundance and the average SST anomaly 3-months prior to sampling ($p < 0.05$, Table 4.5). No other significant relationships were found between *Ostreopsis* spp. and the remaining variables.

Table 4.4. Overview of the significant results of the best-fit GLMM testing for the effect of different variables on *Ostreopsis* spp. concentration in Lagos Bay. Significant *p*-values are shown in bold; potentially important *p*-value is shown in italic.

Variables	Estimate	Standard Error	*p*-value
SST average	-0.979	0.582	0.093
SST anomaly	4.360	1.310	**0.001**
Low SWH	-1.820×10^{1}	6.330	**0.004**
High SWH	7.280	4.150	*0.079*
N wind	-3.970	1.650	**0.016**
NE wind	-1.830	2.760	0.507
NW wind	-6.680	2.090	**0.001**
SE wind	-1.520	2.970	0.609
SW wind	-8.080	3.170	**0.011**
W wind	-6.900	2.480	**0.005**
WSTR	-4.660×10^{1}	6.140×10^{1}	0.448
PAR	0.000	0.000	**0.002**

Table 4.5. Overview of the significant results of the best-fit GLMM testing for the effect of different variables on *Ostreopsis* spp. concentration in Lisbon Bay. Significant *p*-value is shown in bold.

Variables	Estimate	Standard Error	*p*-value
SST average	0.410	1.750	0.814
SST anomaly	-9.160	4.100	**0.025**
Low SWH	-9.210	8.180	0.261
High SWH	0.229	3.100	0.941
N wind	1.480×10^{2}	7.790×10^{3}	0.998
NE wind	-1.040×10^{1}	2.080×10^{4}	1.000
NW wind	-1.080×10^{1}	9.000×10^{3}	0.999
S wind	-4.390	9.360×10^{3}	1.000
SE wind	-1.860	2.080×10^{4}	1.000
SW wind	1.470×10^{1}	7.790×10^{3}	0.998
W wind	-1.450×10^{1}	1.830×10^{5}	1.000
WSTR	1.440×10^{2}	1.010×10^{2}	0.157

4.4. Discussion

4.4.1. Benthic and planktonic *Ostreopsis* abundances

The species of the benthic genus *Ostreopsis* can colonize a wide range of substrates, from macroalgae to hard substrates and sand (see Parsons et al., 2012 for a review). They can also be considered as tychoplanktonic species since their occurrence in the water column is frequently reported (Vila et al., 2001; Simoni et al., 2003; Aligizaki and Nikolaidis, 2006; Mangialajo et al., 2011; Giussani et al., 2017; Jauzein et al., 2018) associated with water turbulence and diel vertical migrations (Jauzein et al., 2018). From the perspective of public health protection, the presence of toxic *Ostreopsis* spp. in the plankton is a major concern since the reported health problems are related to the inhalation of marine aerosols or direct contact in bathing water (Berdalet et al., 2017). Human health problems have been associated with planktonic concentrations of *Ostreopsis* spp. above 3.0×10^{4} cells L^{-1} (Mangialajo et al., 2011; Vila et al., 2016). According to the more recent Italian guidelines for the management of *O.* cf. *ovata* blooms, an alert phase of the monitoring plan should be implemented when cell concentrations are recorded in the water column between $1.0 \times 10^{4}$and 3.0×10^{4} cells L^{-1} together with optimal environmental conditions (Funari et al., 2015, Asnaghi et al., 2017). The monitoring of planktonic samples presents several advantages in relation to benthic

sampling, including ease of sampling, non-disturbance of habitat and the possibility of being integrated in ongoing HAB monitoring programs, which leads to optimized resource management.

In the present study, the analysis of a 7-year long time series of weekly data collected in two coastal sites, included in the national monitoring program of HABs, reveals that *Ostreopsis* spp. concentrations in the water column above 1.0 x 10^4 cells L^{-1} were only recorded once (1.7 x 10^4 cells L^{-1}), on the S coast. These values are consistent with the absence of reported cases of respiratory illnesses or skin irritations from bathers or workers in the studied area. In agreement with previous studies (Aligizaki and Nikolaidis, 2006; Mangialajo et al., 2011; Giussani et al., 2017; Hachani et al., 2018; Jauzein et al., 2018), the abundance of planktonic *Ostreopsis* spp. showed a high correlation with cell abundances in the benthos. Both these results are encouraging and support the use of plankton surveys for rapid assessment of toxic risks associated with *Ostreopsis* blooms (Jauzein et al., 2018). Yet further work is needed to characterize the relation between *Ostreopsis* spp. concentrations in the benthic and the planktonic compartments and eventually define alert and alarm threshold concentrations in the plankton.

4.4.2. *Ostreopsis* temporal and spatial trends

Since the first detection on the SW Iberian Portuguese coast in 2008 (Amorim et al., 2010), *Ostreopsis* has been reported from different sites of the Iberian Portuguese coast (Amorim et al., 2012; David et al., 2012, 2013; Mateus et al., 2012; Ramos et al., 2015). In the present work, two species were identified in Lagos Bay (South coast), namely, *O.* cf. *ovata* and *O.* cf. *siamensis*, the latter also found in Lisbon Bay (West coast). Both species belong to the clades of *O.* cf. *ovata* and *O.* cf. *siamensis* of the Atlantic/Mediterranean/Pacific group, in accordance with previous studies in the same area (David et al., 2013; Ramos et al., 2015). Accoroni and co-workers (2016) hypothesized the presence of the new species *O. fattorussoi* along the Atlantic coast of Iberia but this could not be confirmed by results of the present work.

Both *O.* cf. *ovata* and *O.* cf. *siamensis* are present in the Mediterranean Sea, where the former has a much wider distribution range than the latter (see Accoroni and Totti, 2016 for a review). In the NE Atlantic, the known distribution of *O.* cf. *siamensis* suggests that this species has a wider distribution than *O.* cf. *ovata*, with records from NE Spain to the Atlantic

Moroccan coast (Amorim et al., 2012; Bennouna et al., 2012; David et al., 2013). These two *Ostreopsis* species are known to co-occur (Battocchi et al., 2010; Mangialajo et al., 2011), which was also observed in this study.

Results of the present study indicate that *Ostreopsis* spp. abundance and frequency is higher in Lagos Bay than in Lisbon Bay. In Lagos Bay, a significant positive relationship was found between *Ostreopsis* spp. abundances and the higher PAR observed in the 3-months before the sampling, which may reflect the seasonality of species occurrence. In fact, highest concentrations of *Ostreopsis* spp. (above 5.0×10^3 cells L^{-1}) were recorded during late-summer/early-autumn period (September), intermediate densities (between 5.0×10^2 and 5.0×10^3 cells L^{-1}) in mid-autumn (October/November) and few or no cells recorded between winter and early-summer. In Lisbon Bay, the highest concentration (6.2×10^2 cells L^{-1}) was also recorded in early-autumn (September/October). This seasonal pattern agrees with that described from the northern Adriatic Sea, where the maxima were generally observed in September-October (Monti et al., 2007; Totti et al., 2010; Mangialajo et al., 2011; Accoroni et al., 2015), but contrasts with observations in the geographically closer coast of Catalonia (NW Mediterranean), where blooms are predominantly recorded in summer (Mangialajo et al., 2011). In other temperate regions, as in the Sea of Japan and New Zealand waters, *Ostreopsis* spp. blooms have been recorded from summer to autumn (Shears and Ross, 2009; Selina and Orlova, 2010; Selina et al., 2014).

The much lower abundance or even the absence of *O.* cf. *siamenis* in most samples from Lisbon Bay cannot be explained by the difference in sampling method used at this site. The National Monitoring Program of HABs analyzed surface samples (2001 to 2012) and net samples (2001 to 2017) from the same site and results were not different from the ones obtained in the present study (IPMA, I.P., data not shown).

4.4.3. Relationship between planktonic *Ostreopsis* and environmental conditions

Little is known on the ecology of *Ostreopsis* species along the Atlantic Iberian coast, and particularly on the mechanisms that may favor their high concentrations in the plankton. In the following sections, the main factors suggested as key parameters for the *Ostreopsis* bloom dynamics in the Mediterranean Sea, namely temperature (Mangialajo et al., 2008; Scalco et al., 2012) and hydrodynamics (Totti et al., 2010), are discussed.

4.4.3.1. Water temperature

Temperature is a main factor governing the geographic range of dinoflagellates and particularly of cyst-forming ones, whereby the distribution boundaries tend to follow maximum summer and minimum winter isotherms (Dale, 1996). Until further evidence, the distribution of *O*. cf. *ovata* in the Atlantic Iberian coast is apparently restricted to the South coast of Portugal, which is south the latitude crossed by the 20 ºC isotherm for maximum summer SST (Dale, 1996). Given the distribution of *O*. cf. *ovata* in other temperate areas with winter minima below 0 ºC but summer temperatures reaching 25 ºC (Selina and Orlova, 2010; Selina et al., 2014), it is here hypothesized that it is not the minimum winter SST but the maximum summer SST that limits the spread of *O*. cf. *ovata* further north.

The importance of water temperature on *Ostreopsis* blooms has been described in some studies, but in other cases no clear correlation was found (see Accoroni and Totti, 2016 for a review). In the present work, it was not possible to discern a pattern of temperature change, or optimal temperature, leading to the onset of planktonic populations. These were detected both after an increasing temperature tendency (from 20 to 24 ºC in Lagos Bay and from 15.5 to 19 ºC in Lisbon Bay) and a decreasing temperature tendency (e.g. from 24 to 19 ºC in Lagos Bay), and peaks were associated with variable temperature values (17-23.5 ºC). Studies in the northern Adriatic Sea report peaks of *Ostreopsis* not always coinciding with maximum temperature values, whereas the onset of the bloom was related to a threshold value of around 25 ºC, achieving peak values generally 70–100 days after this threshold was reached (Accoroni et al., 2015). This observation was related to the attainment of the optimal temperature for cyst germination of *O*. cf. *ovata* (Accoroni et al., 2014). Regarding *O*. cf. *siamensis*, cyst germination is reported to occur between 10 and 20 ºC, while encystment takes place at values lower than 10 ºC (Pearce et al., 2001). In Lagos Bay, in 2013 and 2016, temperatures above 25 ºC were reached between 60-80 days before the *Ostreopsis* spp. maximum in plankton, in agreement with the results of Accoroni et al. (2015) and suggesting a possible role of cysts in the dynamics of Ostreopsis spp.. So far, no studies on cysts of *Ostreopsis* spp. exist for the S and W Iberian coasts and further work is needed to understand the role of temperature in modulating the overwintering seed populations and how this affects the onset of blooms.

In the present work, in Lagos Bay, a significant relationship was found between the high concentrations of *Ostreopsis* spp. in the plankton and positive SST anomalies in the months

preceding these events, suggesting that seasonal temperatures play a major role in population dynamics.

The occurrence of *O*. cf. *siamensis* in Lisbon Bay has been sporadic and always with low concentrations, suggesting that environmental conditions are close to the tolerance limits of the species. In Iberia, this species has been reported further north, in the southeastern Bay of Biscay, in an area where summer temperatures reach 25 ºC (Laza-Martinez et al., 2011). The record of the highest planktonic density of *O.* cf. *siamensis* in Lisbon Bay in the present study was in 2017, concomitant with the first detection of a benthic bloom of the species in the same area (David et al., 2018). David et al. (2018), found higher concentration of *O.* cf. *siamensis* in plankton (2.1 x 10^3 cells L^{-1}) in Lisbon Bay, but on a rocky beach, which they suggests as being a hotspot to this species. It is now well established that the NE Atlantic has experienced large-scale biogeographical changes in response to climate change, in some cases with a northerly 10º latitude movement of warmer water plankton in 50 years (Edwards, 2016 and references therein). This suggests that the presence of *O*. cf. *siamensis* in Lisbon Bay, being the known northern limit in the W Iberian coast, may also be a reflection of a warming trend in the NE Atlantic. The few, short, and low abundance occurrences of *O*. cf. *siamensis* in this Bay may correspond to an early colonization stage of the invasion process, when populations are restricted to short periods of favorable environmental conditions or spatially constrained to favorable micro-habitats (Walther et al., 2009). This, combined with the few events recorded, may contribute to the difficulty in understanding the relation between *O.* cf. *siamensis* and seasonal temperature in the Lisbon Bay.

4.4.3.2. Hydrodynamics

Several studies refer that higher abundances of *Ostreopsis* occurred in sheltered areas when compared with areas exposed to high hydrodynamics (Vila et al., 2001; Shears and Ross, 2009; Totti et al., 2010). The influence of hydrodynamics on *Ostreopsis* proliferations is actually difficult to assess since in the literature this environmental feature is usually defined subjectively and several authors use different reference parameters (e.g. Shears and Ross, 2009; Selina et al., 2014; Giussani et al., 2017).

Lisbon and Lagos Bays presented quite different sea state conditions during summer/autumn periods, when *Ostreopsis* cells were recorded in the water column. Lisbon Bay was characterized by wave height generally above 1 m, while in Lagos this value was seldom

reached. In Lagos Bay, a significant correlation was found between high planktonic *Ostreopsis* concentrations and low wave height recorded in the second and third weeks before sampling. This low sea state conditions are considered by several authors to favor cell growth on the benthic substrata (Mangialajo et al., 2008; Shears and Ross, 2009; Bennouna et al., 2012; Accoroni et al., 2015). It was also found that the relaxation of upwelling favorable winds along both West and Southern coasts (northerly and westerly winds, respectively) were favorable conditions to the *Ostreopsis* spp. occurrence. In addition, results suggest that after the calm period mentioned above, two short events (1-2 days each) of moderate wave intensity, mostly caused by onshore winds, seem to be favorable conditions for re-suspension of *Ostreopsis* cells to the water column. Nevertheless, the occurrence of cells in the water column in 2017 could not be related to the occurrence of moderate wave events. Turbulence caused by wave events can play a role in the re-suspension mechanism to the water column, but the existence of a benthic population is a pre-requisite, and other processes such as diel vertical migration should also be considered. The complex interplay between hydrodynamics and biological variables may justify the difficulty in finding a clear relation between hydrodynamics and planktonic populations of *Ostreopsis*. This enhances the importance of implementing surveys on both the benthic and planktonic compartments, when investigating benthic HABs.

4.5. Conclusions

The present study focusing on planktonic *Ostreopsis* along the Portuguese coast is an important step towards the understanding of the local population dynamics. Present results on the species range suggest that the highly toxic *O.* cf. *ovata* is restricted to the South coast, possibly related to temperature thresholds that do not allow its expansion northwards. The low toxicity species *O.* cf. *siamensis* has a wider distribution range, with Lisbon Bay representing its current known northern limit in western Iberia. In Lagos Bay, where *Ostreopsis* spp. have been detected since 2011 in the water column, peaks occur with a pattern of positive SST anomalies but within a wide range of seawater temperatures. In addition, high *Ostreopsis* spp. concentrations in water column are favored by of a period of about 2-weeks with low sea conditions in the previous weeks. The presence of *Ostreopsis* cf. *siamensis* in Lisbon Bay may correspond to an early colonization stage of an invasion process that, if it follows the classic sequence, may be followed by an increase in frequency and duration of the species'

occurrences. So far, *Ostreopsis* spp. have not been responsible for human illnesses or harmful environmental effects along the Atlantic Iberian coasts. Nevertheless, the recent history of *Ostreopsis* blooms in the Mediterranean Sea is an indication of the need to implement preventive management strategies to safeguard coastal ecosystem services. In the present work, data obtained through the national monitoring program of HABs allowed the detection of planktonic *Ostreopsis* well below thresholds considered of human concern, showing the cost-effective value of this monitoring approach. There is an urgent need to understand the ecology and bloom dynamics of benthic populations of *Ostreopsis* spp. and understand how they relate to planktonic populations, in order to enable forecasting models and effective prevention measures.

Acknowledgments

Financial support of M. Santos was provided by a Portuguese PhD grant from FCT (SFRH/BD/52560/2014). This work was financially supported by IPMA, I.P. (SNMB-Monitor/MARE2020), MARE (UID/MAR/04292/2019) and CCMAR (UID/Multi/04326/2013). A. Silva also acknowledges former FCT funding (SFRH/BPD/63106/2009) and current IPMA funding (IPMA-BCC-2016-35), and H. David acknowledges FCT funding (SFRH/BPD/121365/2016). The authors would like to thanks to "Fundação Vodafone Portugal" for the *in situ* summer temperature data at D. Ana beach, and to "Testa & Cunhas, SA", "SOPROMAR" and "Marina de Lagos" for logistic support during fieldwork. A special thanks to João Paulo Medeiros and José Lino Costa for all orientation and help on the statistical analyses, and to Ricardo Melo for help in macroalgae identification. The authors also thank Luciano Júnior and Vera Veloso for help in field and laboratory work, and IPMA colleagues that ensured the observation of 2017 samples. The authors also acknowledge all the other technicians and colleagues from IPMA for sample collection and fieldwork support. M. Santos appreciates the support provided by colleagues at SZN during the stay in Naples, and Elvira Mauriello and the Molecular Biology Service for the LSU sequences. The authors wish to acknowledge the use of the Ferret program, a product of NOAA's Pacific Marine Environmental Laboratory (information is available at http://ferret.pmel.noaa.gov/Ferret/). The authors thank the two anonymous reviewers for their comments and suggestions to improve this work.

References

Accoroni, S., Romagnoli, T., Pichierri, S., Totti, C., 2014. New insights on the life cycle stages of the toxic benthic dinoflagellate *Ostreopsis* cf. *ovata*. Harmful Algae 34, 7–16. http://dx.doi.org/10.1016/j.hal.2014.02.003

Accoroni, S., Glibert, P.M., Pichierri, S., Romagnoli, T., Marini, M., Totti, C., 2015. A conceptual model of annual *Ostreopsis* cf. *ovata* blooms in the northern Adriatic Sea based on the synergic effects of hydrodynamics, temperature, and the N:P ratio of water column nutrients. Harmful Algae 45, 14–25. http://dx.doi.org/10.1016/j.hal.2015.04.002

Accoroni, S., Romagnoli, T., Penna, A., Capellacci, S., Ciminiello, P., Dell'Aversano, C., Tartaglione, L., Abboud–Abi Saab, M., Giussani, V., Asnaghi, V., Chiantore, M., Totti, C., 2016. *Ostreopsis fattorussoi* sp. nov. (Dinophyceae), a new benthic toxic *Ostreopsis* species from the eastern Mediterranean Sea. J. Phycol. 52, 1064–1084. http://dx.doi.org/10.1111/jpy.12464

Accoroni, S., Totti, C., 2016. The toxic benthic dinoflagellates of the genus *Ostreopsis* in temperate areas: a review. Adv. Oceanogr. Limnol. 7, 1–15. http://dx.doi.org/10.4081/aiol.2016.5591

Akaike, H., 1973. Information theory and an extension of the maximum likelihood principle. in: Petrov, B.N., Csaki, F. (Eds.). Proceedings of the 2nd International Symposium on Information Theory. Budapest, Akademiai Kiado, pp. 267-281.

Aligizaki, K., Nikolaidis, G., 2006. The presence of the potentially toxic genera *Ostreopsis* and *Coolia* (Dinophyceae) in the North Aegean Sea, Greece. Harmful Algae 5, 717–730. http://dx.doi.org/10.1016/j.hal.2006.02.005

Amorim, A., Veloso, V., Battocchi, C., Penna, A., 2012. Occurrence of *Ostreopsis* cf. *siamensis* along the upwelling coast of Portugual (NE Atlantic), in: Pagou, K.A., Hallegraeff, G.M. (Eds.), Proceedings of the 14th International Conference on Harmful Algae. International Society for the Study of Harmful Algae and Intergovernmental Oceanographic Commission of Unesco, pp. 10–12.

Amorim, A., Veloso, V., Penna, A., 2010. First detection of *Ostreopsis* cf. *siamensis* in Portuguese coastal waters. Harmful Algae News 42, 6–7.

Asnaghi, V., Pecorino, D., Ottaviani, E., Pedroncini, A., Bertolotto, R.M., Chiantore, M., 2017. A novel application of an adaptable modeling approach to the management of toxic microalgal bloom events in coastal areas. Harmful Algae 63, 184–192. http://dx.doi.org/10.1016/j.hal.2017.02.003

Barone, R., 2007. Behavioural trait of *Ostreopsis ovata* (Dinophyceae) in Mediterranean rock pools: the spider's strategy. Harmful Algae News 33,1–3.

Battocchi, C., Totti, C., Vila, M., Masó, M., Capellacci, S., Accoroni, S., Reñé, A., Scardi, M., Penna, A., 2010. Monitoring toxic microalgae *Ostreopsis* (dinoflagellate) species in coastal waters of the Mediterranean Sea using molecular PCR-based assay combined with light microscopy. Mar. Pollut. Bull. 60, 1074–1084. http://dx.doi.org/10.1016/j.marpolbul.2010.01.017

Bennouna, A., EL Attar, J., Abouabdellah, R., Chafik, A., Penna, A., Oliveira, P.B., Palma, S., Moita, M.T., 2012. *Ostreopsis* cf. *siamensis* blooms in Moroccan Atlantic Upwelling waters (2004-2009), in: Pagou, P., Hallegraeff, G. (Eds.), Proceedings of the 14th International Conference on Harmful Algae. International Society for the Study of Harmful Algae and IOC of UNESCO. pp. 19–22.

Berdalet, E., McManus, M.A., Ross, O.N., Burchard, H., Chavez, F.P., Jaffe, J.S., Jenkinson, I.R., Kudela, R., Lips, I., Lips, U., Lucas, A., Rivas, D., Ruiz-de la Torre, M.C., Ryan, J., Sullivan, J.M., Yamazaki, H., 2014. Understanding harmful algae in stratified systems: Review of progress and future directions. Deep. Res. Part II Top. Stud. Oceanogr. 101, 4–20. http://dx.doi.org/10.1016/j.dsr2.2013.09.042

Berdalet, E., Tester, P., Chinain, M., Fraga, S., Lemée, R., Litaker, W., Penna, A., Usup, G., Vila, M., Zingone, A., 2017. Harmful Algal Blooms in Benthic Systems: Recent Progress and Future Research. Oceanography 30, 36–45. http://dx.doi.org/10.5670/oceanog.2017.108

Bolker, B. M., Brooks, M. E., Clark, C. J., Geange, S. W., Poulsen, J. R., Stevens, M. H. H., and White, J. S. S., 2009. Generalized linear mixed models: a practical guide for ecology and evolution. Trends Ecol. Evol. (Amst.) 24, 127–135. http://dx.doi.org/10.1016/j.tree.2008.10.008

Carnicer, O., Guallar, C., Andree, K.B., Diogène, J., Fernández-Tejedor, M., 2015. *Ostreopsis* cf. *ovata* dynamics in the NW Mediterranean Sea in relation to biotic and abiotic factors. Environ. Res. 143, 89–99. doi:10.1016/j.envres.2015.08.023

Ciminiello, P., Dell'Aversano, C., Iacovo, E. Dello, Fattorusso, E., Forino, M., Grauso, L., Tartaglione, L., Guerrini, F., Pistocchi, R., 2010. Complex palytoxin-like profile of *Ostreopsis ovata*. Identification of four new ovatoxins by high-resolution liquid chromatography/mass spectrometry. Rapid Commun. Mass Spectrom. 24, 2735–2744.

Cohu, S., Mangialajo, L., Thibaut, T., Blanfuné, A., Marro, S., Lemée, R., 2013. Proliferation of the toxic dinoflagellate *Ostreopsis* cf. *ovata* in relation to depth, biotic substrate and

environmental factors in the North West Mediterranean Sea. Harmful Algae 24, 32–44. http://dx.doi.org/10.1016/j.hal.2013.01.002

Crawley, M.J., 2007. The R Book. John Wiley & Sons Ltd., The Atrium, Southern Gate, Chichester, West Sussex, England, 951 pp.

Cullen, A.C., Frey, H.C., 1999. Probabilistic Techniques in Exposure Assessment: A Handbook for Dealing with Variability and Uncertainty in Models and Inputs. Plenum Press, Plenum Publishing Corporation, New York, USA, 335 pp.

Dale, B., 1996. Dinoflagellate cyst ecology: modeling and geological applications., in: Jansonius, J., McGregor, D.C. (Eds.), Palynology: Principles and Applications. American Association of Stratigraphic Palynologists Foundation, Dallas, pp. 1249–1275.

David, H., Laza-Martínez, A., Miguel, I., Orive, E., 2013. *Ostreopsis* cf. *siamensis* and *Ostreopsis* cf. *ovata* from the Atlantic Iberian Peninsula: Morphological and phylogenetic characterization. Harmful Algae 30, 44–55. http://dx.doi.org/10.1016/j.hal.2013.08.006

David, H., Moita, M.T., Laza-Martínez, A., Silva, A., Mateus, M., de Pablo, H., Orive, E., 2012. First bloom of *Ostreopsis* cf. *ovata* in the continental Portuguese coast. Harmful Algae News 45, 12–13.

David, H., Nascimento, P., Caeiro, M.F., Melo, R., Amorim, A., 2018. Bloom of *Ostreopsis* cf. *siamensis* in the Bay of Lisbon. Harmful Algae News 60, 11–12.

Doyle, J., 1991. DNA Protocols for Plants, in: Hewitt, G.M., Johnston, A.W.B., Young, J.P.W. (Eds.), Molecular Techniques in Taxonomy. NATO ASI Series (Series H: Cell Biology). Springer, Berlin, Heidelberg.

Edwards, M., 2016. Impacts and effects of ocean warming on plankton, in: Laffoley, D., Baxter, J.M. (Eds.), Explaining Ocean Warming: Causes, Scale, Effects and Consequences. Full report. Gland, Switzerland: IUCN, pp. 75–86. http://dx.doi.org/10.2305/IUCN.CH.2016.08.en

Fiúza, A.F.D., de Macedo, M.E., Guerreiro, M.R., 1982. Climatological space and time variation of the Portuguese coastal upwelling. Oceanol. Acta 5, 31–40.

Fournier, D. A., Skaug, H. J., Ancheta, J., Ianelli, J., Magnusson, A., Maunder, M. N., Nielsen, A. , Sibert, J., 2012. AD Model Builder: using automatic differentiation for statistical inference of highly parameterized complex nonlinear models. Optim Method Softw 27, 233–249. https://doi.org/10.1080/10556788.2011.597854

Fox, J., Monette, G., 1992. Generalized collinearity diagnostics. J Am Stat Assoc. 87, 178–183.

Funari, E., Manganelli, M., Testai, E., 2015. *Ostreospis* cf. *ovata* blooms in coastal water: Italian guidelines to assess and manage the risk associated to bathing waters and recreational activities. Harmful Algae 50, 45–56. http://dx.doi.org/10.1016/j.hal.2015.10.008

GEOHAB, 2012. Global Ecology and Oceanography of Harmful Algal Blooms: Core Research Project - Harmful Algal Blooms in Benthic Systems. IOC of UNESCO and SCOR, Paris and Newark.

Giussani, V., Asnaghi, V., Pedroncini, A., Chiantore, M., 2017. Management of harmful benthic dinoflagellates requires targeted sampling methods and alarm thresholds. Harmful Algae 68, 97–104. http://dx.doi.org/10.1016/j.hal.2017.07.010

Granéli, E., Vidyarathna, N.K., Funari, E., Cumaranatungac, P.R.T., Scenati, R., 2011. Can increases in temperature stimulate blooms of the toxic benthic dinoflagellate *Ostreopsis ovata*? Harmful Algae 10, 165–172. http://dx.doi.org/10.1016/j.hal.2010.09.002

Hachani, M.A., Dhib, A., Fathalli, A., Ziadi, B., Turki, S., 2018. Harmful epiphytic dinoflagellate assemblages on macrophytes in the Gulf of Tunis. Harmful Algae 77, 29–42. http://dx.doi.org/10.1016/j.hal.2018.06.006

Hafdahl, A.R., 2008. Combining Heterogeneous Correlation Matrices: Simulation Analysis of Fixed-Effects Methods. J. Educ. Behav Stat. 33, 507-533. https://doi.org/10.3102/1076998607309472

Hall, T.A., 1999. BioEdit: a user-friendly biological sequence alignment editor and analysis program for Windows 95/98/NT. Nucleic Acids Symp. Ser. 41, 95–98.

Hankin, S., Harrison, D.E., Osborne, J., Davison, J., O'Brien, K., 1996. A Strategy and a Tool, Ferret, for Closely Integrated Visualization and Analysis. J. Vis. Comput. Animat. 7, 149–157. http://dx.doi.org/10.1002/(SICI)1099-1778(199607)7:3<149::AID-VIS148>3.0.CO;2-X

Hasle, G.R., 1978. The inverted microscope method, in: Sournia, A. (Ed.), Phytoplankton Manual, Monographs on Oceanographic Methodology 6. UNESCO, Paris, pp. 88–96.

Janssen, P.A.E.M., 2004. The interaction of ocean waves and wind. Cambridge University Press.

Jauzein, C., Fricke, A., Mangialajo, L., Lemée, R., 2016. Sampling of *Ostreopsis* cf. *ovata* using artificial substrates: Optimization of methods for the monitoring of benthic harmful algal blooms. Mar. Pollut. Bull. 107, 300–304. http://dx.doi.org/ 10.1016/j.marpolbul.2016.03.047

Jauzein, C., Açaf, L., Accoroni, S., Asnaghi, V., Fricke, A., Hachani, M.A., Saab, M.a.,

Chiantore, M., Mangialajo, L., Totti, C., Zaghmouri, I., Lemée, R., 2018. Optimization of sampling, cell collection and counting for the monitoring of benthic harmful algal blooms: Application to *Ostreopsis* spp. blooms in the Mediterranean Sea. Ecol. Indic. 91, 116–127. https://doi.org/10.1016/j.ecolind.2018.03.089

Kumar, S., Stecher, G., Tamura, K., 2016. MEGA7: Molecular Evolutionary Genetics Analysis Version 7.0 for Bigger Datasets. Mol. Biol. Evol. 33, 1870–1874. https://doi.org/10.1093/molbev/msw054

Laza-Martinez, A., Orive, E., Miguel, I., 2011. Morphological and genetic characterization of benthic dinoflagellates of the genera *Coolia*, *Ostreopsis* and *Prorocentrum* from the south-eastern Bay of Biscay. Eur. J. Phycol. 46, 45–65. https://doi.org/10.1080/09670262.2010.550387

Lim, H.C., Leaw, C.P., Su, S.N.P., Teng, S.T., Usup, G., Mohammad-Noor, N., Lundholm, N., Kotaki, Y., Lim, P.T., 2012. Morphology and molecular characterization of *Pseudo-nitzschia* (Bacillariophyceae) from Malaysian Borneo, including the new species *Pseudo-nitzschia circumpora* sp. nov. J. Phycol. 48, 1232–1247. https://doi.org/10.1111/j.1529-8817.2012.01213.x

Litaker, R.W., Vandersea, M.W., Faust, M.A., Kibler, S.R., Nau, A.W., Holland, W.C., Chinain, M., Holmes, M.J., Tester, P.A., 2010. Global distribution of ciguatera causing dinoflagellates in the genus *Gambierdiscus*. Toxicon 56, 711–730. https://doi.org/10.1016/j.toxicon.2010.05.017

Lobel, P.S., Anderson, D.M., Durand-Clement, M., 1988. Assessment of Ciguatera Dinoflagellate Populations: Sample Variability and Algal Substrate Selection. Biol. Bull. 175, 94–101. https://doi.org/10.2307/1541896

Mangialajo, L., Bertolotto, R., Cattaneo-Vietti, R., Chiantore, M., Grillo, C., Lemee, R., Melchiorre, N., Moretto, P., Povero, P., Ruggieri, N., 2008. The toxic benthic dinoflagellate *Ostreopsis ovata*: Quantification of proliferation along the coastline of Genoa, Italy. Mar. Pollut. Bull. 56, 1209–1214. https://doi.org/10.1016/j.marpolbul.2008.02.028

Mangialajo, L., Fricke, A., Perez-Gutierrez, G., Catania, D., Jauzein, C., Lemee, R., 2017. Benthic Dinoflagellate Integrator (BEDI): A new method for the quantification of Benthic Harmful Algal Blooms. Harmful Algae 64, 1–10. https://doi.org/10.1016/j.hal.2017.03.002

Mangialajo, L., Ganzin, N., Accoroni, S., Asnaghi, V., Blanfuné, A., Cabrini, M., Cattaneo-Vietti, R., Chavanon, F., Chiantore, M., Cohu, S., Costa, E., Fornasaro, D., Grossel, H.,

Marco-Miralles, F., Masó, M., Reñé, A., Rossi, A.M., Sala, M.M., Thibaut, T., Totti, C., Vila, M., Lemée, R., 2011. Trends in *Ostreopsis* proliferation along the Northern Mediterranean coasts. Toxicon 57, 408–420. https://doi.org/10.1016/j.toxicon.2010.11.019

Mateus, M., Riflet, G., Chambel, P., Fernandes, L., Fernandes, R., Juliano, M., Campuzano, F., De Pablo, H., Neves, R., 2012. An operational model for the West Iberian coast: Products and services. Ocean Sci. 8, 713–732. https://doi.org/10.5194/os-8-713-2012

Moita, M.T., Oliveira, P.B., Mendes, J.C., Palma, A.S., 2003. Distribution of chlorophyll *a* and *Gymnodinium catenatum* associated with coastal upwelling plumes off central Portugal. Acta Oecologica 24, 125–132. https://doi.org/10.1016/S1146-609X(03)00011-0

Monti, M., Minocci, M., Beran, A., Iveša, L., 2007. First record of *Ostreopsis* cfr. *ovata* on macroalgae in the Northern Adriatic Sea. Mar. Pollut. Bull. 54, 598–601. https://doi.org/10.1016/j.marpolbul.2007.01.013

Nei, M., Kumar, S., 2000. Molecular evolution and phylogenetics. Oxford university press., New York.

Oliveira, P.B., Moita, T., Silva, A., Monteiro, I.T., Palma, S., 2009a. Summer diatom and dinoflagellate blooms in Lisbon Bay from 2002 to 2005: Pre-conditions inferred from wind and satellite data. Prog. Oceanogr. 83, 270–277. https://doi.org/10.1016/j.pocean.2009.07.030

Oliveira, P.B., Nolasco, R., Dubert, J., Moita, T., Peliz, Á., 2009b. Surface temperature, chlorophyll and advection patterns during a summer upwelling event off central Portugal. Cont. Shelf Res. 29, 759–774. https://doi.org/10.1016/j.csr.2008.08.004

Parsons, M.L., Aligizaki, K., Bottein, M.Y.D., Fraga, S., Morton, S.L., Penna, A., Rhodes, L., 2012. *Gambierdiscus* and *Ostreopsis*: Reassessment of the state of knowledge of their taxonomy, geography, ecophysiology, and toxicology. Harmful Algae 14, 107–129. https://doi.org/10.1016/j.hal.2011.10.017

Pearce, I., Marshall, J.A., Hallegraeff, G.M., 2001. Toxic epiphytic dinoflagellates from East Coast Tasmania, Australia., in: Hallegraeff, G.M., Blackburn, S.I., Bolch, C.J., Lewis, R.J. (Eds.), Harmful Algal Blooms 2000. Intergovernmental Oceanographic Commission UNESCO, pp. 54–57.

Penna, A., Fraga, S., Battocchi, C., Casabianca, S., Giacobbe, M.G., Riobó, P., Vernesi, C., 2010. A phylogeographical study of the toxic benthic dinoflagellate genus *Ostreopsis* Schmidt. J. Biogeogr. 37, 830–841. https://doi.org/10.1111/j.1365-2699.2009.02265.x

Penna, A., Vila, M., Fraga, S., Giacobbe, M.G., Francesco, A., Riobó, P., Vernesi, C., 2005. Characterization of *Ostreopsis* and *Coolia* (Dinophyceae) isolates in the western Mediterranean Sea based on morphology, toxicity and internal transcribed spacer 5.8s rDNA sequences. J. Phycol. 41, 212–225. https://doi.org/10.1111/J.1529-8817.2005.04011.x

R Core Team, 2016. R: A Language and Environment for Statistical Computing, R Foundation for Statistical Computing. Vienna, Austria.

Ramos, V., Salvi, D., Machado, J.P., Vale, M., Azevedo, J., Vasconcelos, V., 2015. Culture-independent study of the late-stage of a bloom of the toxic dinoflagellate *Ostreopsis* cf. *ovata*: Preliminary findings suggest genetic differences at the sub-species level and allow ITS2 structure characterization. Toxins (Basel). 7, 2514–2533. https://doi.org/10.3390/toxins7072514

Ramos, V., Vasconcelos, V., 2010. Palytoxin and Analogs: Biological and Ecological Effects. Mar. Drugs 8, 2021–2037. https://doi.org/10.3390/md8072021

Relvas, P., Barton, E.D., 2005. A separated jet and coastal counterflow during upwelling relaxation off Cape São Vicente (Iberian Peninsula). Cont. Shelf Res. 25, 29–49. https://doi.org/10.1016/j.csr.2004.09.006

Relvas, P., Barton, E.D., 2002. Mesoscale patterns in the Cape São Vicente (Iberian Peninsula) upwelling region. J. Geophys. Res. 107, 3164. https://doi.org/10.1029/2000JC000456

Relvas, P., Peliz, A., Oliveira, P.B., da Silva, J., Dubert, J., Barton, E.D., Santos, A.M.., 2007. Physical oceanography of the western Iberia ecosystem: latest views and challenges. Prog. Oceanogr. 74, 149–173.

Rossi, R., Castellano, V., Scalco, E., Serpe, L., Zingone, A., Soprano, V., 2010. New palytoxin-like molecules in Mediterranean *Ostreopsis* cf. *ovata* (dinoflagellates) and in *Palythoa tuberculosa* detected by liquid chromatography-electrospray ionization time-of-flight mass spectrometry. Toxicon 56, 1381–1387. https://doi.org/10.1016/j.toxicon.2010.08.003

Sansoni, G., Borghini, B., Camici, G., Casotti, M., Righini, P., Rustighi, C., 2003. Fioriture algali di *Ostreopsis ovata* (Gonyaulacales: Dinophyceae): un problema emergente. Biol. Ambient. 17, 17–23.

Sato, S., Nishimura, T., Uehara, K., Sakanari, H., Tawong, W., Hariganeya, N., Smith, K., Rhodes, L., Yasumoto, T., Taira, Y., Suda, S., Yamaguchi, H., Adachi, M., 2011. Phylogeography of *Ostreopsis* along west Pacific coast, with special reference to a novel

clade from Japan. PLoS One 6 (12), e27983. https://doi.org/10.1371/journal.pone.0027983

Scalco, E., Brunet, C., Marino, F., Rossi, R., Soprano, V., Zingone, A., Montresor, M., 2012. Growth and toxicity responses of Mediterranean *Ostreopsis* cf. *ovata* to seasonal irradiance and temperature conditions. Harmful Algae 17, 25–34. https://doi.org/10.1016/j.hal.2012.02.008

Scholin, C.A., Herzog, M., Sogin, M., Anderson, D.M., 1994. Identification of group- and strain-specific genetic markers for globally distributed *Alexandrium* (Dinophyceae) species: I. Restriction fragment length polymorphism analysis of small subunit ribosomal RNA genes. J. Phycol. 30, 999–1011. https://doi.org/10.1111/j.0022-3646.1994.00999.x

Schwing, F.B., O'Farrel, M., Steger, J.M., Baltz, K., 1996. Coastal Upwelling Indices, West Coast of North America, 1946-1995, NOAA Tech. Rep., NMFS SWFSC, 231, 144p.

Selina, M.S., Morozova, T. V., Vyshkvartsev, D.I., Orlova, T.Y., 2014. Seasonal dynamics and spatial distribution of epiphytic dinoflagellates in Peter the Great Bay (Sea of Japan) with special emphasis on *Ostreopsis* species. Harmful Algae 32, 1–10. https://doi.org/10.1016/j.hal.2013.11.005

Selina, M.S., Orlova, T.Y., 2010. First occurrence of the genus *Ostreopsis* (Dinophyceae) in the Sea of Japan. Bot. Mar. 53, 243–249.

Shears, N.T., Ross, P.M., 2009. Blooms of benthic dinoflagellates of the genus *Ostreopsis*; an increasing and ecologically important phenomenon on temperate reefs in New Zealand and worldwide. Harmful Algae 8, 916–925. https://doi.org/10.1016/j.hal.2009.05.003

Silva, A., Brotas, V., Orive, E., Neto, A.I., 2010. First records of *Ostreopsis heptagona*, *O.* cf. *siamensis* and *O.* cf. *ovata* – in the Azores archipelago, Portugal. Harmful Algae News 42, 1–2.

Silva, T., Caeiro, M.F., Costa, P.R., Amorim, A., 2015. *Gymnodinium catenatum* Graham isolated from the Portuguese coast: Toxin content and genetic characterization. Harmful Algae 48, 94–104. https://doi.org/10.1016/j.hal.2015.07.008

Simoni, F., Gaddi, A., Di Paolo, C., Lepri, L., 2003. Harmful epiphytic dinoflagellate on Tyrrhenian Sea reefs. Harmful Algae News 24, 13–14.

Skaug, H., Fournier, D., Nielsen, A., Magnusson, A., Bolker, B., 2013. glmmADMB: Generalized Linear Mixed Models Using AD Model Builder. R Package Version 0.8.3.3. http://glmmadmb.r-forge.r-project.org; http://admb-project.org.

Tamura, K., 1992. Estimation of the number of nucleotide substitutions when there are strong transition-transversion and G+C-content biases. Mol. Biol. Evol. 9, 678–687.

https://doi.org/10.1093/oxfordjournals.molbev.a040752

Taylor, F.J.R., 1979. The description of the benthic dinoflagellate associated with maitotoxin and ciguatoxin, including observations on Hawaiian material, in: Taylor, D.L., Seliger, H.H. (Eds.), Toxic Dinoflagellate Blooms. Elsevier Scientific, New York, pp. 71–76.

Tester, P.A., Kibler, S.R., Holland, W.C., Usup, G., Vandersea, M.W., Leaw, C.P., Teen, L.P., Larsen, J., Mohammad-Noor, N., Faust, M.A., Litaker, R.W., 2014. Sampling harmful benthic dinoflagellates: Comparison of artificial and natural substrate methods. Harmful Algae 39, 8–25. https://doi.org/10.1016/j.hal.2014.06.009

Tichadou, L., Glaizal, M., Armengaud, A., Grossel, H., Lemée, R., Kantin, R., Lasalle, J.-L., Drouet, G., Rambaud, L., Malfait, P., de Haro, L., 2010. Health impact of unicellular algae of the *Ostreopsis* genus blooms in the Mediterranean Sea: experience of the French Mediterranean coast surveillance network from 2006 to 2009. Clin. Toxicol. 48, 839–844. https://doi.org/10.3109/15563650.2010.513687

Totti, C., Accoroni, S., Cerino, F., Cucchiari, E., Romagnoli, T., 2010. *Ostreopsis ovata* bloom along the Conero Riviera (northern Adriatic Sea): Relationships with environmental conditions and substrata. Harmful Algae 9, 233–239. https://doi.org/10.1016/j.hal.2009.10.006

Utermöhl, H., 1958. Zur Ver vollkommung der quantitativen phytoplankton-methodik. Mitteilung Internationale Vereinigung Fuer Theoretische unde Amgewandte. Limnol. 9, 1–38. https://doi.org/10.1080/05384680.1958.11904091

Vassalli, M., Penna, A., Sbrana, F., Casabianca, S., Gjeci, N., Capellacci, S., Asnaghi, V., Ottaviani, E., Giussani, V., Pugliese, L., Jauzein, C., Lemée, R., Hachani, M.A., Turki, S., Açaf, L., Saab, M.A.A., Fricke, A., Mangialajo, L., Bertolotto, R., Totti, C., Accoroni, S., Berdalet, E., Vila, M., Chiantore, M., 2018. Intercalibration of counting methods for *Ostreopsis* spp. blooms in the Mediterranean Sea. Ecol. Indic. 85, 1092–1100. https://doi.org/10.1016/j.ecolind.2017.07.063

Vila, M., Abós-Herràndiz, R., Isern-Fontanet, J., Àlvarez, J., Berdalet, E., 2016. Establishing the link between *Ostreopsis* cf. *ovata* blooms and human health impacts using ecology and epidemiology. Sci. Mar. 80, 107–115.

Vila, M., Garcés, E., Masó, M., 2001. Potentially toxic epiphytic dinoflagellate assemblages on macroalgae in the NW Mediterranean. Aquat. Microb. Ecol. 26, 51–60. https://doi.org/10.3354/ame026051

Walther, G.R., Roques, A., Hulme, P.E., Sykes, M.T., Pysek, P., Kühn, I., et al., 2009. Alien species in a warmer world: risks and opportunities. Trends Ecol. Evol. (Amst.) 24, 686–

693. https://doi.org/10.1016/j.tree.2009.06.008

Wooster, W.S., Baku, A., McLain, D.R., 1976. The seasonal upwelling cycle along the eastern boundary of the North Atlantic. J. Mar. Res. 34, 131–141.

Wu, L., 2010. Mixed Effects Models for Complex Data. Monographs on Statistics and Applied Probability, Chapman and Hall/CRC, USA.

Zingone, A., Berdalet, E., Bienfang, P., Enevoldsen, H., Evans, J., Kudela, R., Tester, P., 2012. Harmful Algae in Benthic Systems: A GEOHAB Core Research Program. Cryptogam. Algol. 33, 225–230.

Zuur, A.F., Ieno, E.N., Elphick, C.S., 2010. A protocol for data exploration to avoid common statistical problems. Methods Ecol Evol. 1, 3-14. https://doi.org/10.1111/j.2041-210X.2009.00001.x

Chapter 5.

Concluding Remarks

5.1. General Conclusions

The main driver of the present thesis was the increasing concern in Portugal with the observed global expansion of several HAB species, particularly of benthic HABs, and their increase in frequency and magnitude. The Portuguese continental coast is influenced by upwelling (Iberia/Canary Current System) with several challenging features, namely the topography, the existence of prominent capes and headlands that, together, lead to different patterns of phytoplankton accumulation/dispersion. Within this scope, two sheltered wide-open bays, located at small latitude distances but in different coastline orientations, were studied to characterize the phytoplankton communities and biomass and the underlying meteorological and oceanographic conditions (MetOc).

To attain these objectives, a nine years time series of *in situ* Chl-*a* data was collected weekly in Lisbon Bay and studied together with different satellite Ocean Color datasets (Chapter 2). This region, due to the great optical variability and complexity, is among the most challenging regions for the performance of satellite Chl-*a* estimates. This resulted in a low correlation coefficient (r = 0.42) between both datasets. After this first approach using the *in situ* Chl-*a*, the OC product that best represented the *in situ* data in Lisbon Bay was used to extract the Chl-*a* data for Lagos Bay, in the same period. This work, based on the results from a Chl-*a* sinusoidal model applied to a decade-long time series, characterizes for the first time, for the SW coast of Iberia, the most likely phytoplankton biomass periodicity. The comparison between satellite and *in situ* Chl-*a* datasets revealed that satellite estimates overestimated the *in situ* biomass and that OC data anticipated the beginning (~15 days) and the end (~1 month) of Chl-*a* maximum concentrations observed *in situ*. A high spatial and interannual variability was found in phytoplankton biomass and, despite the small latitudinal distance between the two bays, different temporal variability patterns were observed: Lisbon Bay showed a long period of high biomass (~5 months), changing from uni- to bi-modal pattern since it was slightly higher in spring than in summer; and Lagos Bay was characterized by a uni-modal seasonal cycle reaching the maximum in June. This work also showed that phytoplankton biomass seasonal curves could be divided in both bays into 3-main periods: (i) the spring bloom period when the increase in phytoplankton biomass occurs; (ii) the early-spring/summer (or spring/summer in Lagos Bay) period characterized by the highest phytoplankton biomass values; and (iii) the late-summer/autumn period characterized by the decline in phytoplankton biomass.

In this study, *in situ* SST time series with unprecedented temporal resolution were also recorded (Chapters 2 and 4). These datasets were recorded on a daily basis in Lagos Bay and every week in Lisbon Bay. The comparison between these datasets and the remote-sensing data showed a strong correlation between them ($r > 0.90$). However, the high temporal resolution of the dataset collected in Lagos Bay allowed to realize that satellite data could not reproduce faithfully the summer sea surface cooling events. In several upwelling events, satellite observation overestimated SST in more than 3 ºC.

In Chapter 2, the time series were studied on a weekly scale. The use of short time-scales has a high relevance when investigating the patterns of phytoplankton biomass and their relation with processes of high variability, such as upwelling. To quantify the significance of several MetOc variables on Chl-*a*, cross-correlation analyses were used within a maximum 1-month time period (from 0 up to 4 weeks apart: lags 0-4). The significant relationship observed between the increase of Chl-*a* and the increase of PAR, at both lags 0 and 1, indicated that light was the main limiting driver in winter/early-spring in both bays. During late-spring/summer period, the increase in upwelling and the associated decrease of SST (both at lag 0 and in some cases at lag 1) were the drivers that most explain the increase of Chl-*a* in both bays. This study reinforces the relevance of the intensity and persistence of seasonal upwelling induced by northerly winds on phytoplankton biomass in Lisbon Bay. In Lagos Bay, the role of each wind component and the differences in the weight of those components at different lags should be further investigated. Due to the proximity to the upwelling filaments generated at CSV under northerly winds, Chl-*a* in this bay is still affected by zonal transport (M_x). However, in this bay, the intensity and persistence of local upwelling events that occur under westerly winds (M_y, meridional transport) have a stronger influence on phytoplankton biomass than the caused by northerly winds.

Following the study on the relationship between MetOc drivers and phytoplankton biomass, the phytoplankton communities were analyzed for one year based on fortnightly data (Chapter 3). Within the identified phytoplankton groups, diatoms were the dominant group and the main contributor to high phytoplankton biomass levels in both bays. Different patterns in coccolithophores and dinoflagellates characterized the studied bays. The second most abundant group in Lisbon Bay belongs to coccolithophores, which were more abundant from late-summer to autumn during the transition from upwelling to downwelling favorable conditions was observed. Nevertheless, despite the lower contribution of this group in Lagos Bay, the magnitude of coccolithophores blooms reached significantly higher concentrations in

this bay. The second most abundant group in Lagos Bay was the dinoflagellates with higher abundances recorded from spring to autumn. The presence of warmer temperatures, stable sea state conditions and a recurrent warm coastal countercurrent favored dinoflagellates development in this region (a fact also highlighted in Chapter 4).

Significant spatial and temporal differences were observed in phytoplankton assemblages (Chapter 3). Lisbon Bay was characterized by a higher contribution of euglenophytes, of several diatom species, particularly *L. minimus* and *C. curvisetus*, and of the harmful dinoflagellate *D. acuta*. Lagos Bay was largely characterized by the high concentration and persistence of cryptophytes and of several dinoflagellate species of which *Amphidium* spp, *Karenia* spp. and *Gyrodinium fusiforme* are worth mentioning. In Lagos Bay, phytoplankton communities observed nearshore did not reflect the phytoplankton present offshore in most oceanographic conditions. An important feature observed nearshore is the high contribution of benthic, epiphytic and tycoplanktonic species, including benthic harmful dinoflagellates (BHABs).

On a seasonal scale, different phytoplankton assemblages were observed in response to the four meteorological seasons (winter, spring, summer and autumn) in both bays (*i.e*. Lisbon and Lagos offshore). Nearshore, in Lagos Bay, only three biological seasons (winter, spring, summer/autumn) could be identified since no differences were recorded between summer and autumn phytoplankton assemblages. In both bays, winter communities were dependent on the water column mixing processes, as well as on precipitation in Lagos Bay. Coccolithophores were the dominant community during this season in Lisbon and in Lagos Bay (offshore), but benthic diatoms were also important in the shallower stations (*i.e.* Lisbon and Lagos nearshore). Chain-forming diatoms dominated the spring community, which showed a relevant dependence with upwelling in Lagos Bay, while in Lisbon Bay possible not studied factors may contribute better to this community. Thermal stratification was the main driver to summer and autumn communities, both mostly composed by dinoflagellates. In addition, the reversal circulation patterns observed in autumn favored a mixed population of diatoms and dinoflagellates in both Lisbon and Lagos (offshore) Bays.

This study showed that Lagos Bay had a higher frequency and abundance of several HAB species (*Pseudo-nitzschia* spp., *D. acuminata*, *D. ovum, Karenia* spp., *Gonyaulax* cf. *spinifera*, *Lingulodinium polyedra, Protoceratium reticulatum* and BHABs) than Lisbon Bay (Chapter 3). Only *D. acuta* seems to be spatially restricted to Lisbon Bay, but had the shortest period of occurrence within *Dinophysis* species. The longest period of occurrence was

observed in *D. ovum*, but this species was spatially restricted to Lagos Bay. This work suggested the presence of ecological differences in seasonality within *Pseudo-nitzschia* genus. Higher concentrations of *P. seriata*-group were observed when *P. delicatissima*-group was scarce or absent. The presence of BHABs during 2015 was recorded in low cell concentrations. Nevertheless, it gives us a first impression of this group ecology that was further investigated in Chapter 4. BHABs were only observed in the nearshore stations of both bays, however in higher cell concentrations and frequency in Lagos Bay.

This thesis, using a seven years time series of weekly water samples, provides novel information on the understanding of the local *Ostreopsis* planktonic population dynamics (Chapter 4). Two species were identified in Lagos Bay (*O.* cf. *ovata* and *O.* cf. *siamensis*) but only one in Lisbon Bay (*O.* cf. *siamensis*). The restriction of the highly toxic *O.* cf. *ovata* to the south coast seems to be related to the maximum summer SST that limits the spread of this species to the west coast. On the other hand, the low toxicity species *O.* cf. *siamensis* has a wider distribution range and was also present in Lisbon Bay.

This study showed that *Ostreopsis* has a clear seasonality, with high cell concentrations recorded during late-summer/early-autumn in both bays. The seasonal temperature has a major role in *Ostreopsis* population dynamics. This was suggested by the significant relationship found between the high cell concentrations in the plankton and positive SST anomalies in the months preceding these events. The relationship between hydrodynamics and planktonic populations of *Ostreopsis* is complex. Notwithstanding, based on significant correlations, a period of low sea state longer than about two weeks was interpreted as favoring bloom development on the substrate, and the following short time events of onshore wind and moderate waves were suggested as causing the re-suspension of *Ostreopsis* cells into the water column. Turbulence caused by wave events can indeed play a role in the re-suspension of *Ostreopsis* to the water column, but the existence of a benthic population is a prerequisite.

This work showed that in Lisbon Bay *O.* cf. *siamensis* was rarely observed. However, at the end of the study, in 2017, the highest planktonic density of *O.* cf. *siamensis* was recorded in this bay. Lisbon Bay, being until now the known northern limit in the W Iberian coast to this species, could be a reflection of a warming trend in the NE Atlantic. However, it is still difficult to understand the relationship between *O.* cf. *siamensis*, seasonal temperature and hydrodynamics in Lisbon Bay, due to the few, short, and low abundance occurrences of this species during the studied period. In Lagos Bay, *Ostreopsis* spp. was frequently observed since the first detection in 2011. So far, concentrations in the water column above the alert

phase accepted by the Italian guidelines (>10 x 10^3 cel L^{-1}) were only observed in 2013 (~17 x 10^3 cel L^{-1}). Several variables, such as substrate, SST and sea state conditions, make Lagos Bay a hotspot to the occurrence of *Ostreopsis* blooms. This urges the implementation of a monitoring plan for these new emergent problems. While the monitoring of planktonic samples has several advantages relative to benthic sampling (e.g. rapid assessment of toxic risks, ease of sampling, non-disturbance of habitat and cost-effectiveness due to the possibility of being integrated in ongoing HAB monitoring programs) there is still the need to characterize the relation between *Ostreopsis* spp. concentrations in the benthic and in the planktonic compartments. Only after this approach, will it be possible to define alert and alarm threshold concentrations in the plankton, and enable forecasting models and effective prevention measures.

Appendix

Appendix A

Table A.2.1. Cross-correlation (CC) analyses between Chl-*a* and each MetOc driver in winter/early-spring for LisB-Sat and LagB-Sat: point estimates of the CCs at different lags; Bonferroni adjusted *p*-values.

		LisB-Sat		**LagB-Sat**	
Variables	**Lag**	**CC**	**Adjusted *p*-value**	**CC**	**Adjusted *p*-value**
Chl-*a* *vs* PAR	0	0.41	0.00	0.37	0.00
	1	0.32	0.01	0.30	0.02
	2	0.24	0.11	0.20	0.30
	3	0.18	0.34	0.14	0.93
	4	0.10	1.00	0.07	1.00
Chl-*a* *vs* SST	0	0.11	1.00	-0.20	0.18
	1	-0.06	1.00	-0.25	0.09
	2	-0.16	0.73	-0.28	0.10
	3	-0.20	0.43	-0.27	0.15
	4	-0.21	0.47	-0.29	0.11
Chl-*a* *vs* M_x	0	-0.01	1.00	0.06	1.00
	1	0.09	1.00	-0.05	1.00
	2	0.14	0.54	-0.03	1.00
	3	0.15	0.52	-0.08	1.00
	4	0.14	0.62	-0.08	1.00
Chl-*a* *vs* M_y	0	0.05	1.00	0.13	0.49
	1	0.05	1.00	-0.01	1.00
	2	0.01	1.00	-0.15	0.33
	3	0.00	1.00	-0.04	1.00
	4	-0.12	0.59	-0.02	1.00
Chl-*a* *vs* MLD	0	-0.23	0.13	-0.02	1.00
	1	-0.14	0.91	0.00	1.00
	2	-0.10	1.00	0.02	1.00
	3	-0.07	1.00	0.09	1.00
	4	-0.06	1.00	0.10	1.00

Table A.2.2. Cross-correlation (CC) analyses between Chl-*a* and each MetOc driver in late-spring/summer for LisB-Sat and LagB-Sat: point estimates of the CCs at different lags; Bonferroni adjusted *p*-values.

		LisB-Sat		**LagB-Sat**	
Variables	**Lag**	**CC**	**Adjusted *p*-value**	**CC**	**Adjusted *p*-value**
Chl-*a* *vs* PAR	0	0.18	0.39	0.13	1.00
	1	0.15	0.66	0.05	1.00
	2	0.08	1.00	0.07	1.00
	3	0.00	1.00	0.03	1.00
	4	0.03	1.00	0.01	1.00
Chl-*a* *vs* SST	0	-0.26	0.06	-0.45	0.00
	1	-0.14	0.76	-0.34	0.00
	2	0.01	1.00	-0.26	0.10
	3	0.09	1.00	-0.31	0.03
	4	0.11	1.00	-0.28	0.07
Chl-*a* *vs* M_x	0	-0.32	0.00	-0.22	0.02
	1	-0.27	0.00	-0.17	0.10
	2	-0.06	1.00	0.01	1.00
	3	0.06	1.00	0.09	1.00
	4	0.05	1.00	-0.01	1.00
Chl-*a* *vs* M_y	0	-0.06	1.00	-0.21	0.01
	1	-0.03	1.00	-0.25	0.00
	2	-0.16	0.13	-0.07	1.00
	3	-0.08	1.00	0.00	1.00
	4	-0.01	1.00	-0.01	1.00
Chl-*a* *vs* MLD	0	0.13	0.93	0.03	1.00
	1	0.09	1.00	-0.01	1.00
	2	-0.07	1.00	-0.03	1.00
	3	-0.13	0.85	0.01	1.00
	4	-0.13	0.86	0.04	1.00

Appendix B

Table. B.3.1. Total number of phytoplankton taxonomic entities and number of samples in which each taxonomic entity is present in LisB, LagB-Offshore and LagB-Beach during 2015. Potentially toxic taxa are pointed with * and the ones that appear in the results of this study are pointed with **. The corresponding abbreviation considered to the multivariate analyses is also shown.

Taxonomic entity	Abbrev.	LisB	LagB Offshore	LagB Beach
Diatoms (Bacillariophyceae)				
Achnanthes spp. Bory, 1822		0	0	1
Achnanthes longipes C.Agardh, 1824		1	0	1
Actinoptychus senarius (Ehrenberg) Ehrenberg, 1843	Ase	2	1	2
Amphiprora spp. Ehrenberg, 1843	AMPHIP	1	0	4
Amphora spp. Ehrenberg ex Kützing, 1844 (< 20 µm)		0	0	1
Amphora spp. Ehrenberg ex Kützing, 1844 */Halamphora* spp. (Cleve) Mereschkowsky, 1903	AMPHO	10	5	7
Asterionellopsis glacialis (Castracane) Round, 1990	Agla	7	3	4
Asteromphalus spp. Ehrenberg, 1844		1	0	0
Asteromphalus flabellatus (Brébisson) Greville, 1859	Afla	1	1	3
Aulacoseira spp. Thwaites, 1848		1	0	0
Bacillaria paxillifera (O.F.Müller) T.Marsson, 1901	Bpax	2	0	4
Bacteriastrum hyalinum Lauder, 1864	Bhya	2	4	0
Bellerochea malleus (Brightwell) Van Heurck, 1885		2	0	1
Biddulphia alternans (Bailey) Van Heurck, 1885		1	0	0
Biddulphia biddulphiana (J.E.Smith) Boyer, 1900	Bbid	5	0	1
Biddulphia spp. S.F.Gray, 1821		2	0	1
Campylodiscus spp. Ehrenberg ex Kützing, 1844		2	0	0
Cerataulina spp. H.Peragallo ex F.Schütt, 1896		1	0	0
Cerataulina pelagica (Cleve) Hendey, 1937	Cpelagica	6	5	3
cf. Cylindrotheca spp. Rabenhorst, 1859 (< 30 µm)	CYL	10	13	8
cf. *Delphineis surirella* (Ehrenberg) G.W.Andrews, 1981	Dsur	2	2	0
Chaetoceros cf. *danicus* Cleve, 1889	Cdan	1	6	2
Chaetoceros curvisetus Cleve, 1889	Ccur	12	0	0
Chaetoceros diadema (Ehrenberg) Gran, 1897		1	0	0
Chaetoceros spp. Ehrenberg, 1844	CHA	22	21	21
Chaetoceros socialis H.S.Lauder, 1864		3	0	0
Climacosphenia spp. Ehrenberg, 1841	CLI	3	2	2
Cocconeis spp. Ehrenberg, 1836		0	0	2
Corethron spp. Castracane, 1886		0	3	0
Corethron hystrix Hensen, 1887	Chys	0	2	2
Coscinodiscus spp. Ehrenberg, 1839	COS	14	11	5
Cylindrotheca closterium (Ehrenberg) Reimann & J.C.Lewin, 1964	Cclo	27	27	25
Dactyliosolen spp. Castracane, 1886	DAC	0	2	3
Dactyliosolen fragilissimus (Bergon) Hasle, 1996	Dfra	4	10	5

Taxonomic entity	Abbrev.	LisB	LagB Offshore	LagB Beach
Dactyliosolen phuketensis (B.G.Sundström) G.R.Hasle, 1996	Dphu	10	15	10
Detonula spp. F.Schütt ex De Toni, 1894		0	2	0
Detonula pumila (Castracane) Gran, 1900	Dpum	12	7	8
Detonula pumila (Castracane) Gran, 1900/Lauderia annulata Cleve, 1873		1	0	2
Dimeregramma spp. Ralfs, 1861/*Plagiogramma* spp. Greville, 1859		0	0	1
Diploneis spp. Ehrenberg ex Cleve, 1894	DIP	8	13	13
Ditylum brightwellii (T.West) Grunow, 1885	Dbri	14	7	2
Eucampia spp. Ehrenberg, 1839		1	0	0
Eucampia zoodiacus Ehrenberg, 1839	Ezoo	8	8	2
Eupyxidicula turris (Greville) S.Blanco & C.E.Wetzel, 2016 (syn. *Stephanopyxis turris* (Greville) Ralfs, 1861)		1	2	0
Fragilaria spp. Lyngbye, 1819	FRA	2	1	5
Fragilariopsis spp. Hustedt, 1913		0	0	2
Grammatophora spp. Ehrenberg, 1840	GRA	15	3	4
Grammatophora oceanica Ehrenberg, 1840		1	0	0
Grammatophora serpentina Ehrenberg, 1844	Gser	5	0	0
Guinardia delicatula (Cleve) Hasle, 1997	Gdel	12	19	15
Guinardia flaccida (Castracane) H.Peragallo, 1892	Gfla	7	11	4
Guinardia striata (Stolterfoth) Hasle, 1996	Gstr	11	13	7
Helicotheca tamesis (Shrubsole) M.Ricard, 1987		1	0	1
Hemiaulus hauckii Grunow ex Van Heurck, 1882	Hhau	6	14	8
Hemiaulus spp. Heiberg, 1863	HEM	2	6	5
Hemiaulus sinensis Greville, 1865	Hsin	1	3	3
Lauderia annulata Cleve, 1873	Lann	7	3	1
Leptocylindrus cf. *danicus* Cleve, 1889	Ldan	10	12	12
Leptocylindrus cf. *minimus* Gran, 1915	Lmin	16	2	4
Leptocylindrus spp. Cleve, 1889	LEP	4	7	11
Licmophora spp. C.Agardh, 1827	LIC	11	9	22
Melosira spp. C.Agardh, 1824	MEL	3	0	1
Meuniera membranacea (Cleve) P.C.Silva, 1996		2	0	1
Navicula cf. *cancellata* Donkin 1872		0	0	1
Navicula spp. J.B.M. Bory de Saint-Vincent, 1822	NAV	15	18	23
Neocalyptrella robusta (G.Norman ex Ralfs) Hernández-Becerril & Meave del Castillo, 1997		1	2	0
Nitzschia spp. Hassall, 1845	NIT	15	15	12
Nitzschia longissima (Brébisson) Ralfs, 1861		0	0	1
Nitzschia longissima (Brébisson) Ralfs, 1861/*Cylindrotheca closterium* (Ehrenberg) Reimann & J.C.Lewin, 1964	Nlon	3	1	6
Odontella spp. C.Agardh, 1832	ODO	6	0	0

Taxonomic entity	Abbrev.	LisB	LagB Offshore	LagB Beach
Paralia sulcata (Ehrenberg) Cleve, 1873	Psul	12	8	5
Pinnularia rectangulata (W.Gregory) Rabenhorst, 1864		0	0	1
Pleurosigma spp. W.Smith, 1852/*Gyrosigma* spp. Hassall, 1845	PLE	17	15	18
Podosira spp. Ehrenberg, 1840		0	0	1
Proboscia alata (Brightwell) Sundström, 1986	Pala	9	14	10
Proboscia indica (H.Peragallo) Hernández-Becerril, 1995	Pind	3	7	3
Pseudo-nitzschia (H.Peragallo, 1900) *seriata*-group**	PSEser	13	16	16
Pseudo-nitzschia (H.Peragallo, 1900) *delicatissima*-group**	PSEdel	19	22	15
Rhizosolenia spp. Brightwell, 1858	RHI	13	14	10
Rhizosolenia cf. *setigera* Brightwell, 1858	Rset	4	10	5
Rhizosolenia cf. *styliformis* T.Brightwell, 1858	Rsty	2	7	2
Scoliotropis spp. P.T.Cleve, 1894		0	0	1
Skeletonema marinoi Sarno & Zingone, 2005	SKE	7	9	10
Stephanopyxis spp. (Ehrenberg) Ehrenberg, 1845		0	0	2
Striatella unipunctata (Lyngbye) C.Agardh 1832	Suni	4	1	3
Surirella spp. Turpin, 1828	SUR	3	3	4
Synedra spp. Ehrenberg, 1830		1	0	1
Thalassionema frauenfeldii (Grunow) Tempère & Peragallo, 1910		1	2	0
Thalassionema spp. Grunow ex Mereschkowsky, 1902		0	2	0
Thalassionema nitzschioides (Grunow) Mereschkowsky, 1902	Tnit	5	7	5
Thalassiosira spp. Cleve, 1873	THA	19	9	7
Thalassiosira subtilis (Ostenfeld) Gran, 1900	Tsub	2	4	2
Thalassiothrix spp. Cleve & Grunow, 1880	THX	9	14	7
Toxarium undulatum Bailey 1854 (syn. *Synedra undulata* (Bailey) W.Smith 1956)		1	0	1
Triceratium spp. Ehrenberg, 1839		1	0	0
Trieres mobiliensis (Bailey) Ashworth & E.C.Theriot, 2013 (syn. *Odontella mobiliensis* (Bailey) Grunow, 1884)	Omob	13	4	5
nº taxonomic entities		**80**	**60**	**75**
Dinoflagellates (Dinophyceae)				
*Akashiwo sanguinea** (K.Hirasaka) Gert Hansen & Moestrup, 2000		0	1	0
Alexandrium affine (H.Inoue & Y.Fukuyo) Balech, 1995		0	1	0
Alexandrium spp. * Halim, 1960	ALE	4	13	12
Amphidinium spp. (< 20 µm)	AMPsmall	0	3	2
Amphidinium cf. *acutissimum* J.Schiller, 1932		0	1	0
Amphidinium cf. *operculatum* Claparède & Lachmann, 1859		0	1	0
Amphidinium spp. Claperède & Lachmann, 1859	AMP	1	20	11

Taxonomic entity	Abbrev.	LisB	LagB Offshore	LagB Beach
Amphidinium spp. Claperède & Lachmann, 1859/*Oxytoxum* spp. Stein, 1883		0	2	0
Amphidinium crassum Lohmann, 1908		0	1	0
Amylax spp. A.Meunier, 1910		0	0	1
Amylax triacantha (Jörgensen) Sournia, 1984		0	2	1
Amylax triacantha var. *buxus* (Balech) Gárate-Lizárraga, 2014		0	1	0
Archaeperidinium cf. *minutum* (Kofoid) Jørgensen, 1912 (syn. *Protoperidinium* cf. *minutum* (Kofoid) Loeblich III, 1970)		2	0	0
Azadinium caudatum var. *caudatum* (Halldal) Nézan & Chomérat, 2012	Acau	2	2	3
Azadinium caudatum var. *margalefii* (Rampi) Nézan & Chomérat, 2012		0	2	0
Ceratocorys magna Kofoid, 1910		1	0	0
Cochlodinium spp. F.Schütt, 1896	COC	3	16	9
Coolia spp. A.Meunier, 1919	COO	0	0	5
Corythodinium spp. Loeblich Jr. & Loeblich III, 1966		0	1	0
Corythodinium reticulatum (Stein) F.J.R.Taylor, 1976	Cret	0	0	4
*Dinophysis acuminata*** Claparède & Lachmann, 1859	Dacum	7	13	5
*Dinophysis acuta*** Ehrenberg, 1839	Dacut	9	1	2
*Dinophysis caudata** W.S.Kent, 1881	Dcau	7	10	7
*Dinophysis fortii** Pavillard, 1924		0	1	1
*Dinophysis hastata** F.Stein, 1883/*Dinophysis odiosa (Pavillard) Tai & Skogsberg, 1934*		0	0	1
*Dinophysis ovum*** F.Schütt, 1895	Dovu	3	14	10
Dinophysis spp. * Ehrenberg, 1839	DIN	4	3	2
Diplopsalis group	DIPLOP	13	12	10
Fragilidium spp. Balech ex Loeblich III, 1965		3	0	0
Gonyaulax cf. *spinifera*** (Claparède & Lachmann) Diesing, 1866	Gspi	5	14	7
Gonyaulax spp. Diesing, 1866	GON	4	13	5
Gonyaulax digitale (C.H.G.Pouchet) Kofoid, 1911	Gdig	3	7	2
Gonyaulax polygramma F.Stein, 1883		1	0	0
Gonyaulax verior Sournia, 1973	Gver	0	6	3
Gymnodinium spp. (chain-forming)	GYMchain	0	7	2
Gymnodinium cf. *filum* Lebour, 1917		0	1	0
Gymnodinium spp. F.Stein, 1878	GYM	12	22	15
Gyrodinium fusiforme Kofoid & Swezy, 1921	Gfus	0	11	5
Gyrodinium spp. Kofoid & Swezy, 1921	GYR	16	26	22
Heterocapsa cf. *circularisquama** Horiguchi, 1995		0	0	1
Karenia spp.** Gert Hansen & Moestrup, 2000	KAR	2	12	4

Taxonomic entity	Abbrev.	LisB	LagB Offshore	LagB Beach
*Karenia mikimotoi*** (Miyake & Kominami ex Oda) Gert Hansen & Moestrup, 2000	Kmik	0	12	1
Katodinium spp. B.Fott, 1957		0	1	0
Kryptoperidinium foliaceum (F.Stein) Lindemann, 1924		0	1	2
Lebouridinium glaucum (Lebour) F.Gómez, H.Takayam, D.Moreira & P.López-García, 2016 (syn. *Katodinium glaucum* (Lebour) A.R.Loeblich III 1965)		0	3	0
*Lingulodinium polyedra***(F.Stein) J.D.Dodge, 1989	Lpol	0	6	3
Naked unidentified dinoflagellate "sp1"	DinNI2	7	9	7
Noctiluca scintillans (Macartney) Kofoid & Swezy 1921	Nsci	3	3	0
Ostreopsis spp.** Johs.Schmidt, 1901		0	0	1
Oxytoxum spp. (< 20 µm)		0	1	0
Oxytoxum scolopax F.Stein, 1883		1	1	1
Oxytoxum spp. Stein, 1883	OXY	4	9	4
Phalacroma rotundatum (Claparéde & Lachmann) Kofoid & J.R.Michener 1911*	Drot	2	7	5
Podolampas spp. F.Stein, 1883	POD	0	6	1
Polykrikos spp. Bütschli, 1873		0	0	1
Pronoctiluca spinifera (Lohmann) Schiller, 1932		0	2	1
Prorocentrum cf. *triestinum* J.Schiller, 1918	Ptri	2	4	1
Prorocentrum compressum (Bailey) T.H.Abé ex J.D.Dodge, 1975		0	3	0
*Prorocentrum cordatum** (Ostenfeld) J.D.Dodge, 1976	Pmin	0	2	3
Prorocentrum dentatum F.Stein, 1883	Pden	1	6	3
Prorocentrum spp. Ehrenberg, 1834	PRO	0	4	3
*Prorocentrum lima*** (Ehrenberg) F.Stein, 1878	Plim	1	0	4
Prorocentrum micans Ehrenberg, 1834	Pmic	12	13	10
Prorocentrum scutellum B.Schröder, 1900	Pscu	10	8	11
*Protoceratium reticulatum*** (Claparède & Lachmann) Bütschli, 1885	Pret	2	10	2
Protoperidinium spp. Bergh, 1881	PROT	17	21	19
Protoperidinium bipes (Paulsen) Balech, 1974	Pbip	5	12	7
Protoperidinium brevipes (Paulsen) Balech, 1974	Pbrevi	2	4	0
Protoperidinium cf. *breve* Unknown authority, nom. inval.	Pbreve	2	3	2
Protoperidinium cf. *cerasus* (Paulsen) Balech, 1973		1	0	2
Protoperidinium cf. *conicoides* (Paulsen) Balech, 1973		0	1	1
Protoperidinium cf. *conicum* (Gran) Balech, 1974		0	2	0
Protoperidinium cf. *leonis* (Pavillard) Balech, 1974		1	1	0
Protoperidinium cf. *marielebourae* (Paulsen) Balech, 1974		2	0	0
Protoperidinium cf. *oblongum* (Aurivillius) Parke & Dodge, 1976	Pobl	1	4	3
Protoperidinium cf. *pallidum* (Ostenfeld) Balech, 1973		1	0	0

Taxonomic entity	Abbrev.	LisB	LagB Offshore	LagB Beach
Protoperidinium cf. *pellucidum* Bergh, 1881		1	0	1
Protoperidinium cf. *pentagonum* (Gran) Balech, 1974		1	0	0
Protoperidinium cf. *pyriforme* (Paulsen) Balech, 1974	Ppyr	1	6	2
Protoperidinium cf. *quarnerense* (B.Schröder) Balech, 1974		0	1	0
Protoperidinium curtipes (Jørgensen) Balech, 1974/*Protoperidinium crassipes* (Kofoid) Balech, 1974	Pcur	6	15	9
Protoperidinium curvipes (Ostenfeld) Balech, 1974		2	0	0
Protoperidinium diabolum (Cleve) Balech, 1974	Pdia	8	16	10
Protoperidinium divergens (Ehrenberg) Balech, 1974	Pdiv	5	5	2
Protoperidinium quinquecorne (Abé) Balech, 1974	Pqui	0	1	9
Protoperidinium steinii (Jørgensen) Balech, 1974	Pste	1	9	4
Pseliodinium vaubanii Sournia, 1972	Gfal	3	5	1
Pyrocystis lunula (Schütt) Schütt, 1896	Plun	0	4	0
Pyrophacus horologium F.Stein, 1883	Phor	2	2	0
Scrippsiellai ispp. Balech ex A.R.Loeblich III, 1965	SCR	23	25	25
Thecadinium spp. Kofoid & Skogsberg, 1928		0	0	1
Torodinium spp. Kofoid & Swezy, 1921		0	1	2
Torodinium robustum Kofoid & Swezy, 1921	Trob	11	22	9
Torquentidium cf. *helix* (Pouchet) H.H.Shin, Z.Li, K.W.Lee & K.Matsuoka, 2019 (syn. *Cochlodinium* cf. *helix* (Pouchet) Lemmermann, 1899)		1	0	0
Triadinium polyedricum (Pouchet) J.D.Dodge, 1981 (syn. *Goniodoma polyedricum* (Pouchet) Jørgensen, 1899)	Gpol	1	2	1
Tripos spp. Bory, 1823	CER	1	3	1
Tripos cf. *macroceros* (Ehrenberg) F.Gómez, 2013	Cmac	3	6	5
Tripos cf. *massiliensis* (Gourret) F.Gómez, 2013		0	1	1
Tripos cf. *minutus* (Jörgensen) F.Gómez, 2013	Cmin	3	3	1
Tripos extensus (Gourret) F.Gómez, 2013		0	1	0
Tripos furca (Ehrenberg) F.Gómez, 2013	Cfur	14	16	10
Tripos fusus (Ehrenberg) F.Gómez, 2013	Cfus	14	17	14
Tripos lineatus (Ehrenberg) F.Gómez, 2013		1	1	0
Tripos muelleri Bory, 1827	Ctri	8	5	7
Tripos teres (Kofoid) F.Gómez, 2013	Cter	1	1	2
Tripos trichoceros (Ehrenberg) Gómez, 2013		0	0	1
Tripos candelabrum (Ehrenberg) F.Gómez, 2013	Ccan	6	6	3
Unidentified dinoflagellate cysts	DinCyst	5	5	1
Protoperidinium cysts	ProtCyst	1	1	2
nº taxonomic entities		**65**	**87**	**77**
Coccolithophores (Prymnesiophyceae)				
Calcidiscus leptoporus (G.Murray & V.H.Blackman) Loeblich Jr. & Tappan, 1978		1	0	1

Taxonomic entity	Abbrev.	LisB	LagB Offshore	LagB Beach
Calciopappus caudatus K.R.Gaarder & Ramsfjell, 1954		0	0	1
Calciosolenia brasiliensis (Lohmann) J.R.Young, 2003		0	2	1
cf. *Coccolithus pelagicus* var *braarudii* (HOL) (Gaarder) Geisen et al., 2002		0	1	0
Cocolithus pelagicus var *braarudii* (HET) (Gaarder) Geisen et al., 2002	Cpel	13	6	0
Coronosphaera spp. Gaarder, 1977/*Syracosphaera* spp. Lohmann, 1902	COR	12	13	8
Coronosphaera mediterranea (Lohmann) Gaarder, 1977	Cmed	4	1	0
Discosphaera tubifer (Murray & Blackman) Ostenfeld, 1900	Dtub	0	3	1
Emiliania huxleyi (Lohmann) W.W.Hay & H.P.Mohler, 1967/*Gephyrocapsa* spp. Kamptner, 1943	Ehux	22	16	5
Helicosphaera carteri (Wallich) Kamptner, 1954	Hcar	6	5	3
Michaelsarsia spp. Gran, 1912		1	0	0
Ophiaster spp. Gran, 1912	OPH	5	5	3
Syracosphaera spp. Lohmann, 1902		0	1	0
Syracosphaera pulchra Lohmann, 1902	Spul	1	4	2
Umbilicosphaera sibogae (Weber Bosse) Gaarder, 1970		0	2	0
nº taxonomic entities		**9**	**12**	**9**
Others				
cf. *Heterosigma akashiwo** (Y.Hada) Y.Hada ex Y.Hara & M.Chihara, 1987		0	2	0
Cryptophytes	CRYsmall	2	21	14
Dictyocha fibula Ehrenberg, 1839	Dfib	5	13	3
Euglenophytes	EUG	24	14	24
Octactis octonaria (Ehrenberg) Hovasse, 1946	Ooct	2	3	4
Octactis speculum (Ehrenberg) F.H.Chang, J.M.Grieve & J.E.Sutherland, 2017		1	2	0
Phaeocystis spp.* Lagerheim, 1893	PHA	2	3	2
Prasinophytes	PRA	0	1	5
nº taxonomic entities		**6**	**8**	**6**
Total		**160**	**167**	**167**

Table. B.3.2. Representation of minima (Min), maxima (Max) and average (Avg) of main HAB species cell concentrations ($x10^3$ cell L^{-1}) by month in each studied site. The national alert and interdiction reference levels are also showed. When the maxima cell concentration occurred above the alert or above the interdiction reference levels are showed, respectively, underline or in bold.

Species	Site		Month												Reference levels	
			Jan	Feb	Mar	Apr	May	Jun	Jul	Aug	Sep	Oct	Nov	Dec	Alert	Interd.
***Pseudo-nitzschia delicatissima*-group**	**LisB**	Min	0	0	0.28	0	0.96	0.60	0	0	0.68	0.12	0.32	0	500	**1000**
		Max	0.08	0	2.00	0	3.08	0.80	5.04	3.76	41.24	1.08	2.16	1.44		
		Avg	0.04	0	1.14	0	2.02	0.70	2.35	2.40	20.96	0.60	1.24	0.72		
	LagB-Offshore	Min	0.08	0.52	0.60	0.68	0.24	0.04	0.60	0	0	0	2.24	0.44		
		Max	0.22	0.72	1.20	21	5.96	0.08	183.65	0.32	0	47.84	2.32	0.84		
		Avg	0.15	0.62	0.81	11	3.10	0.06	68.81	0.16	0	23.92	2.28	0.64		
	LagB-Beach	Min	0	0.20	0.08	0	2.08	0	0	0.32	0	0	0	0.08		
		Max	0	2.02	1.24	24	2.12	0.84	0	59.85	0	2.80	0.16	0.20		
		Avg	0	1.11	0.52	12	2.10	0.42	0	30.09	0	1.40	0.08	0.14		
***Pseudo-nitzschia seriata*-group**	**LisB**	Min	0	0	0	0	0	0.36	0	0	0	0	1.08	0	80	**200**
		Max	0	0	1.88	0.04	1.00	0.56	2.04	8.48	0.52	0	2.60	2.12		
		Avg	0	0	0.94	0.01	0.50	0.46	1.05	2.87	0.26	0	1.84	1.06		
	LagB-Offshore	Min	0	0	0	0.76	0	0	0.08	0.20	52.72	0	1.24	0		
		Max	1.28	0.08	27	2.24	0.52	0	0.40	0.32	68.31	0	1.68	0		
		Avg	0.64	0.40	11	1.50	0.26	0	0.27	0.26	60.53	0	1.46	0		
	LagB-Beach	Min	0	0.06	0	0.32	0.08	0	0	0.24	0	0	0	0		
		Max	0	0.28	1.44	2.08	2.04	1.04	0	2.96	107.61	0.08	0.48	0.16		
		Avg	0	0.17	0.57	1.20	1.06	0.52	0	1.60	36.24	0.04	0.24	0.08		
Dinophysis acuminata	**LisB**	Min	0	0	0	0	0	0	0	0	0	0.04	0	0	0.2	**0.5**
		Max	0	0	0	0.12	0.02	0	0	**0.56**	**0.60**	0.32	0	0		
		Avg	0	0	0	0.04	0.01	0	0	0.32	0.30	0.18	0	0		
	LagB-Offshore	Min	0	0	0	0.08	0	0	0	0.12	0.02	0.04	0	0		
		Max	0	0	0.04	2.40	0.04	0.32	0.08	0.24	0.12	0.04	0	0		
		Avg	0	0	0.01	1.24	0.02	0.16	0.03	0.18	0.09	0.04	0	0		
	LagB-Beach	Min	0	0	0	0.04	0	0	0	0	0	0	0	0		
		Max	0	0	0	0.08	0.12	0.32	0	0	0	0.04	0	0		
		Avg	0	0	0	0.06	0.06	0.16	0	0	0	0.02	0	0		
Dinophysis ovum	**LisB**	Min	0	0	0	0	0	0	0	0	0	0	0	0	0.2	**0.5**
		Max	0	0	0	0	0	0.04	0	0	0.28	0.36	0	0		
		Avg	0	0	0	0	0	0.02	0	0	0.14	0.18	0	0		
	LagB-Offshore	Min	0	0	0	0	0	0.04	0.00	0.04	0.12	0.32	0.04	0.00		
		Max	0	0	0	**0.96**	0	0.06	0.08	0.40	**1.84**	0.48	**2.64**	0.28		
		Avg	0	0	0	0.48	0	0.05	0.03	0.22	1.20	0.40	1.34	0.14		
	LagB-Beach	Min	0	0	0	0	0	0	0.02	0	0.02	0	0	0		
		Max	0	0	0	0.04	0.02	**1.84**	0.08	0.08	**1.36**	0	0.04	0		
		Avg	0	0	0	0.02	0.01	0.92	0.05	0.04	0.47	0	0.02	0		

Species	Site		Month												Reference levels	
			Jan	Feb	Mar	Apr	May	Jun	Jul	Aug	Sep	Oct	Nov	Dec	Alert	Interd.
Dinophysis acuta	**LisB**	Min	0	0	0	0	0	0.48	0	0.16	0	0	0	0	0.2	**0.5**
		Max	0	0	0	0.02	0.24	**0.52**	0.08	0.48	0.08	0	0	0		
		Avg	0	0	0	0.01	0.12	0.50	0.03	0.29	0.04	0	0	0		
	LagB-Offshore	Min	0	0	0	0	0	0	0	0	0	0	0	0		
		Max	0	0	0	0	0	0	0	0	0.02	0	0	0		
		Avg	0	0	0	0	0	0	0	0	0.01	0	0	0		
	LagB-Beach	Min	0	0	0	0	0	0	0	0	0	0	0	0		
		Max	0	0	0	0	0.04	0.04	0	0	0	0	0	0		
		Avg	0	0	0	0	0.02	0.02	0	0	0	0	0	0		
***Karenia* spp.**	**LisB**	Min	0	0	0	0	0	0	0	0	0	0	0	0	n.a.	**n.a.**
		Max	0	0	0.04	0	0	0	0	0	0	0	0.04	0		
		Avg	0	0	0.02	0	0	0	0	0	0	0	0.02	0		
	LagB-Offshore	Min	0.02	0	0	0.08	0.18	0	0	0	0	0	0.04	0		
		Max	0.12	0.02	0.16	0.24	0.52	0	0	0.08	0.16	0	0.20	0.12		
		Avg	0.07	0.01	0.09	0.16	0.35	0	0	0.04	0.07	0	0.12	0.06		
	LagB-Beach	Min	0	0	0	0	0	0	0	0	0	0	0	0		
		Max	0	0	0.14	0.04	0.08	0	0	0	0.04	0	0	0		
		Avg	0	0	0.05	0.02	0.04	0	0	0	0.01	0	0	0		
Gonyaulax* cf. *spinifera	**LisB**	Min	0	0	0	0	0	0	0	0	0	0	0	0	1	**> 1000**
		Max	0	0	0.04	0.02	0	0.02	0	0.04	0.04	0	0	0		
		Avg	0	0	0.02	0.01	0	0.01	0	0.01	0.02	0	0	0		
	LagB-Offshore	Min	0	0	0	0	0.02	0	0	0.28	0.12	0	0	0.10		
		Max	0	0	0	0	0.04	0.04	0.32	2.00	0.44	0.20	0.04	0.16		
		Avg	0	0	0	0	0.03	0.02	0.17	1.14	0.27	0.10	0.02	0.13		
	LagB-Beach	Min	0	0	0	0	0	0.04	0	0	0	0	0	0		
		Max	0	0	0	0	0.04	0.16	0.08	0.08	0.24	0	0	0		
		Avg	0	0	0	0	0.02	0.10	0.04	0.04	0.13	0	0	0		
Lingulodinium polyedra	**LisB**	Min	0	0	0	0	0	0	0	0	0	0	0	0	1	**> 1000**
		Max	0	0	0	0	0	0	0	0	0	0	0	0		
		Avg	0	0	0	0	0	0	0	0	0	0	0	0		
	LagB-Offshore	Min	0	0	0	0	0	0	0	0.20	0	0	0	0		
		Max	0.02	0	0.02	0.36	0	0	0.02	1.52	0	0	0	0		
		Avg	0.01	0	0.01	0.18	0	0	0.01	0.86	0	0	0	0		
	LagB-Beach	Min	0	0	0	0	0	0	0	0	0	0	0	0		
		Max	0	0	0	0.04	0	0	0.04	0	0.08	0	0	0		
		Avg	0	0	0	0.02	0	0	0.02	0	0.03	0	0	0		

Species	Site		Month												Reference levels	
			Jan	Feb	Mar	Apr	May	Jun	Jul	Aug	Sep	Oct	Nov	Dec	Alert	Interd.
Protoceratium reticulatum	LisB	Min	0	0	0	0	0	0	0	0	0	0	0	0	1	> 1000
		Max	0	0	0	0.08	0	0	0	0.16	0	0	0	0		
		Avg	0	0	0	0.03	0	0	0	0.05	0	0	0	0		
	LagB-Offshore	Min	0	0	0	0	0	0	0	0.08	0.08	0	0	0		
		Max	0	0	0.12	0.32	0	0.04	0.04	0.36	0.24	0	0	0		
		Avg	0	0	0.04	0.16	0	0.02	0.03	0.22	0.15	0	0	0		
	LagB-Beach	Min	0	0	0	0	0	0	0	0	0	0	0	0		
		Max	0	0	0	0	0	0	0	0.04	0.08	0	0	0		
		Avg	0	0	0	0	0	0	0	0.02	0.03	0	0	0		
Ostreopsis spp. + *Prorocentrum lima*	LisB	Min	0	0	0	0	0	0	0	0	0	0	0	0	n.a.	n.a.
		Max	0	0	0	0	0	0	0	0	0.04	0	0	0		
		Avg	0	0	0	0	0	0	0	0	0.02	0	0	0		
	LagB-Offshore	Min	0	0	0	0	0	0	0	0	0	0	0	0		
		Max	0	0	0	0	0	0	0	0	0	0	0	0		
		Avg	0	0	0	0	0	0	0	0	0	0	0	0		
	LagB-Beach	Min	0	0	0	0	0	0	0	0	0	0	0	0		
		Max	0	0	0	0.08	0	0.02	0.08	0.04	0	0	0	0		
		Avg	0	0	0	0.04	0	0.01	0.04	0.02	0	0	0	0		